A Virtual Hand Assessment System for Efficient Outcome Measures of Hand Rehabilitation

By
Bilal Nasser

THESIS SUBMITTED IN FULFILMENT OF THE REQUIREMENTS
FOR THE DEGREE OF

DOCTOR OF PHILOSOPHY

in the

DEPARTMENT OF BIOMEDICAL ENGINEERING
UNIVERSITY OF STRATHCLYDE

January 2016

DECLARATION OF ORIGINALITY

Title of Thesis: *A Virtual Hand Assessment System for Efficient Outcome Measures of Hand Rehabilitation.*

This thesis is the result of the author's original research. It has been composed by the author and has not been previously submitted for examination which has led to the award of a degree.

The copyright of this thesis belongs to the author under the terms of the United Kingdom Copyright Acts as qualified by University of Strathclyde Regulation 3.50.
Due acknowledgement must always be made of the use of any material contained in, or derived from, this thesis.

Name   :

Signature   :   21/10/2016

Abstract

Hand rehabilitation is an extremely complex and critical process in the medical rehabilitation field. This is mainly due to the high articulation of the hand functionality. Recent research has focused on employing new technologies, such as robotics and system control, in order to improve the precision and efficiency of the standard clinical methods used in hand rehabilitation. However, the designs of these devices were either oriented toward a particular hand injury or heavily dependent on subjective assessment techniques to evaluate the progress. These limitations reduce the efficiency of the hand rehabilitation devices by providing less effective results for restoring the lost functionalities of the dysfunctional hands.

 In this project, a novel technological solution and efficient hand assessment system is produced that can objectively measure the restoration outcome and, dynamically, evaluate its performance. The proposed system uses a data glove sensorial device to measure the multiple ranges of motion for the hand joints, and a Virtual Reality system to return an illustrative and safe visual assistance environment that can self-adjust with the subject's performance. The system application implements an original finger performance measurement method for analysing the various hand functionalities. This is achieved by extracting the multiple features of the hand digits' motions; such as speed, consistency of finger movements and stability during the hold positions.

Furthermore, an advanced data glove calibration method was developed and implemented in order to accurately manipulate the virtual hand model and calculate the hand kinematic movements in compliance with the biomechanical structure of the hand.

The experimental studies were performed on a controlled group of 10 healthy subjects (25 to 42 years age). The results showed intra-subject reliability between the trials (average of cross-correlation $\rho = 0.7$), inter-subject repeatability across the subject's performance ($p > 0.01$ for the session with real objects and with few departures in some of the virtual reality sessions). In addition, the finger performance values were found to be very efficient in detecting the multiple elements of the fingers' performance including the load effect on the forearm. Moreover, the electromyography measurements, in the virtual reality sessions, showed high sensitivity in detecting the tremor effect (the mean power frequency difference on the right

extensor digitorum muscle is 176 Hz). Also, the finger performance values for the virtual reality sessions have the same average distance as the real life sessions (RSQ =0.07).

The system, besides offering an efficient and quantitative evaluation of hand performance, it was proven compatible with different hand rehabilitation techniques where it can outline the primarily affected parts in the hand dysfunction. It also can be easily adjusted to comply with the subject's specifications and clinical hand assessment procedures to autonomously detect the classification task events and analyse them with high reliability. The developed system is also adaptable with different disciplines' involvements, other than the hand rehabilitation, such as ergonomic studies, hand robot control, brain-computer interface and various fields involving hand control.

Publications

The research in this thesis has contributed in part or full for the following publications:

Proceedings:

Bilal Nasser, Heba Lakany, Bernard Conway. (2014) A Virtual Hand Assessment System for Efficient Measures of Hand Rehabilitation. In European Orthopaedic Research Society.

Book Chapter:

Aikaterini D. K., Susanna S., Bilal N.,Josefina G. M. and Muthukumaran T. (2014) Upper Limb Neuroprostheses: Recent Advances and Future Directions. 207. In Emerging Therapies in Neurorehabilitation. Biosystems&Biorobotics Vol. 4.

Article:

Madeleine G., Bilal N. (2013) The Use of Virtual Reality in Assisting Rehabilitation. 19-20. In Advances in Clinical Neuroscience & Rehabilitation (ACNR) Vol. 13, Issue 6

Acknowledgements

Firstly, I would like to thank Dr. Heba Lakany for all her continuous patience, motivation, guidance, invaluable advice, and significant contribution to my Ph.D.

I also would like to thank Prof. Bernard Conway for giving me the opportunity to be part of the Biomedical Engineering Unit and be able to deploy my skills and passion in the medical rehabilitation field.

In addition to my supervisors, I would like to thank the senior researchers in the lab: Dr. Sujay Galen, Dr. Gopal Valsan, Dr. Campbell Reid and Dr. Sylvie Coupaud,for their insightful feedbacks that contributed in widening my research perspectives and optimizing my research outcomes.

I am thankful to Prof. Madeleine Grealy who provided me the opportunity to join the Psychology department, in a parallel to my research, and develop a virtual reality system for Psychological rehabilitation. This post has come in a great support to fund my PhD.

My thanks also go to the research communities, who I have come to know in conferences, seminars, journal papers or other methods, for stimulating significant discussion that helped me to strengthen my research work.

My sincere thanks and appreciations also go to all my lab colleagues in Neurophysiology: Ange Tano, Hifisyambinahmadjamil Syahrull, Chi-Hsu Wu, Dr. Bahman Nasseroleslami, Pauline Axford, Dr. Danial Kahani, Dr. Alejandra Garza, Catherine MacLeod, Jamie O'Reilly, Sibani Mohanty, Lijo Varughese Chacko, Radhika Menon and everyone else, for adding great moments to my work in the lab, for the circle discussions that were full of learning and reflections, for the late working nights and weekends, and for their encouragements and contribution to my research and experiments.

And big thank you to Mrs. Sarah Day for lending me the SHAP system, in order to conduct the experiments and achieve the study outcome.

Also my great thanks to all the staff and students who helped me in the Biomedical Engineering department, University of Strathclyde.

Last but not least, I would like to thank my family: parents, brother and sisters for their love and support throughout my life. And the warmest thanks to the one and only, my fiancé Maya Yazbeck, for her patience, intelligence, kindness and support throughout all the years of my work on this project.

Table of Contents

List of Figures

List of Tables

Glossary and Abbreviations

Abduction	Lateral movement of finger away from the axial line (middle finger).
Activities of Daily Living (ADL)	Daily activities that people perform without requiring assistance. It includes eating, opening the door, typing etc.
Adduction	Medial movement toward the axial line.
Arm Robot	Robot device that mimic the structure and kinematic of the arm.
Artificial Neural Network (ANN)	A machine learning technique to analyse large dataset and extract specific patterns and features.
CAM	Continuous Active Motion technique for hand rehabilitation.
CIMT	Constraint-Induced Movement Therapy for hand rehabilitation.
Collision Detection	In graphics, collision detection is a computational model to detect the intersection of graphical objects when they come in contact.
CPM	Continuous Passive Motion technique for hand rehabilitation.
cross-coupled sensors	Sensors which are dependent of each other. The variation of one sensor will affect the other.
Data glove	A glove device that compromises sensorial utensils to measure the motion and other characteristics of the hand.
Degree of Freedom (DoF)	A number of independent parameters that describes the system motion and constraints.
Dexterity	Hand skills in performing tasks.
Denavit-Hartenberg (D-H)	A set of properties that define the four convention parameters which attach the links and joints together in a kinematic chain.
DIM	Dorsal Interosseous Muscle
Distal Interphalangeal (DIP)	Joint between intermediate and distal phalanges.
Electromyography (EMG)	A tool that measures the muscle responses by reading the electrical activities.
End-Effector	A point or object at the end of the system to interact with the

	environment. (i.e. Fingertip)
Extension	Straightening the finger joints resulting increase of angle.
Finger Performance Value (FPV)	A metric value to calculate the performance value of the finger using the methods described in this thesis.
Flexion	Bending the finger joints resulting decrease of angle.
Forward Kinematic	A mathematical model that determines the end-effector position with pre-defined joint parameters.
Functional Electrical Stimulation (FES)	A technique that electrically stimulate a nerve to improve mobility.
Genetic algorithm	A recursive method to find the best solution by optimising the parameters. It is based on natural selection process found in biological evolution.
Graphical Display	A device or system to present visual presentation of data or images.
Graphical User Interface (GUI)	An interface to allow user to interact with the application.
Grasp event	A defined event in the experiment to move the fingers to grasp a virtual or real object. (Shown in the fingertip displacement between the Grasp start and Hold start)
Grasp Task	A defined task in the experiment to grasp a spherical shape (i.e. ball), virtual or real object.
Hand Robot	Robot device that mimic the structure and kinematic of the hand.
Hold event	A defined event in the experiment to maintain the fingers at a certain position without moving. (Shown in the fingertip displacement between the Hold start and Relax start)
Home Position	In this thesis Home Position is referred to the finger position at the start of each Grasp event. The fingers are usually fully extended in this position but depend on the subject configurations.
HVDC	High Voltage Direct Current, electrical technique for hand rehabilitation.

Inverse Kinematic	A mathematical model that calculates the joint parameters that move the system end-effector to a desired position.
Kinematic	A mechanical definition that describes the motion of objects, points and systems of bodies.
Kinematic chain	An assembly of rigid bodies connected by joints.
Lateral task	A defined task in the experiment to move the fingers to a certain posture in order to hold a virtual or real plate object.
Learning Pattern	A sequence of functions or motor skills learned by repeating a task for a number of times.
Metacarpophalangeal (MCP)	Joint between the metacarpal bone of the finger and the phalange.
NES	Neuromuscular Electrical Stimulation, electrical technique for hand rehabilitation.
non cross-coupled sensors	Independent sensors.
PNF	Proprioceptive Neuromuscular Facilitation, electrical technique for hand rehabilitation.
Point task	A defined task in the experiment to move the fingers to a certain posture in order to point on a specific spot.
Principal Component Analysis (PCA)	A statistical method that converts a set of correlated variables into set of linearly uncorrelated variables. It is used to reduce the complexity dimensions of a set of data.
Proximal Interphalangeal (PIP)	Joint between the proximal and intermediate phalanges.
Range of Motion (ROM)	The full range of flexion and extension for a joint.
RAP	Right Abductor Pollicis Muscle
RED	Right Extensor Digitorum Muscle
Relax event	A defined event in the experiment to return the fingers and hand to the start position. (Shown in the fingertip displacement between the

	Relax start and Finish)
RFD	Right Flexor Digitorum Muscle
RL session	Real Life session. It involves interacting with real objects.
RL+Load session	Real Life with Load session. It involves interacting with real objects, and with a weight added on the forearm.
RL+Tremor session	Real Life with Tremor session. It involves interacting with real objects, and with tremor movement.
rloess	Regression of locally weighted scatterplot smoothing filter.
Scene Graph	Graphical architecture to organise the different models and objects in a scene in a structural and interactive method.
See-Through	A graphical display technique that allows to reduce visibility of specific graphical objects in order to see different layers or components in the presentation.
Self-Organising Map (SOM)	An artificial neural network type to organise the data in low-dimensional representation by using unsupervised learning method.
Simulator	A computer generated program that provides an imitation of specific conditions or properties of the real world in an advanced graphical display.
Start Position	It is the position to place the hand on the table with extended finger at the start of each task.
Finger Smoothness	It is the consistency of the finger displacement (or trajectory), and measured by applying smoothing or signal noise ratio techniques. It is used in this thesis method calculation.
Southampton Hand Assessment Procedure (SHAP)	A clinical assessment procedure to measure hand performance, using a toolbox.
Finger Speed	It is the finger displacement over time used in this thesis method calculation. Also, known as slope or gradient in mathematics and

graphical definitions.

Finger <u>S</u>tability	It is the stability (or also steadiness) level of the finger movement during and only during the Hold event. It is measured by using data signal smoothing technique and used in this thesis method calculation.
TENS	Transcutaneous Electrical Nerve Stimulation, electrical technique for hand rehabilitation.
Thumb Interphalangeal (IP)	The end joint of the thumb.
Tripod task	A defined task in the experiment to hold a virtual or real prismatic object.
Virtual Environment	A program that manages and controls multiple graphical objects in separate places. It defines the items properties in order to simulate a virtual world similar to realistic.
Virtual Model	A graphical model that defines the interactivity with the virtual environment and the motion properties of different virtual objects.
Virtual Object	A graphical object that includes specific characteristics and properties in the virtual world.
Virtual Reality	A machine system that involves a simulator and technological devices to interact and visualise the imitated world.
Visualisation	A graphical representation of numerical data, in graphs/charts or different formats such as Virtual Reality.
VR session	Virtual Reality session. It involves interacting with virtual objects in the graphical display.
VR+Load session	Virtual Reality with Load session. It involves interacting with virtual objects and with a weight added on the forearm.
VR+Tremor session	Virtual Reality with Tremor session. It involves interacting with virtual objects and with a tremor hand movement.

Chapter 1 Introduction

"The hand is an extension of the human brain." Immanuel Kant

The main scope of the project is to develop an objective measurement system for assessing hand performance during rehabilitation. In this chapter it is essential to begin by explaining the physiology and characteristics of the human hand. The existing medical challenges faced by clinicians and researchers must also be considered before the project's main aims and objectives are described. The purpose of this is to introduce the reader to the main aspects of the project and explain the motivating factors for the author and the associated researchers.

The following sections start by introducing the hand's role and significance in human life. It then discusses the diseases and injuries that can cause loss of hand functionality and severely affect life. Following this, the proposed approach is illustrated, along with the project's objectives and aims. The research hypotheses are then defined. The chapter ends by listing the author's contributions to this field. This includes a virtual reality, human hand outcome measurement, and transferring signal processing and robotics technologies into medical rehabilitation.

1.1. Research Context

1.1.1. Human Hand: Role and Significance

The human hand has a complex anatomical structure and highly articulated mechanisms, giving it the flexibility to perform complex postures with smooth and decisive movements. The hand plays a major role in human life. It has delicate capabilities in sensing, orienting and immersing humans in the external world. Without the hand, there would be no Beethoven, Mozart, or Picasso.

The hand provides the precision and reliability to perform skillful arts, and manipulate sophisticated equipment and tools to construct, write, undertake surgical operation, and perform complex manual tasks. It allows a person to interact with surrounding objects and estimate their distances and positions from the body. It also facilitates communication with

others (i.e. sign languages or gestures), and helps us to identify each individual person from their unique biometric information.

The non-dominant hand is commonly used in emotional and social interactions, such as reaching out to others and making expressions. For a right-hand dominant person, the right hemisphere of the brain, which controls the left side of the body, manages the emotions when reacting to unpredictable incidents and hazards. The left hemisphere manages the structure details and functional control (Forrester et al., 2013).

The fingertips' high touch sensitivity is considered the pinnacle of hand function. They have the highest concentration of touch receptors for sensing vibrations, pressure and textures. This could be tested by trying to identify an object on the forearm or the fingertip without using visual perceptions. Fingertips also have proprioception sensors within the muscles and tendon layers to perceive the location of surrounding objects, in addition to many other external sensations, such as temperature. This could be tested by closing the eyes and placing the fingertip close to a noise, without using any visual feedback.

1.1.2. Hand dysfunction

The hand's significant involvement in a human's daily activities, and contribution to almost 90% of the upper limb function (Magee, 2007), makes it the most mobile joint in the human body. This means it is continuously exposed to high risks of joint dislocations and wear.

Hand dysfunction may be caused by multiple conditions, including carpal tunnel syndrome (nerve compression), injuries (resulting in fractures and ruptured ligaments), or diseases leading to tendinitis (tendon irritations) and osteoarthritis (wear-and-tear arthritis causing deformity).

Hand injuries, such as burns, high-pressure injuries, infections, lacerations, fractures, and dislocation, can also contribute to causing dysfunctions or disability of the hand. The most common cause of hand injuries is blunt trauma (50%), followed by injury from a sharp object (25%) (OSHA, 2015).

Strokes can also play a major role in hand dysfunction. As Stroke (NHS, 2014) is a brain attack which occurs when the blood supply to part of the brain is cut off. Stroke victims often

experience hand impairment, with approximately 38% (Duncan et al., 2003) of stroke survivors reported to have difficulty in hand function.

A stroke patient may suffer a number of weaknesses affecting hand motor functions and dexterity, such as decreased tactile sensation, and diminished proprioception caused by the inability of muscles to produce forces for fine control movements. Patients may experience the need for extra cognitive and motor effort to control limb movement and can suffer from poor task coordination due to the lack of sensory feedback (Lum et al., 2012).

Stroke and injuries survivors generally show a certain ability to recover their lost hand functions (eMedicineHealth, 2013), while application of immediate care significantly reduces the effects of long-term disorders. Therefore, efficient and quick administration of hand rehabilitation is essential in recovering the lost functions.

1.1.1. Hand Rehabilitation
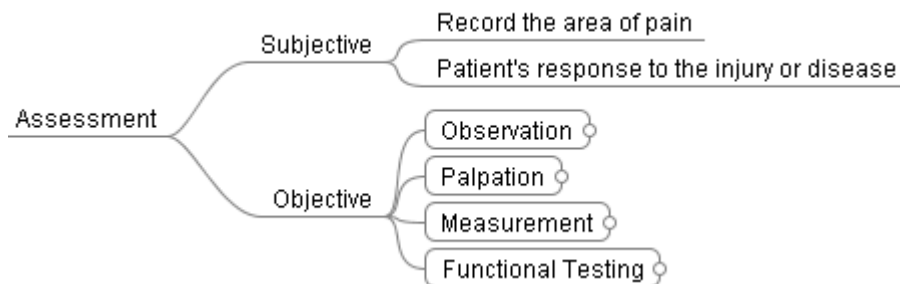
Figure 1-1 Taxonomy of the hand assessment process , combining the subjective and objective evaluations (This diagram is produced by the author. The information is taken from Chapter: Implications for Practice (Florence and Jane, 1988)).

In the case of hand dysfunction, the therapist/surgeon examines the patient's hand, using a set of assessment procedures, and determines whether the hand requires surgery, prosthetic employment or a rehabilitation programme.

The hand assessment process, shown in Figure 1-1, is divided into subjective and objective evaluation. The subjective method identifies the location and nature of the symptoms (pain, swelling, redness and stiffness). It also identifies the patient's physical and psychological reactions to the affected hand in daily activities. The objective method examines the hand

using four techniques: observing the posture and using the hand in simple activities; examining hand abnormalities or locating the pain using palpation; performing measurements on hand dexterity and range of motion using instruments or manual tests; and carrying out functional testing by simulating tasks from daily activities.
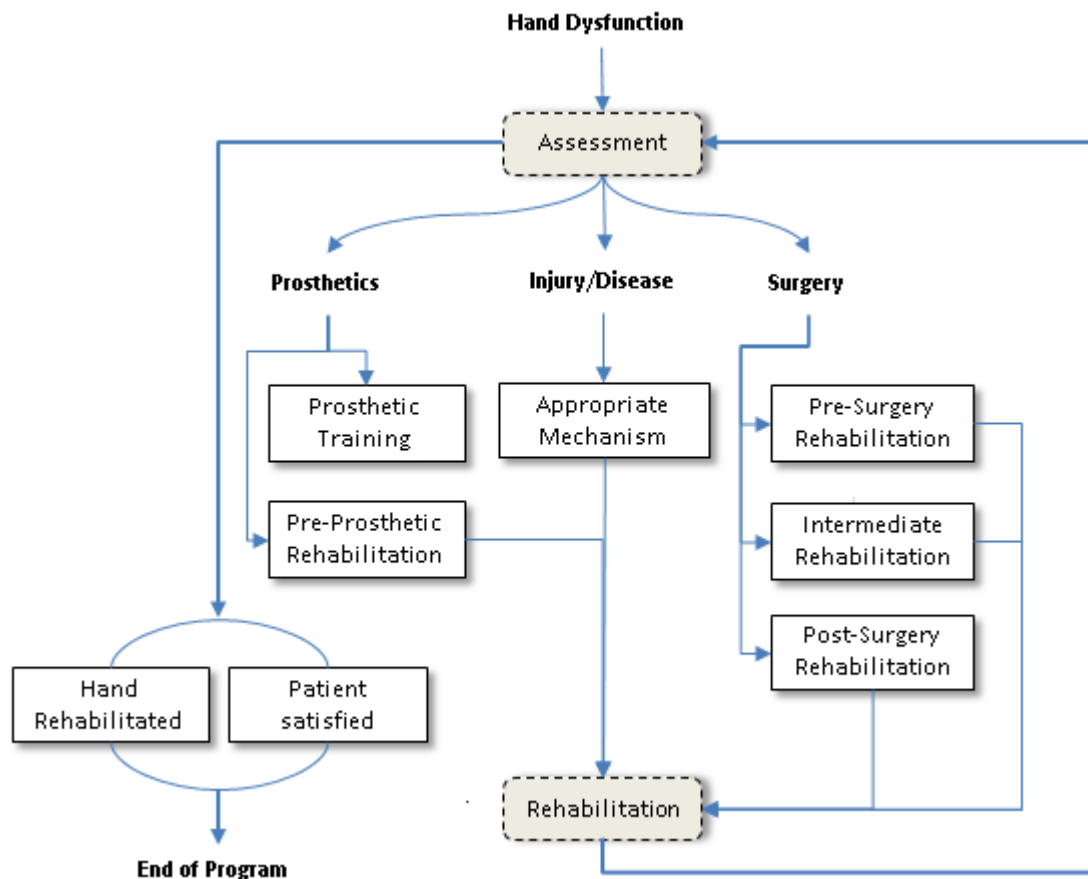
Figure 1-2 Flow diagram of the hand rehabilitation process illustrates the procedures performed in the rehabilitation process for a dysfunctional hand. (This diagram is produced by the author© 2015. The information is taken from Chapter Implications for Practice (Florence and Jane, 1988)).

Rehabilitation programs involve multiple steps and were defined based on the hand's capabilities and the level of dysfunction.

The different techniques involved in the rehabilitation process were psychological support (Florence and Jane, 1988) to patients; education on the anatomy/physiology of the hand, and awareness of the treatment goal with the expected outcome; positioning and immobilising certain hand functions by using items to prevent deformity; manual techniques by occupational therapists, including stretch, massage and vibration, to restore the range of motion of the joints; electrical techniques such as Neuromuscular Electrical Stimulation (NES), High Voltage Direct Current (HVDC), Ultrasound, and Transcutaneous Electrical Nerve Stimulation (TENS); Proprioceptive Neuromuscular Facilitation (PNF) techniques with light to heavy resistance on the fingers applied from different active items (i.e. sponges, putty exercises etc.); and functional activities which allow the integration of treatment modalities with daily living (ADL). The above stages were usually executed consecutively and in repetitive cycles (see Figure 1-2). This serves to provide an efficient restoration of hand functions and accurate transfer of the learned/restored functions from training exercises to real world daily activities (Florence and Jane, 1988).

1.2. Research Motivation

1.2.1. Problem Definition

There are various drawbacks in the hand rehabilitation methods currently used to restore hand functionality. This is mainly due to the inefficiency of the hand model tools in addressing lost function; deformation limits (stiffness, inconsistent durability and elasticity, strength, fatigue, life, and ductility etc.) and inability of materials to adapt with hand performance; and complex mechanics, including sophisticated technologies, which make the device cumbersome and difficult to adjust to while performing gross and fine hand motor movements (Tai, 2007).

An efficient assessment method is required to objectively measure the hand's performance before, during and after the rehabilitation sessions. This would improve rehabilitation results and reduce the limitation level. This method also needs to include quantitative evaluation in order to relevantly adjust the system/programme and make the process self-adaptable. At present, the clinical assessment methods used are still subjective (see section 3.1.1) and

depend only on the therapists' observations. In addition, the objective measurement data provided by the research and hand societies – American Society for Surgery of the Hand (ASSH)(ASSH, 2015), British Society for Surgery of the Hand (BSSH) (BSSH, 2015), and National Institute of Arthritis and Musculoskeletal and Skin Diseases (NIH)(NIH, 2015) – are not sufficient to make decisive conclusions to improve hand performance.

1.3. Research Objectives

Further to the challenges described previously, this thesis aims to provide an advanced hand assessment system that is compatible with the numerous different hand rehabilitation techniques and seeks to reduce many of the existing drawbacks.

The proposed system combines clinical techniques and virtual reality (VR) technologies to return objective and dynamic measurements of the hand's performance. Researchers and therapists can then use these to improve rehabilitation systems. They will also allow the programme to be adjusted depending on patient performance.

There are a number of advantages provided by the VR technology, such as being able to track individual hand digit's range of motion (RoM) and constantly measure the fingers' movements. The system can dynamically measure and evaluate hand performance, compare the subject's performances with the normative dataset, self-adapt with the subject's improvement during the rehabilitation, and provide consistent exercises with high precision and motivation to the patient.

In order to produce this system with high accuracy and efficient results, the following objectives are defined:
1- Specify a compatible and clinically validated hand classification method.
2- Develop a robotic simulator that will comprise the virtual environment for the experiment.
3- Design a biomechanical virtual hand model that can accommodate the different hand kinematics and functions.
4- Develop a robust and reliable interface between the real hand movement and virtual hand display that accounts for the existing discrepancies between different dysfunctions/paralysed hands and the physiological structure of the hand.

1.4. Research Hypotheses

This study hypothesises that the proposed approach of the virtual hand assessment system, quantitatively measures the performance of the hand during rehabilitation.

1.5. Contributions

The author's contributions are:

❖ A novel method is developed that efficiently measures the finger performance value using multiple ROM features (i.e. stability, speed, smoothness). The method is dynamic, objective, automated, modular, and mobile.

❖ This is the first time, to the best of the author's knowledge, a VR system is developed with a clinically validated hand assessment procedure (kinematic, calibration, model, interface).

❖ A unique and robust calibration algorithm is developed to map the sensorial data inputs into the VR model, adapt with the physiological variations and validate the data glove outputs.

This method, unlike others, does not require large data sets or long duration (>5 mins), plus it is inclusive to the different joints DoFs.

❖ An advanced cross-compatible application is developed which can be easily integrated and used in the motor control, sign language and gestures recognition, ergonomics, and system/robotics control studies.

❖ An extensive literature review is produced on clinical, robotics, virtual reality, data glove/exoskeleton and synthetics applications in the hand rehabilitation and assessment.

1.6. Organisation of the Thesis

This thesis is divided into eight chapters with references and appendices. The structure of the chapters is as follows:

Chapter 2: Begins by defining the background of hand anatomy, structure, and pertinent details of the muscle activities essential to hand function. The hand kinematic model and structure are outlined with a review of the multiple implementations and constraints used to define the joints' range of motion.

Virtual simulation is discussed in this chapter, as it is one of the two main elements involved in

the project. A review of various existing robotic simulators is highlighted, with a discussion of their advantages and relevance to the project aims. The selected simulator, GraspIt!, is described separately and in full detail, with an attention drawn to the relevant existing features affiliated with project requirements.

The chapter then pinpoints the list of developments to the robotic simulator that are needed to integrate it into the bioengineering field.

Lastly, hand motor control is described, which highlights the contributions of the project to neurophysiological rehabilitation.

Chapter 3: Starts with a literature review of the existing systems for hand rehabilitation and assessment. This chapter presents some of the devices primarily applied in rehabilitation, including clinics and therapy, robotic assistance, virtual reality, electrical simulation and synthesis applications. The chapter concludes with a discussion on the reviewed methods and proposes the new approach of this project, which tackles the existing limitations in the field.

Chapter 4: Discusses the experimental protocol in depth, as well as the inclusion criteria of the specified subjects and the various procedures undertaken in each task and session.

Chapter 5: Provides a review of the existing computational modelling calibration methods. The calibration approach of the project is provided, including the multiple equations and procedures. At the end of the chapter, the conducted experiment is explained with a discussion of the outcome reliability.

Chapter 6: Illustrates the results of the experiment and the observations made during the data analysis and measurement. The results are analysed using different statistical methods.

Chapter 7: Provides a discussion of the observations validating the repeatability and efficiency of the outcome measurements. The results are compared with other work, and the final outcome is examined in relation to the hypotheses claims. The chapter concludes with the project's contributions.

Chapter 8: Summarises the work and achievements of the project. This chapter also highlights the advantages of the features developed in the system and illustrates a number of potential improvements for implementation in different research fields.

1.7. Summary of the Introduction Chapter

In this chapter the role of the human hand was introduced with its significance, and main medical challenges. This is along with a list of procedures consulted in case of hand dysfunction, associated with the existing techniques for hand performance assessment and hand rehabilitation. This chapter also highlighted that, although there are many techniques in rehabilitation, they have multiple drawbacks.
The project's approach for solving the existing limitations was defined through the hypothesis of developing a virtual reality objective measurement system to assess hand performance.

The chapter concluded by listing the project's contributions to the research community and rehabilitation programmes, along with descriptions of the thesis organisation and content of the chapters.

Chapter 2 Background

This chapter provides extensive details of the project background. It starts by describing the human hand's physiology and anatomy, as well as its role and structure. It then briefly describes muscle activity in the hand and the biological mechanism of the nervous system in terms of its involvement in the hand's functions.

The hand kinematic model and its functions are later described to outline the hand's high articulation and fast adaptability while performing complex tasks and handling different composite tools. This section also includes the algorithms, mathematical models and functional constraints of the hand model.

Following this, an explanation of the virtual model used to perform the hand simulation is provided. An extensive review of its architecture, features, and limitations is provided. This section finishes by listing the developments required on the virtual platform in order to employ this simulator in the project.

The chapter then concludes by exploring the motor control barriers in hand functionality. It gives a background insight of hand dysfunctions and their main effects. This section aims to describe the key elements that should be considered to design an inclusive and cross-compatible system for hand and motor control rehabilitation.

2.1. Hand Anatomy

2.1.1. Structure

Hand structure can be subdivided into five layers: skin, muscles (tendons), nerves, blood vessels, and bones (joints). The layers are intertwined together and any damage to one layer can affect the others and cause impairment to hand function.

2.1.1.1. Muscles

Muscles are the engines that transform energy to produce force and motion. In the hand and forearm, there are 48 extrinsic muscles (Florence and Jane, 1988): 28 in the forearm, 14 in extensor/supinator, and 14 in flexor/pronator, and 20 intrinsic muscles between the wrist and CMC joints, to provide a balancing force between extrinsic extensors and flexors. Forearm

muscles are mainly used for gross hand movements and give strength to the grip. The smaller muscles in the hand control the fingers, support the tendons and refine the movement independently with coordinated timing in order to perform precise and accurate functions. To obtain fine movements, the forearm muscles must be stabilised; this is observed with surgeons when they immobilise their forearms during surgeries, or artists when they use "arm rest" stands during very detailed drawings.

2.1.1.2. Nerves

The hand has median, ulnar and radial nerves to supply the motor control, sensory feedback and autonomic of the hand. Sensory neurons send information signals to analyse and process the command for control. Each muscle is controlled by multiple neurons that transmit the appropriate information to achieve fast, precise and solid results in different activities (Gray, 2015).

2.1.1.3. Arteries

The hand consists of different types of arteries – radial, ulnar and interosseous – that travel alongside nerves to supply the other parts of the hand with blood. There are dorsal and palmar arteries to support the different sides of the hand and fingers (Gray, 2015).

2.1.1.4. Skin

The skin forms a glove over the hand to protect the other components. It is composed of multiple layers including the sensory receptors. It is proficiently structured to ensure suppleness, mobility and elasticity in the different hand movements (Gray, 2015).

2.1.1.5. Nail

The nail apparatus supports and protects the fingertip and provides a mechanism to pick up objects (Gray, 2015).

2.1.1.6. Bones

The hand consists of 27 bones (ElKoura and Singh, 2003); eight carpals – scaphoid, lunate, triquetral, pisiform, trapezium, trapezoid, capitate, and hamate; five metacarpals – proximal base, medial body, and distal head; and 14 phalanges – proximal, medial, and distal on each finger, apart from the thumb which has only proximal and distal. The joints between carpals

and metacarpals are called carpometacarpal (CMC), and, respectively, the others are called proximal interphalangeal (PIP), metacarpophalangeal (MCP), and distal interphalangeal (DIP)
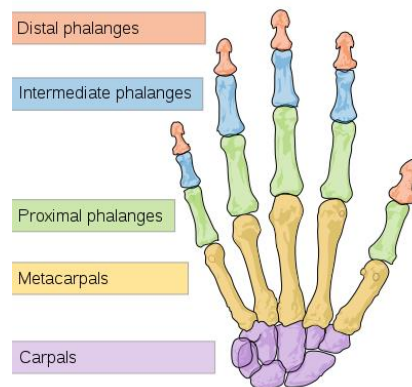
Figure 2-1 Hand skeleton Sketch, dividing the fingers bones into 5 sets: Distal Phalanges, Intermediate Phalanges, Proximal Phalanges, Metacarpals, and Carpals (Gray, 2015).

Elkoura noted that the hand kinematic consists of 27 Degree of Freedom (DoF) (ElKoura and Singh, 2003). There are four in each finger, three for extension and flexion, and one for abduction and adduction. The thumb is more complicated and has five DoF, leaving six DoF for the rotation and translation of the wrist.

Figure 2-2 displays the various hand motions, including degrees of freedom and movements:
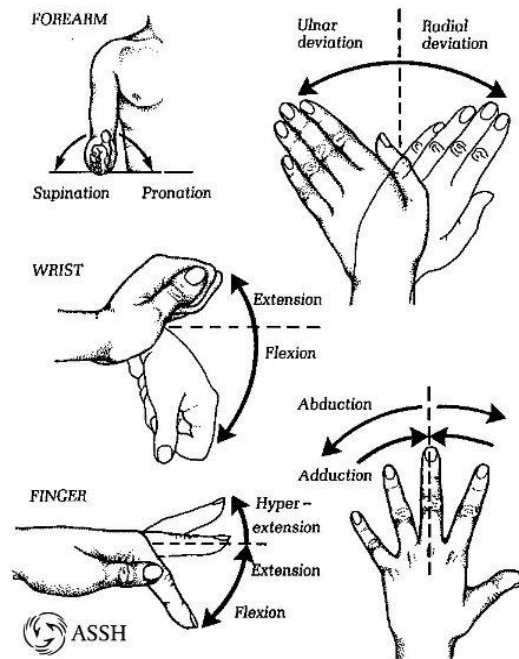
Figure 2-2 Fingers Articulation Diagram, shows the hand motion: wrist/forearm movement: roll (supination, pronation), pitch (flexion, extension) and yaw (ulnar deviation, radial deviation). Finger movement: each finger orient in 2D flexion/extension and abduction/adduction © 2009 American Society for Surgery of the Hand; with permission.

Also, Reiner have measured the normal range of motion of the fingers(Reiner, 2005), presented in Table 2-1:

Table 2-1 Range of movements for the finger joints. The unit used is degree. The DIP minimum is by hyperextension (Reiner, 2005).

Finger	DIP(E/F)	PIP(E/F)	MCP(Ab/Ad)	MCP(E/F)	CMC(E/F)	CMC (Ab/Ad)
Thumb	15H/80	-	0/60	10H/55	25/35	0/60
Index	10H/90	0/100	13/42	0/80	-	-
Middle	10H/90	0/100	8/35	0/80	-	-
Ring	20H/90	0/100	14/20	0/80	-	-
Small	30H/90	0/100	19/33	0/80	-	-

In contrast to other primates (apes, gorillas, baboons, etc.), the thumb of the human hand is longer, stronger and able to move more freely across the hand, giving it unique capabilities with high accuracy and precise grips for manipulating tools and objects (Kivell et al., 2013). The human hand has ulnar opposition capability, where the small and ring fingers can rotate across the palm to meet the thumb and provide a better grip, grasp and torque performance. Also, the opposing thumb can abduct-adduct, flex-extend, and antepose-retropose to touch the other fingers. Almost 90% of the thumb movements happen at the base and it is the most mobile of all the fingers (Fogg, 2015).
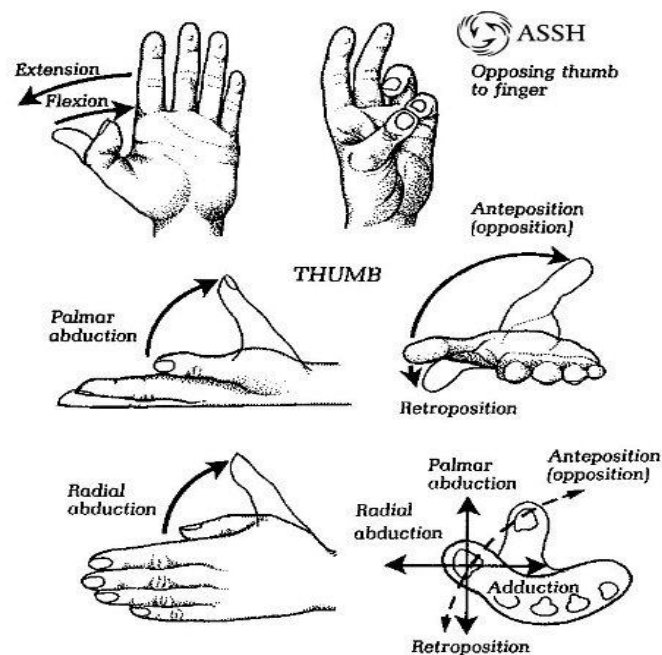
Figure 2-3 Illustration diagram of the thumb motion; the thumb has anteposition/retroposition via radial formation, in addition to the flexion/extension and abduction/adduction; © 2009 American Society for Surgery of the Hand; with permission.

2.1.1.7. Muscle Activities

As previously mentioned the muscles make a large contribution to hand functionality. They act as an engine, transforming energy in to hand motions and dexterous movements.

The hand muscle type is skeletal, which is composed of bundles of muscle fibres. Each fibre is

comprised of many myofibrils, containing repeating subunits of sarcomere, which act as contractile units.

When the muscle receives an electrical signal from the brain via the nervous system, the synaptic terminal of the end nerve cell releases acetylcholine to the neuromuscular junction (motor end plate), binding the nerve with the muscle fibre. This causes depolarization in the synaptic cleft and releases Ca++ (Calcium) elements. The Ca++ travel inside the muscle cells to the actin thin filament, allowing the myosin thick filament to attach to the binding sites and establish cross bridges. The myosin then grabs the actin and pulls it. This phenomenon is known as sliding filament mechanism of muscle contraction (Gray, 2015).

Subsequently, the sarcomere contractions cause muscle shortening and provide the force and motion to perform the desired skeletal movements in the hand.

Hand muscles are subdivided into three groups: the thumb muscles on the radial side, the little finger muscles on the ulnar side, and the middle of the hand and between the metacarpals.

To measure the muscles' contractions during hand activities, specific measurement electrodes can be placed on the muscle that read the summation of the electrical potential from the muscle fibres. This is known as electromyography (EMG).

EMG can be performed using surface electrodes to read high potentials from large muscle activities, or with needle electrodes (intramuscular EMG) to read exclusive potentials from smaller muscles.

Figure 2-4 shows a schematic for EMG recording: the bipolar electrodes are placed on the targeted muscles with the reference electrode on the wrist bone. The signal output is passed to an amplifier to return the raw EMG signals, subtract the baseline from the reference, and remove electrical noises that cause arbitrary voltage variations. The EMG signal is then processed through high pass/low pass filters and signal processing techniques.
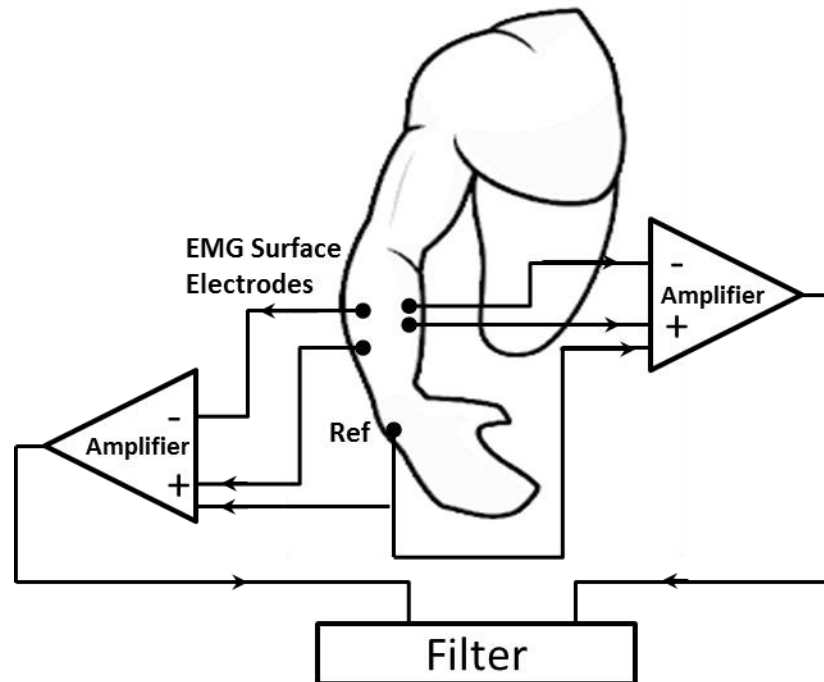
Figure 2-4 EMG recording system diagram; Four electrodes are placed on the forearm of the subject. The system reads the muscle activity by combining two EMG electrodes that are placed on the same muscle. The signal is processed through an amplifier, which multiplexes both electrodes signals and uses the third input as a reference (The reference electrode is placed on the wrist bone). The signal is then processed with applied filter techniques. This diagram is produced by the author.

EMG signal processing focuses on extracting the significant features from the reading which relate to each study purpose (Popović and Sinkjær, 2000). For example, the fast Fourier transform (FFT) is applied on EMG signals to analyse the stability level (hand shaking) during a task, the time domain series is used to measure the duration and force exertion to differentiate the performance of each task or movement, while peak detection and sub-spacing (lowering the dimension level of the multiple properties) methods are employed to analyse the level of muscle involvement.

EMG measurements are used in many tasks (Al-Jumaily and Olivares, 2009): to control prosthetic hands, robotic arms and devices; to monitor and diagnose motor control disorders

or hand dysfunctions; to read isometric muscle activities associated with force and strength applied; to determine the level of fatigue in muscle by measuring the variation of the mean absolute value of the signal; and to identify the level of tremor or involuntary muscle contractions for an impaired hand.

However, EMG measurements, particularly the surface interface electrodes, have multiple limitations, including the produced variation of the EMG signal amplitude from different skin impedance, which reduces the electrical potential level acquired from the muscle (Al-Jumaily and Olivares, 2009). The overlapping muscles cause interferences in the signal activities' reading, plus it is very difficult to identify a specific muscle's involvement. The sub-layered muscles are obstructed resulting in less reliability in readings. In addition, movement in the skin layer is not consistent with muscle movement, which causes deviation from the signal readings of different allocated muscles under the electrode surface (Platz, 2003).

2.2. Hand Kinematic Model

The hand kinematic model is used in different disciplines (Butterfass and Hirzinger, 2001), (ASSH, 2015), (BSSH, 2015) and applications due to its high performance and precision. It is used in manufacturing and construction processes, providing the ability to make the precise movements and critical grips performance required to create high definition objects, buildings, or crafts with complex shapes and designs. It is also used in robotics applications for surgeries and prosthetic limbs, which combine high precision tasks and adaptive coordination between force, stability, and speed, with other control elements. Recently, it has been employed in computer vision for hand tracking and gestures recognition. In addition, the hand kinematic is continuously being investigated as part of rehabilitation objectives, to define the appropriate training techniques to restore the lost functionality and performance for patients' hands.

2.2.1. Hand kinematic development

Hand control and precise finger formation are developed at a very young age (Kivell et al., 2013). This process is achieved and improved upon by exposure to multiple objects and toys in the surrounding environment. During these multi-level interactions, the hand is trained to manipulate objects with complex shapes and perform very articulated tasks, such as hand writing and drawing (Kivell et al., 2013).

17

These training exercises comprise: fine motor strength, involved in activities that strengthen the small muscles by interacting with materials and tools that create resistance for the fingers (clay, putty, interlocking construction toys); pincer grasp whereby only the thumb and index fingers are used to pick up items; hand arches which involve utilising the palmar to control the power of grasping objects of different sizes and shapes; complex fine motor skills, such as thumb opposition to grasp objects and operate tools, and finger isolation to move each finger separately and manipulate objects with one hand only; bilateral coordination, or multitasking by using multiple parts of the body simultaneously with hand operation; and visual motor integration, allowing the manipulation of objects by hand with visual guidance (Florence and Jane, 1988).

2.2.2. Hand Kinematic Model: Functional Development

Despite the latest achievements and advanced technologies, and further examination of hand structure and kinematic discipline, the exact replication of the hand, with all its complex functionalities, is still not accurately presented. Usually, researchers subdivide the multi-dimension layers in hand functions and motor control in order to address specific parts of the hand characteristic in reproduction (Edgar SS, 2014).

Hence, the computer vision and graphics researchers use the 27 degrees of freedom (DoF) model – five DoFs for the thumb, four for each finger and six for the wrist position and orientation (Kanade, 2009) – as necessary parts for gesture recognition and visual interactions. (Yasumuro et al., 1997) added one DoF for each CMC joint of the fingers to allow additional abilities in the fingers' manipulation.

Biomechanical researchers use optical and magnetic motion capture devices for finger measurements and so their alternative adapted model is 31 DoFs. This is obtained by adding four DoFs for the carpometacarpal (CMC) flexion and adduction of the ring and pinkie finger, to the above model. The difference, by including the four fingers' CMC motion during object manipulation and grasping, is represented in the palm involvement.

In this study, the model used has 22 DoF: three flexions/extensions (distal interphalangeal (DIP), proximal interphalangeal (PIP), metacarpophalangeal (MCP)) and one abduction/adduction for each finger. The thumb has two flexions/extensions (MP and IP) and

one abduction/adduction. The remaining three DoFs are the wrist rotations. This is mainly to reduce the complexity of the graphical model in the simulation and address the involvement of dexterity.

The finger joint angles are characterised by flexion-extension (pitch), abduction-adduction (yaw) and axial rotation (roll). The proximal transfer movement from the end joint to the root coordinate system at the wrist can be described by homogenous matrix multiplication (Buchholz and Armstrong, 1992). (An et al., 1979) used classical Eulerian angles to define the relationship between the joints. The transformation matrix from the coordinate (global) system to the proximal (local) is shown in Equation (2-1).

$$A = \begin{bmatrix} cos\emptyset_{ij}cos\theta_{ij} & -cos\,\varphi_{ij}sin\emptyset_{ij}cos\theta_{ij} + sin\varphi_{ij}sin\theta_{ij} & sin\varphi_{ij}in\emptyset_{ij}cos\theta_{ij} + cos\varphi_{ij}sin\theta_{ij} \\ sin\emptyset_{ij} & cos\varphi_{ij}cos\emptyset_{ij} & -sin\varphi_{ij}cos\emptyset_{ij} \\ -cos\emptyset_{ij}sin\theta_{ij} & cos\varphi_{ij}sin\emptyset_{ij}sin\theta_{ij} + sin\varphi_{ij}cos\theta_{ij} & -sin\varphi_{ij}sin\emptyset_{ij}sin\theta_{ij} + cos\varphi_{ij}cos\theta_{ij} \end{bmatrix} \quad \text{(2-1)}$$

Where θ is the abduction-adduction angle; $\emptyset$ is the flexion-extension; and φ is the axial rotation (Buchholz and Armstrong, 1992).

The fingertips curve through a spiral shape not circle, and the finger bones' lengths can be related in a Fibonacci mathematical series, where the approximate ratio is 2, 3, 5 and 8.

(Buchholz and Armstrong, 1992) have provided parametric functions (see Table 2-2) to calculate the length of the bones for each finger in relation to hand length and hand breadth (Reiner, 2005).

Table 2-2 Bones length parametric functions (HL is hand length) (Buchholz and Armstrong, 1992).

	Proximal	Middle	Distal
Thumb	0.196*HL	-	0.158*HL
Index	0.265*HL	0.143*HL	0.097*HL
Middle	0. 277*HL	0.170*HL	0.108*HL
Ring	0.259*HL	0.165*HL	0.107*HL
Pinkie	0.206*HL	0.117*HL	0.093*HL

The hand movements can be classified as prehensile movements, when manipulating objects that include grip and pinch actions, and non-prehensile movements, such as pushing, lifting, tapping and punching with the fingers, (Reiner, 2005). Prehensile movements include precision and power patterns, which are both defined based on the activity rather than the shape or size of the gripped object. The first pattern is when the thumb is opposing one or more fingers, and the second is when the thumb is against the palm. The opposability index of the thumb with the other fingers is measured by (2-2):

$$Finger\_Opposability = \frac{100 * Length\_of\_thumb}{Length\_of\_finger} \qquad \text{(2-2)}$$

Where $Length\_of\_thumb$ is the length of the thumb is *finger from the MCP to the tip, and* $Length\_of\_finger$ *is the length of the opposed finger from the MCP to the tip.*

2.2.3. Hand kinematics: Constraints and Synergies

The hand and fingers have multiple constraints that express the range of motion (RoM) workspace and hand prehensile. These constraints are defined in the physiological structures of the hand, including skin deformation and the mechanical connectivity between joints. Some examples of these restrictions are the thumb's particularity in opposing the other fingers (Kanade, 2009); the joints' extension and flexion limits; the dependency and cross-coupling where, for instance, bending the middle finger MCP joint will cause partial bend to the adjacent fingers' MCP joints; and finger motion being restricted in the positive Sagittal plane only.

Lin has divided the above constraints into three types: Type I static constraints, which are the limitations derived from the hand anatomy; Type II dynamic constraints are limitations to the joints during motions; and Type III natural motion constraints (Lin et al., 2000).
Type I constraints are usually represented by minimum-maximum joint variations in free movements (without applying external forces). The ranges suggested for the flexion-extension joints of the middle finger are shown in equations (2-3), (2-4), (2-5).

$$0^o \leq \theta_{MCP} \leq 90^o \qquad \text{(2-3)}$$

$$0^o \leq \theta_{PIP} \leq 110^o \qquad \text{(2-4)}$$

$$0^o \leq \theta_{DIP} \leq 90^o \qquad \text{(2-5)}$$

Those for the abduction-adduction joints are illustrated in equation (2-6)

$$-15^o \leq \theta_{MCP} \leq 15^o \qquad \text{(2-6)}$$

Where θ_{MCP} is the abduction-adduction; θ_{MCP}, θ_{PIP}, θ_{DIP} are the flexion_extension angle for the MCP, PIP and DIP joints consecutively.

Type II constraints are subdivided into intra-finger and inter-finger.

Intra-finger is when a joint in the finger bends, causing another joint of the same finger to bend as well. An example of this is between the DIP and PIP where the relations can be described using (2-7):

$$\theta_{DIP} = \frac{2}{3}\theta_{PIP} \qquad \text{(2-7)}$$

Inter-finger describes the correlation between joints of different fingers, for example, the effect on the adjacent MCPs joints of bending an MCP. This is represented in terms of a similar relation to the equation above (Lin et al., 2000).

Furthermore, Shuai has acquired the joints movement data measurement using the following equations of constraints in (2-8), (2-9), (2-10), and (2-11) (Shuai et al., 2010).

$$\begin{cases} flex(\theta_{DIP}) = \frac{2}{3}flex(\theta_{PIP}) & \text{(2-8)} \\ flex(\theta_{CMC}) = 2flex\left(\theta_{MCP(T)} - \frac{\pi}{6}\right) & \text{(2-9)} \\ abd(\theta_{CMC}) = \frac{5}{7}abd(\theta_{MCP(T)}) & \text{(2-10)} \\ flex(\theta_{IP(T)}) = \alpha . abd(\theta_{MCP(T)}), \alpha \leq 0 & \text{(2-11)} \end{cases}$$

Where α is the relation value between the flexion-extension bending angles of IP and MCP joints ($\alpha \leq 0$), T indicates Thumb.

In addition, CMCs joints have a related connection with the MCPs. This is exemplified when the

fingers flex, the palm curves to make a finer grasp posture and all the fingertips aim to the thumb base point without obstruction.

This can be represented by equation (2-12).

$$\theta_{finger\_CMC} = k.\theta_{finger\_MCP}$$
(2-12)

Where k is the relation value between the flexion-extension angle of the CMC and MCP joints.

(Wang and Dai 2009) have determined the k values by performing the least square regression method on multiple natural positional tendencies of the hand (such as having the thumb and ring/pinkie fingertip make contact in front of the palm and measuring the variations of CMC-MCP with other positions). The calculated relative values are listed in the equations group in (2-13).

$$\begin{cases} \theta_{Idx\_CMC} = 0.046 * \theta_{Idx\_MCP} \\ \theta_{Mid\_CMC} = 0.0055 * \theta_{Mid\_MCP} \\ \theta_{Rin\_CMC} = 0.14 * \theta_{Rin\_MCP} \\ \theta_{Pin\_CMC} = 0.21 * \theta_{Pin\_MCP} \end{cases}$$
(2-13)

Where θ_{Idx_CMC} is the flexion-extension angle of CMC joint for index finger, θ_{Idx_MCP} is the flexion-extension angle of MCP joint for index finger, θ_{Mid_CMC} is the flexion-extension angle of CMC joint for Middle finger,θ_{Mid_MCP} is the flexion-extension angle of MCP joint for Middle finger, θ_{Rin_CMC} is the flexion-extension angle of CMC joint for Ringer finger, θ_{Rin_MCP} is the flexion-extension angle of MCP joint for Ringer finger, θ_{Rin_MCP} is the is the flexion-extension angle of MCP joint for Ringer finger,θ_{Pin_CMC} is the flexion-extension angle of CMC joint for the Pinkie finger, θ_{Pin_MCP} is the flexion-extension angle of MCP joint for the Pinkie finger.

On the other hand, Type III constraints are caused by those common and natural movements that unify every person. For example, hand writing postures and motions, sequence movements for opening-closing fingers and performing different tasks, and the involved patterns in the motions of grasping or performing daily activities which combine multiple joint movements between different digits (Mouri and Kawasaki, 2008).

Furthermore, there are varying levels of dependencies between the different fingers. The middle and ring fingers have closer relative movements compared to the others. This is

determined in cross-couple joints motion observed while performing free movements (without object interaction or external forces on the hand).

This correlation is due to multiple factors involving functional control of the hand, such as the passive mechanical connections between the joints, the structure of finger muscle tendons, and the neural control distribution in the upper limb and hand. Subsequently, this is divided into different constraint types and unique patterns of motion. The relationship parameters are dependent on each joint angle.

Ideally, these constraints include significant details about the hand movements, but they are very difficult to define in a model equation. Hence, different techniques are required in order to capture these factors.

Different researchers have used the finger dependencies rule with principal component analysis (PCA) to lower the number of DoF involved in representing hand motion or pose (Shuai et al., 2011, Housman et al., 2009).

The strength of the hand in gripping and grasping objects is produced by different factors within its structure, such as the strength of the muscle, bone structure and density (mineral content), and the thickness of the tendons attached to the fingers' bones (Callender, 2015).

These constraints give harmonic contribution to the hand and reliability in its ability to perform precise and smooth movements in daily life activities.

(The static constraints values used in this project are available in the CodeSnippet III-1. The dynamic or natural constraints are implemented in the calibration methods which are further discussed in the calibration Chapter 5)

2.2.4. Finger Contribution

Multiple studies were performed to assess fingers' contributions. Methot has performed a study on a controlled group to determine the ulnar digits contribution to overall grip strength, using a calibrated dynamometer (Methot et al., 2010). The study indicated that the ulnar index and middle digits' contribute significantly to the overall grip strength of the entire hand. On the other hand, other research has found that the normal digital contributions in grip strength were 25%, 35%, 26% and 15% for the index, long, ring, and small fingers respectively (Talsania and Kozin, 1998).

In another study, it was concluded that the total grip forces for the index, middle, ring, and little fingers were 42.0%, 27.4%, 17.6% and 12.9%, respectively in a static grip force (Kinoshita et al., 1995).This distribution showed that the fewer the number of fingers involved in the grip mode, the greater the grip forces were. However, the middle and ring fingers were influenced by the mode of the grip; but not the index finger.

2.2.5. Contact

The force exerted and the motor control determines the velocity of the fingers. Robotics researchers (González-Quijano et al., 2015) include the contact model in the hand kinematic when interacting with objects. The contact is defined as an interface between two bodies where the forces, f, and moments, M, are transmitted. The two variables are usually denoted in a single vector, called wrench, as represented in equation (2-14).

$$w = \begin{bmatrix} f \\ M \end{bmatrix}$$

(2-14)

In the case of contact frame c, the wrench basis of the transmission is equation (2-15).

$$w_c = B_c f_c$$

(2-15)

where: f_c is the contact force intensity; B_c is the wrench basis matrix; $B_c \in \mathbb{R}^{p*m_i}$, p is the space dimension (p = 6 for 3D) and m_i is the number of independent forces on a contact area.

In frictionless contact (Figure 2-5), the B_c matrix is defined by equation.
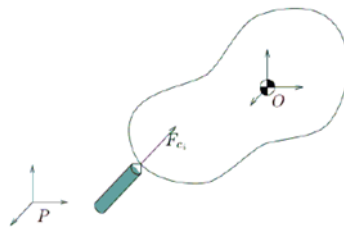
Figure 2-5 Contact force applied on the contour of the object. O is the centre mass. P is the world original

$$B_c = \begin{bmatrix} 0 \\ 0 \\ 1 \\ 0 \\ 0 \\ 0 \end{bmatrix} \qquad \text{(2-16)}$$

Friction contact is represented by equation (2-17).

$$B_c = \begin{bmatrix} 1 & 0 & 0 \\ 0 & 1 & 0 \\ 0 & 0 & 1 \\ 0 & 0 & 0 \\ 0 & 0 & 0 \\ 0 & 0 & 0 \end{bmatrix} \qquad \text{(2-17)}$$

Aside from this, the force applied in a contact is dependent on the finger kinematics and configuration of the contact. This is described using Jacobian J_h relation between the joints' angular velocities $\dot{\theta}$ with the fingertip's (Cartesian endpoint of the joints chain) velocities by the equation (2-18) .

$$v = J_h(\theta)\dot{\theta} \qquad \text{(2-18)}$$

Torque of the joints is calculated by using the Jacobian transpose with f_c fingertip forces on the contact points, equation **(2-19)**.

$$\tau = J_h^T(\theta)f_c \qquad \text{(2-19)}$$

The hand Jacobian is determined in the matrix of the equation (2-20)

$$J_h(\theta) = \begin{bmatrix} J_1(\theta_{f_1}) & & 0 \\ & \ddots & \\ 0 & & J_n(\theta_{f_k}) \end{bmatrix} \qquad \text{(2-20)}$$

Where: $J_{pf_1}^8$ is the Jacobian for the ith finger in spatial coordinates, in reference to the palm. This is calculated in equation (2-21).

$$J_i\left(\theta_{f_k}\right) = B_c^T J_{pf_1}^8 \qquad\qquad \text{(2-21)}$$

2.3. Virtual Simulation

The robotic simulator offers low-cost development time for new robotic simulations as well as more reliable components (Andrew and Matei, 2015). In order to address the complexity of the hand and implement both the mechanical and graphical kinematic models to the virtual simulation, it is efficient to develop the approach basing on a base robotic simulation platform that is already validated and upgraded with various physics and graphics elements for analysis, rather than starting from scratch and focusing on supplemental components for the application. However, most simulators are designed to concentrate on specific elements of robotic analysis, such as grasping mechanism, automation control for industrial applications, or for pathfinding and trajectory planning.

Numerous different categories of 3D robotic simulators are available: open source and research simulators, such as OpenSim (OpenSim, 2015), Simbad (cross platform for scientific and educational, support Java) (Tim, 2015), Robotics Toolbox for MATLAB (Matlab), V-REP (very advanced 3D simulator for industrial robots, also supports many languages) (v-rep, 2015), Gazebo (cross-platform and compatible with ROS, with a large database of robots) (Gazebo, 2015), UWA Robot Simulators and GraspIt! (developed by Columbia University for measuring the grasp quality); and commercial simulators, such as Worspace5 (Worspace5, 2015), Microsoft Robotics Developer (a free simulator that is compatible with visual studio) (StudioRoboticsDeveloper, 2015), Easy-Rob (EASY-ROB, 2015), AnyKode (cross platform and offers a high level of reality) (anyKode, 2015), and Virtools (Virtools, 2015).

The robotic simulator's structure is based on scene graph elements that contain graphical geometries and transformation definitions. The scene graph is a scene management interface whose role is to organise the scene data in a hierarchical order. The data is presented in a tree structure, composed of multiple nodes, where one of them represents the parent and one or all of the others are children to this parent node. The latest applications of these elements serve to combine the graph nodes with the transformation matrix and the grouping properties, making it simpler and more practicable to modify the orientation and geometry of the scene

objects.

Each object is presented as a node, comprising multiple geometric properties and transformation details from the global (world) to the local (object) coordinates. This facilitates the manipulation of each object separately, and connects the multiple groups (collection of nodes characteristics) together by those that share similar values.

Figure 2-6 shows the structure involved in managing the geometrical information, rendering it and displaying it on the visual device.

The scene graph focuses mostly on haptic and dynamic operations, with little consideration of the graphic rendering, which is used in design and animation.

Various scene graphs APIs are available, including Open Inventor (Group-Visualization-Sciences, 2015), Performer (OpenGL-Performer, 2015), OpenGL Optimizer (OpenGL, 2015), DirectX (GeForce, 2015), Gizmo (Gizmo3D, 2015), Coin3D (Coin3D, 2015), OGRE (Ogre3D, 2015), QtQuick(Quick-Qt, 2015) and VRML97 (Vrml, 2015). These APIs are commonly used in graphics and provide multiple features and built-in components to create interacting visual applications (either in C++,.Net, Java, or C# language) with advanced rendering techniques and high performance. Some of the essential components included in these APIs are graphical objects (cubes, polygons, spheres, etc.), text, materials, cameras, lights and 3D viewers (Group-Visualization-Sciences, 2015). The Open Inventor and Coin3D are open sources with cross compatible platforms.
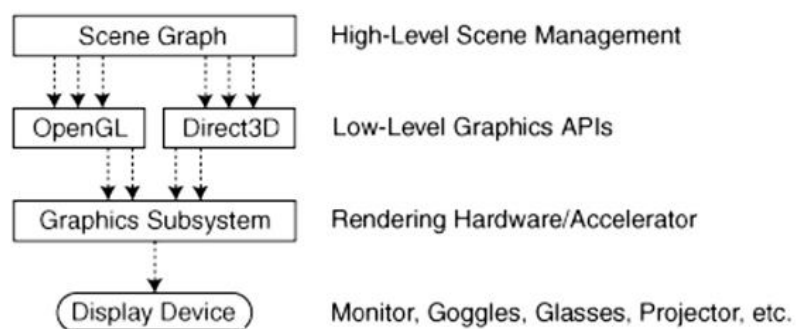
Figure 2-6 Architecture diagram of the scene graph; This figure illustrates the process executed to produce 3D graphical displays. The process starts by acquiring the high-level

details of the 3D graph, it then transfers the information into instructions for the graphical engines and subsystem rendering.

The API libraries also include physics engines for simulating the virtual interaction properties of objects of different sizes, weights, dynamics, and mechanisms. Two of the available physics engines are the ODE (ODE, 2015) and PhysX (PhysX-Nvidia, 2015), used mainly for producing realistic movements in the scene.

The imported world elements within the robotics simulators are designed with external modelling tools such as AutoCAD (AutoCad, 2015), Autodesk 3dsMax (3dsMax, 2015), Autodesk Maya (Maya, 2015) and Blender (open source tool with features of robotic simulation and animation) (Blender, 2015). However, some simulators like Virtual Robot Experimentation Platform (v-rep, 2015), Webots (commonly used in research and education) (Webots, 2015), and R-Station (H., 2015) support built-in creation tools.

CyberGlove® has developed its own Virtual Hand Simulator (VHT) (CyberGlove, 2013) that includes a virtual human hand model, object manipulation and interaction, and graphical rendering. In addition to the scene graph, the application has an event model and physical simulation component, but they are very complex to develop or update with newly designed models. The endorsed physics engine is basic and lacks multiple robotic features, such as databases references with different kinematic mechanisms, and the possibility to include different 3D models with differing formats and structures.

2.3.1. GraspIt! Robotic Simulator

GraspIt! (Andrew and Matei, 2015) is a robotic simulation platform offering multiple features in research and development that support the project's aims. It is an open source application, initially designed for measuring the robotic's grasp quality. The application was developed by a group of researchers at the University of Columbia and implements multiple robotic models such as DLR, Barrett, Robonaut, and other designs commonly used in automation and industrial control.

GraspIt! offers a generic and easy platform to import robots of various structures. It supports a robust 3D manipulation interface to connect multiple robots, links and objects, specifically

designed for an experimental virtual environment; a basic hardware and software communication interface to interact with sensors and analytical applications (MATLAB); a large database with robotic hand models and simple analysis functions to test lower dimension spaces; and a set of pre-developed algorithms for grasp optimisation, trajectory generation and planning, joints control, and dynamic simulation with a physics engine.

2.3.1.1. GraspIt!: Review

The application, GraspIt!, is not fully developed and requires improvement on the dynamic engine processing, virtual hand manipulation with hardware devices, and kinematic modifications. However, this application is selected for this project because of the multiple features implemented in the API, which correspond closely with the project objectives.
The application provides a rich and varied platform of robotic structures, accommodating arbitrary hand and robot design employment; it allows easy configuration of the simulated world, so is suitable for the needs of the experiment and the requirement for different aspects in robotic analysis. GraspIt! has multiple advanced units which implement machine learning, Principal Component Analysis (PCA) sub-spacing, soft finger contact, and a large grasping database for testing and training newly implemented algorithms; GraspIt! is an open source scientific research platform that has multiple implementations for robotic hands and provides a more straightforward system to implement newly designed models and kinematic configurations; and it also offers the ability to manipulate robotics joints through the sensory device.
In addition, it is different from the other available robotic simulators as it is designed for qualitative analysis of robotic grasping with robust rendering and user interface systems.

In order to implement GraspIt! in the experimental studies of the project, there are multiple elements requiring new development or improvement:

- Hand Model: GraspIt! supports multiple robot hands with different designs and kinematic chains, but for bioengineering application models, it needs to be addressed in a different perspective to the robotic and industrial fields.

- Collision detection: This requires improvement to create more matching boundary volumes of the newly designed hand model. The performance process requires development, as the engine slows the real time update of the robotic joints' movements, which in turn causes delays between the actual hand movement (wearing the data glove) and the visualisation system. This must also be addressed as it significantly affects hand performance analysis and results in inaccuracy in the speed, stability and smoothness of the hand movement.

- Multiple contacts: GraspIt! allows only one collision contact at a time, so in a static mode when multiple contacts are produced, the application stops all the joints until the first contact is resolved. This makes the process unreliable, as it causes an asynchronous reaction with the finger movements and external manipulation. A handling list of contacts needs to be implemented in order to address the multiple contacts case and allow it to grasp and move objects in the static mode, without interruptions.

- Dynamic view: Following multiple investigations and consultation with the application developers, the implemented dynamic engine was found to be fragile in applying appropriate forces on the robot links and detecting collision with multiple objects. The DoF motor controllers used are very difficult to calibrate in order to obtain the desired motion, which causes instability in the bodies' motions. In addition, the robot link connections produce many errors if they are set incorrectly and without the precise time-step for the integration.
Furthermore, the robotic hands cannot be externally manipulated by a data glove or user interaction, during the dynamic mode, which is a key criterion for the purpose of this study. Hence, further developments are required on the engine performance; suggestions have been made to replace the LCP solver due to its instability and the long computation time. An additional layer also needs to be included in order to give control to the robot joints without modifying the implemented motor controllers and joint connections process.

- Hardware connection: Although GraspIt! has a hardware connection feature, this is, unfortunately, basic and only implemented in older versions, which lack the dynamic state

features and multiple kinematic chains in the new version. Thus, a hardware interface needs to be re-implemented to manipulate the hand model with the data glove and the DoF angle values have to be configured appropriately with sensor inputs. This leads to the next development procedure in this list.

- Calibration: Calibrating the hand model with data glove sensory inputs is a vital element in obtaining accurate results and precise visual simulation with the hand movement. GraspIt! does not support a calibration method. In light of this, a robust method needs to be implemented to control the model DoF by the data glove with a precise and consistent movements display.

- Experimental Setup: The role of the application in this project is to run hand performance experiments. This requires a set of interactive procedures with the virtual world, instructions to follow concurrently with the trials, and a new classification algorithm with appropriate object simulations to match the defined clinical hand classification method in this project.

2.4. Motor Control

The hand is controlled by the brain through signals sent via the nervous system to the muscles, which lead to contraction or expansion reactions (Kanade, 2009).

The motor cortex, located in the frontal lobe of the brain, is responsible for generating order signals to the limb, with all the relevant information (force, position, speed, etc.) for executing a motor function. The transformation process from sensory signals, provided by exteroceptors and/or proprioceptors, to motor commands is determined within the central nervous system (CNS).

Recent research has focused on understanding the steps involved in the transformation process (Kanade, 2009). This is because a number of complexities and sub-layers are involved in the reception, planning and control. For example, the spherical task – which involves moving the hand to grasp the ball, grasping it, moving it to a new position and relaxing it back to start position – has a very complex multi-dimensional coordination between sensory and motor

movements. This entails specifying the position between local and world coordinates; the orientation and adjustments of the many DoF between the arm and hand; the indeterminate assignments of specific DoF from large range in the control system; the cross-coupled DoF which require selective patterns; the involvement of muscles and the forces gathered by more than 30 muscles and thousands of fibres' coordination; the infinite trajectories or paths which could be selected to perform the task; and the analysis of the defined velocity and force.

The above motor control process can be divided into four stages: Plan, Control, Estimation and Learning, Execution. A brief overview of these stages is presented in the sections below.

2.4.1. Plan

Pas literature suggests that the method used to plan the movement in the CNS is attained by creating optimal control processes, based on self-supervised models (fed with the sensory inputs and previously learned functions), in maximising the smoothness of the hand trajectory and torque commands (Flash and Hogan, 1985, Uno et al., 1989). However, this method doesn't consider the multiple motor systems involved and only addresses the optimised factors of smoothness and trajectory levels, which still need further investigation in this approach.

2.4.2. Control

Some of the methods in the motor command process suggest that the CNS specifies spatial parameters using the concept of the spring-like properties of muscles and reflex loops (Feldman, 1966, Hogan, 1984). This is where the muscles that are used and the spinal cord properties act as a feedback controller to adjust the hand to the desired trajectory and perform the movement with multiple successive equilibrium positions.

Another method suggests the inverse model construction in mapping each point's state of the trajectory into motor commands (Kawato et al., 1987). A more recent method proposes the combination of the inverse model to achieve the desired position, with the implementation of muscle activation patterns to simplify the command (Giszter et al., 1993).

The above highlights the different explanations of the brain neurons' mechanism to encode the trajectory properties such as the direction, velocity, acceleration, posture and torques.

However, other explanations propose that the trajectory properties are rather resolved in the cortical activity, muscle filtering properties and movement kinematics' overall relations.

2.4.3. Estimation and Learning

The CNS has great capacity in estimating the next movement state of the hand by mentally simulating the movement of the hand and objects (Miall and Wolpert, 1996), with less sensory feedback delays and higher accuracy of the next estimated state. Sensory prediction is involved in cancelling the noises or sensory effects of movements and enhancing the more relevant sensory information. This is mainly applied in self-motion to determine whether a movement is externally or internally produced, which may increase the accuracy of the prediction (Blakemore et al., 1999).

The neural mechanism is continuously learning and improving movement accuracy. The properties of the sensory feedback system are captured in the forward and inverse model, and an error signal is derived from the variation between the predicted and actual sensory feedback of the movement (Bell et al., 1997), to improve the control model and make adjustments in response to the dynamic changes.

2.4.4. Execution

The neural system delivers the command signals to the muscle fibres, which in turn contract and expand with specific velocity and force to control the skeleton bones of the hand and arm for reaching, grasping the ball, moving it to a new position and relaxing back to the starting position.

The relationship between the developed application in this project and the above-mentioned is very significant, as the motor control of hand function is very comprehensive and is the origin of the initial causes for hand performance or dysfunction. Further to this, the application is developed with the intention of being used in future projects involving the neurophysiology of the hand movement.

Hand movement classification of brain activities is a very complex process and requires specific analysis algorithms to divide the multi-dimensional details of the neural control signal. This section aims to simplify or breakdown the aspects of using the developed application, in

the project, with the possible classification methods for the hand gestures. This can be used in Brain-Computer Interface (BCI) analysis or brain activity pre-processing.

An example of hand classification is to define a set of known postures, such as spherical, tripod, point and lateral, which can be used in the feature selection of the algorithm. This will train the algorithm to identify specified posture properties encapsulated in the brain signal variations and recognise new hand functions as they are added to the system.

The existing challenges in this process are the high dimensionality of the involved parameters in each task. This includes the wide range of motions for the joints, the large number of hand and arm DoF instructions involved, and the dependencies and constraints defined in the natural movements.

Therefore, the regression analysis method is not applicable in this specification and more advanced techniques are required in order to subspace the level of details in the hand function and continuously adapt, with new inputs that cover the different variations of the joints' workspace.

Santello has suggested that most grasping hand postures derive from a relatively small group of discrete pre-grasp shapes (Santello et al., 2002). They have selected 57 objects (umbrella, wrench, apple, door key, etc.), encountered in day-to-day life, to impose multiple defined hand postures. To determine the extent of each posture, a discriminant analysis (Johnson and Wichern, 1992) method is applied and the generated outcome is used to construct a confusion matrix (instructed postures X objects), representing the hand posture prediction for each grasped object. The optimal association of the hand postures with appropriately shaped objects are positioned on the diagonal of the matrix.

Regression analysis is then used to assess the level of angular covariance between the multiple DoF. To investigate the covariations of the hand patterns and undefined constraints, the principal component analysis (PCA) was computed using the eigenvectors and eigenvalues of the coefficient covariance matrix from the postures (waveforms).

The results showed that the first two PCA's principal of components account for 80% of the variation range for all 57 postures. Therefore, the high dimensionality of the hand postures in daily activities can be reduced to obtain the relevant DoF space. The rest of the principal

components (which form 20%) are still very critical to count as 1- they are not noises and 2- it could be suggested that they are included in the initial grasp planning stages, as this specific study was performed in the absence of the real objects and by reproducing it from memory.

This method was also implemented using the GraspIt! application on robotic hand postures (Ciocarlie and Allen, 2009). Each posture p is described as in (2-22):

$$p = [\theta_1 \ \theta_2 \ ... \ \theta_d] \in \mathbb{R}^d \qquad \text{(2-22)}$$

Where d is the number of DoF; and θ_i is the angular value of the i-th DoF.
Also p is calculated using equation (2-23):

$$p = \sum_{i=1}^{b} a_i e_i \qquad \text{(2-23)}$$

Where b is the number of principal components (eigengrasp) in the defined subspace of the hand posture; a_i is the i-th amplitude vector, as represented in equation (2-24):

$$a = [a_1 \ a_2 \ ... \ a_b] \in \mathbb{R}^b \qquad \text{(2-24)}$$

and e_i is the principal component for i-th posture, represented by equation (2-25).

$$e_i = [e_{i,1} \ e_{i,2} \ ... \ e_{i,d}] \qquad \text{(2-25)}$$

Alternatively, to optimise the parameters of the grasp postures in edge grasp (principal of components) space, by decomposing the hand posture (intrinsic) and position (extrinsic) details, the energy function is of the form shown in equation (2-26):

$$E = f(a, w) \qquad \text{(2-26)}$$

Where $a \in \mathbb{R}^2$ is the vector of eignengrasp amplitudes (2 as only two eigengrasps counted); and $w \in \mathbb{R}^6$ contains the position and orientation of the wrist.
This function attempts to define selected contact points on the robotic hand in contact with the object.

Table 2-3 Eigengrasps defined for the robotic hand models, which is used in GraspIt! (Matei et al., 2007).

Model	DOFs	Eigengrasp 1			Eigengrasp 2		
		Description	min	max	Description	min	max
Barrett	4	Spread angle opening			Finger flexion		
DLR	12	Prox. joints flexion Finger abduction			Dist. joints flexion Thumb flexion		
Robonaut	14	Thumb flexion MCP flexion Index abduction			Thumb flexion MCP extension PIP flexion		

Although this method identifies a large range of hand postures, it still needs improvement in different aspects. Firstly, it covers only a limited range of daily life common postures; this could return inaccurate definitions for the myriad different postures that are less frequently used. Secondly, the rest of eigengrasp (~20%) postures are not defined (Santello et al., 2002) and these could be part of the grasp planning or the object shape restrictions that force the hand to change from natural movements.

An interesting concept, which could be used to complement to the above method, is the self-organising map (SOM), which allows the extension of the hand posture variations to include all the varied motions without eliminating any of the patterns or natural movements that are unique to every individual.

The SOM is a neural network method used for data analysis, dimension reduction, classification, and predictions, among others. The method concept acts similarly to the PCA through non-linear projection of the data into lower dimensions, but the reduction is performed in the first stage by clustering the data with similar properties or features. It is an unsupervised training system that uses competitive learning, where the network neurons organise themselves by activating only one output neuron, based on the connections' weights and negative feedbacks, at the time.
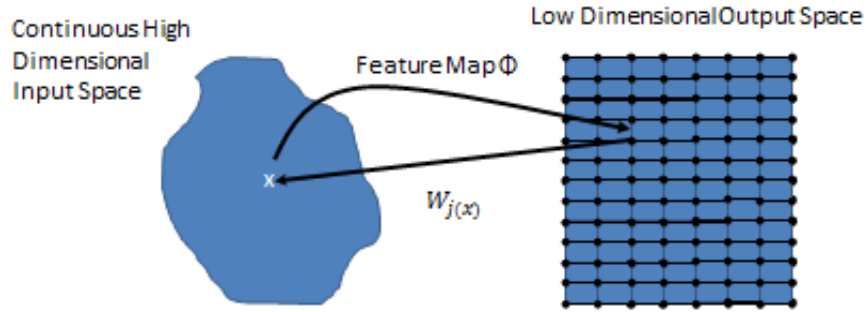
Figure 2-7 Self-organizing map schematic; x is the input in high dimensional space, I is the output that is organised in low dimensional space, and w is the connectivity weight. (The output dimension can extend from 1 to N dimensions, but always less than the input's).

The process of the SOM could be described in the below steps (Kohonen, 1997):

1- Initialisation: collecting all the input nodes with random weights vector.

2- Competition: selecting the neuron with weight vector being the closest to the input vector to be activated, known as a best matching unit (BMU). This is obtained by finding the smallest value of the discriminant function, using the Euclidean distance in equation (2-27).

$$d_j(x) = \sum_{i=1}^{D}(x_i - w_{ji})^2 \qquad \text{(2-27)}$$

Where x is the input vector; D is the input dimensional space; and w_{ji} is the connection weights between the input units i (1 to D) and the neurons j in the low dimensional space (1 to N).

3- Adapting: Adjust the network by pulling the neighbour nodes of the BMU closer to the input vector. This is done by updating the weights using the equation (2-28).

$$\Delta w_{ji} = \eta(t)T_{j,I(x)}(t)(x_i - w_{ji}) \qquad \text{(2-28)}$$

Where $\eta(t)$ is a learning restraint due to iteration progress; and $T_{j,I(x)}$ is the topological neighbourhood function for the neurons in the SOM, which is commonly a Gaussian function that depends on the lateral distance between input data and BMU.

37

4- Continuation: keep repeating until the feature map stops changing.

Therefore, by utilising the above process to identify the hand gesture, the network is first trained by multiple hand postures to find the optimally organised map, which is then applied on new hand motions to recognise the gesture.

The SOM method has multiple advantages, as it is adaptable with new inputs and patterns, which are usually difficult to derive from the hand movements. The method counts these components in the network map organisation in response to the negative feedback updates. Shuai and colleagues have used SOM to recognise the hand gestures from dataglove readings, but only two gestures are defined for classification, as it is used for simple tasks in the virtual interaction (Shuai et al., 2010).

However, the SOM method requires extensive investigation, specifically in the pre-processing phase, to choose the relevant input data to determine the adequate features that are suitable for the classification interests. Santello and colleagues suggested using a sensorimotor index (SME), a ratio between the actual information transmitted by the hand posture and the maximum possible amount of information that could be transmitted, in order to differentiate the hand postures(Santello et al., 2002). This can also be used as an additional parameter for more efficient map rearrangement in order to obtain the desired outputs.

2.5. Summary of the Background Chapter

In this chapter, multiple elements of the hand anatomy, structure and complex kinematical model have been reviewed. Also, as the project aim is to develop a virtual reality system for hand assessment, the author explained in extensive detail the selected robotic simulator architecture and compliance with the project requirements. The hand motor is later described to provide a further background of injury causes and hand functionality.

In the following chapter, multiple systems used in hand rehabilitation and the affiliation of the proposed approach with the various systems of architecture and end outcomes will be reviewed.

Chapter 3 Literature Review

Research into hand rehabilitation is continuously increasing due to the high demands in clinics for advanced applications to address the multiple aspects of hand physiology and anatomy (Florence and Jane, 1988). The regularly updated devices implemented in surgical procedures require different and more consistent strategies to restore lost function in the affected area, in addition to the technological improvements which provide the driving factor for continued research to develop more advanced hand rehabilitation systems.

First, it is important to note that this project has a very diverse scope. The initial idea of the project was to develop a system for hand rehabilitation by using a data glove device. Therefore, in this chapter the existing hand rehabilitation techniques used in research and clinics are reviewed, beginning with the basic and traditional clinical tools/exercises to the very advanced technological systems that use robotic assistance, virtual reality, Neuroprosthesis and other technologies (this is covered in sections 3.1.1 to 3.1.8). In addition, I illustrated some of the robotics devices and exoskeleton technologies, and the latest technologies in tracking the hand motion (visual based, optical, mechanical and data glove devices) to give a deeper understanding of the new system mechanisms.
But remarkably, during the review of these systems, it is noticed that nearly all of them depend on subjective assessment of hand improvement during rehabilitation, or on assessment techniques that are limited toward specific tasks only or account for the general hand posture which varies between each case.
Thus, it is later reviewed, in section 3.2, the existing hand assessment techniques covering the basic clinical methods to the most advanced technological devices.

Also, descriptions and review of each individual system are provided. The chapter concludes by specifying the selected methods and devices for the project, and illustrates the uniqueness of the project's approach and advantage in supporting the hand rehabilitation research. At the end, the Experimental Chapter 4 is introduced, where the materials and the key advantages of choosing these equipment and devices are provided.

The literature review search was conducted by focusing on controlled randomized studies, reviews and meta-analysis, published in English between 2005 and 2016. The research was

conducted in MEDLINE, IEEE, ACM, ProQuest and Compendex, JREF with the following keywords: ''human hand rehabilitation'', ''human hand assessment'', ''human hand outcome measures', 'human hand assessment tests', 'virtual reality hand rehabilitation', 'robotics hand rehabilitation', 'robotic arm', 'virtual robotic hand', 'Neuroprosthesis upper limbs', 'data glove', 'motion tracking', 'tracking sensors', 'hand exoskeleton', 'virtual reality hand assessment', 'clinical therapy', 'clinical hand assessment methods', and 'EMG hand movement'.

3.1. Hand Rehabilitation

This section lists the hand rehabilitation techniques applied for hand motor function damage. It includes the Clinical Therapy, Robotic Assistance, Virtual Reality, Neuroprosthesis, and Synthesis.

3.1.1. Clinical Therapy

Studies have proven that arm therapy has positive effects on the rehabilitation progress, and it is essential to implement hand therapy in the early stages of hand diagnosis to obtain efficient outcomes. Improving motor coordination and inhibiting consequent complications, i.e. spasticity or joint degeneration, would serve to enhance the hand motor skills and give patients confidence and independence in their lives (Florence and Jane, 1988).

In general, the patients with paralyzed arms receive arm therapy to rehabilitate the hand motor function through learning new skills which facilitate the transfer from training activities to daily life activities (ADL) (Florence and Jane, 1988).

3.1.1.1. Physiotherapy

Figure 3-1 highlights the rehabilitation methods used in clinics, with reviews of the advantages and disadvantages.
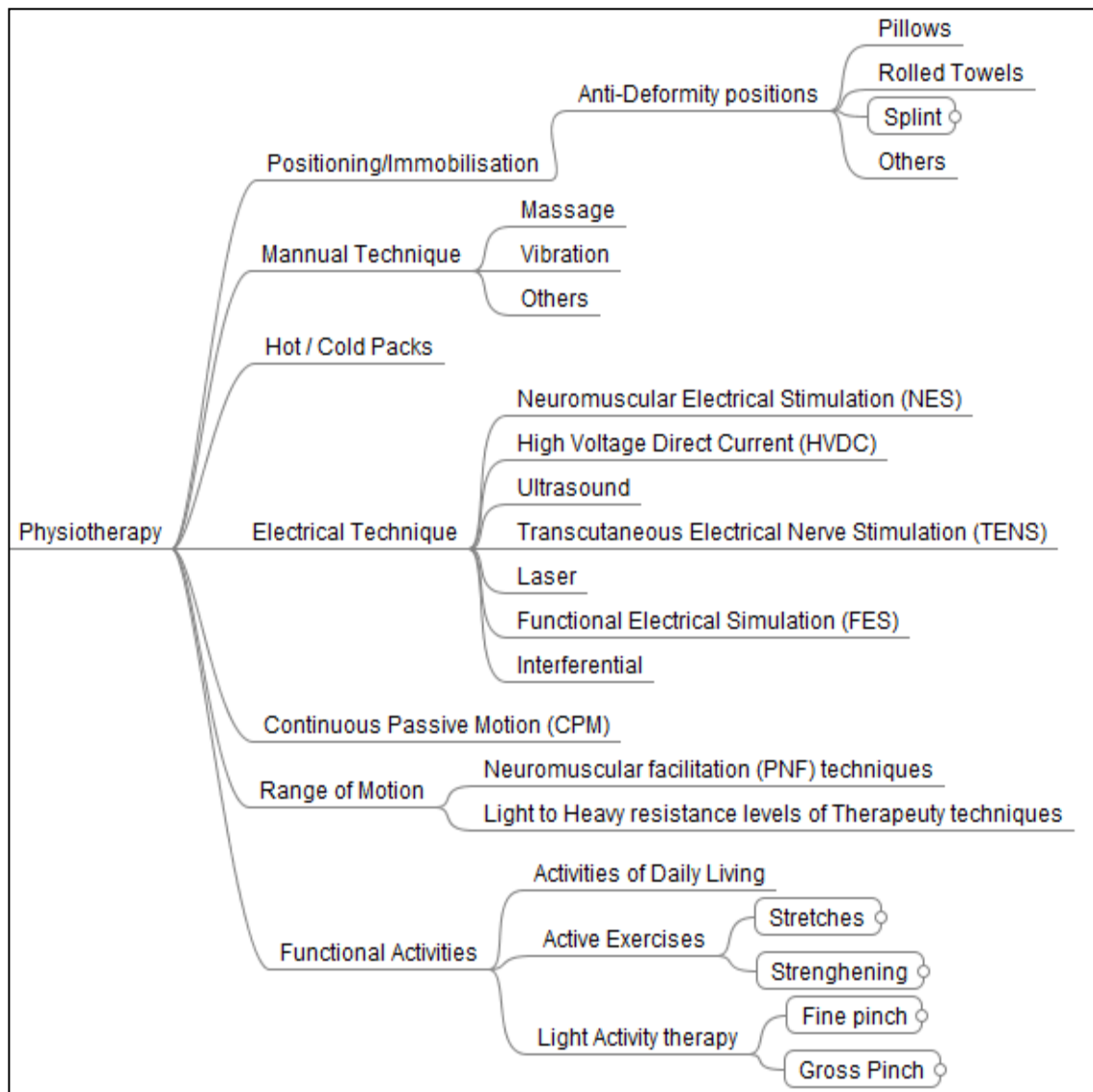
Figure 3-1 Taxonomy of the physiotherapy techniques applied in human hand rehabilitation sessions. (This taxonomy is produced by the author© 2015. The information is taken from Chapter Implications for Practice in (Florence and Jane, 1988)

Physiotherapy is a type of therapy used in clinics; it involves training exercises, manual therapy techniques such as stretching, digit flex hand and grip strengthening to relieve muscle pain and stiffness, and hand massage on targeted area to encourage blood flow (Wu et al., 2006).

Figure 3-1 shows the most common techniques used in physiotherapy. Positioning and immobilisation are applied to prevent deformation of the hand's natural movement, by using

pillows, rolled towels or splints (Brosseau et al., 2003); manual techniques such as massage or vibration are performed on the patient's hand to soften or restore the range of movement; electrical techniques stimulate selective areas of the hand to restore neurons or muscles functions, and this may include neuromuscular electrical stimulation (NES) (Lake 1992), high voltage direct current (HVDC) (Maria et al., 2010), ultrasound, transcutaneous electrical nerve stimulation (TENS) (Brosseau et al., 2003), functional electrical stimulation (FES) (Kawashima et al., 2013) and interferential pads (Fuentes et al., 2010); range of motion (ROM) helps to remodel the affected part of the hand and provides proprioceptive feedback on the hand movement to the patient. Techniques included in ROM are proprioceptive neuromuscular facilitation (PNF) techniques, for relaxation and mobility, and light to heavy resistance levels of therapeutic techniques by using objects with different shapes, textures and weight (i.e. temper foam sponges); functional activities to promote active range of motion by multi-modal activities: exercises involving activities of daily living (ADL), such as pouring water, opening a door handle, grasping a mug or ball etc.; active exercises such as stretching the joints full range in isolation or as mass movement; and strengthening the muscles by using different tools (static bike, rowing machines, putty exercises, ball games, etc.), or light activity therapy, fine pinch (pick-up sticks, quilling, etc.) and gross pinch (solitaire, dominoes, Scrabble, etc.).

3.1.1.2. Occupational therapy

Unlike physical therapy, occupational therapy focuses on evaluating and diagnosing movement dysfunctions, the occupational therapy focuses on improving life skills and incorporating adaptive tools. It includes different treatment practices such as wound and scar management, splinting, fracture healing, dynamic activities (require repetitive grasp and release and include putty exercises, open a door handle, pick up coins, play checkers, put puzzle together, pick up can, fill bowl with rice, large beadwork) and static activities (focus on endurance building and sustained tool use and may include painting, drawing and writing skills) (Florence and Jane, 1988).

3.1.1.3. Mirror therapy

It consists of a mirror projecting the functional arm in order to create the illusion of normal movement for the patient while training the dysfunctional arm. This technique was initially used to treat phantom limb pains for patients with amputated arms, but recently it was employed in post-stroke rehabilitation as it has an optimistic and psychological impact (Altschuler et al., 1999, Sathian et al., 2000, Yavuzer et al., 2008). Mirror therapy provides finer motor capacity and autonomy scores for tasks involving upper limb functions.

3.1.1.4. Pharmacological technology

It uses drug and chemical properties to restore perceptual, cognitive and motor functions. Drugs have a broad effect on the biological system and facilitate the rehabilitation progress. Additionally, studies have found that combining specific chemical treatments (amphetamine) with rehabilitative training may enhance neural signals and return beneficial effects in restoration of hand function (Barbay and Nudo, 2009a).

3.1.1.5. Constraint-induced movement therapy (CIMT)

It uses the concept of learned non-use, by applying intensive exercises on the affected limb whilst the healthy limb is restrained from moving by a splint, light cast or sling, (Taub and Morris, 2001). It is used as a treatment for post-stroke patients in cases where the motor and sensory deficits of the affected limb are not too severe.

3.1.1.6. Continuous Passive Motion (CPM) and Continuous Active Motion (CAM)

The CPM, (Birch et al., 2008), is a device that provides early post-operative passive motion to maintain a gentle range of movement in the hand. CAM is a device used in rehabilitation after CPM to provide active resistance on hand motion. Recently, CPM and CAP have been employed in robot assistance device structures, which are discussed in detail in the next section.

3.1.1.7. Mental imagery

It is a form of rehabilitation based on subliminal activation of the motor neuron system by inducing imagining actions, recognising the surrounding environment, observing, and learning by comprehending other people's actions. It is referred to as a conscious representation of an action (Jeannerod and Frak, 1999).

3.1.1.8. Review of the Clinical Therapy Methods

The above mentioned methods have multiple drawbacks in practical application as they require intensive work from both therapist and patient, they entail long and weary training sessions which prevent patients from gaining optimal therapeutic outcomes, they lack repeatability and they rely largely on observations and verbal feedback for assessment (Huang and Low, 2008). The level of efficiency of verbal encouragement and feedback, provided by the therapist, is dependent on the patient's interactivity, with regards to their cognitive ability and motivation. The majority of patients find training sessions tedious and boring and this demotivates them and prevents them from continuing the sessions (Damush et al., 2007, Johnson et al., 2006) .

In contrast, robotic-aided systems reduce many of the above drawbacks by providing effective training with repeatability and purposeful exercises. This eventually increases the likelihood of gaining optimal motor function and compliment the therapist's intensive work by providing autonomous exercises, which have higher consistency and efficiency (Reiner, 2005).

3.1.2. Robotic Assistance

Robotic assistance devices have multiple advantages in rehabilitation. They apply regulated forces on the hand, replace the therapist's assistance, produce repetitive training movements throughout the hand range of motion (ROM) and prevent inappropriate movements which could cause abnormality to the original form of motor function (Huang and Low, 2008, Prange et al., 2006). Brain injury is also found to be influenced by the sensorimotor experience, where repetitive robotic assistance therapy exercises after injury have a positive impact in speeding up the recovery of hand functions (Sale et al., 2014).

Various robotic devices were developed to address the different challenges in hand movements and multiple DoF, with different designs which adjust to the patient's hand performance during training, cover a wider range of the patient's ability, suit the hand size and consistently target the appropriate ROM.

Chalon and colleagues presented a list of functional specifications to consider while developing a high performing arm rehabilitation system, that would return positive effects on hand restoration as well as adaptability with the patient's hand size and affected part (Chalon et al., 2010). The following parameters are considered in the functional specification priority: human size, tendon-driven system, good object enveloping, fingertip manipulation, human range of motion, flat hand configuration, correct magnitude of the thumb forces, large power grasp, large opening angle, maximum contact surface and proper orientation, and minimal control complexity.

Several clinical test studies (Zariffa et al., 2011), performed on patients after using robotic-aided systems during rehabilitation training, have displayed efficient improvements on the motor function movements with higher impact. Clinical studies (Zariffa et al., 2011) showed that the piloted robot-aided devices are safe, feasibly adaptable by patients, and can enhance restoration in motor control of proximal arm function.

In the section, the robotic devices are divided into three subsets: robots which are used mainly as therapy aids, exoskeleton devices, and assistive robots.

3.1.3. Therapy aid robot

Therapy aid robot devices are used in combination with therapeutic exercises and work on improving hand performance and reducing the dysfunction level. They provide individual control for each hand digit by applying active and passive forces on the distal segments of the digits. The robot is designed on the self-adapting system, whereby the level of assistance to the patient's hand is reduced in correspondence with hand improvement, with the aim of training the hand towards independent functions.

Table 3-1 lists some of the commonly used robotic aid devices in hand therapies.

3.1.4. Exoskeleton

Exoskeleton devices take the form of external skeletons on the hand and the finger joints. They are comprised of components which expand and contract and have direct control of the digits' movements. The device's DoF are aligned with the hand joints. The challenges encountered with these devices, as shown in the examples given in Table 3-5, lie in their being not very comfortable on the hand, their difficulties to apply on a large ROM, and that they involve a complex process for joint control (Nef et al., 2007).

3.1.5. Assistive robot

Assistive robot devices support patients in their daily activities but do not promote rehabilitation. These devices are used to assist aging people or for generic purposes, but there is scope for them to be employed in rehabilitation i.e. exploring the environment, manipulating objects from a distance, lifting heavy objects, etc. It is important to highlight that there are common bases between these devices and industrial robots. However, employment of the latter in rehabilitation requires them to be adjustable and oriented to the newly instructed activities as there is difference in the system and structure of these robots (Munih and Bajd, 2011).

Table 3-1 List of robotic devices used in assisting with therapy exercises (this table is produced by the thesis author © 2015)

Device	Developer	Description	Review
RUPERT	Kinetic Muscles Inc. (Krebs et al., 2007),(Volpe et al., 2000)	A robotic device that uses pneumatic muscles to perform repetitive therapeutic exercises to the upper extremity. It undergoes a self-regulation in the amount of force needed for normal feeding and reaching movements, which allows the muscles to function independently through exercises.	
Haptic MASTER	Moog FCS Corporation	A force-controlled robotic device that provides force feedback to the hand. It has three degrees of freedom (yaw, pitch and roll). The device measures the velocity, endpoint position and forces exerted to the admittance by the hand.	The device helps to interact with various rehabilitation applications.
Reha-Digit	(Hesse et al., 2003)	A controlled electromechanical trainer for sensorimotor rehabilitation of paralysed fingers. It has four mutual independent rolls with powered cam shaft to move the four fingers (apart from the thumb) in a repetitive range of movements.	
GENTLE/s	(Loureiro et al., 2003b)	A robotic rehabilitation system for neural and physical therapy rehabilitation. It has haptic components: frame, shoulder support, wrist connection, elbow orthosis, keypad and HapticMaster (a three-dimensional haptic interface device with three DoF), and Virtual Reality system.	The system includes motivation factors by incorporating training exercises, contributing to physical movement with visual perceptions.
Hand Rehab. Machine	(Yamaura et al., 2009)	A hand rehabilitation system that uses a wire-driven mechanism. It has a hand rehabilitation device, placed on the dysfunctional hand, which moves finger joints with the motor. A data glove is worn on the healthy hand, to control the movement of the finger joints on the other hand.	
Bristol Robotics Hand System	(Tzemanaki et al., 2011)	A finger rehabilitation device. It has one linear actuator for each finger with a force sensor at each fingertip. The device gives repetitive training exercises by passively extending and flexing the fingers in order to regain flexibilities.	
InMotion HAND™ robot	Interactive Motion Technologies (InMotion, 2015)	It is used with the InMotion ARM™ Robot and forms a neurorehabilitation platform that delivers strength, sensorimotor, sensory and continuous passive motion training in the grasp and release of the hand.	

Table 3-2 List of assisting robot systems in hand rehabilitation (this table is produced by the author © 2015)

Device	Developer	Description	Review
TWENDY-ONE	(Iwata and Sugano, 2009)	A human symbiotic robot. The robot has dual arms with a compact passive mechanism and mechanical softness in joints and skins. The arms are supported with tactile sensors to adequately manipulate objects through contact with the fingers and palm.	This robot was initially developed for enhancing the quality of life for the elderly by providing them physical support in their daily life activities.
KH Hand type S	(Mouri and Kawasaki, 2008)	An advanced robot hand. It has a low force robotic manipulator to guide the human user's movement to place a tool at specified positions. The robot returns faster responses than human fingers, provides dexterity in manipulating objects, and enables compliant pinching with distributed tactile sensors.	This application is used for industrial purposes but entails many advanced robotic technologies in designing anthropomorphic hand device (Kikuuwe et al., 2007).
ActivMedia Pioneer 2-DX mobile	(Gockley and Matarić, 2006)	A self-guided mobile robot system used for exploration of unknown environment and indoor applications. It has wheels with sensing and navigation components.	Used by Rachel Gockley et al. in the study to assist and encourage the patient. The device demonstrated the extent to which patients comply with their physical therapy.

Table 3-3 List of hand exoskeleton used in hand rehabilitation (produced by author © 2015)

Device	Developer	Description	Review
SKK Hand Master	(Sung, 2000)	An exoskeletal haptic device that is semi-directly driven by linkage with ultrasonic motors. It has two finger-like modules attached on the index and thumb. The device can produce high torque without the need for gear transmission.	This method avoids the problems in integration of the weight and actuation to generate sufficient forces for rehabilitation requirement.
Rutgers Master II	(Bouzit et al., 2002)	A tendon driven exoskeleton, providing control for four fingers with one degree of freedom each. The device is used to assist in performing rehabilitation exercises supported by Virtual Reality.	It was employed in a study of the rehabilitation of stroke patients. The performed exercises, supported by virtual reality, showed measurable success (Jeannerod and Frak, 1999).

Device	Developer	Description	Review
CyberGrasp®	(CyberGrasp, 2015)	A force feedback exoskeleton system on the fingers and hand. It has a network of tendons to the fingertips with five actuators for each finger. The device is designed for virtual interactions and lets the patients perceive the hand size and 3D object's shape.	It restricts motion by pull cables with brakes on their distant end. (Further review on this device is explained in the haptic devices below).
Hand Exoskeleton Rehabilitation Robot (HEXORR)	(Godfrey et al., 2010),(Schabowsky et al., 2010)	A hand exoskeleton device that has two modular components to control the fingers and thumb movements separately. The device serves to restrict movement in correspondence with the specification, produces static force and allows free movement. It provides hand motor therapy.	
Hand rehabilitation exoskeleton	(Wege et al., 2013a)	An exoskeleton hand robotic device that has four units: actuator and controller, orthopedic attachment, and mechanical leverage. The device supports bidirectional movement, has four degrees of freedom for each finger, and no tools on the palm to permit interaction with objects.	The device is designed for hand rehabilitation. It can be used to diagnose hand injuries with fitted sensors on the leverage. And it can be easily attached and adjusted to damaged hands.
iHandRehab	(Li et al., 2011)	A hand rehabilitation system that is composed of hand exoskeleton, controller and virtual environment. The exoskeleton has wires attached to the joints and is connected by actuation modules to drive hand movements and receive feedback of the joints' movements, forces and variation angles via integrated sensors. It provides both active and passive rehabilitation motions on the thumb and index fingers.	The device is lightweight, has low inertia, independent control of the finger joints, mechanical safety design and can accommodate different hand sizes with variable ROM.
Index finger rehabilitation exoskeleton	(Wang et al., 2009)	An exoskeleton with four DoF. It has four modules on the joints of the index fingers and uses a double slider mechanism to achieve the flexion/extension of the joints. The device provides angles and force measurements of the joint during finger rehabilitation.	The design of the device can be extended to adopt the other fingers, but it does not provide sufficient ROM because of the constraints of the modules (Li et al., 2011).
HANDEXOS	(Azzurra et al., 2009)	A wearable exoskeleton device that allows independent actuation of all fingers. It has active rotational joints for flexion/extension, passive rotational joint for abduction/adduction, and passive translational joint for the kinematic coupling for each finger. The device trains the impaired hand to perform safe extension motions.	The device still needs clinical studies on the biomechanical assessment of stroke hand.
T-WREX	(Sanchez et al., 2006)	Is a passive orthosis training system. It has a robotic arm exoskeleton with elastic bands and no robotic actuators. It gives five DoF and interacts with computer simulations. The device provides gradable anti-gravity support for the arm and measurement for arm and hand grasps during functional activities.	

Device	Developer	Description	Review
Fin motion assist equipment	(Satoshi et al., 2011)	Self-motion control rehabilitation equipment. It has motion assistance devices for the fingers, wrist and mobile base. The device contains active and passive joints to allow bilateral rehabilitation assistance. It provides symmetrical motions control between the affected and unaffected hands. The unaffected hand commands the device using a data glove device, which feeds back joints posture to the equipment actuators. The device also returns hand motion visual feedback through computer graphic displays and has forced measurements.	
AMADEO	Tyromotion (Amadeo, 2015)	Fingers mechatronic rehabilitation device. The device consists of finger slides that transpose the flexion-extension movement. It has three different modules that could be set depending on the progress: passive, active and active variants.	It allows measurement of fingers' movement and interacts with virtual objects, but the wrist is stable and addresses fingertip positions only.
DLR Hand II	(Huang and Low, 2008)	An advanced robotic system that is attached to the patient's hand and regulates the inputs/outputs to transmit full support in movement and rehabilitation exercises of the hand.	
ARMin	(Nef et al., 2007), (Staubli et al., 2009)	A haptic display and arm therapy robot with semi-exoskeleton kinematics. It provides patient-cooperative assistance by considering his/her activity and the level of support needed. The robot is combined with an audiovisual to display the tasks and movements.	The system increases the motivation and activity of the patient during rehabilitation sessions.
Hand exoskeleton	Andreas Wege and Günter Hommel (Wege et al., 2013b)	A hand exoskeleton device designed for hand therapy, which supports bidirectional movements. It has four degrees of freedom for each finger, and no tools attached to the palm, to allow free interaction with objects.	The device can be easily set up and adjusted to the deformed and damaged hand.
Biomimetic orthosis Neurorehabilitation for Elbow and Shoulder (BONES)	(Klein et al., 2008b)	A shoulder and arm rehabilitation exoskeleton that offers support on three degrees of freedom, for shoulder movement and shoulder internal/external rotation.	

Despite the positive outcomes of robotic device applications in hand rehabilitation research, their use is still not spread across clinics. This is mainly because very few clinical tests have been performed on hand robots (<25% of devices are tested), and also many of the devices are not compatible with the clinical environment (Lum et al., 2012).

However, clinical test studies are not conclusive on the advantages of using robotic devices in rehabilitation and the analyses show variances and inconsistency. Some researchers have demonstrated that robotics are very effective in hand training Reha-Digit (Hesse et al., 2013) and the Hand Wrist Assistive Rehabilitation Device (Takahashi et al., 2008), but others have not supported these advantages (Fischer et al., 2007, Connelly et al., 2010, Lo et al., 2010, Kutner et al., 2010). In addition, review papers suggest multiple reasons for these discrepancies between studies:

a. Inefficiency in the device design, where the dysfunctional hand's motor control is not addressed accurately. Most of these devices can provide simple grasping and releasing (Wege et al., 2013b). Their initial design addresses only one or two fingers and considers the rest (fingers and wrist) as one part, resulting in a contrast with normal hand movement.

b. Uncomfortable and difficult to set up on the hand, which might demotivate the patient from using it. Most of these devices place the motors or the mechanical structure on the forearm, and this makes it undesirable and adds unwanted weight to the hand during rehabilitation training.

c. Incompatible with the clinical environment, as the study shows that less than 25% of hand robots have been tested specifically in clinics. Most robotic devices are not able to support daily living activities (ADL) due to their design and physical/hardware limitations (Huang and Low, 2008).

d. Technological limitations in the hardware and materials, including inertia, strength, force-control ability, and range of motion (RoM). This decreases the viability of the device in rehabilitation (van der Smagt et al., 2009).

e. The muscle lag issue, as patients start to adjust their hand functions by relying more on robotic assistance in performing the training movements. This happens after using the

robot aided device for a period of time. This issue results in failure to transfer the skills into the hand from robot exercises to the ADL tasks (Klein et al., 2008a).

f. The complex mechanism used in the advanced robot devices. This allows the device to self-adapt the level of assistance it provides based on the patient's cognitive and hand performance. However, this has the effect of increasing the level of complexity (van der Smagt et al., 2009).

3.1.6. Virtual Reality

Virtual reality technology has been used extensively in multiple disciplines, such as psychology (provide cognitive tasks and simulation), architecture (test and interact with 3D structures), industrial engineering (robot and machine simulation), bioengineering (rehabilitation and assessment), plus many others. It provides a platform to develop an immersive virtual world and offers the ability to interact with 3D objects in a safe, cheap and creative environment without limitations (Holden et al., 2005).

VR has recently been deployed in different rehabilitation research due to its capability in offering multiple advantages in comparison with traditional methods. The system development is cheap, safe, entertaining (encouraging), efficient, progressively adjustable, has controllable real-time feedback, and returns impulse stimuli similar to real life reactions, that is very significant for learning new skills and transferring these into ADL task performance (Shen et al., 2008).

Holden has listed four advantages for using VR in motor rehabilitation while being conducted in clinical studies. The patients are able to learn motor skills in VR (Holden, 2005). The skills are transferrable from VR to the real world and can simplify untrained tasks. There are no cyber sickness effects generated by using the VR in motor training.

Other studies also found that the VR is capable of offering a task oriented environment where the patient concentrates on key elements of the training with fewer distractions interfering with the rehabilitation progress (Brooks, 2010). The VR environment can be easily customised and adjusted in order to adaptively assist the patient with their progress.

A notable study was conducted on the activities of the brain with VR usage and this illustrated that VR has an influence on mirror neuron inputs by initiating visual inputs during imitation

display (Holden, 2005). Learning by imitation is very efficient in rehabilitation, as it provides visual feedback and accurate repetition of tasks to facilitate the correct pattern formation of cellular activity in CNS.

Hand rehabilitation programs require precise hand digit movement detection to study performance variation and to describe the appropriate task movements needed in each case, which would assess the self-adjustment of the executed activities in each session. As such, the glove offers a better solution for diagnosis and hand analysis from the motion tracking system and markers, as it doesn't require long and tedious calibration or complex considerations on sensitivity issues and light reflections in the surrounding region. The hand motion measurements obtained by the glove while interacting with real (Kikuuwe et al., 2007, Luo et al., 2005, Holden et al., 2005, Reinkensmeyer et al., 2002), imaginary (Holden et al., 2005), or virtual objects would make it feasible to quantify the variations and performance between different subjects.

This review focuses on VR research employed for hand and upper extremity rehabilitation. Therefore, since the project involves the use of the data glove system, in the following, the existing VR methods are divided into two parts: data glove systems, and other VR systems with different approaches.

Starting with the data glove, this system is very commonly used to monitor hand movements and motions. Its exclusivity is in returning precise detection of the digits' movements and joints' variations, and many data glove applications have been produced or are still under development.

Researchers and engineers have used the data glove in multiple disciplines, as it offers the ability to interact with computer-generated environments and machines. In manufacturing engineering, data glove is used for testing tools and environments before construction; for virtual training and 3D objects modelling; and for testing artefacts in simulated equipment. Aside from this, the data glove is used in robotics for different objectives: to control and tele-operate (Oujamaa et al., 2009, Lam et al., 2004, Mascaro and Asada, 2001) robot devices, to manipulate multiple DoF simultaneously; and to teach robots natural skills by demonstrating the movements (Hernandez-Rebollar et al., 2002, Su et al., 2003) and self-learning with semi-

supervision (Szelitzky et al., 2013, Sakurai et al., 2013).

In data visualisation, it is used to interact with large scale data presentations for spatial (Godfrey et al., 2010), geospatial (Shen et al., 2008), statistical, and medical display (Brooks, 2010).

The device is also used in entertainment fields, such as musical performance (Didjiglove, 2013)(Saggio et al., 2009, CyberGlove, 2013, Jack et al., 2001), to control acoustic parameters or play games (Lam et al., 2004), in order to identify natural body movements without using complex hardware attachments.

Additionally, it is found in sign languages (Huenerfauth and Lu, 2010, Lu and Huenerfauth, 2009) and haptic emoticons (Krishna et al., 2010), to translate sign languages into text or vocals and to communicate with deaf users by automatically understanding gestural languages (Oujamaa et al., 2009).

Wearable technologies use the data glove to execute commands and to interact with other devices and applications. The aim of this application is to replace the traditional interaction devices which use computers, such as mouse and keyboard, and provide hand movement interactions that are more natural and may facilitate the control of computer software and hardware (i.e. Virtual keyboard KITTY (Rovetta et al., 2009), Scurry (Bovend'Eerdt et al., 2004), (Earhart et al., 2011), Fingering (Wolf et al., 2001)).

In terms of relating this work to medical application, the data glove device is combined with hand exercises and therapies to restore lost motor control, and with virtual reality (Volpe et al., 2000)(Al-Jumaily and Olivares, 2009)(Merians et al., 2011) as it allows interaction with virtual objects while training the hand to perform visual exercises (Housman et al., 2009, Sanchez et al., 2006, Yoshiyuki et al., 2013, Adamovich et al., 2009a, Zariffa et al., 2011, Endo et al., 2009) . Another instance of using the glove with virtual reality is medical education and training, through manipulation of 3D anatomical data (obtained by MRI or CT (Volpe et al., 2000, Desrosiers et al., 1994)) and performing virtual surgery (Kikuuwe et al., 2007, Linde et al., 2002).

The glove is also used in ergonomics to monitor patients', athletes' and subjects' performances in order to test and design better equipment or devices for the group (Gregson et al., 1999,

Kowalczewski et al., 2011b).

To develop or select a glove system that is appropriate for hand rehabilitation, various characteristics of the device should be considered: the sensor information (if it is continuous or discrete); the number of sensors; the sensor location, whether on the joints, fingertip, or a variable range surrounding the joint; the type of sensor mounting (cloth support or attached to the fingers by mechanical structure); the technology used (fibre optic, hall-effect, piezoresistive); the interface and connection with other machines (serial, parallel, USB, wireless, Bluetooth etc.); the materials of the glove (differs in surgery, sport, fMRI and others); and the performance precision, repeatability and sampling (number of records/sec).

Table 3-4 Data gloves used for general purposes including hand rehabilitation, virtual reality interaction, robot control and others (this table is produced by the author © 2015).

Device, Developer	Description	Review	
ATLAS glove, developed by (Sivak et al., 2012)	It is a bimanual rehabilitation glove that applies Angle Tracking system. It consists of five potentiometer bend sensors at the back of the four fingers and thumb, inertial measurement units, and magnetic base to track the position.	It has a close concept to the CyberGlove© device (discussed in section 4.1.1) for measuring the joints angles; however it is designed to reduce the complexity and it allows the base to be wire-free, but this also reduces the information of the dexterity details with less number of tracked joints.	Figure 3-2 (Sivak et al., 2012) © 2012 ICDVRAT
MusicGlove, developed by Flint Rehabilitation Devices (MusicGlove, 2016)	Is a visual interactive music-based therapy device. It consists of conductive touch sensors placed on the tip of each finger and interact with a visual display to play music key notes by contacting the right fingers. The device also provides score system of the number of correct fingers performed.	The device is lightweight, motivating, very easy to wear, adjustable with the size of the hand and does not require calibration. But it does not measure the joints angles and limited feedbacks on finger performance.	Figure 3-3 (MusicGlove, 2016) © 2016 Flint Rehabilitation Devices with permission
Human Glove, developed by (Chalon et al., 2010)	Consists of 20 hall-effect sensors that measure flexion-extension and abduction-adduction of the fingers. Available in 3 sizes. It uses the serial port connection.	Custom design available. However, difficult recording from thumb and DIP joints (Dipietro et al., 2008).	Figure 3-4 (Chalon et al., 2010) © 2010 IEEE.

Device, Developer	Description	Review	
5DT Data Glove, developed by (Fifth-Dimension-Technologies, 2013)	Uses proprietary fibre flexor sensors. Each fibre loop is connected with an LED at one end, and the light sent is sensed by a phototransistor at the other end. It uses serial, USB, and adapter port connection.	It has multiple versions, and is wireless and MRI compatible. However, has only 1 size and requires calibration.	Figure 3-5 (Fifth-Dimension-Technologies, 2013) Image courtesy: www.5DT.com.
Pinch Glove, developed by (Fakespacelabs, 2015)	Pinch Glove consists of flexible cloth gloves augmented with conductive cloth into the tips of the fingers. Upon contact of two fingers, signals are generated from the conductive pieces and sent to the host machine. It uses the serial port connection.	The glove can detect over 1000 postures and doesn't require calibration. However, it doesn't record joint angles.	Figure 3-6 (Fakespacelabs, 2015) with permission.
Didjiglove, developed by (Didjiglove, 2013)	Consists of 10 bend sensors around the hand to record the fingers' flexion. It is used to operate cameras, lights, rigged animation characters, and driver controls. It uses the serial port connection.	The device is mainly used for animation and has a basic calibration method. There is no abduction-adduction measurement.	
StrinGlove, developed by (Hesse et al., 2003), (Loureiro et al., 2003a)	Consists of 24 induct coders to record flexion-extension of the fingers and abduction-adduction angles, plus wrist motion. It has also nine magnetic sensors. It uses the serial port connection.	Sensors can be easily removed to wash the device; it has three sizes, embed DSP based encoding system for hand posture recognition. However, the sensors are fragile and require accurate calibration.	Figure 3-7 (Hesse et al., 2003) With permission.

Device, Developer	Description	Review	
Finger Nail Glove developed by **(Mascaro and Asada, 2001)**	Uses electro-optics to track the coloration of fingernail changes due to touching, bending/extension and shear.	It can predict finger postures or forces from the measured data, but it requires complex calibration algorithms.	 **Figure 3-8 (Mascaro and Asada, 2001) © 2001 IEEE.**
Colour tracking Glove developed by **(Wang and Popovic, 2009)**	Uses colour patterns to track hand movement. The research study applies Hamming-Distance and other classification methods on the camera images. It uses the camera to capture the glove's motion and feed it back to the host machine.	It is accurate and affordable but cumbersome. Its main use is in animation.	 **Figure 3-9 (Wang and Popovic, 2009) © ACM transaction with permission.**
AcceleGlove, developed by (Hernandez-Rebollar et al., 2002)	The device attaches accelerometers to a leather glove for each finger and tracks the fingers' motion. It is used in physical therapy and hand signal recognition. It uses the serial port to connect to the host machine.	There is no calibration required and it has low cost, but it does not detect horizontal postures.	 **Figure 3-10 (AcceleGlove, 2015) © ACM SIGGRAPH with permission.**

Device, Developer	Description	Review	
3D motion data glove developed by **(Su et al., 2003)**	Uses 3D electromagnetic sensors attached to the glove to detect the position of the fingers. It is used to present a 3D motion system for Parkinson's disease.	This glove returns high precision in position and orientation, but it is complex and has a low sampling rate 10Hz, which returns disrupted synchronisation between the glove and application.	
Data glove developed by **(Szelitzky et al., 2013)**	Uses low cost resistive flex sensors. The system offers 3D hand visualisation that captures the hand movement and simulates the sensation of grasping rigid and elastic objects. It uses USB communication.	The device has low cost and independent GUI with synchronous visualisation. However, it only fits on limited hand sizes and has low precision.	 **Figure 3-11 (Szelitzky et al., 2013) © 2013 IEEE.**
StretchSense developed by **(StretchSense, 2015)**	It has stretch sensors on each finger. Each sensor is wireless and uses Bluetooth protocol. The development kit supported by the device includes sensors, circuitry and software to interact with different devices (smartphones, tablets). It can also be used to measure hand motion for animation, augmented reality, healthcare and the prosthetics industries.	The device provides precise measurements and stable readings that don't require constant calibration, but it tracks the fingertips only. Further work needs to be implemented in designing a full glove from these sensors.	 **Figure 3-12 (StretchSense, 2015) Image courtesy of StretchSense Ltd www.stretchsense.com.**
Force feedback data glove developed by **(Sun et al., 2011)**	It has a bidirectional force feedback data glove actuated by pneumatic artificial muscles. The device offers a simple exoskeleton structure and the bidirectional force is exerted on fingertips. It also applies resistance on the finger's movement to exercise the muscle and strengthen its power.	The device is large, cumbersome and designed only for one finger.	

Device, Developer	Description	Review	
Tactile sensing glove, developed by **(Sagisaka et al., 2013)**	Composed of the thin elastic base glove. The glove enables pressure measurement on a human hand.	It is durable, low cost and accommodates deformation; however, it is limited to tactile sensing only.	Figure 3-13 (Sagisaka et al., 2013) © 2013 IEEE.
PneuGlove, developed by **(Connelly et al., 2009)**	It is a servo-controlled glove that assists the extension of individual finger digits in grasping/releasing activities. The glove permits free movement in the arm workspace and has a specially designed VR environment for training simulations.	The device returns beneficial effects on the hand during training with adaptive adjustment to the level of resistance, but has only one size and requires accurate calibration.	Figure 3-14 (Connelly et al., 2009) © 2009 IEEE.
Haptic device developed by **(Daud et al., 2010)**	A five-bar linkage haptic device with two active and three passive DoF. The device is combined with a graphic simulation interface to produce a VR rehabilitation environment. It can generate forces of up to 20 N in the fingers and hand, and supports both high manipulability and low inertia.		
ProGlove developed by **(Impressum, 2015)**	A device that scans, senses and tests the equipment used in the manufacturing and mechanical industries. The glove interacts with objects and returns result of temperature, size and pressure, on the display attached at the back of the hand.	The glove is a prototype and used for manufacturing.	Figure 3-15 (Impressum, 2015) Image courtesy of Proglove www.proglove.de

Device, Developer	Description	Review	
Conversational Glove, developed by **(Rachel, 2015)**	Has two Arduino Megas to track the finger positions and hand rotation and a Kinect to track each hand movement through space. It also works on digitizing gestural communication using emerging technology.	It is used in animation and entertainment.	
3D Printed motion sensing glove, developed by **(Leigh et al., 2012)**	Comprised of embedded sensing strips in each finger with carbomorph that is both piezoresistive and conductive to measure finger movements.	The glove materials are created using a 3D printer, and it is open source.	 **Figure 3-16 (Leigh et al., 2012) (Open access).**
Fiber Optic Finger-Flexion Data Glove, developed by **(MimuGloves, 2015))**	Uses optical fibres and photosensors to track the finger flexion-extension movement. It communicates with a host machine by the standard RS232 serial port.	The device application is cross-platform compatible and presents fast and robust tracking of the hand movement. However, it is expensive and requires complex calibration.	 **Figure 3-17 (MimuGloves, 2015) with permission.**
TUB-Sensor glove, developed by (Platz, 2003).	Uses inductive length encoders. It is comprised of 12 or 22 sensors for finger flexion-extension and pressure sensors(Langhammer and Stanghelle, 2000). It uses the serial port to communicate with the host machine. The glove is used for health science and robot control.	The device has robust measurement and is available in multiple sizes.	 **Figure 3-18 (Platz, 2003) With permission.**

Device, Developer	Description	Review	
SIGMA glove, developed by **(Kowalczewski et al., 2011b)**	Consists of 30 carbon ink bend sensors for flexion-extension and abduction-adduction movements. It uses parallel port communication.	The device is low cost and is available in multiple sizes. It is also used for motor performance analysis.	
Robo-glove, developed by **NASA** and **General Motor**. **(Wright, 2013)**	Composed of multiple actuators for each finger and pressure sensors. The glove assists users in repetitive tasks such as grasping and holding heavy tools or objects. It also helps users to reduce the force that they need to apply in the action.	The device is portable and includes an embedded microcontroller, but it adds weight to the arm. It is designed mainly for manufacturing and operations that require a large force.	Figure 3-19 (Wright, 2013) © NASA 2013 With permission.

3.1.6.2. Hand therapy data gloves with haptic feedback

Table 3-5 Data glove systems with Haptic feedback support (this table is produced by the author)

Device, Developer	Description	Review	
X-Glove developed by (Triandafilou et al., 2011)	It consists of flexion/extension motors on each finger. The motors are actively actuated using microprocessor. This is controlled with either voice recognition software or muscle activation, measured by electromyography sensors.	The device is portable. It allows controlling each of the fingers' digits independently.	Figure 3-20 X-Glove (Triandafilou et al., 2011) with permission
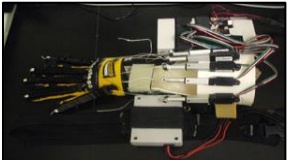
Device, Developer	Description	Review	
J-Glove developed by (Ochoa et al., 2011)	It consists of multiple actuators on the fingers joints. The motor are actively actuated using the microprocessor. It offers three control modes: voice recognition activation, muscle activation (electromyography) and manual. It assists in finger and thumb extension.	This device is portable and allows the user to use the three control model synchronously or separately. It provides force and position feedbacks to the fingers.	 Figure 3-21 J-Glove (Ochoa et al., 2011) © 2011 IEEE.
SCRIPT developed by **(Amirabdollahian et al., 2014)**	The device has passive actuation mechanism and it cannot actively generate or control movements. It consists of a wrist-torque transfer mechanism to allow wrist flexion-extension but block the rotations; a torque-generation for the motor, a micro-controller, and integrated measurements units (IMUs) to measure the hand posture.	It is portable and can passively offset the undesired torques on the fingers.	 Figure 3-22 SCRIPT (Amirabdollahian et al., 2014) with permission
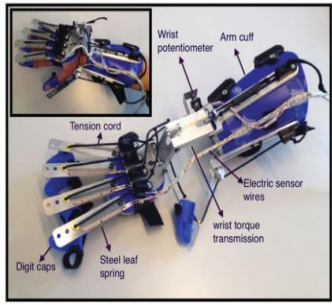
63

Device, Developer	Description	Review	
YouGrabber developed by **(YouGrabber, 2015)**	Consists of three flex sensors on the thumb, index and middle fingers. It supports patients with sensory-motor and cognitive impairments during rehabilitation. The device provides interactive therapy exercises. It uses wireless communication.	The glove can be adjusted to various sizes and individual patient's needs. It is portable and can be used in computer interactive training.	Figure 3-23 (YouGrabber, 2015) With permission.
Gloreha glove, developed by **(Idrogenet, 2015)**	Consists of 5 electric actuators on each finger, and an electronic control system to adjust the length of the cables and the effective range of motion. It offers force feedback on the fingers while interacting with objects. It uses a serial port to connect with the host machine to interact with the visual display. It is used in hand therapy.	The device is light, has no intrusive exoskeleton and keeps the palm free. It is easy to operate, with a user-friendly interface to adjust the level of forces. However, it only provides active assistance in extensions. It has a Lite and Professional version, with different costs.	Figure 3-24 (Idrogenet, 2015) With permission.
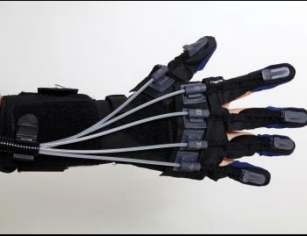
Device, Developer	Description	Review	
HandTutor, developed by **(MediTouch, 2015)**	Consists of electro-optical sensors for finger flexion-extension movements and speed wrist. It uses USB communication with the host machine. The glove allows biomechanical evaluation of the hand's speed, the passive-active range of motion and motion analysis for the wrist and fingers.	The device is validated under medical standard approval. It has robust measurements and accommodates multiple sizes. However, it does not measure joints' angles and does not support the abduction-adduction finger movements.	Figure 3-25 (MediTouch, 2015) With permission.
SaeboFlex, developed by **(Saebo, 2016)**	It consists of a wrist splint and hand mount. The fingers are attached with a lead mount that is connected back to a finger spring to exert force on the flexion of the finger end. The thumb has a separate spring and a line guide to constraint the range of motion.	Saebo offers other devices SaeboGlove (attach fingers joints with tensioners), SaeboReach for the forearm therapy. The device is mechanical only and has simple structure in comparison to the other devices, but does not provide force regulators or joints motion measurement.	Figure 3-26 SaeboReach and SaeboFlex, (Saebo, 2016) with permission
ExoGlove, developed by **(Hong et al., 2015)**	It is based on a novel concept of using soft robotic actuators. The glove consists of soft pneumatic actuator attached to the back of the fingers. The pneumatic actuator, controlled by the air feed, is contracted by the reduction of the air pressure. This causes the soft actuator to close, in a circular loop shape, and extend the finger. In contrast, increase of air pressure causes the finger to flex.	The device offers variable stiffness at different locations of the finger. However, the actuator has a singular shape trajectory when it bends that does not comply with all the grasping forms, has open loop control with no feedback sensors and low accuracy.	Figure 3-27 (Hong et al., 2015) © 2015 IEEE
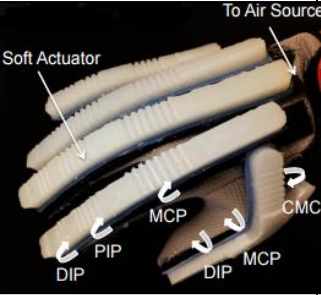
Device, Developer	Description	Review	
CyberGrasp, developed by **(CyberGlove, 2013)**	A force feedback system for the fingers. It consists of an exoskeleton that mounts five actuators on each finger, and exerts forces to the fingertips throughout the ROM. It can be separately specified for individual fingers. It connects to an instrumentation unit, consisting of an actuator module and force control. The connectivity with the host machine is through the Ethernet.	The device allows full ROM movement without obstruction. It is fully adjustable to different hand sizes and allows sensory feedback of the virtual objects. However, it is cumbersome, has complex coding control, and causes traffic loads during Ethernet communication.	 **Figure 3-28 (CyberGlove, 2013) With permission.**

3.1.6.3.Data Glove Devices Review

The selection of the appropriate device from this list should be based on the project objectives and possible implementations. The starting point of this process is to define the glove application class: whether it is a monitoring application or a communication system. The latter is applied in robotics control, sign language detection and games interactions, while the former is applied mainly in health care and medical approaches requiring more specific detail on the hand movements.

To assist the selection of the glove, other factors are considered, such as cost, accuracy, ability to monitor large and small ROM of the fingers/joints' movement, comfort, accurate repeatability, safety approval by medical standards and regulations, portability, and the length of time required to fit on the hand.

Although, the methods in Table 3-4 have multiple advantages, such as simplicity, adjustability, comfort of the user's hand, and accurate recording in motion tracking, they are not all appropriate for hand rehabilitation due to many complications.

In the instance of gloves (MimuGloves, 2015) with fibre optic sensors, the fibre optic cables measure the intensity, phase, frequency and polarisation of the light passing through the cable from one end to the other, by internal reflection. If the cable is bent then the light rays are refracted, and return the bending angle. Fibre optic gloves have numerous disadvantages, including high costs, interference of their light region, occlusion caused by the cross-fingers, and the lack of fine detection of excessively bent/flexed fingers (very often occurring in the case of paralysis). Many are designed for games and virtual reality interaction purposes that require less accuracy in the DoF measurements (Burdea et al., 2011, Lightglove, 2013).

Alternative gloves use capacity sensors (Didjiglove, 2013), electromagnetic (Su et al., 2003), magnetic (StrinGlove, 2015), printed circuit wires (Touch-Typing, 2015), piezoresistive (Leigh et al., 2012), electrical contacts (Zariffa and Steeves, 2011) among other methods.

A more efficient approach in data glove application is to use carbon ink bend sensors to track the joints' movements. These bend sensors are made of plastic film, wafered with coating substrate, which makes them electrically conductive. The ink increases resistance with the application of more bend.

This method offers a high level of robustness, accuracy, less complexity and lower cost. However, it is more likely to be damaged if it is bent more than 90 degrees, and has fixed lengths with less repeatability and accuracy in comparison to the fibre optic method (Dunne et al., 2007).

Saggio and colleagues developed a bending sensor data glove, which is mainly used for recording digits' movement data and assessing hand performance (Saggio et al., 2009). However, a more advanced and well-designed device, used in multi-disciplinary areas, can be found with CyberGlove® (CyberGlove-Systems-Spec, 2013). It has 90Hz data rate, presents good reliability in finger and haptic applications, and supports the CyberGrasp® hand exoskeleton for haptic feedback.

A number of rehabilitation research studies that have made use of CyberGlove® are listed in the section below:

Jack and colleagues produced a VR system which interacts with two input devices, CyberGlove® and Master II-ND force feedback glove (Jack et al., 2001). The system is designed for recovering hand function in stroke patients.

Ueki et alalso produced a VR system that use CyberGlove® to track the motions of the healthy hand of the patient and reproduce these, via an assistant device, in the impaired hand. Cooperative and skilled movements are created with self-motion control in the VR environment.

The PianoVR (Aguiar, 2007), as its name indicates, is a different and entertaining approach that uses a VR piano in interaction with CyberGlove® (or other data gloves). It allows interactive music to play on screen, aiming to create an entertaining environment to motivate patients. It only supports visual feedback (Ueki et al., 2008).

Adamovich and his group have developed a virtual simulations system that uses CyberGlove® and CyberGrasp for hand tracking and haptic feedback, by applying flexion resistance to the adjacent fingers (Adamovich et al., 2009b). This system also has an arm tracking device, Flock of Birds (Ascension Technologies), and an admittance controlled robot, Haptic Master (more details are provided in the robot-aided section), for arm feedback to produce haptic objects such as walls, blocks, cylinders, spheres, springs, dampers and global forces.

The system employs four different virtual simulations used for varying approaches in rehabilitation schemes.

o   Plasma Pong: Trains the upper arm and hand by integrating appropriate shoulder flexion and finger extension in the game.

o   Hummingbird Hunt: Employs audio-visual feedback in the environmental elements. The game provides practice in reach, hand shape and grasp. Different progressions in the range of motion are allowed.

o   Hammer Task: Trains 3D reaching together with repetitive finger flexion/extension. The game provides audio-visual and haptic feedback, and force feedback is produced by the robot through object collision and gravity forces.

o   Virtual Piano (Adamovich et al., 2009a): Provides training for detailed finger flexion/extension movements, accompanied by audio-visual feedback and tactical feedback from the CyberGrasp®.

Data glove systems are widely used in hand rehabilitation as they allow continuous and discrete hand joints recording and simpler VR interaction methods. However, the gloves have different limitations as they create a barrier between the hand and the object, limiting the sensory element and natural flow of the movement. The cloth's support of the glove is also found to affect the pattern creations in gesture formations and measurement performance (Ottobock, 2013, Bionics, 2013, Viau et al., 2004). In addition, the majority of gloves require complex calibrations, and the strength of the recording is very much related to the materials' price.

Nevertheless, different approaches have been suggested to monitor hand movements using various methods to resolve some of the previously mentioned limitations:

McLaughlin has developed a VR assisted motor training system for post-stroke patients (McLaughlin, 2007). The system can be regulated by the therapist to drive the patient's kinetic behaviour, in relation to predefined training, and accurately captures the human kinetic performance. The system tracks the hand position and transfers the details to the VR.

In another study, Liu has presented a motor rehabilitation system that uses a Falcon force feedback joystick and a 3D virtual reality environment ,which interact with a flight simulation (Liu et al., 2013). The tasks exercise the pronation and supination of the arms. Morrow have developed a rehabilitation VR system based on a game console and VR glove (Morrow et al., 2006). This is cheaper than other systems but not as feasible or immersive as 3D applications. Wang has addressed the cost of VR rehabilitation by controlling the game using a simple artefact input device (Wang et al., 2010). The system reads user action when squeezing the rubber ball via the attached sensors. The Handcopter Game, developed by (Souza and Santos, 2012), is designed for treating patients suffering from post-stroke paralysis. The system tracks the hand's movement through a low-cost vision-tracking device.

Finally, Xu have presented a haptic handwriting and Ten Pin Bowling game which interacts with a Novint Falcon, a parallel robot with three servo arms connected to a detachable grip (Xu et al., 2010). The system aims to improve the rehabilitation process by motivating patients and creating more effective tasks.

The device generates low force and low resolution. Both the Novint Falcon and Phantom Omni devices are designed to measure the endpoint motion (position or velocity), exerted by the hand, and to output the force feedback.

Digits device, developed by Kim and his group in contribution with Microsoft Research, is a gloveless wrist-worn sensor that captures the full 3D pose of the user's hand (Kim et al., 2012). The electronics are self-contained on the user's wrist and they emit a light from the device (visual, infrared or camera imaging) to scan the full palm and sense the wrist, hand and fingers.
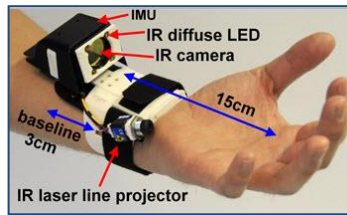
The system uses a new signal-processing pipeline to sample key parts of the hand, such as the tips and lower regions of each finger, and retrieves the full finger motion. It uses a wireless connection with the host machine, enabling a variety of freehand interactions on the move.

The glove is highly precise, but it is complex, has low sampling rates and requires compound algorithms. It is mainly used for interaction with virtual reality objects, but in the case of real objects it causes interference with the IR projection.

In summary, there are many VR systems that have been developed for rehabilitation. Most of the systems introduced are still in the field of research and have not been clinically adapted for rehabilitation sessions (Holden et al., 2005). Additionally, studies have not validated the efficiency of VR in treating motor disabilities. However, it is recommended as an assistance tool for therapies and an efficient tool for data monitoring (Popescu et al., 2000).

Therefore, to design an effective VR system in rehabilitation, it must be very precisely adjusted in relation to the involved exercises for each specific patient's case (Holden et al., 2005); have an ability to provide perceptive coordination between the clinicians-patients and virtual environment (Nathaniel and Anne, 1994); and provide a significant link to transfer motor skills into real world activities by addressing existing motor disorders (Kozak et al., 1993).

Recently augmented reality has been introduced to visualisation technology by combining both real and virtual worlds. This method has numerous features that seek to resolve the existing VR limitations. It provides more stimuli and realistic feeling to the subject, gives

versatility to transfer improvements into real world situations, and offers fatigue reduction during intensive practices (Shen et al., 2008).

Another method in hand rehabilitation is incorporating regulated electrical stimulation during physical training and this is explored further in the following section.

3.1.7. Neuroprosthesis

Neuroprosthesis (NP) treatment involves devices that substitute the damaged motor, sensory or cognitive modality. NP systems are distributed by different techniques and functions.

Electrical stimulation (ES), a very common NP application used in biomedical engineering, is a type of system that employs the peripheral nervous system (PNS) and reads muscle activation, aiming to replace the central nervous system (CNS) in some hand function instructions.

ES is frequently used with physical motor training, particularly for wrist and finger extensors, and this is known as functional electrical stimulation (FES). FES delivers trains of electrical charge pulses, similar to those excitation signals generated by CNS in healthy structures (Popovic et al., 2002), and its operations use multi-channel electrical stimulation that can be regulated appropriately.

An alternative use of ES is in combination with therapy, known as therapeutic electrical stimulation (TES). Both TES and FES are used to strengthen the muscles and assist in functional tasks (Gritsenko and Prochazka, 2004, Stein and Prochazka, 2013).

An example of these systems is the Stimulus Router System (SRS) (Gan et al., 2007), a Neuroprosthesis (NP) consisting of a conductive pick-up terminal, subcutaneously implanted under one of the surface electrodes, and a delivery terminal implanted near or on the target nerve (Gan and Prochazka, 2010).

Another type is the daily neuroprosthetic, NESS Handmaster, a functional electrical stimulation used in sub-acute stroke, consisting of a wrist-hand orthosis (WHO) with a non-invasive microprocessor controlled simulation system. The system is set up on the limb of the patient and supported with a 5 electrode array (Ring and Rosenthal, 2005).

A further type of NP system is brain magnetic resonance (MR). Its function is to target motor and cognitive modulations. An example of this approach is the MR_CHIROD v.2 (Khanicheh et al., 2008), a hand rehabilitation device with one degree of freedom. It uses electrorheological fluids (ERFs) to provide computer-controlled resistive force generation. It consists of three subsystems: ERF based resistive element, handles, and two sensors for hand motion and force measurement.

Another example is high-frequency transcranial magnetic stimulation (TMS) (Berlim et al., 2013). The system stimulates the ipsilesional motor cortex for inhibiting excitation, associated with motor re-learning training (Barbay and Nudo, 2009b).

The last of these NP systems is EMG Imagery, a mental process imagery where the patient simulates a given task to control the hand prosthesis. Many applications use this process, such as Ottobock's SensorHand, 2008 (Ottobock, 2013) and Touch Bionic's i-Limb, 2007 (Bionics, 2013).

The abovementioned NP systems make a significant contribution to rehabilitation, although further studies are required to improve their efficiency. Moreover, the NP devices are expensive and cause discomfort to patients. ES systems, in particular, can cause pain and edema in some sessions. The current systems also offer inadequate selections for the varying sizes and locations of muscles. Additionally, the simulation-forces are very difficult to regulate because of their complexity (Popović and Sinkjær, 2000).

Considering the various approaches in hand rehabilitation – from basic clinical techniques to robotic assistance, virtual reality and neuroprosthesis – and pointing to the currently existing drawbacks, it is clear that extensive further research and thorough analysis are required in order to produce proficient devices for rehabilitation.

A new investigative area has been highlighted, combining the different approaches and using the various advantages of each in order to resolve the encountered limitations.

3.1.8. Synthesis

The synthesis approach combines multi-disciplinary approaches in order to create a synthetic device that has higher efficiency with fewer drawbacks. The purpose of this

system is to use the benefits encountered in each method to counteract the drawbacks, and to carefully join different methods to maintain the proficiency of rehabilitation.

Below are some of the available systems that have used this approach:
Conventional ET and ReJoyce ET combine electrical stimulation with training efforts. The former comprises strength training, trackball computer games and therapeutic electrical stimulation (TES) (Kowalczewski et al., 2011b); and the latter consists of computer games associated with ADL activities that are controlled by a joystick (Kowalczewski et al., 2011b).

An alternative is the combination of robot-aided systems with EEG, by which S. B. Fok et al. have developed an EEG-based brain-computer interface for hand control rehabilitation post-stroke, using ipsilateral cortical physiology (Fok et al., 2011).
A different approach in this field is to combine the robot-aided systems with electrical stimulation, also known as hybrid systems**.** The idea is to associate the FES with the mechanical structure using the human muscles as actuators. It aims to replace the heavy actuators in the exoskeletons and invoke functional solutions in wearable robotics.
An example of a hybrid system is the smartFES (sFES), which is a non-invasive FES assistive rehabilitation system. The electrical stimulation is controlled by a neural inverse dynamics model and is provided to the patient in order to assist in the execution of specific arm movements (Goffredo et al., 2008).

Robot-aided systems are also tested in combination with EMG. The EMG-driven exoskeleton hand robotic training device consists of a robotic hand module and embedded controller. The robotic hand module is attached to the hand using finger rings and Velcro straps. The device detects the patient's intention by measuring EMG signals of the hand muscles, and assists in the opening and closing of the hand (Ho et al., 2011).
A further example of an EMG-driven system based on VR has been developed by Al-Jumaily.The VR provides exercises in the virtual environment accompanying the patient's movement intentions (Al-Jumaily and Olivares, 2009).

Combining robotics systems with virtual reality has garnered the interest of many researchers, and there are many examples that could be listed in this section.
The Virtual Curling System (Yoshiyuki et al., 2013), is a robotic rehabilitation system for upper limbs that uses the handle of an impedance-controlled robot to move a virtual object

while predicting its transient behaviours upon release. The system generates human hand trajectory models in the virtual curling and transfers these into the robotic device to assist in teaching smooth movements relevant to the performed task.

Various applications of this method have been provided by SV Adamoich et al. and these were discussed in the Virtual Reality Section, 3.1.6. Their proposed systems depend on combining interactive gaming simulation with adaptive robots in order to provide a multi-faceted environment (Merians et al., 2011, Adamovich et al., 2009b), and are being investigated further.

Armeo Spring®, Hocoma AG (Zariffa et al., 2011) is a passive upper limb rehabilitation device. The device provides adjustable anti-gravity force feedback to the patient's upper arm and forearm, supported with a VR display that controls a virtual arm. The device provides adjustable anti-gravity arm support, adjustable ROM, and optional grip module to control the strength and adaptability to various forms of limb impairment.

The HIRO system (Endo et al., 2009) consists of a five-fingered robot hand and a robot arm. It provides force and tactile feedback to the five fingertips of the human hand. HIRO consists of a 6 DoF arm and a 15 DoF hand and can reproduce 3-directional haptic forces at the hand.

Ueki has developed a hand rehabilitation system that provides symmetric master-slave motion assistance, allowing the impaired hand to be driven by the healthy hand, while displaying effective VR exercises (Ueki et al., 2008).

Kikuuwe has provided a virtual fixture device that is based on simulated plasticity (Kikuuwe et al., 2007). The VR fixture guides the hand in path-tracing tasks and obstructs movement inside specified boundaries. The fixture is always passive and acts as a hard fixture when the hand's force is smaller than the yield force.

As mentioned in the Virtual Reality section, a more advanced technology in computer graphics is augmented reality (AR), which is the combination of VR with therapeutic movement. AR technology augments the user's view of the real world by displaying virtual objects in the physical world and provides visual and haptic feedback, allowing the user to interact with virtual objects in a real environment.

Unlike VR, the AR provides tasks that resemble real life activities and allows for a more efficient transfer of the learned motor skills from AR to ADL. Arms Guide and PUMA robot

are two existing systems that employ this technology (Luo et al., 2005).

Lastly, Telerehabilitation is a combination of VR with therapeutic training, with a long range of distance between the VR and the objects. It is a newly developed technology that allows for easier access to rehabilitation training services, as it is less expensive and more portable for patients. The system uses the internet to connect therapists with patients, provide assistance during training exercises and supervise progress and performance from the clinics.

Holden et al. developed a VR system augmented with Telerehabilitation capability. It provides real-time interactive treatment sessions between the patient at home and the therapist in the clinic (Holden, 2005). Several other groups have also developed similar systems in teletherapy and web-based therapy from home-to-clinic (Holden et al., 2005), (Reinkensmeyer et al., 2002, Holden et al., 2005, Bowman and Speier, 2006, Kowalczewski et al., 2007) and clinic-to-clinic (Burdea et al., 2000, Popescu et al., 2000).

3.2. Hand Assessment

Rehabilitation methods require careful assessment and validation as they can cause a severe impact on the hand if they are not applied appropriately. Inaccurate employment of these techniques can distort the motor functions of the hand (Klein et al., 2008a), and mal-transfer the learned skills from the training exercises to daily activities (Huang and Low, 2008). These side effects can be caused due to the system design, which is difficult to customise to the patient's performance, is inefficient in addressing specific individual cases and has low precision in training each finger separately (Li et al., 2011). It is also important to note that the patient's satisfaction with the application (Wang and Popovic, 2009) plays a major role in evaluating the system success.

In this section, multiple hand assessment applications that are currently used in clinics and research have been reviewed. This is divided into four hand assessment categories: clinical, hand motion, robotics, and virtual reality. The section then concludes with a brief introduction to the proposed approach.

3.2.1. Clinical Hand Assessment Methods:

These methods are usually basic and have limited outcomes, but they are still frequently used to assess the patient's performance in clinics due to the cost and lack of technological applications that are appropriate for clinical settings. There are many existing techniques, for this purpose, which consist of either a set of instructions and questionnaires to verbally assess the rehabilitation, or a variety of traditional equipment, such as dynamometers and stop watcher, to record details and analyse hand movement by using velocity and time parameters.

These methods mainly include hand tasks that can be categorised as a small movement, mass grasp (balls and spherical objects), key pretension (jug pouring), palmar pretension (food cutting, opening door handle), and individual finger movement (using keys, trays, or a finite movement).

Different methods are presented below:

Modified Ashworth scale (Gregson et al., 1999) is a set of instructions defined with specific movements to assess the shoulder, elbow, wrist, fingers and thumb.

Box and Blocks Test is a set of instructions where the patient is asked to move a set of blocks across partitions to test the functional use of the hand (BBT) (Desrosiers et al., 1994),

(Miltner et al., 1999).

Jebsen-Taylor hand tests (Jebsen et al., 1969) are a set of tasks where the patient is asked to complete a subset; results are obtained by measuring the time of completion. The test includes simulated eating, providing a quantifiable activity of daily living, lifting large light objects and lifting large heavy objects.

Hand grip strength (Davis et al., 2000) uses a handgrip dynamometer to measure the maximum isometric hand strength.

Action Research Arm Test (ARAT) (Carroll, 1965) is a set of tasks such as grasping, lifting, placing objects, and pouring water from one glass to another. Results are measured by the therapist, based on task completion and the naturalness of the motion.

Graded and Redefined Assessment of Strength, Sensibility and Prehension (GRASSP) tests three aspects on the upper limb – strength (manual motor testing), sensibility (sensory testing using monofilaments), and prehension – qualitatively by examining the different hand postures that the subject is able to assume, or quantitatively with functional tasks such as pouring water, turning a key, and moving pegs on a pegboard.

FuglMeyer Assessment (Gladstone et al., 2002) is a quantitative test to measure sensorimotor changes during recovery after stroke.

Wolf Motor Function Test (Wolf et al., 2001) is a set of instructions that measure motor ability through timed, functional tasks and strength.

Jebsen Test of Hand Function (JTHF) (Bovend'Eerdt et al., 2004) measures the hand motor skills by using seven items that measure fine motor skills, weighted functional tasks, and non-weighted functional tasks.

Nine Hole Peg Test (9HPT) (Earhart et al., 2011) evaluates manual and finger dexterity by measuring speed, accuracy, quality, and finger use following set of instructions.

Five-rung grip strength test (Shechtman et al., 2005) is a therapeutic test used to determine the sincerity of the effort exerted by the injured hand. The test is employed to measure the quality of the injured hand in applying a force and to regulate the differences in the shape of the curve during hand gripping.

Southampton Hand Assessment Procedure (SHAP) (Light et al., 1999) is a set of tasks that involve finite and gross movements: Tip, Lateral, Tripod, Spherical, Power and Extension (Light et al., 1999). These tasks are performed using eight abstract objects and 14 activities of daily living (ADL).

(More details on this method can be found in Experimental Chapter 4)

The above methods provide only subjective observation or measurement to the time or duration to complete tasks, which are not sufficient to efficiently evaluate hand improvement.

3.2.2. Measuring Activities of Daily Living (ADL):

There are different clinical methods used to measure the ability to perform the ADL activities and ensure the transfer from rehabilitation exercises to daily life functions. These methods merely rely on the subjective assessments from the health care professionals. The therapist observes the patient while performing different ADL tasks such as dressing, easting, bathing, toileting, transferring (standing, walking)

The therapist evaluation is based on a score that marks each task. There are different scoring methods implemented to reduce the subjective variations between the physicians' observations. Katz Index of Independence, (Katz et al., 1970), defines each task and the bases on which the patient is awarded a point. The score of the patient's independency, (Katz, 1983), is calculated by summing the total points of the tasks.

Likewise, the Barthel Index of Activities of Daily Living, (Wade and CoNin, 1988), scores the tasks to reveal the patient's ability to self-care or perform the ADL tasks.

Although, both methods have similarities , (Hartigan, 2007), they lack test reports to validate their reliability and precision. In addition, very often, the scoring evaluation introduces variability between assessments, this is mainly due to the different experiences between the therapists observing the patient, (Shelkey and Wallace, 2000).

3.2.3. Hand Motion Assessment Systems:

Motion assessment is a newly adopted technique for acquiring explicit information from hand movement.

The kapandji test (Chalon et al., 2010) is the standard test system that is used to assess the range of motion for fingers. It measures the fingers' motion during movement within predefined gestures. All fingers' motion directions are included in this test in order to make it applicable for testing the hand's sufficiency during the grasp function.

Some studies (Hester et al., 2006) use accelerometers to measure motion trajectories. The raw data is used in data mining techniques to predict clinical scores for standard tests. This usually requires a therapist's evaluation.

Another method captures the range of motion by using optical markers that are placed on defined locations in the body to track and monitor the motion (Shurtleff et al., 2009). The patient who is wearing these markers is asked to perform specific movements, such as reaching, moving arms around the field and interacting with the object. After recording the motion capture, data is compared between sessions to determine the level of changes and motion quality (Viau et al., 2004).

3.2.4. Robotics Devices Hand Assessment:

On the whole, the robotic devices have displayed more accurate measurements than the clinical observation techniques. This is mainly due to the precise and repetitive measurements that the robotic devices provide for data performance analysis. Some of the existing approaches are listed below:

Daphne system (Rovetta, 2009) is a neuromotor assessment system that measures the time response in the motion of one finger from the hand, the velocity of phalanxes, and the force exerted by the finger against a button.

Jamar device (Chalon et al., 2010) allows pinch grasp and power grasp forces. It provides relevant information for defining the force requirements at the fingertip in a half flexed hand.

Omni®, Sensible with VR application developed by Haptic library (SIRS-Lab, Siena) (Meary and Baud-Bovy, 2009) is used for developing a robot-assisted assessment system for hand motor control.

The system uses the tasks, including the handedness questionnaire, to describe the patient's hand performance in rehabilitation procedures in less than half an hour. The assessment evaluates effects in accordance with the use of feed-forward/feedback control, learning and hand dominance.

The wrist-RoboHab (Baniasad et al., 2011) can be used for evaluating: forearm supination/pronation, wrist flexion/extension, and ulnar/radial deviation. The device, aside from measuring the spasticity of elbow and wrist flexors at a constant velocity, measures the hand's active range of motion by moving the handle with low impedance and end points, considered as ROM.

Passive ranges of motion are evaluated by allowing the handle to be free to move, and the therapist drives the patient's hand while he/she grips the handle.

Although robotic systems return more accurate and precise assessments, they are expensive and are exclusively designed for the specific device.

3.2.5. Virtual Reality in assessment

Alternatively, several researchers focused on using VR in assessment, as it returns very efficient measurements with lower cost and higher robustness.

VR Kitchen, developed by the group in Texas (Viau et al., 2004), is one of the specified methods which works on evaluating patient performance by emulating ADL tasks. The test involves meal preparation tasks, such as making soup, sandwiches, etc.. These tasks are consequently divided into subtasks for acquiring more profound and detailed evaluation. This test was compared with real kitchen tasks and indicated efficient reliability.

Davies has developed multiple VR systems for the purpose of kitchen-based training (making coffee, setting the table), vending machine interaction (i.e ATM), and path finding using VR representations of the local hospital and university buildings **(Davies et al., 2002)**.

Albani has developed an application which assesses the patient's performance while navigating through a flat surface using a joystick **(Albani et al., 2002)**. The three factors monitored are speed, object identification, and object recall. This test measures the performance of patients with Parkinson's disease.

The VR systems mentioned above are developed for general purposes of rehabilitation. However, there are some dedicated projects that primarily target hand rehabilitation:

The **ReJoyce automated hand function test (RAHFT) (Kowalczewski et al., 2011a)** consists of three parts: function range of motion (fROM), grasp, key-grip, pronation-supination tasks and placement tasks. The system is connected with a workstation to interact with generated computer games.

It efficiently measures a set of specified tasks, but this makes it limited and incompatible with other hand rehabilitation systems.

The restriction of RAHFT is that it targets tasks that are not common with other techniques or devices, and this makes it very general. Also, the tasks covered do not usually transfer to ADL activities.

A remote rehabilitation system developed by (Burdea et al., 2011) comprises of multiple interactive virtual hand games with a modified PlayStation 3 and a 5DT data glove. The system measures the patient's performance at the start and end of the system usage;

during this time the grasping strength, hand function and bone health are monitored.

A similar approach can be found with **(Huber et al., 2008)**. This system shows positive outcomes but with some limitations, as the glove size is not customisable; it uses one fibre optic sensor per finger, which restricts it to only "global flexing" measurements; and each of the sensors requires a separate calibration curve, which tends to dislodge when wearing the glove. These drawbacks make the data measured inaccurate and more difficult to communicate.

In addition, there are various limitations found in the above VR systems. The virtual games use game consoles that are old and not cross-platform compatible. The remote rehabilitation is also not as beneficial as expected; this is because it depends on internet speed, the compliance of the surrounding environment, and the continuous need of therapist observation to ensure that the data measured is deducted from the appropriate tasks and procedures.

3.2.6. Hand Assessment Approach

After reviewing the above methods, the key elements that need to be addressed in order to ensure reliable and efficient development of the hand assessment method can be summarised: 1- The developed system should be compatible with other rehabilitation systems and not be specified to only one particular technique or application. 2- The data measurements should not be dependent on eye observation only, as this is inconsistent and does not return accurate data. 3- The designed applications or devices should not restrict the active ROM space of the patient's hand as this could limit the task workspace.

By having these elements in considerations, this project aims to implement a clinical hand assessment classification method inside a virtual reality system, where the hand motion can be tracked using a data glove sensorial device and visualised on the 3D display.

The virtual reality system offers a safe interactive environment, significant visual feedback for the hand movement containing high details of the environment with some analysis (Grealy and Nasser, 2013), and remarkably increase the motivation of the patient while performing exercises (Eletha, 2008).

In addition, the data glove device can return efficient measurements of fine and gross finger joint movements, with high accuracy and robustness; dynamic measurements of

hand motion without having overlap issues between the fingers or mixtures of reference points (Yamaura et al., 2009); and constant reading of the hand velocity, smoothness of the hand digits trajectory while performing a task, and stability of the fingers.

The data glove also does not cause any inconvenience as it is easy to wear, comfortable on the hand, and it does not prevent the subject's hand from interacting with real objects.

In conclusion, employing the data glove device and virtual reality for hand assessment, will provide a safe and robust system that can objectively measure the different properties of the fingers motion and functionality.

3.3. Summary of the Literature Review Chapter

As the initial scope of this project is wide and covers multiple disciplines in hand rehabilitation, which involve standard clinical methods, robotics and advanced technologies, it has been decided to divide the review subjects into five categories in hand rehabilitation: clinical therapy, robotic assistance, virtual reality, neuroprosthetics, and synthesis.

Each method/device is given with a description of the system properties and the existing challenges/drawbacks that affect the patient's hand or the general setup effort, mobility, and costs. In general, most of the clinical methods require extensive effort from the patient and the therapists. In contrast, advanced systems such as robotic, virtual reality and synthesis provide mobility and repeatability; it also reduces the intensity of the exercises. Although the advanced technological systems have more advantages than the conventional techniques, they are expensive and not adaptable with the patient performance, and still require further adjustments and research.

In conclusion, this chapter points to the necessity of developing an advanced and efficient hand assessment system that supports the conventional and advanced rehabilitation methods, with objective and dynamic measurements of hand performance.
Multiple methods were reviewed in the hand assessment and conventional methods were found to be non-automated, not adaptive and highly reliant on subjective assessments.

In the following Experimental Chapter 4, more details of the materials and methods used to conduct the analysis were provided. The CyberGlove® data glove device, which was reviewed in this chapter, was selected for the study because of the many advantages it has

over the other reviewed systems; including the portability, robustness, and feasibility, where different recording sensors cover most of the hand DoFs and do not produce high noises or disruption with surrounding devices.

Also, the clinical assessment method SHAP has been reviewed with supportive information to illustrate the advantage of this system and highlight the reasons behind using it in this study.

Chapter 4 Experimental

This chapter describes the setup and methods used in building the outcome measurement system to assess hand functions. It starts with an explanation of the system architecture and the various components involved in the hardware, graphics and data processing layer. The chapter then describes the experimental protocol, with the subjects' inclusion criteria and the experiment structure and regulations. It then concludes by outlining the procedures for calibrating the systems, recording the data and processing it for analysis.

4.1. Experimental Setup

The project system architecture, shown in Figure 4-1, consists of three grouping layers:

- The hardware layer: consists of the hardware connectivity between the devices (CyberGlove®, EMG reading devices, Dome® and computer screen) and the software display.
- The data processing layer: consists of the data collection component for storing the data, and the data analysis. The data is analysed using the developed algorithms to calculate the outcome measurements and perform the statistical analysis.
  It also includes the experimental software setup and the classification procedures application.
  The data processing layer contains part of the graphic display. This includes the virtual model's data structure and kinematic, collision detection, object interaction, and data calibration.
- The graphics layer: consists of the 3D virtual graphics engine that is responsible for 3D rendering, texturing and rasterization.

Graphics

- Buffer Objects
- Vertex Shader
- Primitive Assembly
- Rasterizer
- Textures
- 3D projection
- Results

Data Processing

- Scene Graph
- Collision
- Simulation
- Objects, Obstacles
- HumanHand
- Kinematic
- Calibration
- Virtual Manipulation
- Experiment Setup
- Data Recording

Data Collections

- Statistics
- Math Calculation
- Algorithms
- Data Export
- Report

Hardware Layer

- Update Output
- Synchronise
- Handshake
- Read Inputs
- GPU

| Serial Port | USB | Parallel Port | VGA |

CyberGlove ®

Interface Unit

Flex Sensors

EMG

CED 1401

Neurolog

Electrodes

Dome

Screen

Figure 4-1 Schematic of the full system architecture presents the structure with the different involved components. The top layer is the graphical and display process unit; the second top layer is the data processing for calculating the hand model kinematic and experimental data collection/analysis; the bottom layer is the hardware part which involves data glove sensor components, graphical devices and EMG data recording; the bottom layer acts as an intermediate between the subject and the system graphics.

The hardware components of the system and the visual display are shown in Figure 4-10.The visual display is placed in front of the subject with an immersive screen. The subjects interact with the visual world using the data glove device with the objects located on the table and virtual reality.
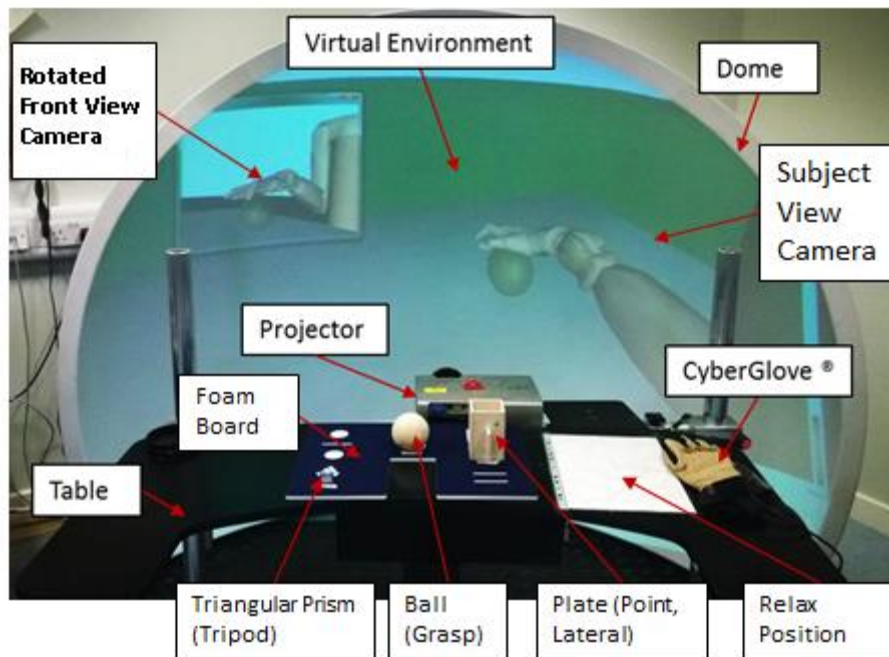
Figure 4-2 Hardware/software components used by the subject during the experiment; the system includes Graphical Display Dome® to show the VR environment along with both the camera views (front and subject virtual cameras), the table that holds all the experiment

Before illustrating the components of the system, it is important to note that alternative devices or methods could be used to perform the experiment. The only condition for using any different equipment is that it must be compatible with the system architecture displayed in Figure 4-1. In this project, the devices and methods were selected based on their efficiency in measuring the required data, compatibility with other devices, and availability in the neurophysiology research lab, at the Biomedical Engineering Unit of the University of Strathclyde.

4.1.1. Data Glove

The data glove device used in this experiment is the CyberGlove® (CyberGlove, 2013). This device was created by Immersion Corporation and later acquired by CyberGlove® systems. The glove is designed for measuring the movements of the joints of the hand. It consists of 18 or 22 sensors (the latter is for the latest version) mounted over or near the joints of the hand and wrist.

In this project the device is combined with the hand assessment classifications method to measure the multiple digits' movements during the experiment. The signals recorded from the glove incorporate many properties for the fingers while performing tasks of gross and fine movements, such as stability, speed, and smoothness of the motion.

Figure 4-3 Full kit display of CyberGlove® device with its components, including the interface module, serial connector to the machine (CyberGlove, 2013).

The CyberGlove® (CyberGlove, 2013), Figure 4-3, model used in this project is CyberGlove I. It consists of glove fitted with flexible sensors, wired to the interface unit that contains the digital signal processing and amplifier, and a serial port to communication with a computer machine. The glove specifications are listed below:

- The glove has 22 flex sensors (three flexion sensors per finger, four abduction sensors, and three palm-arch sensors to measure the wrist flexion and abduction (Figure 4-4).The sensors are thin and flexible to make the glove lightweight and elastic.
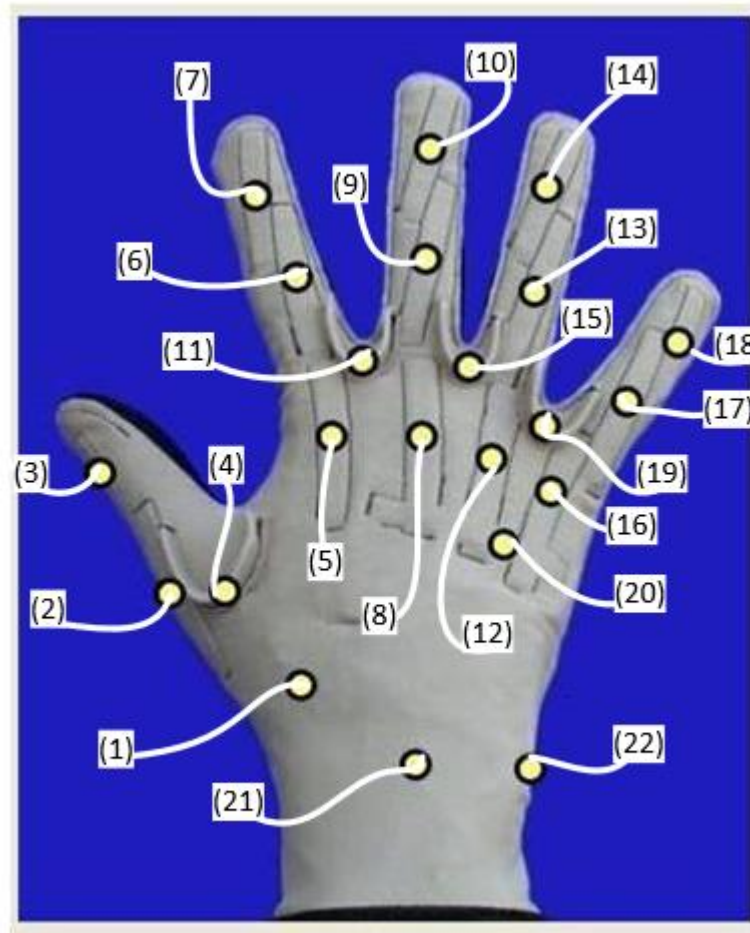
Figure 4-4 Display of the 22 sensors' positions on the CyberGlove® device; (1) Thumb Rotate, (2) Thumb MCP, (3) Thumb IP, (4) Thumb Abd, (5) Index MCP, (6) Index PIP, (7) Index DIP, (8) Middle MCP, (9) Middle PIP, (10) Middle DIP, (11) Middle-Index Abd, (12) Ring MCP, (13) Ring PIP, (14) Ring DIP, (15) Ring-Middle Abd, (16) Pinkie MCP, (17) Pinkie PIP, (18) Pinkie DIP, (19) Pinkie-Ring Abd, (20) Palm arch, (21) Wrist Flexion, (22) Wrist Abd. The different sensors positions allow for measurement of the multiple range of motion of the human hand(CyberGlove, 2013).

The sensors used in CyberGlove® are flex sensors, designed to withstand typical ranges of bending and radii of curvature of natural finger motion. It provides a proportional angle output relative to the joint and joint radius, independent of the sensors' locations. In order to obtain an accurate reading, it is essential that the sensor covers

the arc of the joint between the adjacent bone segments.

The output voltage (0-5V) for each sensor varies linearly with the bend angle. It is processed through an ADC converter to return digital output (0-255). Each sensor has hardware offset and gains value, set in the CGIU unit, for modifying the digitisation output and producing a sub-range of 40-220. This sub-range is set to exclude high or low saturation for the sensors in extreme cases.

The glove sensors have resolution <1 degree, repeatability 3 degrees (average standard deviation between glove wearing), linearity of 0.6% maximum nonlinearity over the full joint range and a typical sample data rate 90 records/sec.

Further information on the flex sensors' definition and properties can be found in the Literature Review, Chapter 3.

- The glove size is regular male hand size.
- Operating temperature: 10-45°C
- Medical approvals: CE, FCC, Japan Technical Regulations Conformity Certification of Specified Radio Equipment

The data acquisition is performed using an interface unit (CGIU). It reads the flex sensors' output, digitises it, and feeds it back to the machine via a DE-9 male connector with RS232C serial communication.

CyberGlove® offers a basic virtual application to display glove interaction with the hand model.

Hence, as the CyberGlove® is a medically approved device, has high frequency, provides high resolution and repeatability, and mounts multiple bending sensors on the significant DoFs (Flexion/Extension, Abduction/Adduction) of the hand, the device is found very compatible for measuring the fingers' motion and analysing the sensorial data in this project.

Moreover, in comparison with the other devices, covered in the Literature Review Chapter 3 section 3.1.6.1, the CyberGlove ® is more robust and its bending sensors do not require complex calibrations nor suffers from interference with surrounding devices, in contrast to the fibre optics sensors' sensitivity and complex calibration. Furthermore, the bending

sensors, unlike the vision based sensors, do not get obstructed by grasped objects and crossing fingers.

4.1.2. Hand Assessment Classification

The classification method selected in this project is SHAP (Light et al., 1999). It is a clinically validated device that consists of a set of procedures covering a wide range of prehensile tasks for evaluating hand functions.
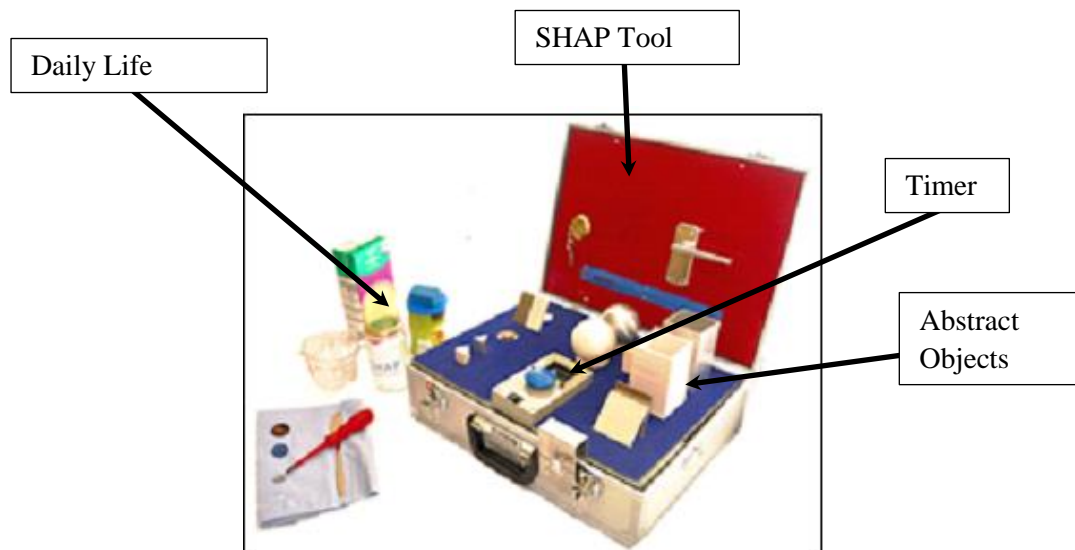
Figure 4-5 SHAP toolbox includes the multiple classification objects for hand assessment and timer button to measure the performance speed (SHAP, 2013).

The device is a portable toolbox, shown in Figure 4-5, containing 26 assessment items of abstract and daily activities. The items are listed in Table 4-1.

The toolbox also includes a two-sided board and a timer (Figure 4-6) controlled by a push button. The system requires access to an online web-based interface to obtain the hand function evaluation scores from the session data.

Table 4-1 List of SHAP Items available in the tool box

Quantity	Item
1	Test case containing all SHAP equipment
1	Backboard mounted in case with lock & key, door handle and zip
1	SHAP form-board
1	Foam insert containing all objects
1	Timer unit
6	Lightweight abstract objects
6	Heavyweight abstract objects
1	Lock and key mounted on backboard
1	Zip mounted on backboard
4	Coins (2 x 1p and 2 x 2p)
1	Button board with 4 buttons attached
1	Plasticine block
1	Knife
1	Note card
1	Glass jar with lid
1	Glass jug
1	Cardboard juice carton
1	Empty tin with plastic lid
1	Door handle mounted on backboard
1	Metal arrow unit
1	Screwdriver
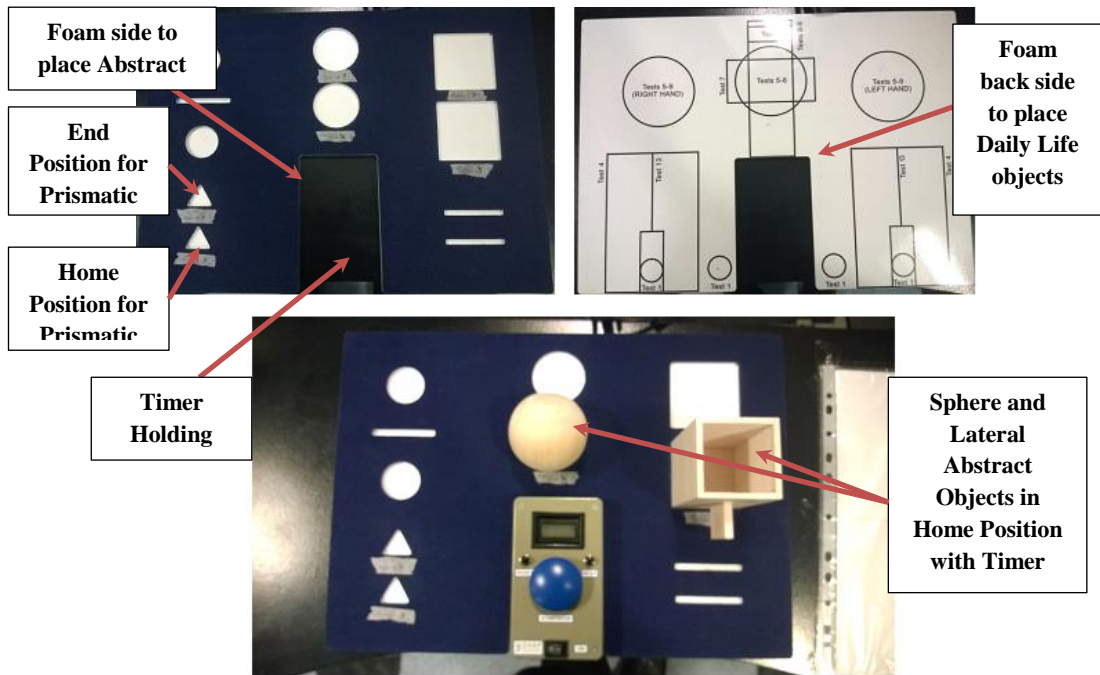
Figure 4-6 SHAP foam plate which is used to place the classification objects (the top figures shows the two sides of the plate).

The two types of object in the toolbox are abstract and activities of daily living (ADL) tasks.

a. SHAP Abstract Objects

This consists of a set of 12 different objects not found in daily life activities (Figure 4-7). The inclusion of the abstract objects aims at removing the prejudicial psychological effects that exist in daily tasks. These lead to intermediate grip patterns or adverse evaluation effects by the subject.

In this part of the test, subjects with impaired hand function are forced to make compensations in their fingers' movements in order to carry the abstract objects with abnormal shapes. This will vary the movement from the natural patterns found in ADL tasks. The abstract objects are comprised of non-compliant dense materials and marginally compliant low-density materials for creating variation in the weight and yield in hand movement.

These tasks are designed to assess grip patterns, as well as the strength and compliance of the grip involved in performing the task.
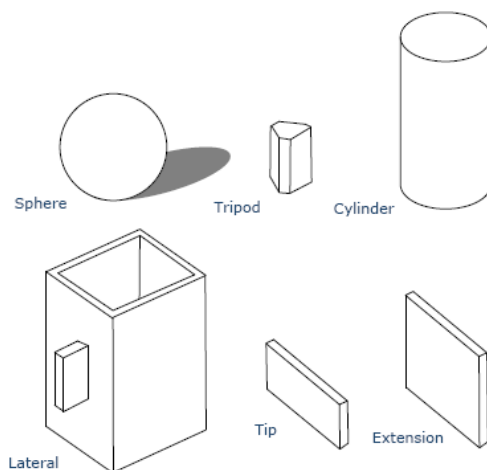
Figure 4-7 List of SHAP Abstract Objects: Sphere, Tripod, Cylinder, Cup (Lateral), Plates (Tip, Extension). Top row labels describe some of the objects, bottom row labels describe some of the task related to the object © SHAP Business Enterprise – the University of Southampton, with permission.

b.   SHAP ADL Objects

This consists of 12 daily living tasks (Figure 4-8), selected from the most commonly occurring daily activities (Sollerman and Ejeskar, 1995). They don't require subjective assessment or large variability of timing and are all unilateral.
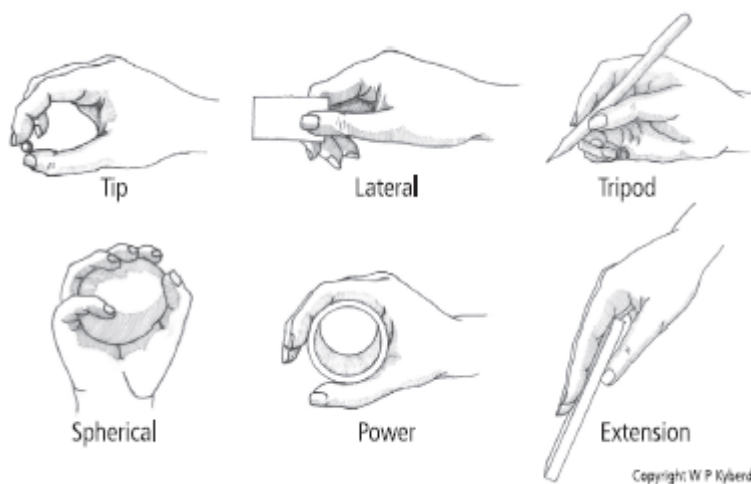
Figure 4-8 List of SHAP grip classifications postures: Tip, Lateral, Tripod, Spherical, Power and Extension. © SHAP Business Enterprise-University of Southampton, with permission.

The percentages of the required grips in the ADL tasks are: 10% spherical, 10% tripod, 25% power, 20% lateral, 20% tip and 10% extension (Light et al., 2002). Table 4-2 lists the selected ADL tasks associated with the grip classification.

Table 4-2 SHAP daily living tasks (ADL) addressing the human hand natural grip classifications

No.	Task	Natural Grip Classification
1	Pick up coins	Tip
2	Undo buttons	Tip/tripod
3	Simulate food cutting	Tripod/power
4	Simulate page turning	Extension
5	Remove jar lid	Spherical
6	Pour water from jug	Lateral
7	Pour water from carton	Spherical
8	Move empty tin	Power
9	Move full jar	Power

4.1.2.1. SHAP Outcome Measure

The outcome measure, score or Index of Functionality (Light et al., 2002), is calculated and correlated with the normal hand function outcome. This is important for comparing hand performance throughout the treatment and rehabilitation and between different groups.

C. M. Light et al. have created a normative dataset on a controlled group of 24 subjects with healthy hand functions. The selection criteria used applied to this are: the subjects' ages range from 18 to 50 years old and they do not have any adverse hand trauma, neurologic conditions, or disability of the upper limb.

The SHAP (Light et al., 1999) classification method is selected for this project based on the following:

- SHAP test can be used in conjunction with other tools such as CyberGlove®.
- Reliability in measuring the hand function where an ANOVA test on the controlled group has revealed an F-value of 0.39 and P value of 0.68 (Light et al., 2002).
- The tasks in SHAP are designed to address the prehensile ability in fine movement, with a limited concentration on the gross movement, due to the minimal arm transport requirement. This corresponds with the data glove measurement, as it is specifically limited to the dexterous range of motion.

- The scoring method not only assesses the level of performance throughout rehabilitation, but it also returns the level of function in respect to the benchmark (from a pre-established normative dataset). This satisfies the project objectives in providing dynamic and static assessment during the rehabilitation process.
- Index of Functionality (IoF) indices can be calculated for the overall hand functions or specific prehensile pattern to illustrate in closer detail the level of function for each task.
- SHAP outcome measurement is a standardised and clinically validated method and has been used in various research studies focusing on upper limb rehabilitation.

4.1.2.2. SHAP in the Project Approach

4.1.2.2.1. Specifying the Three Fingers for analysis

To reduce the complexity of hand classification, this study focuses on three fingers: index, middle, and thumb.

The thumb is the most versatile and important finger in the hand. Its opposable direction with the other fingers and its wide range of motion, equip the hand with the ability for precision and appropriate force in manipulating objects and using tools effectively for tasks (kitchen tools, construction, mechanical, etc.).

At first glance, it may appear that the other four fingers of the hand are all equal in function and that the second most important finger for hand involvement, after the thumb, is the index finger. However, this is not accurate as the little finger (also known as the pinkie) is more significant for several reasons: 1- it is essential to the grip as it can approach the thumb to a higher degree than any other finger, 2- it has an identical group of slimmer and finer muscles that perform similar functions to those dedicated to the thumb, 3- the little finger approaches the thumb effectively to give the thumb more precision and strengthen the grip action, and 4- it is the most mobile finger after the thumb.

The above concept is based on the consideration of which fingers would be the most significant to exclude from overall hand functions.

However, this project considers the fingers that are used most in daily life activities, where the patients rely heavily on them to perform any day-to-day task. As mentioned in the SHAP definition, the patients have natural prehensile pattern skills. They possess pre-learned skills for performing ADL tasks and their recovery makes hand rehabilitation easier,

faster and more efficient for restoring the lost functions.

It is essential to note that the right-hand side is selected for studies in this project due to the materials design, and its prevalence among the subjects.

4.1.2.3. Classifications

To reduce the dimensionality of the fingers' involvement in different tasks and to specifically address the three selected fingers, four classification methods were selected from the SHAP procedures: Spherical, Lateral, Point and Tripod (Figure 4-9)
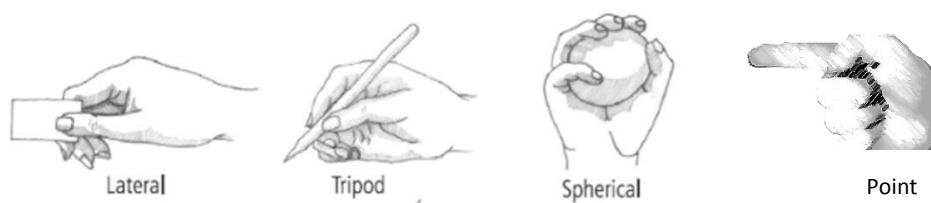
Figure 4-9 List of classification postures selected for assessing the index, middle, and thumb performance (Lateral, Tripod, Spherical and Point); This figure is based on © SHAP Business Enterprise – University of Southampton, with permission. (The point figure is included by the author).

Before defining the fingers' involvement in each task, it is important to differentiate between the two terms used in task performance – "depending on the finger" and "involving the finger". The former implies that the task requires the movement or formation of the finger in the performance. The latter indicates that the task doesn't require a specific finger movement but, because of the finger joints' dependencies and mechanism in some movements, it involves the adjacent finger in performing the task. In other words, performing the task doesn't depend on the finger's movement, but rather, it involves it in the full hand function. To further illustrate this, for performing the lateral task, the hand depends on the index and thumb fingers. Correspondingly, it involves the extension of the middle finger as the middle-MCP extension is closely related to the index-MCP extension.

Tripod and spherical tasks rely on the three fingers, index, middle, and thumb, while, in point tasks, the hand depends on the index and middle fingers.

4.1.3. Virtual Hand Simulator

As discussed in the Virtual Simulation section 2.3, Background Chapter 2, different robotic simulations can be employed. However, the GraspIt! (Andrew and Matei, 2015) simulator most closely matches the project aims, as it incorporates the following features:

- GraspIt! provides a basic communication interface library to interact with CyberGlove®.
- It includes a robot library with several hand robot models, including a Puma arm (Billingsley, 2006).
- It has the ability to import new obstacle models. This is specifically required for adding the newly developed classification models to interact with the virtual hand during the hand assessment process.
- It supports a dynamic engine with basic collision detection methods.
- It is endorsed under the GNU General Public License (Gnu, 2015).
- It has a detailed online manual of the system structure for developers.

However, the GraspIt! application still requires a number of developments in order to utilise it in the project for assessing hand performance: 1- data communication and calibration improvement, 2- collision detection improvement, 3- human hand and objects modelling, 4- classification procedures and experimental setup implementation.

4.1.3.1. Data communication

The virtual simulation application is required for communication with the CyberGlove®, via a serial port data connection, in order to manipulate the virtual hand with the subject's hand wearing the data glove. It needs to synchronise with the CED Micro 1401 EMG recording device, using the parallel port, in order to instantaneously coordinate the event occurrences with the instructions and EMG data recording.

For the requirements above, the development is implemented in the hardware connection layer of the application. This is where the appropriate serial, parallel communication protocols and handshaking phases are included. The CyberGlove® data communication procedures and CED Micro 1401 data handshaking protocol can be found in the EMG section 4.1.4.

4.1.3.2. Calibration

The calibration between the virtual model and data glove is an essential phase to ensure accuracy in data acquisition. This will result in reliability and robustness for any analysis performed and conclusions drawn.

The GraspIt! application has a basic calibration method of calculating the linear relations between the raw glove sensors and the virtual hand DoF. This method does not include independent/dependent sensor variations and joint relations. The calibration configuration is impractical as it requires manual generation and configuration to the intercepts and offsets parameters of the linear equation. The saved configuration file also needs to be loaded at the beginning of each launch.

The CyberGlove® virtual application calibration method is cumbersome and depends on manual adjustment for the variables in the linear equation and the DoF correspondence value. The defined poses for mapping the calibration are also limited and do not cover the full extent for the joints' variability. Hence, a more advanced method of calibration is applied in GraspIt! to overcome the unreliability and complexity of the existing process. This chapter focuses on the implementation of the calibration method and procedure with the GraspIt! application. The algorithm is covered in detail in the Calibration Chapter 5.

At the beginning of the experiment, the calibration procedures are performed by the subject by using a group of predefined gestures (Calibration Chapter 5, section 5.3). These are saved into .xml format and used in the experiment for the same subject and as a reference for the data analysis.

4.1.3.3. Collision Detection

The collision detection mechanism implemented in GraspIt! (Andrew and Matei, 2015) uses a basic approach. It creates bounding boxes around each object and continuously measures the distances between both bodies. There is a notable difference in the application between collision and contact. Collision refers to when interpenetrations occur between two objects, and contact refers to the closest point having the shortest distance between both bodies, that is bigger than or equal to the threshold limit.

In the case of a collision, the application works to solve it by interpolating the DoF angle values between the initial joint position and the final joint position until the bodies'

distance reaches a level less than the contact threshold. If the initial position is not collision free it will return to 0.

Although the GraspIt! application has a multi-threading feature for collision detection to speed up the collision detection process, it still requires various developments as it is very fragile, especially in dynamic simulation.

The method also returns multiple contact points but does not support multiple collision detection i.e. if the system detects a first collision with the body then it stops all the joints' movement until this particular collision is resolved. In the real world, it is assumed that other joints are free to move and are independent from the collision effects of unrelated joints.

Therefore, the necessity to implement a faster collision detection algorithm arises, to avoid delay between the real world task performance and visual display. This would also include multiple collision detections to avoid jams in the virtual hand joints when interacting with other objects.

In the Background chapter, various collision detection approaches are explored and correlated with the project requirements.

The developments also included readjusting the initial method of handling multiple collisions to process each one separately in the interpolation function. This was achieved by creating a list of all occurring collisions with the corresponding joints. This created a parallel resolutions process for all occurring collisions.

4.1.3.4. Virtual Hand Model and Kinematic

In contrast to robotic arms, the human hand requires acute designs and joint connections in order to represent realism when interacting with the virtual simulation. In response to this, a new hand model is designed and implemented by applying the existing robotic hand kinematic chains to other robotic models in GraspIt!

The kinematic interactions and modelling are also adjusted accordingly with the project aims. Further discussion on the depth of the human hand kinematic is found in the Background Chapter 2.

The hand model that has been designed, Figure 4-10, is based on the DLR robotic hand. Its

total size is approximately that of a medium-sized male hand, and the fingers have relative sizes corresponding to real hand variations. Each finger consists of three joints: one between the proximal and medial links, one between the medial and distal links, and one at the base. It has 20 degrees of freedom, five universal joints (ten DoF) on the metacarpal joints (linking the fingers to the palm), and ten revolute joints (ten DoF) for the proximal and distal. For further information on the virtual hand model and configurations structure code please see Appendix III and Appendix IV.
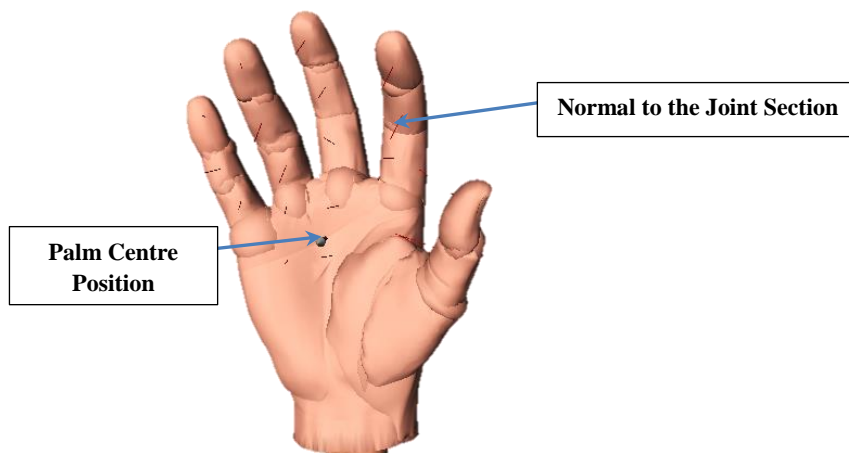
Figure 4-10 Human hand model 20 DoF. Red Lines represent the Normals for each finger section. Joints are designed to adapt with the fingers orientation without deformation.
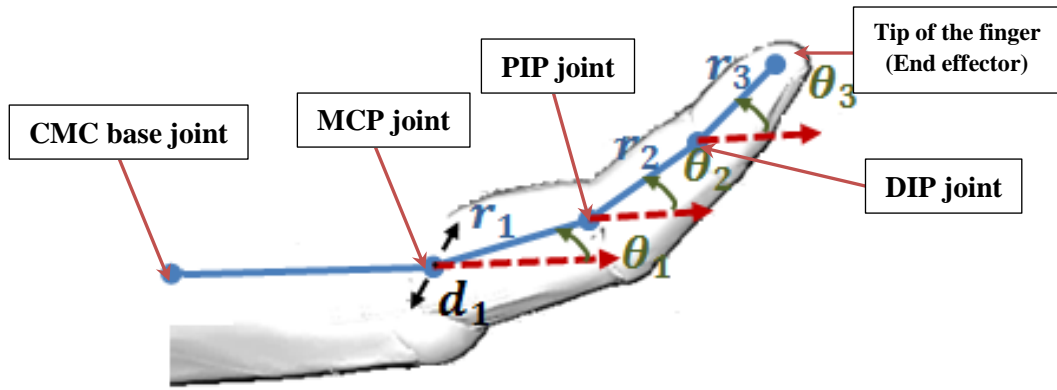
Figure 4-11 D-H parameters representation of the hand finger kinematic; where $\theta_1, \theta_2, \theta_3$ are the angles of the finger joints; $r_1, r_2, . r_3$ are the length of the common normal; and d_1 is the offset along the previous joint.

In kinematics, the Denavit-Hartenberg (D-H) parameters are a commonly used convention for selecting reference frames to the links in the kinematic chain, Abdullah et al., (2013), Figure 4-11. The D-H transformation Ť used for locating the end link of the chain is presented in the cross-product equation (4-1)

$$[\check{T}] = [\check{Z}_1][\check{R}_1] ... \check{Z}_{n-1}\check{R}_{n-1}\check{Z}_n \tag{4-1}$$

Where i the joint is number from 1 to n; $\check{Z}_i$ is the first part transformation matrix, combining rotation angle θ and translation d along z axis, presented in equation (4-2).

$$[\check{Z}_i] = \begin{bmatrix} cos\theta_i & -sin\theta_i & 0 & 0 \\ sin\theta_i & cos\theta_i & 0 & 0 \\ 0 & 0 & 1 & d_i \\ 0 & 0 & 0 & 1 \end{bmatrix} \tag{4-2}$$

$\check{R}_i$ is the second part transformation matrix, combining rotation angle $\acute{\alpha}$ and translation r along x axis, presented in (4-3).

$$[\check{R}_i] = \begin{bmatrix} 1 & 0 & 0 & r_{i,i+1} \\ 0 & cos\ \acute{\alpha}_{i,i+1} & -sin\ \acute{\alpha}_{i,i+1} & 0 \\ 0 & sin\ \acute{\alpha}_{i,i+1} & cos\ \acute{\alpha}_{i,i+1} & 0 \\ 0 & 0 & 0 & 1 \end{bmatrix} \qquad \text{(4-3)}$$

The four parameters of D-H in the transformation matrix $\check{T}$, are derived from the common normal between both joints' z axes (z axis is the rotational axis for the joint):

d : is the offset distance along the previous joint z axis to the common normal with the new joint z axis

θ : is the angle about the previous joint z axis to align its x axis with the new origin.

r : is the length of the common normal.

$\acute{\alpha}$: is the angle about common normal, from previous z axis to new z axis.

In the case of finger flexion-extension joints, d is the variable between 0 and the maximum flexion angle; θ is 0 as the x axes are parallel; r is fixed with the finger length between joints; and α is 0 as the z axes are parallel. These parameters are entered to the virtual simulation with the hand robot configuration file. More details are available in the Background Chapter, Kinematic Hand Model section 2.2.

In order to manipulate the virtual hand position in the virtual world, the hand model is mounted on the end link of the Puma560 robotic arm. The Puma560 arm has three "universal" joints, with six DoF.

Linking the hand to the arm is similar to joints kinematics procedures. It involves parent-child chain link settings, in addition to a set of inverse kinematics routines used in the transformation matrix between the last joint of the arm (the wrist) and the base joint of the hand (palm).

The transformation matrix for the palm of the hand, corresponding to the Puma560 world, is T_{h1}. This is calculated using equation (4-4).

$$T_{h1} = T_{h0}.T_{j1} \qquad \text{(4-4)}$$

T_{j1} is the transformation matrix for the last joint of the Puma560 arm, in the final position. T_{h0} is the initial transformation matrix of the hand palm in reference to Puma560. This is defined in the below equation (4-5) .

$$T_{h0} = T_{w0}.T_{j0}^{-1} \tag{4-5}$$

T_{j0}^{-1} is the inverse of the initial transformation matrix for the last joint of Puma560. The T_{j0}^{-1} gives the transformation matrix required to transform the hand model from the scene world to the Puma560 world.

T_{w0} is the transformation matrix of the palm in reference to the scene world, at the initial position.

The role of T_{h0} is to convert all the palm 'transformation matrix' parameters to the new world, where the Puma560 is the reference point. This then makes it possible to transform to any desirable location using the T_{h1}.

The mounting of both models (Human Hand and Puma560) to each other uses the world configuration file, see Appendix III .The Puma560, parent robot in the chain, configuration is added in the first <robot> node robot and the Human Hand, child robot of the chain, configuration is then added in the following <robot> node.

Ultimately, the <connection> node, responsible for connecting both robots, includes three elements: 1- the index of the parent robot in the world, 2- the kinematic chain number on the Puma560 robot to attach the Human Hand, and 3- the initial transformation offset between the last link of Puma560 and the palm (base link) of the Human Hand. Figure 4-12 shows the Human Hand model connected with the arm base, resembling the human arm's manipulation of the hand with six DoF.
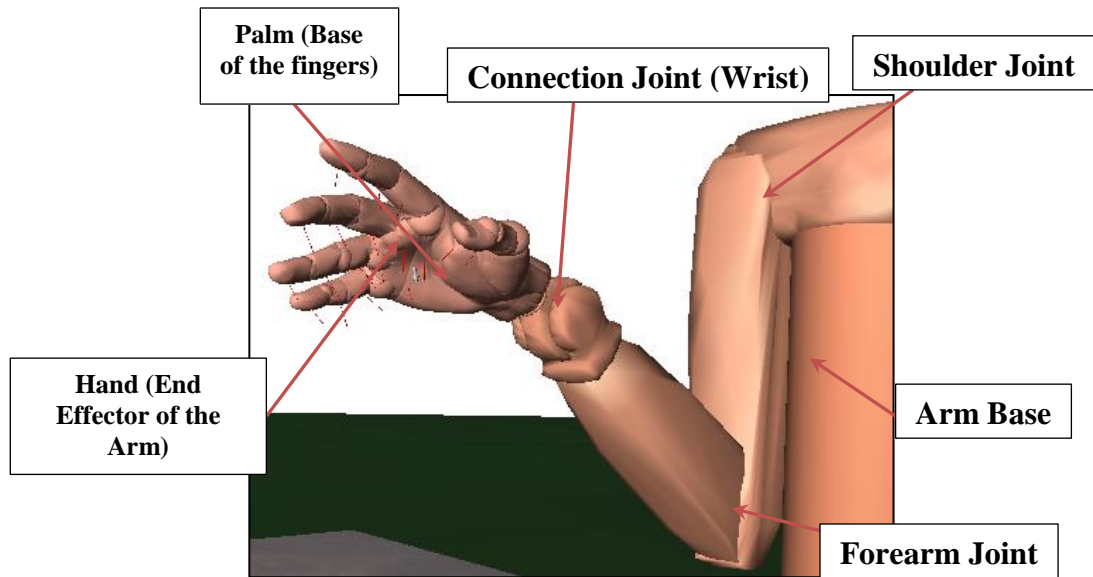
Figure 4-12 Graphical display of the developed Virtual Human Hand mounted at the distal of the Puma560 based arm robot. Hand transformation is calculated using inverse kinematic from the Arm base.

4.1.3.5. Virtual Environment Configurations

To replicate the real world experiment, the virtual scene needs to be configured in order to include tables, background and appropriate graspable objects, similar to SHAP's. GraspIt! (Andrew and Matei, 2015) includes three types of bodies: "Robots", as previously discussed; "Obstacle", a static object such as the floor, table, etc.; and "GraspableBody", a mobile that can be manipulated by the robot, such as balls, cups, etc.

Three specific virtual graspable objects (see Figure 4-13) are designed for the experiments, with similar shapes to those of the real graspable objects. The graspable virtual objects' size relativity to the virtual hand's finger sizes is equal to that of the real objects and real hand's finger sizes. This helps to maintain the grasping formation between both virtual and real worlds.
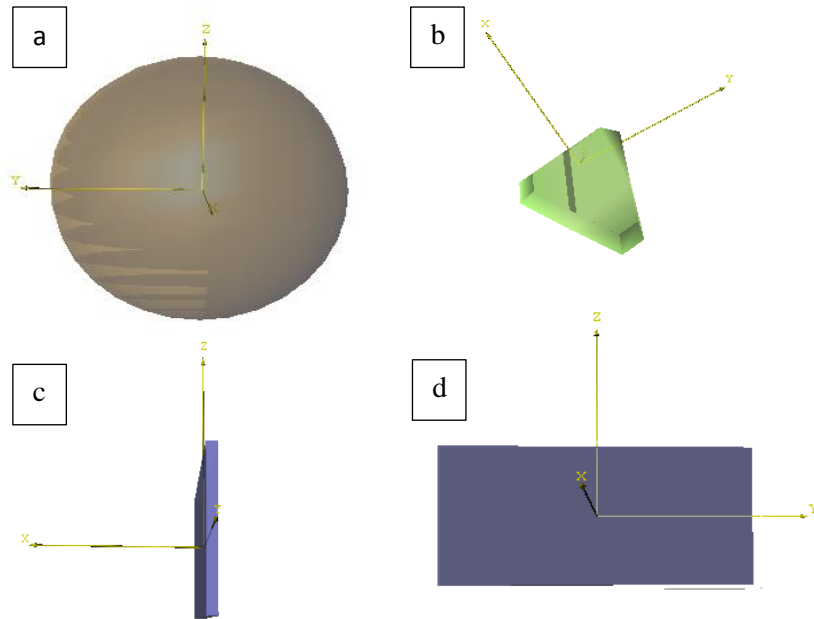
Figure 4-13 Virtual objects used in the hand assessment experiment – (a) ball: used for the spherical task, (b) triangular prism: used for the tripod task, (c) plate: used for the lateral task, and (d) plate: used for the point task.
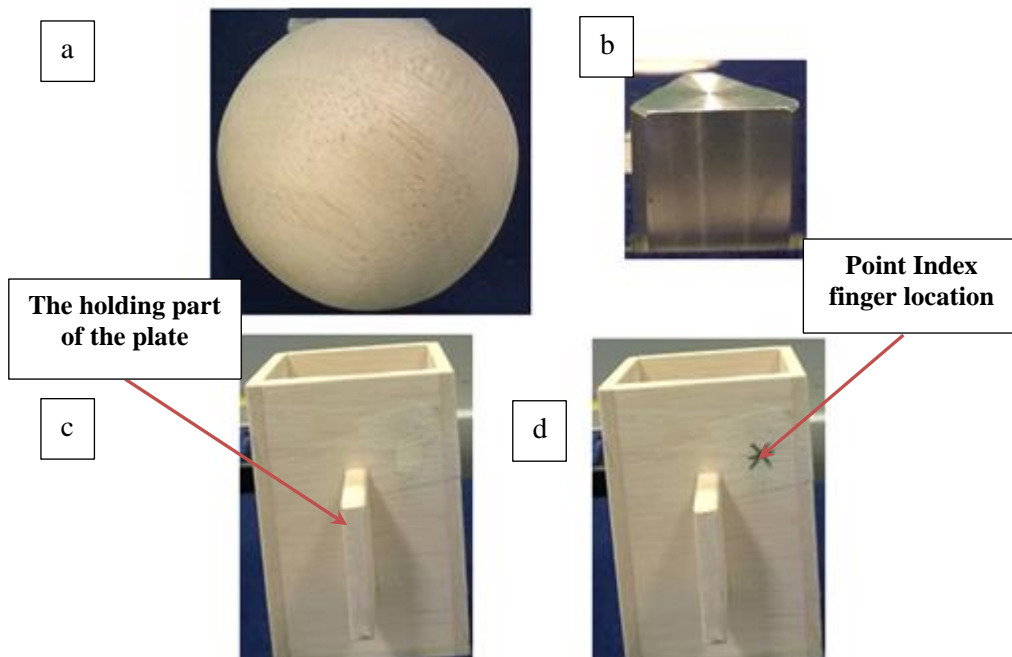
Figure 4-14 SHAP real objects used in the experiments– (a) ball for the spherical task, (b) triangular prism for the tripod task, (c) plate for the lateral task, and (d) plate for the point task (the asterisk shows the place to point to with the index finger).

The virtual reality setups, performed in association with every event during the experiment, are displayed in Table 4-3. This implementation ensures time consistency between the real and virtual tasks and the data analysis focuses on the prehensile pattern formation.

Table 4-3 Virtual reality setup procedures for each event during the experiment.

Event	Virtual Reality World Setup
Relax	The hand moves to the relax position. (Hand movement is performed by configuring the arm joints' (shoulder, elbow, wrist) DoF angle values to the specified positions)
Move Hand	The object that corresponds to the task performed (ball – spherical grasp, plate - lateral, plate - point, triangular prism – tripod, see Figure 1.1.2-5) moves to the position X on the table, close to the arm. The hand moves close enough to the object.
Get Ready	None
Grasp Object (Formation)	None
Hold Hand	None
Move Object and Release.	Object and virtual hand move to position Y. The object then moves to the initial position. Hand returns to the relax position.

The following Figure 4-15 shows the virtual hand position in accordance with each task in the VR.
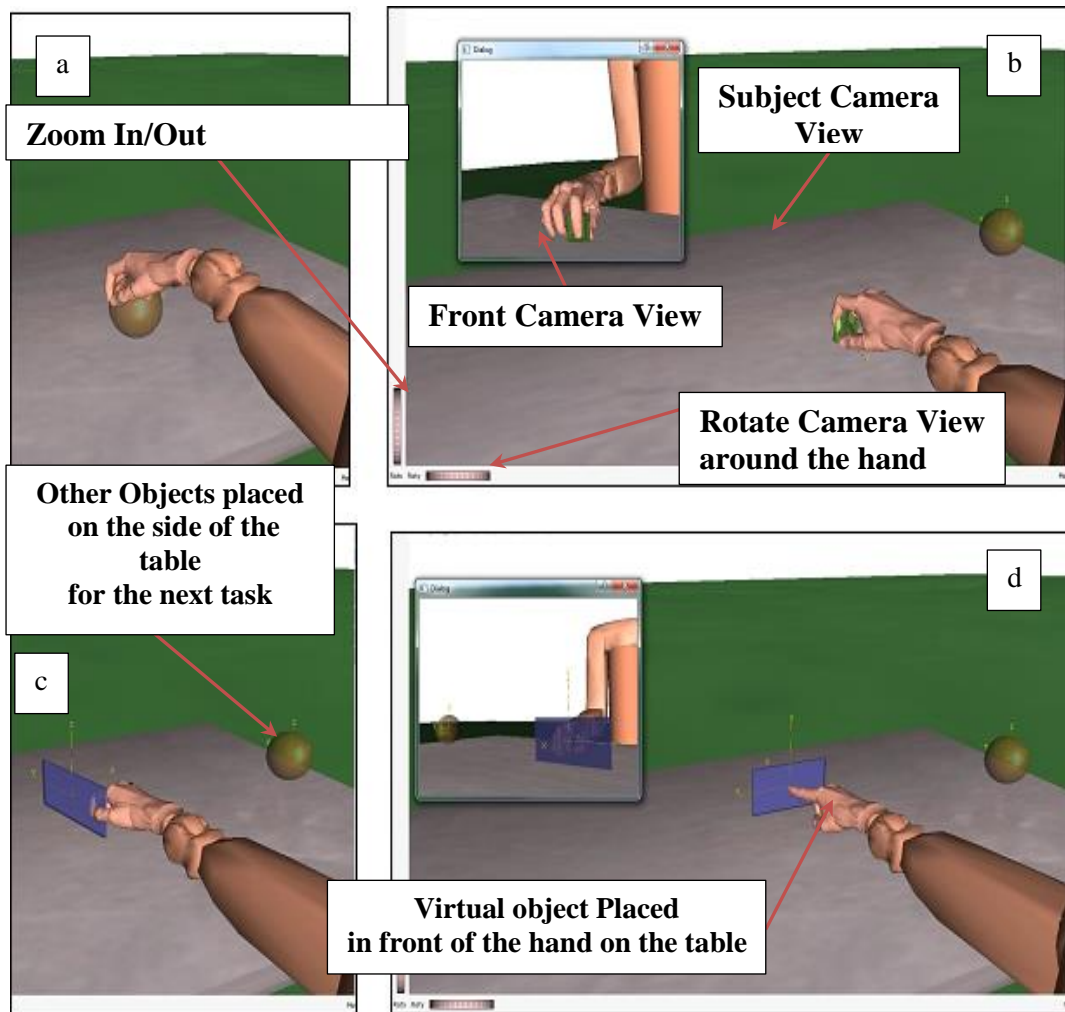
Figure 4-15 Display of the virtual hand positions for each task in the experiment – (a) spherical task, (b) tripod task, (c) lateral task, (d) point task. Objects are moved towards the virtual hand to perform the task. In the (b) and (d) figures, the front camera is added to include front perspective view of the graphical model and assist in the subject's interaction with the VR.

In the VR experiments, the subject is presented with two cameras. The first camera projects the back view of the scene, which is the same angle as that when viewing the hand while performing real tasks. The second camera projects the opposite view to show the fingers and objects from the front side (see Figure 4-16).
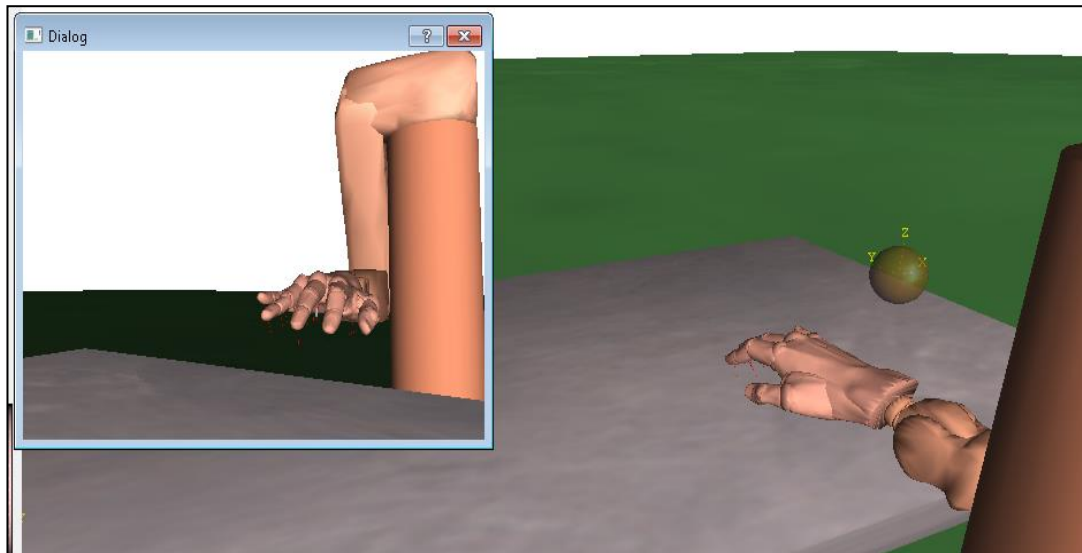
Figure 4-16 Display of the virtual world view during an experiment. The left camera view is the opposite/front view of the hand, and the right camera view is the back/subject view of the hand and VR objects. Introducing both views help the subject to visually assess the interaction level with the VR environment.

The main camera, displaying the subject view, facilitates immersive control of the virtual hand and associates this control as if it were the subject's own hand. The front camera is added to provide a closer view of the fingers' movements to provide more accuracy while grasping the corresponding object.

(Demo method of the VR hand simulator with the experiment setup is available online on https://1drv.ms/f/s!Ag1FSC4ql9qBgViYbJ3kMKJzMbiS)

4.1.4. Electromyography Measurement Device

Electromyography, (EMG, 2015), is the measurement of the muscles' activities, described as muscle response to nervous stimulation. The measurement is performed by detecting the electrical potential generated by muscle cells during contraction.

The surface electrodes are commonly used for reading EMG. These are different from the needle electrodes as they are non-invasive and target readings for the larger muscle contractions. Needle electrodes are used specifically for localised potentials in the muscle. The surface electrode consists of metal and is injected with conductive/adhesive gel. Any dead, dry skin should be removed and the skin should be shaved to provide high conductivity and increase the impedance of the muscles' electrical signals.

Electrode female connector to the amplifier

Amplifier male connector

Electrode's end placed on the skin.
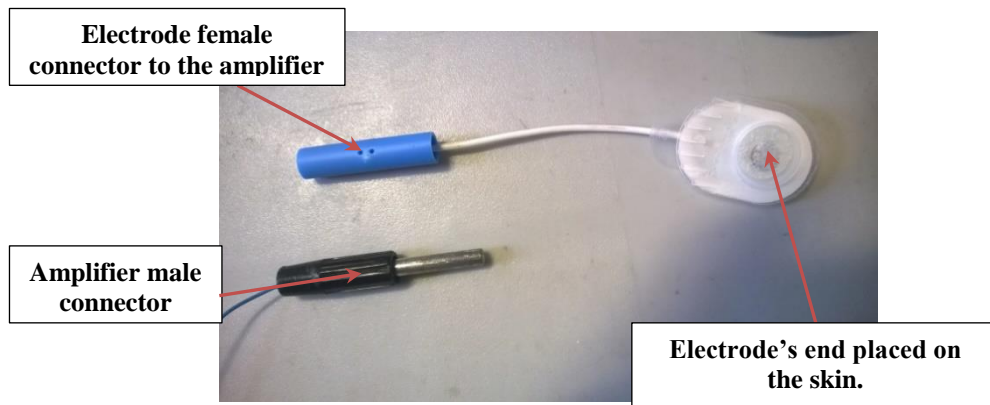
Figure 4-17 EMG Ambu r blue sensor surface electrodes, N-10 A-25; The sensor is placed on the subject's arm and connected back to the amplifier of the EMG.

The EMG (EMG, 2015) surface electrodes use a differential signal mechanism, with three electrodes placed on the hand: two binomial electrodes at both sides of the muscle and a ground electrode on a non-muscled area. In this project, the pisiform wrist bone of the right hand is selected as the location of the ground electrode.

The EMG electrodes are connected with an NL824 amplifier (see Figure 4-18) that provides high impedance differential inputs. The amplifier is used in conjunction with a Neurolog NL820 isolator, connected in turn with four NL125 filters for each channel (see Figure 4-19). This setting allows for individual configuration of each channel: low-cut, high-cut and notch (in/out). The filters are set to frequency range 50Hz-500Hz to match the EMG signal's bandwidth. (See Data Processing section 4.3 for further information)
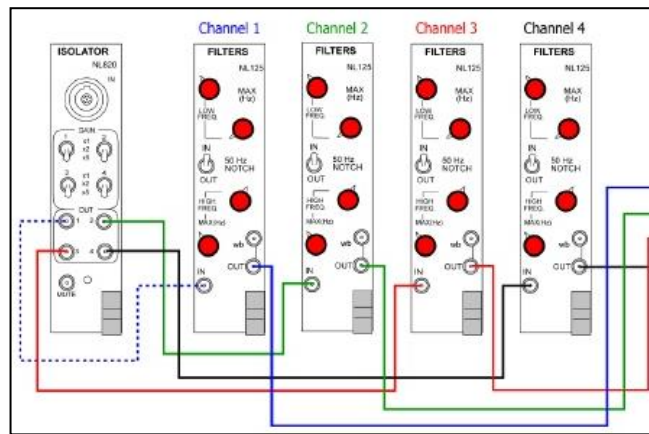
Figure 4-18 Schema of the Neurolog connecting the isolator to the four filters for each channel (the four lines' outputs go to the amplifier).
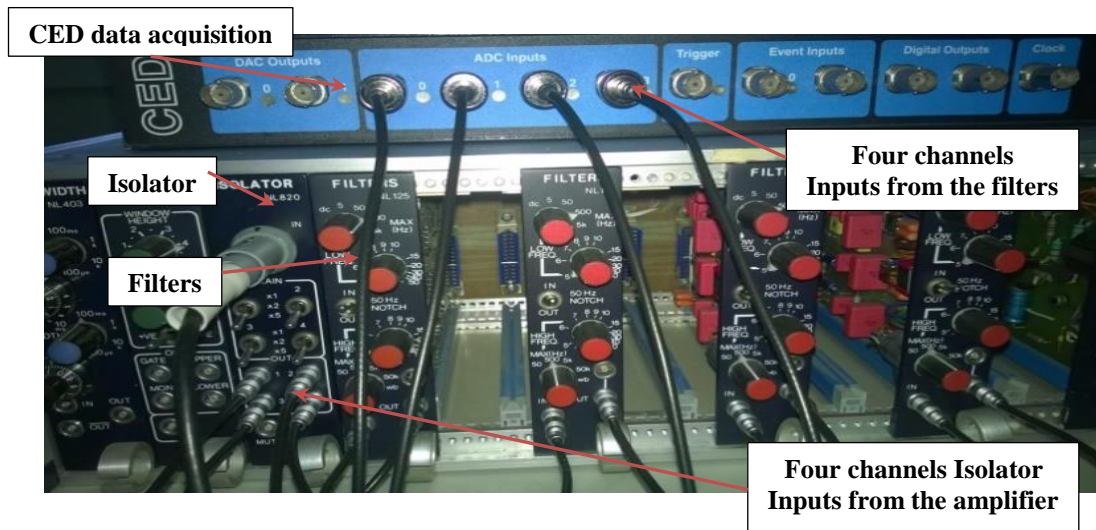
Figure 4-19 Digitimer Neurolog system connecting the CED Micro 1401 (on top) data acquisition unit. This part involves isolators and filters for the transferred signal from each channel.

Data is then transferred to a data acquisition unit, CED Micro 1401 ((CED, 2015)), before being exported to a computer, via USB 2.0 connector. The data is recorded in the machine with Spike 2 software.

Spike 2 (see (CED, 2015)) is a data acquisition software application. It has various features, including data analysis and preprocessing. It provides a user-friendly interface to interact with the data readings, and multiple options to organise the data, navigate through

channels numerous times, detect specific features inside the signal, apply filtering and other signal processing methods, and export the data with channel markers in multiple formats for use in a more powerful analysis application, such as Matlab®.

To ensure that the EMG reading is synchronized with the event instructions in the experiment, a script code is implemented in the virtual application to label the data channels in Spike2 (see Digital marker connections in (Spike2) for information about the parallel port handshaking). The communication is established via a 25-pin parallel port, connected from the printer port of the PC to the CED Micro 1401's digital input (shown in Figure 4-20). The code uses handshake protocol to establish the connection then passes commands to the CED following each event. The data output is labelled before being sent as full package to the PC, via USB.
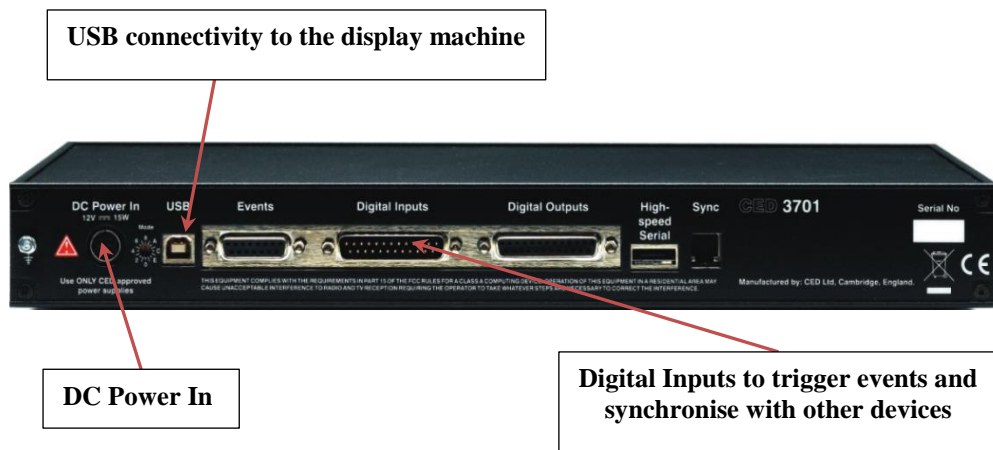
Figure 4-20 Rear view of CED Micro 1401, showing all the peripherals and digital I/O ports.

The Dome® (Figure 4-21) is a 3D immersive visual display. It has a 180° horizontal x 135° vertical field of view. The visual environment is displayed on the dome shaped screen, via a projector connected to a PC. Due to its design, it has advanced immersion levels in comparison to a normal screen, as it surrounds the viewer and delivers high-resolution virtual reality without a headset.
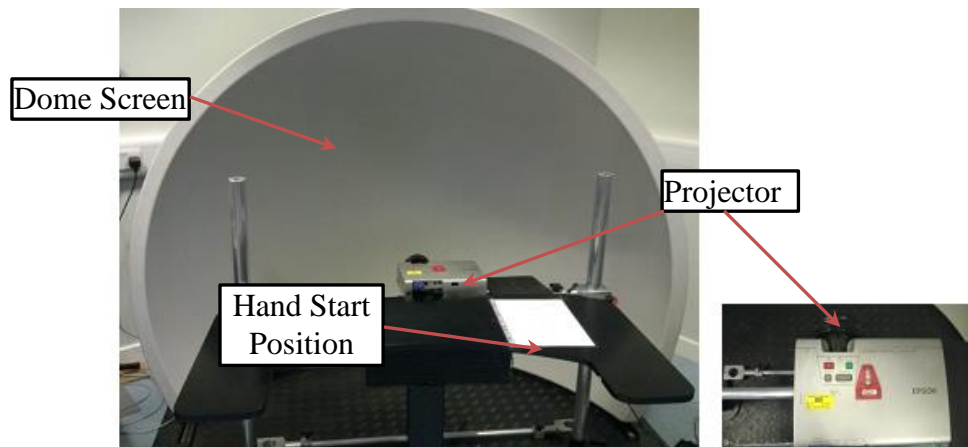
Figure 4-21 Dome® projector for graphical display; it has the curvature form to increase the immersion level when interacting with virtual environment. The projector height and dome distance can be adjusted as necessary with the display.

4.2. Experimental Protocol

The project aim is to produce an efficient outcome measurement for hand performance. The development of a hand outcome measurement method consists of two phases. The first is to validate the reliability and efficiency of the system on healthy subjects, by generating a normative data set to differentiate between the dynamic variation of disabled and healthy hand functions. Secondly, studies must be conducted on patients in order to further validate the method's reliability and efficiency.

Furthermore, the calculated hand progress evaluation results are highly dependent on the baseline analysis. This requires conducting experiments on healthy subjects in order to generate the normative data set and register the level of constraints on healthy hands. Then, the assessment of the hand movement performance for the subjects with dysfunctional hand will be performed by measuring the variation between hand performance (trajectory smoothness, velocity and time) and the normative data set. The measurements data for each subject are stored in individual profiles. This is used later to generate the analytical reports for the hand progress, and outline the improvement and efficiency of the rehabilitation sessions.

Therefore, in the below section, the experiments procedures for validating the proposed methods and generating the normative dataset are described.

4.2.1. Subject Inclusion Criteria

Experiments were conducted on a controlled group of ten subjects who met with the following criteria – male; aged between 23 and 46 years old; both hand and leg are right side dominant; healthy with no neurological disorders; no medical issues; no history of epilepsy; have not received any operations on the upper limb on the right side; have no skin injuries on the right hand and forearm; are not allergic to EMG electrodes; have healthy visual perception with no motion sickness in using VR; right hand is close to medium male hand size and fits appropriately with the CyberGlove® data glove; and are not suffering from any hearing issues that would prevent them from listening to and following the instructions.

The experiment generates a large dataset as it includes multiple trials and sessions for 3 to 4 hours continuously recording data on the three fingers; hence, recording data for 10 subjects was found evident to generate the necessary normative dataset. An advertisement

email was sent in the Biomedical department to recruit the subjects in addition to the neuroscience lab students. The email described the experiment involved and the study criteria. The ethics approval for this study was obtained from the University of Strathclyde's Biomedical Engineering department. Informed consent was obtained prior to the experiment, Appendix VII.

4.2.2. Experiment Process

The subject sits in front of the Dome® station in order to interact with the virtual objects projected on the screen and real objects placed on the table.

The SHAP's foam-board (Figure 4-6) is placed approximately 8cm from the front edge (Light et al., 1999). The subject starts with resting arms and elbows at a 90° angle. The subject is instructed with audio cues to follow each event in the task (see Figure 4-22). The data is recorded continuously throughout, by both the EMG electrodes using Spike and the data glove sensors using the developed application.

The real objects are placed on the SHAP board, with the specified locations labelled as positions X (start position) and Y (end position). In the VR, the virtual hand is automatically moved to the start position, close to the task object. As such, the fingers' grasp movements are only involved in the VR tasks.

There are six sessions involved in the experiment and these include the defined hand classifications, spherical, lateral, point and tripod (previously described in section 4.1.2.2 for SHAP method). The first three sessions involve interaction with the real abstract objects selected from SHAP. The "Real Life" session acts as the benchmark session to relate the new approach with SHAP measurement. The "Real Life + Load" session serves to measure the effect of fatigue on the hand and simulates impairment on the hand movement by adding extra weight (0.5 kg) to the forearm. The "Real Life + Tremor" session is for simulating paresis and studying the sensitivities of the system to detect the level of variability in hand/fingers' movement. Subjects in this session are asked to feign hand tremor movements. The final three sessions are similar to the 'RL' sessions, but use virtual reality instead of real objects. Table 4-4 details the structure for each of the above mentioned sessions.

Table 4-4 Structured details of the experiment sessions.

Session	Evaluation	Description
"Real Life"	20x trials	Interacting with real objects
"Real Life + Load"	20x trials	Interacting with real objects. 0.5kg load is placed on the forearm next to the elbow joint in order to prevent major deviation on the force exertion in movement.
"Real Life + Tremor"	20x trials	Interacting with real objects. Subjects are instructed to simulate a tremor movement, with the following sentence. "Please perform the following procedures while pretending you have what you consider a tremor in the right hand. With your arm in position, please mimic this tremor".
"Virtual Reality"	20x trials	Interacting with virtual objects on the projected screen.
"Virtual Reality + Load"	20x trials	Interacting with virtual objects. 0.5kg load is placed on the forearm next to the elbow joint.
"Virtual Reality + Tremor"	20x trials	Interacting with virtual objects. Subjects simulate tremor movement while performing the tasks.
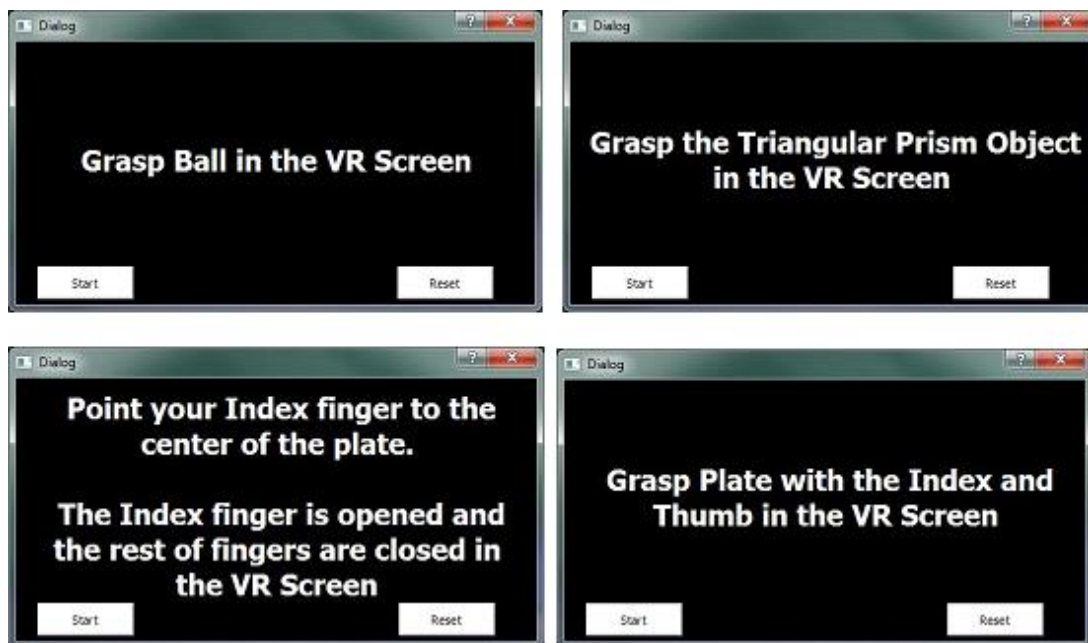
Figure 4-22 Four different audio-visual instructions presented during the experiment.

Each task is demonstrated at the beginning of each experiment, with the prehensile formation and hand movement that are relevant to the particular task's requirements. This ensures repeatability and consistency between the different trials and subjects.
For example, during the demonstration the subject is notified that the lateral task is

accepted only if the thumb's MCP, PIP, DIP are extended and the index's PIP is flexed.

The index finger's tip must not be opposite to the thumb's tip, in order to have the object contact on the index's PIP-DIP left side finger sagittal and the thumb tip finger frontal only.

Likewise, the tripod task is accepted only if the object is grasped where the three fingers' contact points, with the object, are the frontal side of each fingertip.

And the spherical task is accepted if the contact points, with the object, are the three fingers' full frontal side.

The point task is accepted if the index finger is fully extended and middle finger is fully flexed.

The tasks are randomly selected in each session to avoid any pattern developments in the fingers' formation. Such pattern development can distort the fingers' performance analysis and interpretation while performing repetitive tasks in the sessions.

Each trial takes 56 sec (4*14sec) to 72 sec (4*18sec), which is dependent on the time when the subject places the right hand back on the table in the same shape as it was at the start of the trial.

The hand's relax position is detected using the data glove reading. This is done by comparing the sensor values with the original sensor readings from the start of the trial. A +10 degree difference is permitted.

The addition of self-adaptability to the system addresses the difference between impaired and natural hand functions for completing a task.

It is important to note that the above protocol was reviewed and adjusted after performing preliminary studies on four subjects. The four subjects of the preliminary study were selected based on the same criteria as the ones used in experimental study. The four subjects conducted the full experiment, and the collected data were analysed including the subject's feedbacks. Hence, this preliminary study suggested a necessity to reduce the total time of the experiment (four hours) as it is very long and tiring for the subject. The literature review (Light et al., 2002) advised that a maximum number of 18 trials is required for assessment studies, therefore the number of trials is reduced from 30 to 20.

The preliminary studies also indicated that it is important to randomly change the order of the sessions in order to avoid development patterns affected by the preceding sessions, such as load and tremor. In addition, the subjects suggested altering the instructions display

from visual to audio to offer fewer distractions while performing the tasks (see Discussion Chapter 7).

In light of these suggestions, the final estimated total experiment time, including both the initial experiment time plus the setup time is:

Initial Experiment Time = Time of Single Trial * Number of Trials * Number of Tasks * Number of Sessions = (2+1+1+4+4+ (~6)) (sec)*20 *4* 6= ~8640 seconds = ~2.4 hours.

The setup time for the experiment – placing the materials and demonstrating each trial for the subject – takes approximately half an hour. This increases the total estimated experiment time to approximately three hours.

For further explanation of the hardware and software setup for the system and the experiment process used in the multiple sessions see Appendix I.

Table 4-5 Instructions cue for each task of the experiment. The objects used for the tasks are ball for spherical, cup for lateral, triangular prism for tripod, and plate for point.

Task ID	Task	Message Text on Screen	Time	Recording	Description
i	Relax	"Relax hand in start position on the table"	(1+1)s	EMG + data glove	Start position. Record data glove data to detect the stop position. Time of 1 second added if previous trial starts before.
ii	Move Hand	"Move the hand close to the object without moving the fingers"	1s	EMG + data glove	Used for timing the start of the formation and ensuring consistency with the VR.
iii	Get Ready	"Get ready"	1s	EMG + data glove	Relax and get ready.
iv	Grasp Object (Formation)	"Grasp the ball" "Grasp the triangular prism" "Grasp the plate with the index and thumb fingers only" "Point at the plate"	4s	EMG + data glove	This event is used to compare joints' positions between the VR and real life formation.
v	Hold Hand	"Hold hand and fingers "	4s	EMG + data glove	Measure the stability of the hand while holding an object, without moving the hand.
vi	Move Object and Release.	"Move object to position Y. After finishing relax hand in start position"	Detect the time using data glove	EMG + data glove	Relax (if it is not the first run).

4.3. Data Processing

The data analysis process used in this project is illustrated in Figure 4-23:
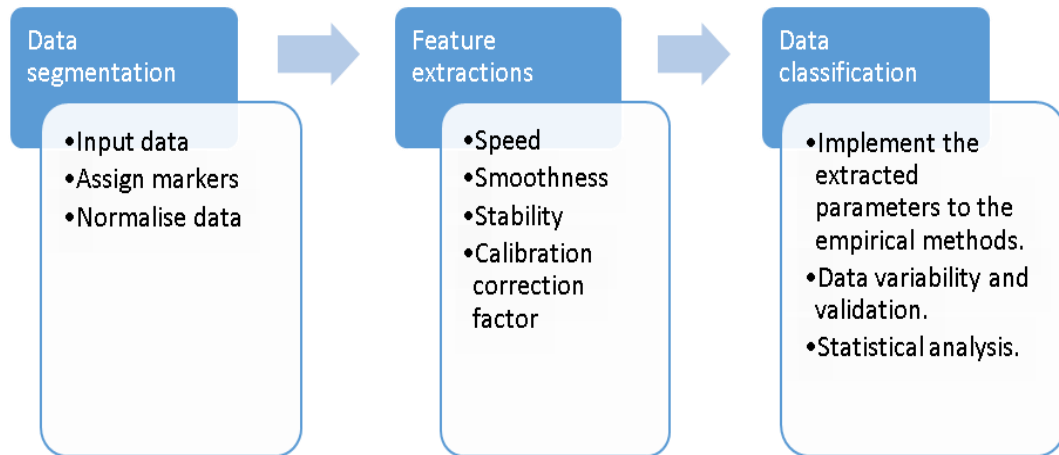
Figure 4-23 Data analysis procedures; The first step includes segmenting the data from the files and marking the multiple events, the second step extracts the features from the signal, which are used in the final step of data classification and statistical analysis to measure the performance.

The data segmentation phase includes, importing the recorded data, dividing it with each event task that is obtained from the marker's details, and normalising the data across the session. The data must be normalised as some trials finish earlier than the rest, due to the variation in returning the hand back to the start position or the noises from the sensors of data glove, and this introduces extra data.

The feature extractions phase obtains the relevant parameters that define the level of performance for each finger in the performed task. The Algorithms section, in the previous chapter, explains the procedures considered to calculate the equation parameters.

In the data classification phase, the derived parameters are applied into the assessment equations. This allows the study of the variability between sessions, users, and tasks, and deduction of the statistical analysis in order to prove the efficiency of the applied method.

4.3.1.1. Data Segmentation

As previously mentioned in the Experiment Process, the recorded data is assigned with markers to synchronise the recording devices and identify the events' occurrences. These markers are triggered by the audio instructions displayed in the experiment. The markers help in analysing the data and determining the event duration and time, as well as

performing intra and inter comparisons between the trials and subjects.

The device synchronisation is performed using a parallel port adapter cable, where the markers are sent in coordination with each event occurrence.

In addition, the data glove recording is transmitted separately through a parallel process, with a data-sampling rate of 50 samples per second. This configuration reduces the delays between each reading and interruption with the graphical and execution processes.

The experiment directory consists of six subdirectories in each session. In the subdirectory, the data is stored in two formats: "comma separated values" for the full DoF session data and markers, and "text" file for the Spike recorded data from the EMG signals, including the digital markers. The stored data is segmented with the markers' timing and task names.

Before starting the feature extraction process, the data is normalised across all the session trials of each subject. This is performed by the following:

1- The start and end of the task is extracted from DoF and sensor values by using mathematical equations to determine the level of threshold window that identifies the beginning and end of movements in the finger's displacement signal.

2- The finger's displacement signal is then interpolated from its time range to the experimental defined range (see Table 4-5 for all the defined timings for each task).

4.3.1.2. Feature Extraction

This section covers the mechanisms applied to extract the features from the data recorded with the data glove and EMG measurement devices.

4.3.1.2.1. Data Glove Feature Extraction Method

The calculation of hand performance outcome measurement focuses on analysing the variation of the three fingers – thumb, index and middle – involved in the four selected tasks – spherical, lateral, point, and tripod.

Calculation of the outcome measurement requires multiple pre-processing steps prior to applying the evaluation equation that has been designed. First, the displacement of the tip of each of the three fingers is calculated to reduce the complexity and return a general overview of the fingers' displacements.

The end effector, or tip of the finger's displacement Figure 4-11, is calculated with the forward kinematic method where:

$$X_{finger} = l_1 \cos\theta_1 + l_2 \cos(\theta_1 + \theta_2) + l_3 \cos(\theta_1 + \theta_2 + \theta_3) \qquad \textbf{(4-6)}$$

$$Y_{finger} = l_1 \sin\theta_1 + l_2 \sin(\theta_1 + \theta_2) + l_3 \sin(\theta_1 + \theta_2 + \theta_3) \qquad \textbf{(4-7)}$$

$$\emptyset_{finger} = \theta_1 + \theta_2 + \theta_3 \qquad \textbf{(4-8)}$$

Where in (4-6), (4-7), and (4-8) l_1, l_2, l_3 are the length between the joints of the finger (unit cm); and θ_1, θ_2, θ_3 are the angles of the three DoFs (unit radiant). Thumb DoFs (CMC (Thumb Abd sensor), MCP (Thumb MCP), IP (Thumb IP)), other fingers DoFs (MCP, PIP, DIP). The joints' angles are the DoF angle values of each joint, acquired from the recordings of the CyberGlove® sensors after calibration.

Equation (4-6) returns the horizontal displacement of the fingertip. Equation (4-7) returns the vertical displacement of the fingertip. Equation (4-8) returns the angle for the fingertip.

Figure 4-24 displays the grand average Y_{finger} for the fingers of each task in the "Real Life" sessions.
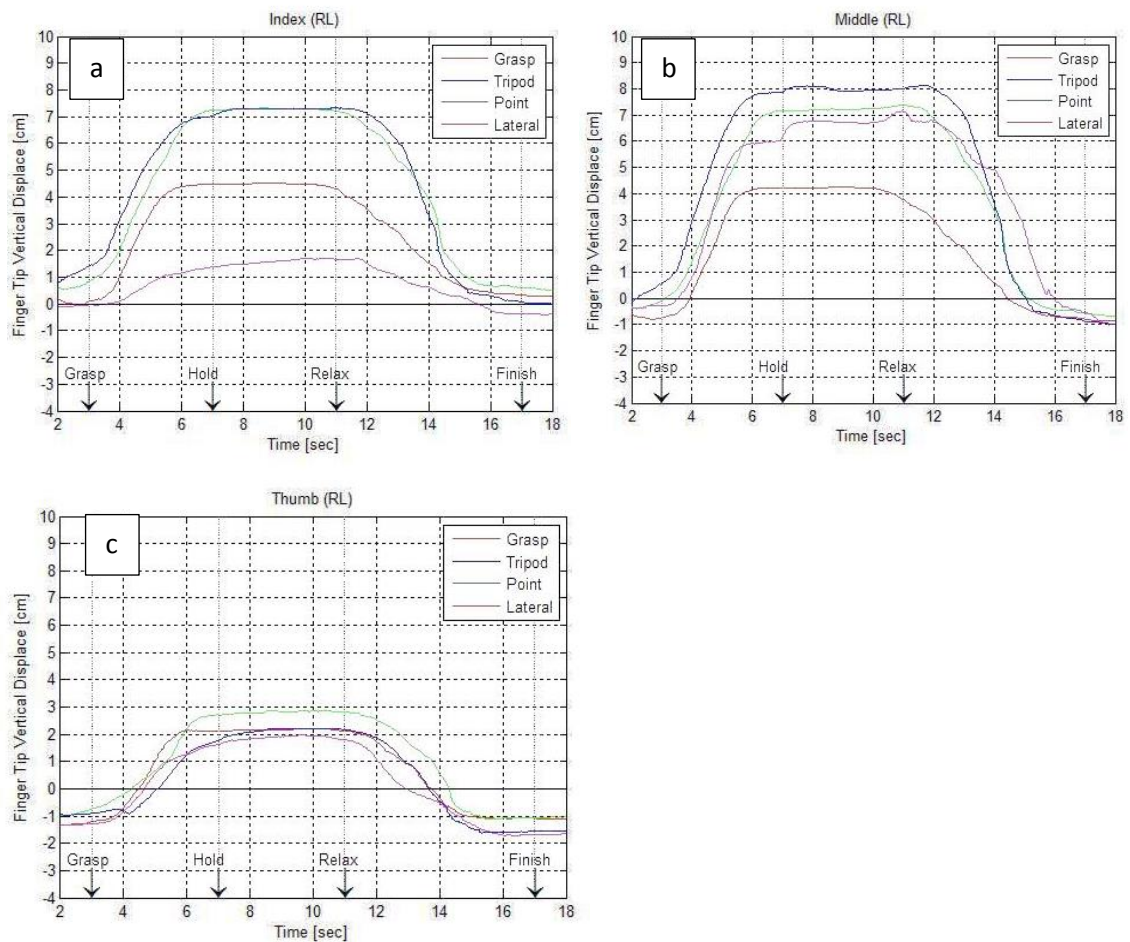
Figure 4-24 **Data graph for the tip of three fingers' displacement during the four different tasks: grasp, tripod, point and lateral. The unit of displacement is cm. (a) graph is the index finger displacement, (b) graph is the middle finger and (c) graph is thumb. The x axis of each graph represents the time in seconds of the task starting and completion times, which are distributed into four sections (grasp, hold, relax and finish).**

The fingertip vertical displacement provides significant information for assessing finger performance. By examining the variations of the finger displacement during the tasks (Figure 4-24), the essential components can be derived for assessing the fingers' movement: speed, stability and smoothness.

Different signal processing techniques are used in this phase, to calculate the above components, from the data displacement signals in Figure 4-24.

The data segmentation variables, which are used in the calculation methods, are defined on the finger's displacement signal data window, shown in Figure 4-25, as following: start of the grasp task (gStart); end of the grasp task (gEnd); start of the Hold task (hStart); end of the Hold task (hEnd); start of the relax task (rStart); end of the relax task (rEnd).

123

The slide-window technique (O'Haver, 2015) is a feasible tool that is used to determine these variables from the data signal.

The technique first extracts a small data vector (window) from the finger's displacement signal that has a defined duration time "ws". Then it calculates the slope of the data in this vector and compares it with the threshold.

If the slope value is bigger than the threshold of finger's displacement signal-start, it indicates that the start of 'grasp' event is detected. If the slope value is smaller than the threshold, then the window is slide across the finger's displacement signal by same time duration "ws", and then the process is repeated until the start of the event is detected. On the other side, to detect the end of the 'grasp' event similar steps are processed until the method finds the data window with slope value less than the end-threshold.

The start of the 'hold' event is detected by finding the first decrease in the slope of the sliding window vector, instead of using the pre-discussed threshold comparison. However, the end of the 'hold' event is detected using the threshold comparison.
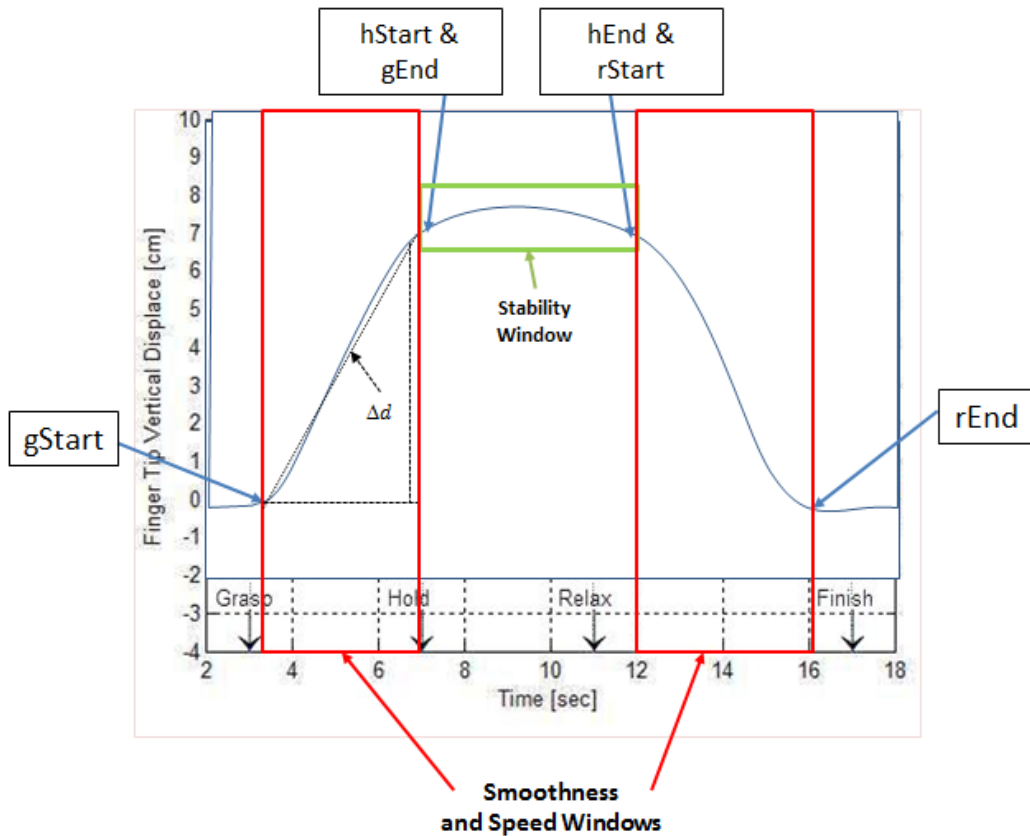
Figure 4-25 Graph display of the defined variables (gStart, gEnd, hStart, hEnd, rStart, rEnd) on the finger's displacement signal curve. The Speed and Smoothness windows are displayed in Red and Stability window is displayed in Green.

The slide-window technique's accuracy is dependent on two elements: the level of noises in the finger's displacement signal and the size of the window duration "ws" to correlate with the finger's displacement signal peak width.

In this project, a low pass filter is used to smooth the finger's displacement signal and avoid the local minima issue.

Plus, the window duration "ws" is defined based on the time markers. The markers are assigned by the virtual simulator by synchronising the data recording with the task instructions (events).

4.3.1.2.1.1.   The Speed Component

The average speed of the finger movement is calculated using equation (4-9).

$$Average\_Speed = \frac{Grasp\_Speed + Relax\_Speed}{2} \qquad \text{(4-9)}$$

Where $Grasp\_Speed$ is the speed of grasping the object or forming the posture, in the time range [gStart gEnd]; and $Relax\_Speed$ is the speed of relaxing the finger back to the initial position after the 'hold' event, in the time range [rStart rEnd].

The *speed* of both 'grasp' and 'relax' events is calculated by finding the slope of the finger's displacement signal data within the time range. This is described in equation (4-10).

$$speed = slope = \frac{\Delta d_{t_e}}{t_e} \qquad \text{(4-10)}$$

Where t_e is the time duration of the event; and Δd_{t_e} is the displacement distance of the tip of the finger for the defined section of the finger displacement signal within the time range of t_e. The unit of the speed is cm/s.

Calculating the slope using equation (4-10) is correct in condition that the finger's displacement signal is linear. However, because the finger's displacement signal is assumed to be of Gaussian shape, the *speed* is calculated by first finding the polynomial equation of finger's displacement event finger's displacement signal and then calculating the slope.

In order to determine the polynomial equation of the data in the selected time range, the Least Square fitting method (LSR) is used. The LSR returns the polynomial parameters of the equation based on the regression of the data.

4.3.1.2.1.2. The Smoothness Component

The smoothness component of the finger's displacement signal measures the consistency level of the finger while performing a posture. The calculation of the smoothness is performed by first smoothing the finger's displacement signal using 'rloess', regression locally weighted scatterplot smoothing, filter (10% span of total data points) and then subtracted from the original using equation (4-11).

$$Smoothness(t_g) = \sqrt{\frac{\sum_{t_{g_0}}^{t_{g_k}}(VD_1(t_g) - VD_2(t_g))^2}{t_{g_k} - t_{g_0}}} \qquad \text{(4-11)}$$

Where t_g is the time range of the 'grasp' or 'relax' event. It varies from t_{g_0} (start time of the event, also noted as gStart or rStart) to t_{g_k} (end time of the event, also noted as gEnd or rEnd); $VD_1(t_g)$ is the original vertical fingertip displacement signal during t_g; $VD_2(t_g)$ is the vertical fingertip displacement during t_g after applying 'rloess' regression loess smoothing filter,

The 'rloess' is similar to lowpass filtering. It is a moving average filter which smooths the finger's displacement signal by replacing the data point with the average of the neighbour points within the span. (Matlab-SMOOTH, 2015); it is calculated using the equation.

$$\ddot{y}_s(i) = \frac{1}{2\acute{N}+1}\sqrt{\ddot{y}(i+\acute{N}) + \ddot{y}(i+\acute{N}-1) + \cdots + \ddot{y}(i-\acute{N})} \qquad \textbf{(4-12)}$$

Where $\ddot{y}_s(i)$ is the smoothed value of the data point; i is the data point number in the finger's displacement signal;
$2\acute{N}+1$ is the span; and $\acute{N}$ is the number of neighbouring data points.

The equation (4-11) calculates the Root Mean Square Error (RMSE) (Holmes, 2000) between the smooth and original finger's displacement signal, to calculate the level of variation in the finger displacement.

Moreover, similar to the speed, the smoothness is calculated on the Grasp and Relax events time duration. The smoothness values are calculated separately by using (4-11) and then averaged. This is described in equation (4-13).

$$Average\_Smoothness = \frac{Grasp\_Smoothness + Relax\_Smoothness}{2} \qquad \textbf{(4-13)}$$

Where $Grasp\_Smoothness$ is the smoothness calculation of the finger's displacement signal for the 'grasp' event, in the duration range [gStart gEnd]; and $Relax\_Smoothness$ is the smoothness of the finger's displacement signal for the 'relax' event, in the duration range [rStart rEnd]. The unit of smoothness is cm.

4.3.1.2.1.3. The Stability Component

The stability component is the level of stability of the finger's displacement signal during only the 'hold' event. To calculate the stability of the fingers, both the low level noises and high level noises are measured and included in the equation (4-14). This is to cover both small and large variations in the finger movements.

$$Stability(t_h) = \sqrt{\frac{\sum_{t_{h_0}}^{t_{h_k}} (VH_1(t_h) - VH_2(t_h))^2}{t_{h_k} - t_{h_o}}} + 0.5 * \sqrt{\frac{\sum_{t_{h_0}}^{t_{h_k}} (VH_1(t_h) - VH_3(t_h))^2}{t_{h_k} - t_{h_o}}} \qquad \text{(4-14)}$$

Where t_h is the time for 'hold' event (between the 'grasp' and 'relax'). It varies from t_{h_0} (start time of the event, also noted as hStart) to t_{h_k} (end time of the event, also noted as hEnd) ; $VH_1(t_h)$ is the original vertical fingertip displacement during t_h; $VH_2(t_h)$ is the vertical fingertip displacement signal during t_h and smoothed using 'rloess' filter (10% span of total data points); $VH_3(t_h)$ is the vertical finger's displacement signal during t_h, smoothed using 'rloess' regression smoothing filter (80% span of total data points).

The equation (4-14) consists of two parts: first it calculates the RMSE of the finger movement's small variations, and the second calculates the large variations during the 'hold' event within time range [hStart hEnd]. The unit of stability is cm.

4.3.1.2.1.4. The Finger Performance Value Equation

The above calculations of the Smoothness, Speed and Stability are combined in equation (4-15) to calculate the Finger Performance Value (FPV).

$$FPV = \frac{\dfrac{Average\_Speed}{\max(Average\_Speed)}}{\dfrac{Average\_Smoothness}{\max(Average\_Smoothness)} + \dfrac{Stability}{\max(Stability)}} * Corr\_Fact \qquad \text{(4-15)}$$

Where $Corr\_Fact$ is the calibration coefficient index for each subject; max(.) is the maximum value of the total data set for all the subjects (used for normalisation).

The $Corr\_Fact$ is calculated by using the Pearson's r correlation coefficient to compare the expected and actual DoF angle values. The DoF angle values are calculated in the calibration process (Chapter 5). The actual DoF angle values are the specified six hand gestures stored data.

The Finger Performance Value (FPV) is a dimensionless value; It is normalised by the maximum value max(.). The maximum value is obtained using the data results of all the subjects.

(Muir et al., 1995) suggests that the maximum speed, for healthy hands, with no external forces or weight, is 5.7 cm/s. To verify the results on CyberGlove®, the small experiment was conducted after calibration, which consisted of flexing and extending all the fingers as fast as the possible. The experiment was repeated five times with 20 second rest in between. The results show that the total average of the speed was 6cm/s.

4.3.1.2.2. EMG Feature Extraction Method

The four muscles selected in monitoring the three fingers' movements (Kanade, 2009) during the experiment are:

1. Dorsal Interosseous Muscle (DIM) – For the thumb opposition-apposition.
2. Right Abductor Pollicis (RAP) – For the thumb opposition-apposition.
3. Right Flexor Digitorum Superficialis (RFD) – For the index and middle fingers' flexion.
4. Right Extensor Digitorum (RED) – For the index and middle fingers' extension.

The EMG electrode signals of the subject's four muscles are filtered using a low pass (500 Hz) filter and high pass (5 Hz) filter. They are then amplified to enlarge the features contained within the signal (De Luca, 2001).

Following this, the data is passed through a digital rectification filter in order to perform the necessary analysis. These procedures are described in Figure 4-26.
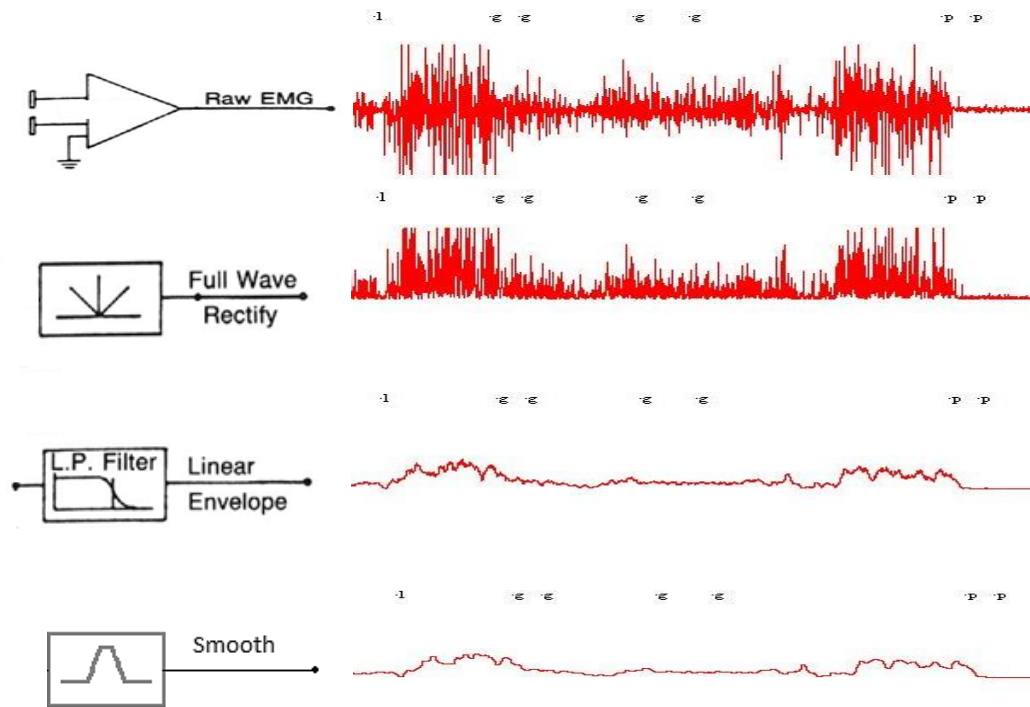
Figure 4-26 A schematic procedure of the EMG data signal processing; In the first, top step the signal is acquired from the digital filters and amplifier; in the second step the signal is rectified using specified equation; in the third step the signal is passed through a linear low pass filter envelope to eliminate the noise; and in the final, fourth step the signal is smoothed using a median filter for data analysis.

The following equation (4-16) is used to rectify the signal.

$$ARV = \frac{1}{T} \int_{i=1}^{T} \left| EMG\ (t) \right| dt \qquad \text{(4-16)}$$

Where ARV is the average rectified value (Stutz, 2012), and $\left| EMG\ (t) \right|$ is the absolute of the EMG signal in time (t).

To build a linear envelope on the EMG, the full-wave rectification is combined with a second order Butterworth low pass filter with a cut off of 400 Hz (Mello et al., 2007). The below equation describes the N order of a low pass analogical Butterworth filter in the frequency domain (Terri et al., 2003).

$$|HM(wf)|^2 = \frac{1}{1+(\frac{wf}{wf_c})^{2N}}$$

<div align="right">(4-17)</div>

Where $|HM(wf)|^2$ is the square magnitude of the frequency response of the filter; wf is the angular frequency; wf_c is the filter's cutoff frequency; and T is the total time. Smoothing techniques, using the digital median filter, are applied to process the signal further. The filter looks at the neighbouring area (usually defined as a window) of each signal data point to determine whether or not it is representative of the surrounding signal. The filter eliminates small noise spikes while keeping the remainder of the signal intact (Florence and Jane, 1988).

The EMG signals are analysed using spectral analysis, by studying the frequency domain of the signal. The approach uses fast Fourier transform (FFT) to deconstruct the signal into multiple sine waves of different frequencies. This shows how the signal frequency varies with time. At this point, the power spectral density (PSD) is used to measure the power contribution of each frequency in the EMG signal. This is calculated by squaring the FFT from each section of the signal and averaging the total. The PSD is then compared between the defined epochs.

The mean power frequency is also calculated from the PSD for all the epochs in order to assess the EMG data quantitatively.

Spectral analysis is used to study muscle fatigue during the sessions that use an added weight. Florence used mean frequency to analyse muscle activity, which is proven to decrease with time during the tasks that induce fatigue (Florence and Jane, 2015) and (NIH, 2015). EMG is also used to measure the level of physiological tremor on the fingers, as it decreases in line with the tremor effect on the hand movement (Conolly, 2015).

4.3.1.2.3. Physiological Features for the Subject Hand

The physiological characteristics of each subject's hand are also included in this project. The physiological features add variability in the results between subjects, and change the kinematic calculations for identifying the fingertip positions from the DoF angle values and fingers length.

The features considered include the subject's hand size, finger lengths, the arm's shoulder to tip length, and the level of usage of the right hand (see Appendix II).

4.3.1.2.4. Subjective Assessment

The aim of the subjective assessment is to supplement the objective's, by outlining the physiological differences between subjects, previous experience with virtual reality and the level of concentration while running the experiments (this endorses the boredom level, incorrect following of instructions and attempting to learn task patterns) .

The subjective assessment is performed during the experiment by observing the subject performance and interaction level with the system. The author was monitoring the subject and taking notes of any noticed actions as well as video recording their performance. The observation included assessing the motivation rate by reviewing the concentration level when following the instructions, questions asked by the subject related to the system functionality and studies, and interaction skills in the real and VR system (besides manipulating the virtual hand, interacting with the 3D objects and synchronous wrist movement with the VR) Appendix VI. The observations and subjective assessment are all performed by the author of this thesis.

4.3.1.3. *Data Classification*

The data classification process involves analysing the features taken from the previous process (Feature Extraction 4.3.1.2) by studying the variability between the subjects, sessions, trials, and tasks. It also involves statistically evaluating the data in order to prove the efficiency of the proposed hand assessment method.

A Pearson's r cross-correlation test is performed, on a trial basis, for each subject to test the intra-subject repeatability of the studies.

To test the inter-subject repeatability for all the subjects in the control group, the ANOVA test is used. The null hypothesis is that there are no significant differences in the assessment values between subjects of the controlled group. The hypothesis is tested at an α level of .05. The confidence interval (CI) for rejecting a true hypothesis (having type I error) is 95%.

This helps in validating the reliability and effectiveness of the developed method.

In this approach, it is very difficult to compare the studies performed on SHAP with the results obtained, as there are variances in the parameters included (range of motion, smoothness, and stability). The experimental protocols also vary as in here the time measurement is performed automatically, while in SHAP this is performed using a timer

button that is pressed by the subject at the start and end of the task to track the time. In addition, trying to exclude the reading of the hold event from the data results does not only confuse the main factor of the SHAP scoring method – the time taken to execute a complete task without obstruction – it also eliminates the subtle factors of the hand function during grasp and release, such as grip strength, stability duration, and proprioception.

Another approach to validate the assessment method is to present the outcome measurements for a group of hand therapists. This allows the subjective assessment of the outcomes in combination with the SHAP scoring values for the same group.

The combination of SHAP scores incorporates the majority of significant factors addressed in the project assessment method.

The efficiency of virtual reality sessions, in comparison to real life sessions, for providing accurate outcome measurements is dependent on multiple factors. Firstly, VR does not include haptic feedbacks (senses of textures, size, temperature, weight), where muscle/nervous contributions differ, as no forces are required to lift objects. Secondly, there are differences in the perception (i.e. visual perception) of the virtual objects that lead to inconsistencies in estimating the size, shape, and distance of the objects. Finally, the VR has numerous limitations in simulating the high articulations and details of the human hand, as well as the complex interactions with real world objects. This reduces the precision and feasibility of the fingers' movement and motor control.

4.4. Experimental Chapter Summary

In this chapter, the experimental setup was described with the various materials used. This included the data glove device, the hand assessment method, the virtual reality system with the developed virtual hand simulator and display devices, and the electromyography measurement application.

The experimental protocol is detailed with information of the inclusion criteria used for the subjects and the different procedures designed to perform the experiments. This included task definitions, session sequences and incorporation, and the time domains.

Following this, the data processing procedures are illustrated involving data segmentation, feature extraction, and data classification for the outcome measurements. The feature

extraction section highlighted the unique approach of this project, as well as the other features and calibration factors that have been considered to remove discrepancies and provide accurate hand assessment analysis.

In the following chapter, the calibration method used for the data glove device with the virtual hand model is explained. Very importantly, during the research the importance of accurately calibrating the device with the subject's performance in order to obtain accurate results was noted. In light of this, a separate chapter has been included which is mainly dedicated to the calibration and development process. The latter covers an extensive review of the available methods, the approach developed and the specific experiments performed on the subjects in order to validate the procedure.

Chapter 5 Calibration

The hand model calibration is considered a key factor in obtaining efficient outcome measurements for the project as it produces consistency and a reliable visual display for hand interactions and manipulations.

The high complexity of the hand kinematics makes it essential to address the calibration and dedicate a separate part of the project process to reviewing and developing different methods. This will serve to provide a reliable approach that closely resembles the actual hand movements and reduces discrepancies.

It is not possible to draw any reliable conclusions on the designed model efficiency, or to conduct any study performing the classification methods, without having an accurate and feasible calibration method.

The calibration method considered in this project is off-line programming, as the aim is to avoid making the process cumbersome and to ensure it is kept independent from any external third party devices.

This chapter begins with a description of the procedures involved in performing calibration, followed by a review of the existing methods. It concludes with the suggested approach and the results obtained.

The main aim of calibration is to address the various discrepancies between the human hand kinematics (fitting with hand), the tracking device method (sensor properties) and the hand model kinematics and manipulations. A reliable and robust calibration is dependent on both its adaptability in addressing the numerical problems of data reading and the deficiencies of the system tracking devices, and its simplicity or independence from additional external tools. Calibration is a cumulative process that involves defining hand model constraints, taking measurements, performing numerical identification for human hand characteristics, and implementing processing algorithms.

The hand modelling procedures, as previously described in the Background chapter, provide an approximate resemblance to the human hand size, shape and constraints. However, users have different hand sizes and finger joint lengths, which require anthropomorphic measurement for each subject and agreed parameters for the adaptive algorithms. The calibration algorithm is then applied to map or translate the sensor reading values from the tracking device to the human hand model DoF.

5.1. Review of different Data Glove Calibration Methods

Several methods have been provided to address the calibration of the data glove reading with virtual models. The large volume of research in this area highlights how challenging the process is and that there is no one solution that can cover the various aspects of adjustments.

The CyberGlove® VirtualHand application offers a basic method to calibrate the virtual hand. This involves manually adjusting the gain and offset parameters of the raw values for each sensor to produce a visually convincing hand pose. This is described in the following equation (5-1).

$$DOF_{Val} = gain * raw_{Val} + offset \qquad \text{(5-1)}$$

Where raw_{Val} is the sensor value; $gain$ is the gain value; and $offset$ is the offset value; and DOF_{Val} is the calculated DOF angle value by using the gain and offset constant values.

This approach has many limitations as it is not accurate and produces spatial differences between users and repetitions. As such, it is not valid for tasks that involve fine finger movements. The process is also cumbersome and lengthy, and does not take the joints'/fingers' dependencies into consideration.

The alternative posture method supported in the application is limited to only two gestures and this does not cover the maximal constraints of the hand movement.

5.1.1. Neural Network Data Glove Calibration Method

The neural network (MachineLearning, 2015) is a commonly used model for calibration. Its main use is to resolve various self-learning mathematical problems used in different applications. Its applications extend to numerous fields, such as pattern recognition and classifications (facial recognition, task identifications, brain activity features in motor control), times series prediction (statistical, finance), signal processing (filter, noise cancellation), control (automation control, robotics), and soft sensor analysis (evaluation of multiple sensory inputs) (NeuralNetwork).

The neural network architecture consists of multiple neurons, which are connected linearly and nonlinearly. A weight is assigned to the link between the neurons to alter the throughput signal appropriately. The model adjusts itself to obtain the desired output by

136

performing continuous evaluations and error parameters calculations. There are three techniques used in the network:

1- A supervised learning network, where the network compares its output with defined (known) values and makes adjustment to its connections.

2- Unsupervised learning, which is where there are no defined values to be used for evaluation. Instead the network separates between different datasets by using learning mechanisms to identify characteristics or remarks for each group. A common application is clustering.

3- Reinforcement learning is a semi-supervised network that is configured with a reward based element, which increases when it gets the correct outputs. An example of reinforcement learning is a robotic hand searching for the optimal posture to grasp an object – the network reward is increased if the object is grasped appropriately and with the relevant force and stability.
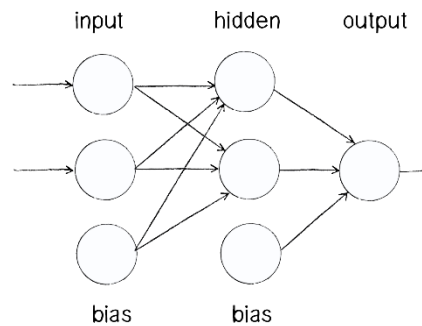
Figure 5-1 Neural network diagram; This figure displays a basic structure of neural network that consists of 3 layers: input, hidden, and output.

The neural network model also has multiple types:

Feed forward neural network (shown in Figure 5-1 Neural network diagram; This figure displays a basic structure of neural network that consists of 3 layers: input, hidden, and output.): this is a very common network. It is composed of multiple layers – input, hidden and output. The input layer is processed with different computational weights to produce the desired output. This network is usually trained with different algorithms, such as genetic algorithms and back-propagation techniques.

Self-Organising Map (SOM) (Kohonen, 1997): consists of two layers. Rather than taking the outputs from all or individual neurons, this model selects only the neuron with highest output to be considered in the process. It is usually used for clustering and is classified as a

137

reinforcement learning technique.

Hopfield Neural Network: a single layer recurrent network that echoes back its updated state to the network. It is a supervised learning technique and is commonly used to recognize patterns.

Simple Recurrent Network (SRN): this has a context later mechanism that holds the previous output from the hidden layer and echoes it back to the hidden layer's input. This network is used for prediction.

The detailed process of a fully connected feed-forward network can be defined as follows: N is the total number of neurons and ne is the neuron's number [1,2…N].

1. Initialize input layer as in equation (5-2).

$$Input\_layer = xNumb \qquad \text{(5-2)}$$

Where xNumb is the number of the layer.

2. Propagate activity forward using equation (5-3).

$$\breve{O}_{ne} = f_{ne}(Weight_{ne} * \breve{O}_{ne-1} + BiasW_{ne}) \qquad \text{(5-3)}$$

Where $\breve{O}_{ne}$ is the output; Weight is the weight assigned for each neuron; $BiasW$ is the bias weight;

3. Then calculate the error in the output layer using equation (5-4).

$$\delta_N = tVal - \breve{O}_N \qquad \text{(5-4)}$$

Where $tVal$ is the target value.

4. Back propagate the error using equation (5-5).

$$\delta_{ne} = \left(1 - y^2_{hUnit}\right) * (Weigth^T_{ne+1} * \delta_{ne+1}) \qquad \text{(5-5)}$$

Where δ is the back propagate error; *hUnit* is the hidden unit; T is the matrix transposition operator; and y is the output of the unit.

5. Update the weights and biases, using equation (5-6) and (5-7).

$$\Delta Weight_{ne} = \delta_{ne} * \breve{O}^T_{ne-1} \qquad\qquad (5\text{-}6)$$

$$\Delta BiasW_{ne} = \delta_{ne} \qquad\qquad (5\text{-}7)$$

(Fischer et al., 2007) have used neural networks for data glove calibration in coordination with a measurement device to evaluate the output. The network model type used is augmented feed-forward (Figure 5-2). This has 23 inputs for each sensor, 12 outputs, and 28 hidden units in a single layer.
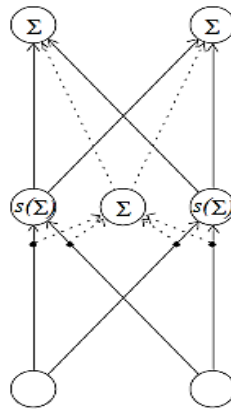
Figure 5-2 A linear augmented feed-forward network diagram; The model augments the feeding process by including the extra hidden node connections between the input and output layers. The dotted connections between the inputs and outputs have an unchanging weight equal 1.

The network outcome was tested on 1,500 samples and compared to the ordinary feed-forward network, where there are no direct connections between the inputs and outputs (shown in the dotted line in Figure 5-2). The results found that the residual error is three times lower than the ordinary network.

(Shuai et al., 2010, Shuai et al., 2011) have used the Self Organising Map (SOM) for hand gesture recognition. This takes raw sensor data from the data glove and maps the hand motion gestures detected to defined data gestures (open/close fist). The network learns the gestures' properties and adapts to identify new gestures that have been inserted. The training step is performed on six subjects, with each gesture repeated ten times. The test is then performed with seven subjects interacting with virtual reality by opening and closing their hand (fist). The SOM method has demonstrated high efficiency in interacting with the

scene. (Further details of this research and the SOM is described in the previous Chapter, Motor Control Section)

5.1.2. Genetic algorithm Data Glove Calibration Method

Another process employed in data glove calibration is genetic algorithm (GA). This method is generally used to optimise parameters by finding the most fitting solution for a defined model. Several processing steps are considered:

1- Define the parameters required to optimise and generate a population of controlled (experiments) or random values.

2- Perform the evaluation of each set of parameters (defined chromosome). The parameters in the equation are replaced and the correlation between the actual (calculated) values and the desired values (usually obtained from a difference measurement device reading, or database of corresponding values) is calculated.

3- The selection step follows this. Probabilities for all the chromosomes in the population are computed. This is usually obtained by first calculating each fitness value = 1 / the pre-calculated evaluation value in the previous step, and then dividing it by the total of all the chromosomes' fitness values – P = Fitness/ Total_Chromosome_Fitness. To avoid dividing by zero, 1 is added to the evaluation value. The selection process method is then applied, to select the fittest chromosomes. For example, the roulette-wheel technique will calculate the cumulative probability and select corresponding chromosomes with the randomly generated x numbers between the range of 0-1. (x is the number of chromosomes in the population)

4- The crossover step is the mating phase between the different parents in the algorithm to provide the fittest chromosome distribution. The parent chromosome selection is performed by choosing the randomly generated values for chromosomes that are below the crossover rate set by the user. A random crossover point is then determined to cut the parent chromosomes and interchange the generations (parameters).

5- Following this, the mutation step is performed to ensure the spread of chromosome selection is distributed fairly across the population and increase the diversity. A number (defined by the mutation rate and total generations' length of time in the population) of randomly defined generations replaces existing generations of the population at random positions.

6- The new generations are then evaluated against the desired values, following the same process as in the evaluation step. If sufficient solution quality is reached, it then stops. If not, it will repeat the same process until it reaches either a sufficient quality of solution or the end of a predetermined number of iterations.
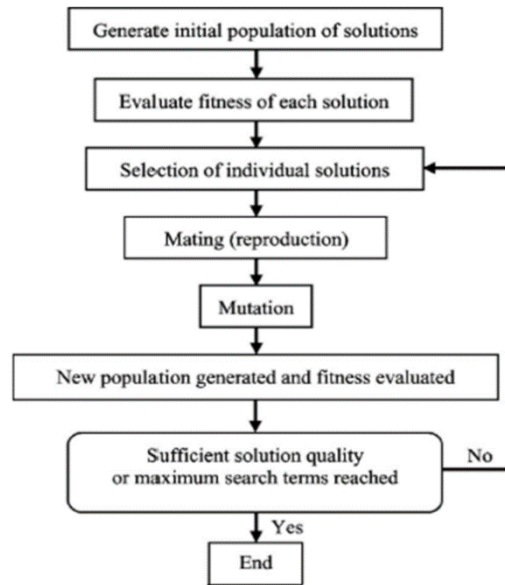
Figure 5-3 Genetic algorithm structure flowchart; This illustrates the iterative process performed by evaluating and optimising the data process to produce the most fit population output (most accurate result).

A larger iteration number will result in a longer process and higher accuracy of output.

(Sun et al., 2011, Sun et al., 2006) have used the GA method to calibrate the data glove by measuring the DoF flexion angles, via a specially designed test device. The measured outcome is then used in the evaluation step of the GA to return the grade value for each process. The population generated consists of 4 generations (parameters) and 40 chromosomes (data conducted on 40 different individuals).

The stochastic (NeuralNetwork) uniform method is applied in the selection step and uses equal sized steps during 400 iterations to obtain the optimal solution.

The GA method returns high accuracy in comparison to the least squared method.

5.1.3. Regression Data Glove Calibration Method

Regression and analytical methods are used to perform glove-hand calibration in numerous pieces of research. Although the calibration of flexion-extension sensors can be performed using linear regression, the coupled sensors require calculations that are more accurate to

the level of constraints.

(Ferenc et al., 2015) have implemented new equations to calibrate the cross-coupling abduction sensors of the glove. The relationship between the independent adjacent fingers' flexion and the abduction sensor is described in equation (5-8).

$$\theta_{Abd} = gainf * (Surf_o(surf_{Flex}^{left}, surf_{Flex}^{right}) - surf_{Abd}) \qquad \text{(5-8)}$$

Where $Surf_o$ (.) is the isosurface function of the abduction sensor; $gainf$ is the gain value; and $surf$ is the sensor readings for $Flex$ (flexion) or Abd (Abduction), also indicates ($left$, $left$) to refer on the adjacent sensor.

The data points collected from the experiments are projected into three trajectories. A fit cubic function is then applied on each trajectory, with equidistant sampling, to get the three point sets in the density space. The parabolas are fitted to the triple point sets and the isosurface of the points is triangulated to get a local linear interpolation of $surf$. The method is compared to the linear independent method, on two trajectories' 0 and 25° abduction movement. It demonstrates higher capability to compensate for the faulty abduction sensor readings for 0 trajectory and similar outcomes with the 25°. A comparison was also performed with the linear regression and showed similar results.

(Shuai et al., 2010) suggested different equations to calibrate the independent and cross-coupled sensors. This takes in to consideration the predefined dynamic constraints in the hand kinematic model (see Type II constraints and synergies in the Hand Kinematic Model Section 2.2 in Chapter 2)

The calibration method used for the independent sensors is presented in equation (5-9).

$$\theta_{out} = \theta_{min} + \frac{val - raw_{min}}{raw_{max} - raw_{min}}(\theta_{max} - \theta_{min}) \qquad \text{(5-9)}$$

Where θ is the DoF angle; val is the current sensor value; and raw_{max}, raw_{min} are the ranges of the sensors' values.

The method applied for crossover sensors uses Laplace natural interpolation. The advantage of this method is that it has more efficient approximation to the underlying "true" function than the nearest neighbour function. Firstly, the process locates the natural neighbours and then computes the coordinates. Finally, it computes the interpolated values for the point.

The results demonstrate an effective method in eliminating crossover effects at the MCPs of the index, ring and little fingers. The index finger results are more accurate than the other two fingers, due to the anatomic constraints.

However, (Weston et al., 2000) and (Wang and Dai 2009) have proposed a similar linear equation for independent sensors, equation (5-10).

$$\emptyset = g * \sigma + \ddot{\Theta} \qquad \text{(5-10)}$$

Where $\emptyset$ is the DoF angle value; g is the gain; σ is the sensor value; and $\ddot{\Theta}$ is the offset value.

However, for the cross-coupled sensors (excluding the thumb) B. Wang et al. used the equation(5-11).

$$\emptyset_{Abd} = (g_{Abd} * \sigma_{Abd} - \ddot{\Theta}_{Abd}) + (k_L * \sigma_L + k_R * \sigma_R + ḩ) \qquad \text{(5-11)}$$

Where g_{Abd} is the gain for the abduction sensor; $\ddot{\Theta}_{Abd}$ is the offset for the abduction sensor; σ_{Abd} is the sensor value for the abduction sensor; k_L is the cross parameter for the left adjacent sensor to the abduction; σ_L is the left adjacent sensor value for the abduction sensor; k_R is the cross parameter for the right adjacent sensor to the abduction; σ_R is the right adjacent sensor value for the abduction sensor; ḩ is the offset for cross-coupled sensors.

The equation (5-11) is composed of a non cross-coupled part and a cross-coupled part. The parameters of the non cross-coupled part are calculated by using the independent sensor calibration approach. Those of the cross-coupled part are calculated by stabilising the abduction sensor in a fixed angle while flexing the MCP joints. The error output of non cross-coupled part, after deriving the cross-coupled part, is defined by the equation (5-12).

$$\Delta\emptyset_{Abd} = \emptyset_{Abd} - (g_{Abd} * \sigma_{Abd} + \ddot{\Theta}_{Abd}) \qquad \text{(5-12)}$$

Where g_{Abd} is the gain value for abduction sensor; and $\ddot{\Theta}_{Abd}$ is the offset value for the abduction sensor.

The method for the thumb calibration is a little more complex, as both groups have used the least square regression iteration for trajectories where the thumb and index fingertips

are connected. This eliminates the need to use an external validation device (i.e. camera or others) to evaluate the outputs. The error difference between the fingertip positions is ±4mm. B. Wang et al. have applied the turning off/on bottle cap method, which differs from the thumb-index fingers' holding, as it connects both fingertips and allows more circumduction motion for the thumb.

The forward kinematics equation of the hand model is applied on the N recorded poses during these trajectories. This generates the error vectors Δd from each calculated index position to the corresponding thumb position. The thumb position is calculated by using both the cross-coupled and non cross-coupled (5-10) methods between the thumb joints.

This method uses the hand model Jacobian (J) to relate the infinitesimal joint angles and operational space motion. J is represented by a function of joint angle $\emptyset$.

The equation used for non cross-coupled, which combines the offsets and gains, is represented in (5-13).

$$\Delta d = J \begin{bmatrix} \Delta\emptyset_1 \\ \dots \\ \Delta\emptyset_n \end{bmatrix} = [J \, Diag(\sigma_i)J] \begin{bmatrix} \Delta\ddot{\Theta}_i \\ \dots \\ \Delta\ddot{\Theta}_i \end{bmatrix} \qquad \textbf{(5-13)}$$

Where $\Delta\emptyset_1, \dots \Delta\emptyset_n'$ is the set of joint angle errors; and $\Delta g_i, \dots \Delta\ddot{\Theta}_i'$ are the parameter offset vectors; and J is the Jacobian matrix;

The Jacobian matrix is extended to include the cross-coupling gains and offsets, by replacing the $\Delta\emptyset_i$ with the corresponding relations in (5-14).

$$\begin{bmatrix} \emptyset_{Thu\_Roll} \\ \emptyset_{Thu\_Abd} \\ \emptyset_{Thu\_Twist} \end{bmatrix} = \begin{bmatrix} g_{Roll} & g_{Roll}^{Abd} \\ g_{Abd} & g_{Abd}^{Roll} \\ g_{Twist}^{Abd} & g_{Twist}^{Roll} \end{bmatrix} \begin{bmatrix} \sigma_{Roll} \\ \sigma_{Abd} \\ \sigma_{Roll} \end{bmatrix} + \begin{bmatrix} \ddot{\Theta}_{com\_Roll} \\ \ddot{\Theta}_{com\_Abd} \\ \ddot{\Theta}_{com\_Twist} \end{bmatrix} \qquad \textbf{(5-14)}$$

Where σ_{Roll} , σ_{Abd} are thumb abduction and flexion sensor readings; g_{Roll}, g_{Abd} are the non cross-coupled gains; $g_{Twist}^{Abd}, g_{Roll}^{Abd}, g_{Abd}^{Roll}$ and g_{Twist}^{Roll} are cross-coupled sensor gains; $\ddot{\Theta}_{com\_Roll}, \ddot{\Theta}_{com\_Abd}$; and $\ddot{\Theta}_{com\_Twist}$ is the angular offset of non cross-coupled and cross-coupled combined together. (σ_{Twist} is not available due to the glove primitives).

Weston has extended the Jacobian function to include the relationship between bone lengths and fingertip positions (Weston et al., 2000). To prevent insignificant closed-loop

solutions, both equations are multiplied by the non-singular matrix V, which consists of vectors to control the parameter deviation.

Further to this, Wang and Dai have performed coarse and fine calibration to insure the numerical stability of the least squares regression (Wang and Dai 2009). This also remove noise by relating the J and $Diag(\sigma_i)J$ and dividing the σ_i by the maximum sensor value, 255.

A visual inspection was performed to investigate the performance of the derived methods. The results showed vast similarities between the constructed hand gestures and the real ones, considerable elimination of the cross-coupling error between MCP flexion and abduction sensors, and high accuracy in fine manipulation of the virtual objects. (See (Michael, 2015) for the above method).

Gesture database

In this review it is worth noting that there are many existing gestures databases and published biomechanics data available for use in testing the calibration or training the network model. Some examples of these are (An et al., 1979) dataset for biomechanical models; and the Columbia Grasp Database (CGDB) (Database), OpenRAVE database package (OpenRAVE, 2015), HandCorpus (HandCorpus, 2014), and the Human Grasping Database(Warnick, 2015) for grasp and 3D robotic hand models (Andrew and Matei, 2015).

5.2. Data Glove Calibration Approach

The suggested neural network method is very efficient in terms of the project's objectives and restraints. However, it requires external input hardware to evaluate the output and adjust the network throughout. It also requires a large dataset (> 1,500 samples) to train the model for high accuracy results, and a lot of time is needed to generate this.

The GA method has similar disadvantages, as it needs to use an external input device to evaluate the output. In addition, it requires a long time to process all the iterations. Conversely, the SOM model has a great advantage over the other methods(Shuai et al., 2011). This is because it performs gesture recognition with little or no supervision during the classification process. However, as with the previous methods, it requires a large dataset to generate. In addition, Shuai and colleagues have included only two gestures (open and close fist) in their approach to train the network (Shuai et al., 2011). In order to

obtain high accuracy, the SOM needs a wider range of gestures to cover all the hand variations and RoM.

In this project, the goal is to find a reliable calibration method that provides accurate outputs that map the sensor readings to the multiple DoFs of the virtual hand model. It should also only require a short time for performance and have no reliance on external devices.

In light of this, the regression method is found to be the most suitable approach as it doesn't require a large dataset to generate and no additional hardware is needed for the system. It does, however, require the development of complex equations in order to consider all the different constraints involved.

The linear interpolation method (Mathematics, 2015) and Laplace natural interpolation method are commonly used for virtual interaction applications that require less accuracy in detailed joint movements. However, when studying hand performance, a high absolute accuracy is required to encompass all of the fine finger movements.
Therefore, the suggested approach is more closely related to the last two regression methods of Weston and Wang, (Weston et al., 2000, Wang and Dai 2009). The equations derived from these are implemented in this application, with further adjustments to cover the existing variations in the virtual model and glove outputs, and thus improve the results.

The natural and dynamic constraints that exist between joints, such as the connection between the DIP and PIP angles (see hand kinematic model Section 2.2 in Chapter 2 for further details), are not included in this project. This is to ensure adaptability between different users' hand sizes and kinematics by avoiding the hardcoded coefficients that define the cross-couple motion of the fingers (such as PIP angle = 2/3 DIP or Right MCP flexion = 1/3 left MCP flexion). The application targets patients with hand dysfunction who wish to restore the lost kinematic functions.

The flexion-extension independent sensors are calibrated using the equations described in (5-10) and (5-11)

Before listing the proposed method for abduction (independent) sensors, there are several important factors that need to be identified and included in the calibration. The factors

listed below are created by the limitations of the hardware and hand kinematic constraints, and measured by complex algorithms:

-   The four fingers' MCP flexion-extension is naturally (without an external force being involved) cross-coupled (Shuai et al., 2010). As an extensive flexion of the index MCP causes a proportional degree of flexion in the middle MCP, a flexion of the middle MCP causes a degree of flexion on the ring MCP. Similarly, a flexion on the middle MCP causes a flexion on the pinkie MCP.
    This rule is considered in unidirectional terms, from left to right only, as a flexion on the middle MCP does not cause a flexion on the index MCP. This case could have internal variation in the palm, but it only appears on a small scale and can be omitted to reduce the complexity of the algorithm.
-   The glove sensors are attached to the soft skin of the hand and can be dislocated during the movements, which may cause inefficiency in the data reading.
-   The first abduction sensor from the left side of the hand can be used to derive the thumb abduction as it is not coupled with the adjacent one (Lin et al., 2000).. However, there are still other factors that need to be considered separately for thumb abduction, as it includes dependent sensors such as roll, abduction and twist.
-   The other four abduction-adduction sensors of the glove (apart from the thumbs') are coupled together and there is a 3->4 mapping in the calculation. The intermediate fingers (middle and ring), between two abduction sensors, are dependent on both the adjacent abduction sensors' variations to determine whether they are abducted (DoF moves left), adducted (DoF moves right) or stable (DoF is neutral or 0).
-   Incorporating the cross-couple equation suggested by (Wang and Dai 2009) (5-9) into the model, by using the least square fit regression analysis to determine k_L and k_R parameters, showed that the equation misses a ratio parameter between abduction and flexion variations. Additionally, there are constraints for each finger that need to be considered individually.

In order to address the above factors, the calibration is designed with flexibility and adaptation features. There are multiple hand postures selected for the procedures to encompass the constraints of the hand kinematics (see section 2.2.3). Therefore, to determine the relationship between the middle flexion DoF and the ring flexion DoF specifically, four hand postures are selected: "Fully Opened Hand", "Holding Object",

"Middle Pinch", and "Fist". The average value of the four postures for the middle and ring flexion DoF determines the coefficient relationship of the specific subject's results. The same concept is applied to calculate the intra (between DoF of same fingers i.e. DIP-PIP) and inter (between DoF of different fingers i.e. MCPs) cross-couple relationships.

The existing deficiency in the abduction sensors' DoF mapping for the intermediate fingers, is caused by the difficulty in identifying both the direction of movement and which finger needs to be abducted or adducted. This is due to the low dimensions of the glove readings. For example, an increase/decrease in the abduction sensor 2 is not enough to predict whether the index finger has moved left or if, instead, the middle finger has moved right. The abduction sensor 2 is the sensor between the index and middle fingers. To avoid confusion when referencing the abduction sensors, they are numbered "1 to 4" from the left to right on the right hand side.

The DoF-sensor mapping of the abduction sensors is critical when grasping objects of different shapes, where some external forces are applied on the fingers to change the movement from the natural RoM. It is possible to identify these directions and parameters by using the variations between the "Full Opened Hand" and "Straight: All Fingers Fully Abducted" posture readings of the adjacent abduction sensors, and by including certain conditions of the hand kinematic,.

Flexion of the MCP joint of the finger causes the adjacent abduction sensor to expand and, therefore, return a bigger value. The noise levels generated by the movement of the glove sensors, which are due to its attachment to the soft skin of the hand, need to be subtracted to avoid inconsistency.

In this approach, the flexion sensors (flexion and extension) are defined as "independent" and linear least square (LSR) regression analysis is applied on different posture readings to determine the gain and offset of the calculated equation.

The abduction sensors (abduction and adduction) are defined as "dependent" and the newly derived equations are used for calibration. The abduction sensors also have two parts – "cross-coupled" (flexion and adjacent abduction sensors) and "non cross-coupled" (abduction sensors). These will be explained in more detail later.

The methods above are explained in detail in the following, using the quoted algorithm

(data processing) codes. While reading the algorithms, it is important to note that the abduction sensors' values increase when they are flexed. This is captured by the maximum values and absolutes.

The algorithm is also working the sensor (in voltage) and the DoF (in radiant angle) on two dimensions, and so extra functions are included to perform the conversion with the appropriate gain-intercept parameters.

5.2.1. Dependent Sensors Data Processing Equations

5.2.1.1. Cross-Coupled Parameters

The k_L and k_R cross-coupled gains for each finger are calculated by stabilising the finger with a fixed abduction angle and moving the MCP to three different positions (Wang and Dai 2009). An alternative method is to move the MCP of the adjacent finger. The three variables (k_L, k_R and common offset θ) are found using the elimination method in three linear equations.

The non cross-coupled gains, g_{Abd} and offset $\ddot{O}_{Abd}$ (or gain, offset), are calculated using the linear least square fit (LSR) (LeastSquareFitting) method for all the values obtained from the postures (5-15).

$$
\begin{cases}
g_{Abd} = \dfrac{np \sum_{i=1}^{np} \sigma_i y_i - \sum_{i=1}^{np} \sigma_i \Omega_i}{n \sum_{i=1}^{n} \sigma_i^2 - (\sum_{i=1}^{np} \sigma_i)^2} \\[4mm]
\ddot{O}_{Abd} = \dfrac{\sum_{i=1}^{np} \Omega_i - g_{Abd} \sum_{i=1}^{np} \sigma_i}{np}
\end{cases}
\qquad \textbf{(5-15)}
$$

Where np is the number of postures; σ_i is the sensor value; and Ω_i is the desired DoF angle value.

5.2.1.2. The Index Abduction DoF angle

The index abduction DoF variable is dependent on the values of abduction sensor 2, within a specified range. The abduction DoF is in neutral position if the MCP flexion is over 1/3 of the maximum flexion.

As the glove abduction sensor 2 value increases with Index MCP flexion, hence the adjacent right abduction sensor (number 3) is included in the equation as it is cross-coupled with the middle finger, and can define the degree of adjustment for both abductions' DoF using equation (5-16).

$$
Index\_Abd\_DOF = (g_{Abd} * \sigma_{Abd} + \ddot{O}_{Abd}) + |k_{li} * \sigma_{li} * \varpi_{li}| - \varsigma * (g_{ri} * \sigma_{ri} + \ddot{O}_{ri}) \qquad \textbf{(5-16)}
$$

Where σ_{Abd} is the abduction sensor 2 with g_{Abd} gain and $\ddot{O}_{Abd}$ offset; k_{li} is the cross parameter for the index flexion sensor; σ_{li} is the index flexion sensor; ϖ_{li} is the ratio to convert from flexion variation to abduction variation; $g_{ri}, \sigma_{ri} \ and \ \ddot{O}_{ri}$ are gain, value and offset for right neighbour abduction sensor 3. The last parameters are derived using

regression analysis for the specific sensor.

ς is constant equal to $\frac{1}{4}$, to limit the amount of variation by the right abduction sensor.

Algorithm 5-1 Algorithm code for calibrating the index abduction DoF

// $\emptyset = g * \sigma + \ddot{\Theta}$. indValue is used for the index, middle, ring, and pinkie fingers
// $Abd\_Sensors[DOF\_nb] - max_{Abd\_Sensors[DOF\_nb]}$ gives the variation value, within the specified range

$DOF_{Sensor[2]} = slopeValue_2 * (Abd\_Sensors[2] - max_{Abd\_Sensors[2]}) + interceptValue_2$

1: **if** $DOF\_nb == Index_{Abduction}$
2:   **if (** $Index\_MCP\_Flexion \leq \frac{1}{3} * max_{Index\_MCP\_Flexion}$ **)**
3:   **// ratio is for relating the flexion variation with the abduction's**
4:     $ratio = \dfrac{Abd\_Sensors[2](max_{Middle\_MCP\_Flexion}) - Abd\_Sensors[2](min_{Middle\_MCP\_Flexion})}{max_{Middle\_MCP\_Flexion} - min_{Middle\_MCP\_Flexion}}$
5:     **// k_l is the slope of index MCP,**
6:     **// $Abd\_Sensors(MCP_0)[2]$ abduction sensor value at current MCP**
7:     **// $Abd\_Sensors(MCP_{max})[2]$ abduction sensor value at maximum MCP**
8:

    $Flex\_Sensor\_Variation = k_l * (Abd\_Sensors(MCP_0)[2] - Abd\_Sensors(MCP_{max})[2]) * ratio$

9:     $Adj\_Abd\_Variation = slopeValue_3 * (Abd\_Sensors[3] - max_{Abd\_Sensors[3]}) + interceptValue_3$

10:     **if (** $min_{DOF_{Sensor[2]}} \leq DOF_{Sensor[2]} \leq max_{DOF_{Sensor[2]}}$ **)**
11:       **// minus $Adj\_Abd\_Variation$ because it moves left and ¼ proportional effect on index**
12:       $DOF[DOF_{nb}] = DOF_{Sensor[2]} + abs(Flex\_Sensor\_Variation) - \frac{1}{4} * abs(Adj\_Abd\_Variation)$
13:     **end**
14:   **Else**
15:     $DOF[DOF\_nb] \cong 0$ **// Neutral position: 0 or DoF angle value in the "Full Opened Hand" posture**
16:   **end**
17: **end**

5.2.1.3. The Middle Abduction DoF

The middle finger is dependent on both abduction sensor variations 2 and 3. Most hand postures have the middle abduction DoF in neutral position. However, the shapes of some objects force the DoF to change (large tripod shaped objects, etc.). To determine this variation, a threshold is set for each of the abduction sensors' values. This is 2/3 of the maximum value.

If abduction sensor 2's value is bigger than the threshold, equation (5-17) is used:

$$Middle\_Abd\_DOF = |k_{lm} * \sigma_{lm} * \varpi_{lm}| + \left(g_{Abd_{lm}} * \sigma_{Abd_{lm}} + \ddot{\Theta}_{Abd_{lm}}\right) - Th_{lm} \qquad \text{(5-17)}$$

If abduction sensor 3's value is bigger than the threshold, equation (5-18) is used:

$$Middle\_Abd\_DOF = -(|k_{rm} * \sigma_{rm} * \varpi_{rm}| + \left(g_{Abd_{rm}} * \sigma_{Abd_{rm}} + \ddot{\Theta}_{Abd_{rm}}\right) - Th_{rm}) \qquad \text{(5-18)}$$

where $g_{Abd_{lm}}, \sigma_{Abd_{lm}}, \ddot{\Theta}_{Abd_{lm}}$ are gain, value and offset parameters for the left sensor from abduction sensor 2.

$g_{Abd_{rm}}, \sigma_{Abd_{rm}}, \ddot{\Theta}_{Abd_{rm}}$ are gain, value and offset parameters for the right sensor from the abduction sensor 2.

$k_{lm}, \sigma_{lm}, \varpi_{lm}$ are the cross parameters, value and ratios for left flexion sensor 'index MCP'.

$k_{rm}, \sigma_{rm}, \varpi_{rm}$ are the cross parameters, value and ratios for right flexion sensor 'ring MCP'.

Th_{lm} is the threshold for left abduction sensor 2, and Th_{rm} is the threshold for right abduction sensor 3.

If index and ring MCPs flex together, the middle finger MCP flexes. This causes the adjacent abduction sensors, 2 and 3, to vary. Furthermore, the middle abduction DoF moves left or right only if the middle MCP is less than 1/3 of the maximum flexion.

Algorithm 5-2 Algorithm code for calibrating the middle abduction DoF

1: **if** $DOF\_nb == Middle_{Abduction}$

2:   **if** $\left(Middle\_MCP\_Flexion \leq \frac{1}{3} * max_{Middle\_MCP\_Flexion}\right)$

3:    $ratio_l = \dfrac{Abd\_Sensors[2](max_{Middle\_MCP\_Flexion}) - Abd\_Sensors[2](min_{Middle\_MCP\_Flexion})}{max_{Middle\_MCP\_Flexion} - min_{Middle\_MCP\_Flexion}}$

4:    $ratio_r = \dfrac{Abd\_Sensors[3](max_{Ring\_MCP\_Flexion}) - Abd\_Sensors[3](min_{Ring\_MCP\_Flexion})}{max_{Ring\_MCP\_Flexion} - min_{Ring\_MCP\_Flexion}}$

5:    **// convert abduction sensor values to DoF**

6:    $DOF_{Sensor[2]} = slopeValue_2 * (Abd\_Sensors[2] - max_{Abd\_Sensors[2]}) + interceptValue_2$

7:    $DOF_{Sensor[3]} = slopeValue_3 * (Abd\_Sensors[3] - max_{Abd\_Sensors[3]}) + interceptValue_3$

8:    **// move right**

9:    **if (** $DOF_{Sensor[2]} \leq Threshold_{DOF_{Sensor[2]}}$ **)**

10:

   $Flex\_Sensor\_Variation =$
   $k_l * \left(Abd\_Sensors(MCP_0)[2] - Abd\_Sensors(MCP_{,max})[2]\right) * ratio_l$

11:

   $DOF[DOF\_nb] =$
   $abs(Flex\_Sensor\_Variation) + (DOF_{Sensor[2]} - Threshold_{Abd\_Sensors[2]})$

12:    **// move left**

13:    **else if (** $DOF_{Sensor[3]} \leq Threshold_{DOF_{Sensor[3]}}$ **)**

14:

   $Flex\_Sensor\_Variation =$
   $k_r * \left(Abd\_Sensors(MCP_0)[3] - Abd\_Sensors(MCP_{,max})[3]\right) * ratio_r$

15:    $DOF[DOF\_nb] = -(abs(Flex\_Sensor\_Variation) + (DOF_{Sensor[3]} - Threshold_{Abd\_Sensors[3]}))$

16:    **end**

17: **else**

18:    $DOF[DOF\_nb] \cong 0$

19: **end**

20: **end**

5.2.1.4. The Ring Abduction DoF

The ring finger is also dependent on two adjacent abduction sensors, 3 and 4. The ring abduction DoF is adjusted using the abduction sensor 3 value, within a specified range. If the abduction sensor 4 is smaller than the threshold, the ring abduction DoF moves to the left side.

The effect on the middle finger of moving the right hand fingers (ring, pinkie) to the right when fully abducted is very small, therefore it is not considered in this equation.

If abduction sensor 3 is within the specified range, equation (5-19) is used:

$$Ring\_Abd\_DOF = (g_{Abd_r} * \sigma_{Abd_r} + \ddot{\Theta}_{Abd_r}) + |k_{lr} * \sigma_{lr} * \varpi_{lr}| \qquad \textbf{(5-19)}$$

Where σ_{Abd_r} is the abduction sensor 3 with g_{Abd_r} gain and $\ddot{\Theta}_{Abd_r}$ offset; k_{lr} is the cross parameter for the ring flexion sensor; σ_{lr} is the ring flexion sensor; and r_{lr} is the ratio to convert from flexion variation to abduction variation.

If the abduction sensor 4 is bigger than the threshold, equation (5-20) is used:

$$Ring\_Abd\_DOF = -(|k_{rr} * \sigma_{rr} * \varpi_{rr}| + (g_{Abd_{rr}} * \sigma_{Abd_{rr}} + \ddot{\Theta}_{Abd_{rr}}) - Th_{rr}) \qquad \textbf{(5-20)}$$

Where $g_{Abd_{rr}}, \sigma_{Abd_{rr}}, \ddot{\Theta}_{Abd_{rr}}$ are gain, value and offset parameters for right abduction sensor 4.

$k_{rr}, \sigma_{rr}, \varpi_{rr}$ are the cross parameter, value and ratio for right flexion sensor 'pinkie MCP'.
Th_{rr} is the threshold for right abduction sensor 4.

Algorithm 5-3 Algorithm code for calibrating the ring abduction DoF

1: **if** $DOF\_nb == Ring_{Abduction}$

2:   **if (** $Ring\_MCP\_Flexion \leq \frac{1}{3} * max_{Ring\_MCP\_Flexion}$ **)**

3:     $ratio_l = \dfrac{Abd\_Sensors[3](max_{Ring\_MCP\_Flexion}) - Abd\_Sensors[3](min_{Ring\_MCP\_Flexion})}{max_{Ring\_MCP\_Flexion} - min_{Ring\_MCP\_Flexion}}$

4:     $ratio_r = \dfrac{Abd\_Sensors[4](max_{Pinkie\_MCP\_Flexion}) - Abd\_Sensors[4](min_{Pinkie\_MCP\_Flexion})}{max_{Pinkie\_MCP\_Flexion} - min_{Pinkie\_MCP\_Flexion}}$

5:   **// convert abduction sensor values to DoF**

6:     $DOF_{Sensor[4]} = slopeValue_4 * (Abd\_Sensors[4] - max_{Abd\_Sensors[4]}) + interceptValue_4$

7:     $DOF_{Sensor[3]} = slopeValue_3 * (Abd\_Sensors[3] - max_{Abd\_Sensors[3]}) + interceptValue_3$

8:   **// move according to the abduction sensor 3 value (after converting to angle).**

9:     **if (** $max_{DOF_{Sensor[3]}} \leq DOF_{Sensor[3]} \leq max_{DOF_{Sensor[3]}}$ **)**

10:

  $Flex_Sensor_Variation = $
  $k_l * (Abd\_Sensors(MCP_0)[3] - Abd\_Sensors(MCP_{max})[3]) * ratio_l$

11:     $DOF[DOF\_nb] = DOF_{Sensor[3]} + abs(Flex\_Sensor\_Variation)$

12:   **// move right**

13:     **else if (** $DOF_{Sensor[4]} \leq Threshold_{DOF_{Sensor[4]}}$ **)**

14:

  $Flex_Sensor_Variation = $
  $k_r * (Abd\_Sensors(MCP_0)[4] - Abd\_Sensors(MCP_{max})[4]) * ratio_r$

15:     $DOF[DOF\_nb] = -(abs(Flex\_Sensor\_Variation) + (DOF_{Sensor[4]} - Threshold_{Abd\_Sensors[4]}))$

16:   **end**

17: **else**

18:     $DOF[DOF\_nb] \cong 0$

19: **end**

20: **end**

5.2.1.5. The Pinkie Abduction DoF

The pinkie abduction DoF (5-21) is similar to the index finger, as it has only one adjacent abduction sensor, 4. The DoF is set by the value reading from the sensor, within a range. When the ring finger is fully adducted to the pinkie finger, the abduction sensor 3 is checked and added to the DoF's final value. Adding the value instead of using the 'if' condition statement helps to verify the sensor reading when the ring finger is in the neutral position.

$$Pinkie\_Abd\_DOF = \left(g_{Abd_p} * \sigma_{Abd_p} + \ddot{O}_{Abd_p}\right) + \left|k_{lp} * \sigma_{lp} * \varpi_{lp}\right| + \varsigma_p * (g_{rp} * \sigma_{rp} + \ddot{O}_{rp}) \qquad \textbf{(5-21)}$$

Where σ_{Abd} is the abduction sensor 4 with g_{Abd_p} gain and $\ddot{O}_{Abd_p}$ offset; k_{lp} is the cross parameter for the pinkie flexion sensor; σ_{lp} is the pinkie flexion sensor; ϖ_{lp} is the ratio to convert from flexion variation to abduction variation; $g_{rp}, \sigma_{rp} \ and \ \ddot{O}_{rp}$ are gain, value and offset for right neighbour abduction sensor 3. The last parameters are derived using regression analysis for the specific sensor.

ς_p is constant equal to $\frac{1}{4}$, to limit the amount of variation by the right abduction sensor.

Algorithm 5-4 Algorithm code for calibrating the pinkie abduction DoF

1: **if** $DOF\_nb == Pinkie_{Abduction}$

2:   **if (** $Pinkie\_MPJ\_Flexion \leq \frac{1}{3} * max_{Pinkie\_MCP\_Flexion}$ **)**

3:     $ratio = \dfrac{Abd\_Sensors[4](max_{Pinkie\_MCP\_Flexion}) - Abd\_Sensors[4](min_{Pinkie\_MCP\_Flexion})}{max_{Pinkie\_MCP\_Flexion} - min_{Pinkie\_MCP\_Flexion}}$

4:     **// convert abduction sensors values to DoF**

5:     $DOF_{Sensor[4]} = slopeValue_4 * (Abd\_Sensors[4] - max_{Abd\_Sensors[4]}) + interceptValue_4$

6:

    $Flex\_Sensor\_Variation =$
    $k_l * \big(Abd\_Sensors(MCP_0)[4] - Abd\_Sensors(MCP_{,max})[4]\big) * ratio$

7:     **if (** $min_{DOF_{Sensor[4]}} \leq DOF_{Sensor[4]} \leq max_{DOF_{Sensor[4]}}$ **)**

8:       **// Note, this could be also implemented in a collision by moving adjacent fingers when**

9:       **// in contact, but it saves computation**

10:     $Adj\_Abd\_Variation = slopeValue_3 * \big(Abd\_Sensors[3] - max_{Abd\_Sensors[3]}\big) + interceptValue_3$

11:     $DOF[DOF\_nb] = DOF_{Sensor[4]} + abs(Flex\_Sensor\_Variation) + \frac{1}{4} * abs(Adj\_Abd\_Variation)$

12:   **end**

13: **else**

14:   $DOF[DOF\_nb] \cong 0$

15: **end**

16: **end**

Alternatively, the influence of the middle finger's movement on the adjacent fingers (index moves to the left, ring and pinkie move to the right) could be resolved in the collision detection algorithm by adding force to move the adjacent fingers appropriately. However, this needs to be implemented in the dynamic mode with the correct mass and force settings.

5.2.1.6. Thumb Abduction and Roll DoFs

The thumb virtual model is limited to four DoF – IP, MCP, abduction and roll – so the mechanisms to calibrate the thumb are more condensed. The abduction, MCP and roll are cross-coupled together, while the others are independent. In addition, the thumb abduction is independent from the adjacent finger's movement and can be calculated simply by using the abduction sensor 1, as in equation (5-22):

$$
\begin{cases}
Thumb\_Abd\_DOF = \left(g_{abd_t} * \sigma_{abd_t} + g_{abd_{roll_t}} * \sigma_{roll_t} + \ddot{\Theta}_{abd_{roll_t}} \right) + |k_{lt} * \sigma_{lt} * \varpi_{lt}| \\
Thumb\_Roll\_DOF = \left(g_{roll_t} * \sigma_{roll_t} + g_{abd_{roll_t}} * \sigma_{abd_t} + \ddot{\Theta}_{abd_{roll_t}} \right) + |k_{lt} * \sigma_{lt} * \varpi_{lt}|
\end{cases}
\tag{5-22}
$$

Where g_{abd_t}, g_{roll_t} are non cross-coupled gains; $\sigma_{roll_t}, \sigma_{abd_t}$ are values for the thumb abduction sensor 1 and roll sensor; $g_{abd_{roll_t}}$ is the cross-coupled gain for the thumb abduction and roll sensor; k_{lt} is the cross parameter for the thumb flexion sensor; σ_{lt} is the thumb flexion sensor; ϖ_{lt} is the ratio to convert from flexion variation to abduction variation; and $\theta_{abd_{roll_t}}$ is the combination offset value of the thumb abduction and roll sensors.

Algorithm code for calibrating the thumb abduction DoF

1: **// calibrating the abduction DoF**
2: **if** $DOF\_nb == Thumb_{Abduction}$
3:      $ratio = \dfrac{Abd\_Sensors[1](max_{Thumb\_MCP\_Flexion}) - Abd\_Sensors[1](min_{Thumb\_MCP\_Flexion})}{max_{Thumb\_MCP\_Flexion} - min_{Thumb\_MCP\_Flexion}}$
4:
     $Flex\_Sensor\_Variation =$
     $k_l * \left(Abd\_Sensors(MCP_0)[1] - Abd\_Sensors(MCP_{max})[1] \right) * ratio$
5:      $abdIndValue = slopeValue_{abd} * Abd\_Sensors[DOF\_nb] + interceptValue_{abd}$
6:      $rollIndValue = slopeValue_{roll\_abd} * Roll_{Sensor} + interceptValue_{roll}$
7:      **if (** $min_{abdIndValue} \le abdIndValue \le max_{abdIndValue}$ **)**
8:
     $DOF[DOF\_nb] = abdIndValue + rollIndValue + abs(Flex\_Sensor\_Variation)$
9:      **end**
10:    **end**
11: **end**

1: **// calibrating the roll DoF for thumb**

2: **if** $DOF\_nb == Thumb_{Roll}$

3: $\quad ratio = \dfrac{Roll\_Sensor(max_{Thumb\_MCP\_Flexion}) - Roll\_Sensor(min_{Thumb\_MCP\_Flexion})}{max_{Thumb\_MCP\_Flexion} - min_{Thumb\_MCP\_Flexion}}$

4:

$\quad Flex\_Sensor\_Variation = k_l * \left(Roll\_Sensor(MCP_0) - Roll\_Sensor(MCP_{,max})\right) * ratio$

5: $\quad abdIndValue = slopeValue_{abd\_roll} * Abd\_Sensors[1] + interceptValue_{abd}$

6: $\quad rollIndValue = slopeValue_{roll} * Roll\_Sensor + interceptValue_{roll}$

7: $\quad$ **if (** $rollIndValue \leq rollIndValue \leq max_{rollIndValue}$ **)**

8:

$\quad DOF[DOF\_nb] = rollIndValue + abdIndValue + abs(Flex\_Sensor\_Variation)$

9: $\quad$ **end**

10: **end**

11: **end**

5.3. Calibration Process in the Virtual Simulator

In order to implement the above calibration method, the following configurations are performed on the virtual simulator.

The calibration process is performed using the CyberGlove® device and the virtual reality system. The VR system includes the virtual hand simulator and the graphical display device, Dome®.

Descriptions of the device specifications and methods of application to the system are provided in the Experimental Chapter 4 – section 4.1.

In order to implement the calibration method in the virtual hand simulator, the following procedures are developed.

A new calibration dialog, Figure 5-4,created in the simulator menu that gives the option to either load an existing calibration file for the virtual hand model or to create new one.
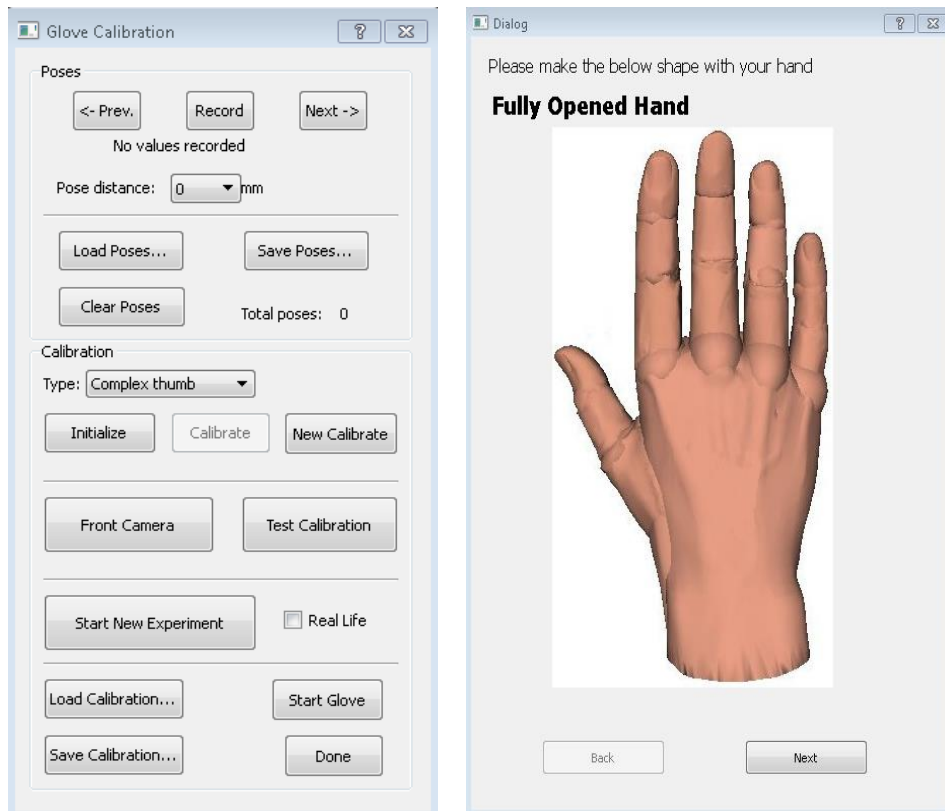
Figure 5-4 Configuration settings added to the simulator. (L) Calibration menu, showing list of options to select in order to toggle between poses, save them and load existing ones. Also gives option to perform a new calibration or load an existing one, and to start the experiment. (R) Calibration procedures displaying the posture with description.

The calibration application gives the option to repeat the posture again without exiting the process.

In order to make the calibration system dynamic and adjustable with the subjects' hand performance, a group of fifteen hand postures (Figure 5-5) are defined and presented in the graphical interface in a sequential order. These postures are carefully selected to include all the constraints and extensions of the joint movements, as well as the different features required to interact with objects.

In posture 2, the subject uses a round hand bolster to assist in forming the appropriate shape and different joint extensions.

It is important to note that each of the postures defined in Figure 5-5 addresses multiple DoFs and sensors. As previously stated, the DoF calculation is dependent on 1 or more sensors. The regression analysis is applied by using all the values of each particular DoF and

including the postures that involve movements on this DoF, or the associated sensors.
Figure 4-4 displays the sensors positions on the CyberGlove® data glove device.
For example, the thumb roll DoF uses the postures 0, 1, 12, 13 and 14 (Figure 5-5) to
calculate the calibration coefficient. A list of all the associations between the selected
postures and the multiple DoFs is presented in Table 5-1.

Table 5-1 List of the DoF with the associated postures that are used to calculate the LSR equation for the calibration method; the list shows the DoF of the cross-coupled sensors.

DoF	Posture
Thumb Roll	0,1,12,13,14
Thumb-Index Abduction/Adduction	0,1,2,3,4,5,7,10,11,13
Index-Middle Abduction/Adduction	0, 3, 4, 6, 9, 10,11
Middle-Ring Abduction/Adduction	0,3,4,7,9,10,11
Ring-Pinkie Abduction/Adduction	0,3,4,7,8,14

"Fully Opened Hand" (posture 0 in Figure 5-5) is used as a reference position for the sensors
and DoF angle values. The three postures, "Fully Opened Hand", "Fist: Thumb under Index"
and "Straight Fist" (Postures 0, 1 and 3), are used to find the cross-parameters of the
adjacent sensors. The postures used for the independent sensors are displayed in Table 5-2.

Table 5-2 List of the DoF with the associated postures that are used to calculate the LSR equation for the calibration method; the list shows the DoF of the independent sensors.

DoF	Posture
Thumb MCP	0,1,2,10,12,13,14
Thumb IP	0,1,2,10,12,13,14
Index MCP	0,10,11,12,14
Index PIP	0,2,9,10,11
Index DIP	0,1,2,9
Middle MCP	10,11,13,14
Middle PIP	0,1,2,9,11
Middle DIP	0,1,9
Ring MCP	0,2,10,14
Ring PIP	0,1,2,9,11
Ring DIP	0,1,9
Pinkie MCP	0,2,9,10,14
Pinkie PIP	0,1,2,9,11
Pinkie DIP	0,1,9

Figure 5-5 The fifteen postures used in glove calibration. Each posture represents the adequate extension/flexion of the sensors and DoF involved in the data glove and the virtual hand model.

5.4. Calibration Experimental Setup

To test the efficiency of the calibration performed, another group of six postures are implemented. This allows for comparison of the calibration coefficient indices between the two datasets.

Figure 5-6 shows the list of the postures used. These postures are selected from the calibration set in order to test the repeatability.

| Posture 0 Open Hand | Posture 1 Hook | Posture 2 Table Top |
| Posture 3 Straight Fist | Posture 4 Pinch | Posture 5 Fist |
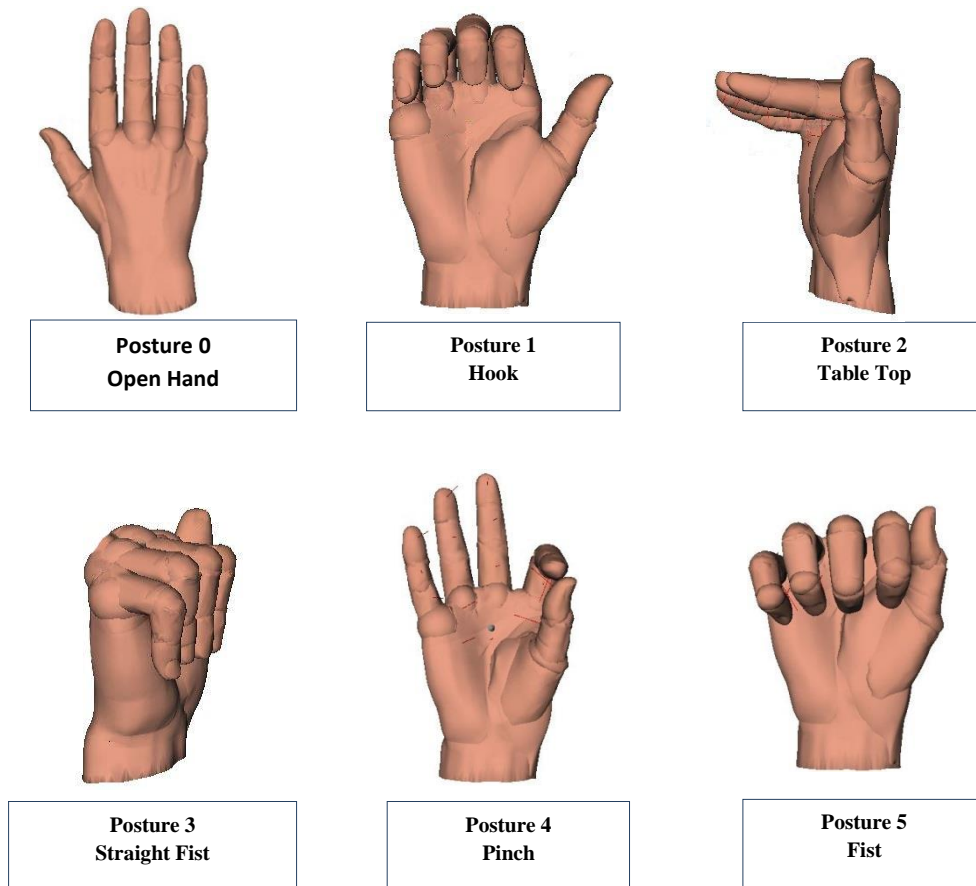
Figure 5-6 List of the six postures used in the experiment for testing the calibration

The list used to associate the six postures with the DoF is provided in Table 5-3.

Table 5-3 List of the DoF with the associated postures that are used in calculating the LSR equation of the test calibration method

DoF	Posture
Thumb MCP	0,2,4,5
Thumb IP	0,2,4,5
Index MCP	0,2,3,4,5

DoF	Posture
Index PIP	0,1,2,3
Index DIP	0,1
Middle MCP	2,3
Middle PIP	0,1,3
Middle DIP	0,1
Ring MCP	0,2,5
Ring PIP	0,1,3
Ring DIP	0,1
Pinkie MCP	0,1,2
Pinkie PIP	0,1,3
Pinkie DIP	0,1
Thumb Roll	0,4,5
Thumb-Index Abduction/Adduction	0,2,3
Index-Middle Abduction/Adduction	0,1,2,3
Middle-Ring Abduction/Adduction	0,1,2,3
Ring-Pinkie Abduction/Adduction	0,5

5.5. Calibration Experimental Protocol

The subject inclusion criteria used in the calibration experiment is the same as that defined for the hand assessment experiment in Chapter 4 Experimental – Section 4.2.

At the beginning of the experiment, the following measurements are performed: size of the hand, length of the finger joints, length of the arm, length of the forearm, height and weight of the subject.

During the experiment the subject sits in front of the graphical display screen and wears the CyberGlove® device on the right hand. A calibration display dialogue is then presented on the screen and the subject follows the procedures. Each step in the dialogue shows a screen shot of the virtual hand postures, along with a description. The subject is permitted to use the left hand, the table or other objects to help in forming the required posture. Clarification and assistance are provided by the operator where required.

Once the subject completes the shape, the operator manually moves the programme to the next hand posture. The process is performed only once and the calibration is saved under the subject's profile for use in the virtual hand control. The calibration process takes approximately 5 minutes.

Following the calibration, the subject forms the 6 test postures to validate the calibration.

5.6. Calibration Experimental Data Processing

Two sets of coefficient indices are produced by the calibration method. The first uses the postures set of the calibration, explained in section 5.3, and the second uses the newly implemented six postures.

ANOVA is used to test the inter-subject repeatability of the sensor readings between the subjects. The independent variable is each sensor and the dependent variables are the reading of the postures for the 10 subjects. The null hypothesis, of having no significant difference in the sensor values between subjects, is rejected when p < 0.01.

Also, before using the data glove device outputs it is very crucial to validate the consistency of the sensors readings. Hence, an ANOVA test is performed by testing the intra-subject repeatability of the data glove sensors readings for each subject. The dependent variables of the sensors' values are obtained from the 15 postures in the calibration tests. This is performed by grouping the postures with the same joint positions (see Figure 55).The null hypothesis, that there are no significant differences in the sensors' readings, is rejected when p<0.05.

The coefficient indices of both the initial and the test posture results are compared using the Pearson r-correlation method (David et al., 2015), described in Equation (5-23).

$$P\_r = \frac{\sum_{i=1}^{N}(U_i - \bar{U})(V_i - \bar{V})}{\sqrt{\sum_{i=1}^{N}(U_i - \bar{U})^2}\sqrt{\sum_{i=1}^{N}(V_i - \bar{V})^2}} \tag{5-23}$$

Where U is the initial posture DoF results, V is the test posture DoF results, $\bar{U}$ and $\bar{V}$ is the mean of the U and V results.

The LSR equation, mentioned previously in this chapter, is used in the calibration method to calculate the regression coefficient value between the different postures. However, the Pearson r-correlation in here is used to statistically test the efficiency of these calculated calibration values. It is then performed by comparing the subject's results between the initial postures set and the test calibration set.

5.7. Calibration Experiment Results

Table 5-4 shows the graphs for the grand average sensor values in each posture of the 15 included in the calibration. (The data table is shown in Appendix IV). The values range from

0 to 255 as they are converted from analogue to digital in the CyberGlove® interface unit.

The S6 sensor (Index PIP) has a mean average 226.12 (sensor values range [0-255]) across all postures (Table 5-5). This large value is seen all the subjects, with a standard deviation equal to 3.12.

In the graphs of posturers 0, 6 and 7, the S11 sensor, for the abduction of the index middle fingers, shows an increase in value as expected. However, an unexpected increase is shown on the S11 sensor in the graphs for postures 3, 5, and 8.

There is an increase in the sensors S7 to S14 in the graphs for posture 1 and 14, while in the graph for posture 11, an increase is seen on all sensors apart from S7, S14, and S15.

In the graph for posture 9, an increase in the sensor values is noticed on sensors S7, S9, S10, S11, S13 and S14, with smaller values for S1, S2, S3 and minimal increase on S4.

Table 5-4 Graphs of the grand average of the 22 sensors' values for all the subjects during the calibration process; the value range for sensors is from 0 to 255 (this is a raw value after it is converted from analogue to digital); the minor tick in the graph is '20'; the axes display range on all the graphs is from 0 to 260; the graphs are ordered by posture 0 to 14; the axis labels S1 to S22 are the sensor IDs, as listed in Table 5-5; the top right figure on each graph displays the corresponding posture; the values are displayed in a radar chart to simplify the visualisation as each axis is associated with a sensor.
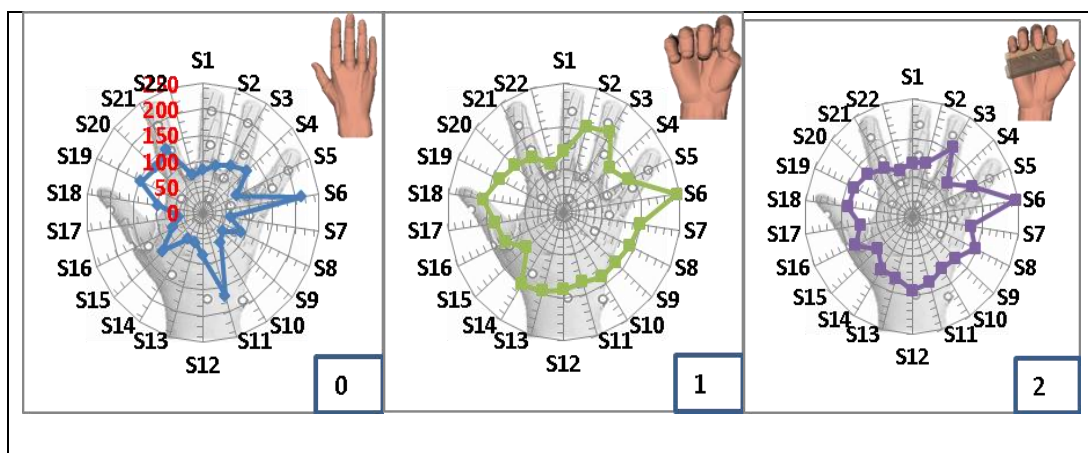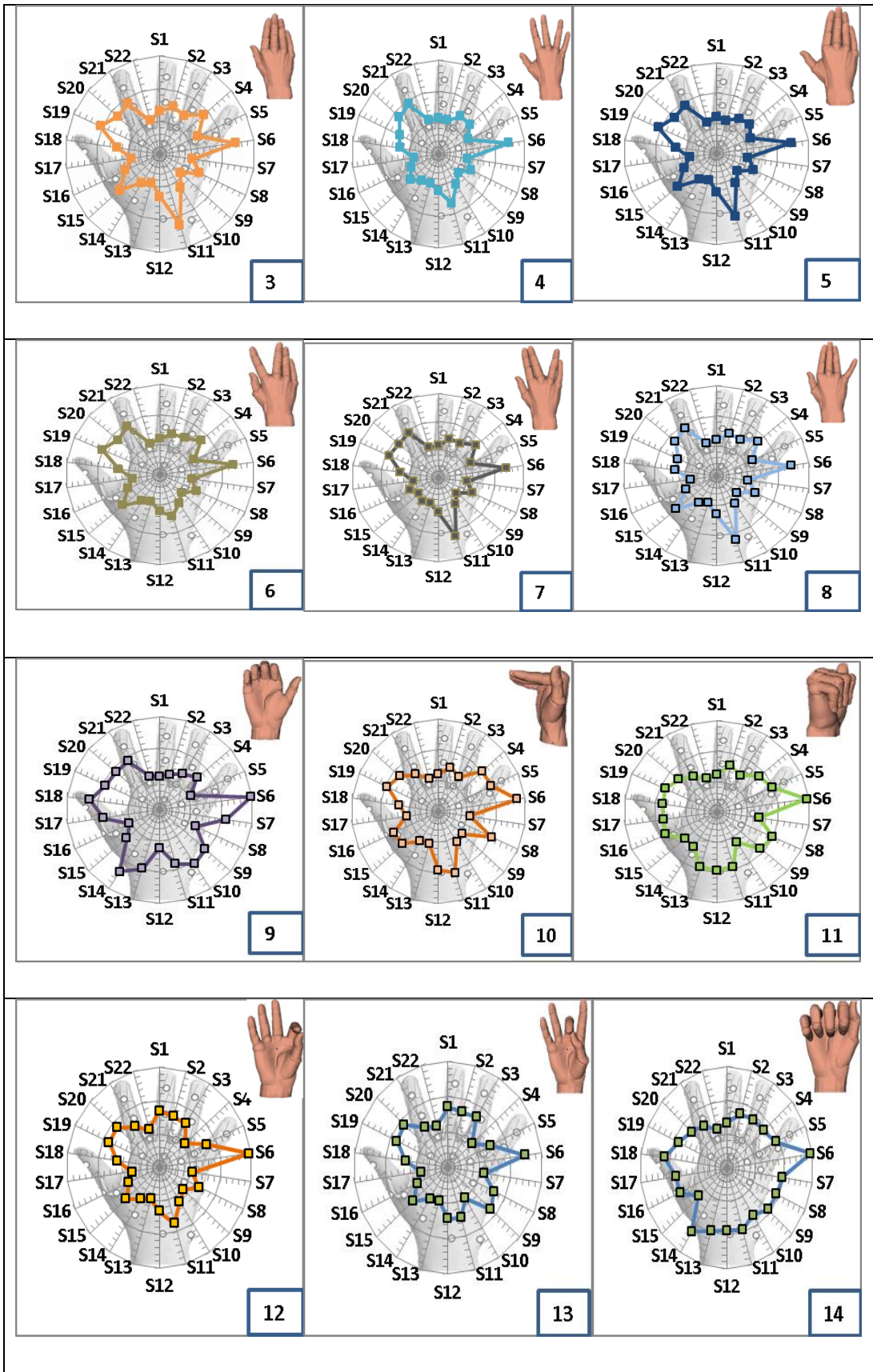
The visual test performances of the calibration virtual hand postures are displayed next to the real hand postures in Figure 5-7. A number of similarities are observed between the VR and real hand postures. The VR DoF shows flexibility in grasping the bolster roller, ball, and pen objects. The flexion-extension and abduction-adduction movements also show corresponding movements across all the postures.

VR Posture	Real Posture	VR Posture	Real Posture	VR Posture	Real Posture
C1		C2		C3	
C4		C5		C6	
C7		C8		C9	
C10		C11		C12	

Figure 5-7 The figures display 12 virtual hand postures compared to the real hand postures formed using the CyberGlove®. The bolster roller and ball objects are used to demonstrate the virtual hand model's flexibility in enacting the real hand movements. Each posture is compared to the real position opposite it.

Further examination of Figure 5-7 highlights that there are variations between the real and virtual hand in a number of postures. In (C1) the fingers in the virtual hand are separated horizontally in the abduction, while in the real hand they sit together. This is also seen in (C5) and (C7). In (C5) the middle finger of the real hand is rotated toward the thumb, while in the virtual hand no opposition can be seen. This is also apparent on the index finger in (C10).

The inter-subject repeatability test results are shown in Table 5-5. The table displays the ANOVA test p values for each sensor. Only the Thumb Rotate sensor (p = 3.84E-07), Palm arch (p = 2.21E-12), Wrist Flexion (p = 5.09E-08) and Wrist Abd (p = 1.08E-32) have

produced a significant difference between subjects. The Middle-Index Abd (p = 0.016055) and Ring-Middle Abd (p = 0.021733) showed low p values.

Table 5-5 The inter-subject repeatability ANOVA test of the data glove sensors between the ten subjects, during the calibration experiment. Highlighted in yellow results with significant variations p <0.01.

ID	Sensor	p Value
S1	Thumb Rotate	3.84E-07
S2	Thumb MCP	0.14784
S3	Thumb IP	0.534584
S4	Thumb Abd	0.363451
S5	Index MCP	0.648977
S6	Index PIP	0.987216
S7	Index DIP	0.953822
S8	Middle MCP	0.873575
S9	Middle PIP	0.999998
S10	Middle DIP	0.189112
S11	Middle-Index Abd	0.016055
S12	Ring MCP	0.986837
S13	Ring PIP	0.999688
S14	Ring DIP	0.971112
S15	Ring-Middle Abd	0.021733
S16	Pinkie MCP	0.907058
S17	Pinkie PIP	0.999976
S18	Pinkie DIP	0.986128
S19	Pinkie-Ring Abd	0.443237
S20	Palm arch	2.21E-12
S21	Wrist Flexion	5.09E-08
S22	Wrist Abd	1.08E-32

Furthermore, the intra-subject repeatability of the data glove sensors results for each subject is shown in Table 5-6. The p values for the ten subjects are much higher than 0.05.

Table 5-6 Intra-subject repeatability ANOVA test results of the data glove sensors for each subject.

Subject	p Value
Subject 1	0.958984
Subject 2	0.998382
Subject 3	0.990565
Subject 4	0.96381
Subject 5	0.895592
Subject 6	0.991092

Subject 7	0.934066
Subject 8	0.99748
Subject 9	0.966978
Subject 10	0.899843

The Pearson-r coefficient values calculated for both the calibration and test postures set is presented in Table 5-7, with a chart display of the variations in both values. The results show high correlation between the coefficient values, with an average of ρ = 0.795 for the calibration postures phase and ρ= 0.8415 for the test postures phase. The mean difference between the two sets is 0.0465.

Table 5-7 Table of the calibration coefficient values for the calibration and test postures set for each subject. Also presented with a histogram chart.

	S1	S2	S3	S4	S5	S6	S7	S8	S9	S10
Calibration Set	0.844	0.74	0.84	0.871	0.833	0.747	0.735	0.793	0.724	0.823
Test Set	0.98	0.869	0.726	0.809	0.723	0.905	0.887	0.836	0.785	0.895
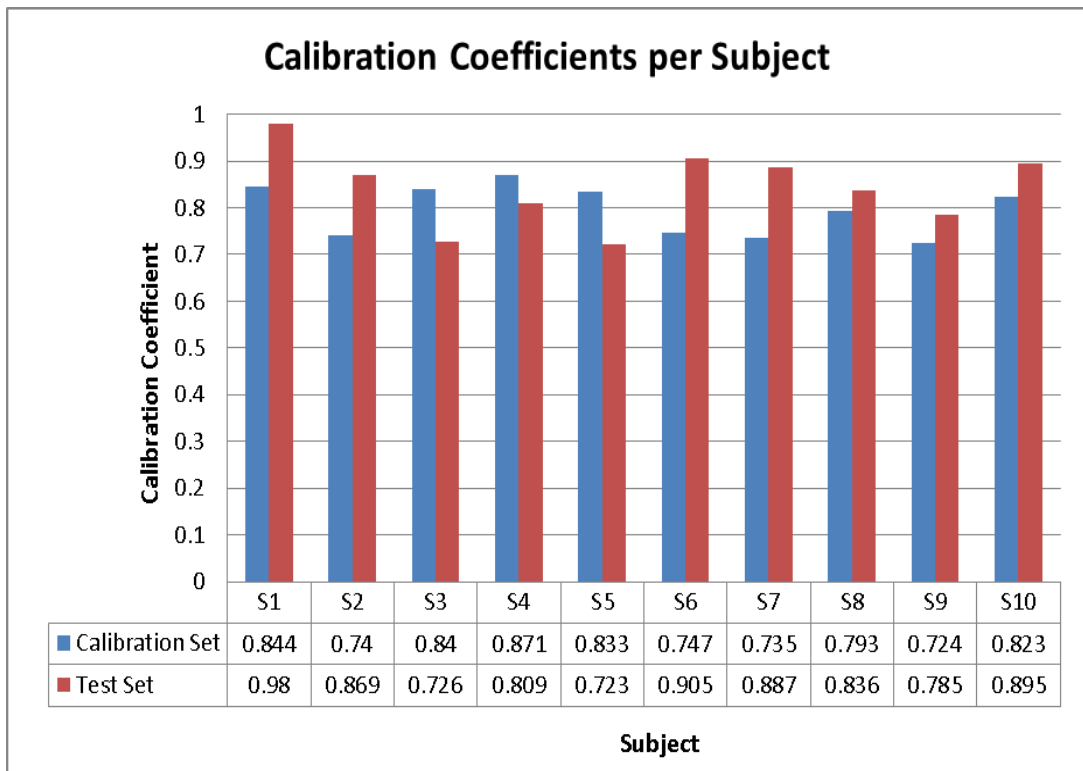
5.8. Calibration Experiment Discussion

Although there are variations in the subjects' hand sizes, the calibration method is seen to be adaptive and efficient in calibrating the sensors' data and registering it into the virtual hand model DoFs.

The large values returned on sensor S16, in Table 5-4, is due to the gain values that are pre-configured in the interface unit of the Cyberglove®. The unexpected increase in the abduction sensor, S11, for the index and middle fingers is because it is cross-coupled with the adjacent sensors. This is also shown for the ring and middle abduction sensor in the graphs of the postures 5, 6, and 8.

The cross-coupled sensor variations have been previously discussed in the calibration method approach, section 5.2.

These equations are validated in the comparison provided between the virtual hand postures and the real hand postures. Many visual-similarities are observed in the virtual hand control and flexibility of the DoF to grasp objects of different shapes. These closely resemble real hand movements.

The variation highlighted in Figure 5-7, on the abduction joints between the real and virtual hand in (C1), (C5) and (C7), is due to the virtual hand model design rather than the calibration. This is because the virtual hand's fingers are not attached to each other in the hand position when abducted. The variation whereby the index and middle fingers do not rotate opposite to the thumb, in (C5) and (C10), is due to limitations of the data glove sensors in measuring this DoF. The rotation of the finger can be compensated for in the virtual hand model by using the normal hand kinematic, but discrepancies can still be seen between the virtual displays and the actual hand movement.

The data glove sensors' reliability was validated using inter-subject repeatability tests on the values recorded. Most of the sensors showed no significant difference, with $p < 0.05$, apart from the ring Thumb Rotate, Palm arch, Wrist Flexion and Wrist Abd sensors. These variations are mainly introduced by the different palm sizes between the subjects that cause the glove to over stretch on the palm, regardless of the lengths of the fingers. The last three sensors are not included in the hand assessment classifications for my project analysis, as the fingers used are the Index, Middle and Thumb. Also the Thumb Rotate is not included in the virtual hand model as the DoF depends on the Thumb Abd only, and finger performance calculation uses the Thumb MPC, IP and Abd only (see section 4.3.1.2.1). Thence, this variation has no effect on the outcome measurements.

On the other hand, the intra-subject repeatability test showed high consistency in the sensors' readings for all subjects with p values greater than 0.89. This indicates that sensors' readings are consistent and have high repeatability for performing data analysis.

The calibration coefficient measurement showed high-correlations between the calibration postures group and the test group. The mean difference between the both groups' coefficient indices is 0.045. The high coefficient indices (average >0.8) demonstrate high reliability in the data glove measurement for repeating postures or forming new ones.

The experiment results have demonstrated that the proposed calibration method is efficient and adaptive to the subject's hand variations. Unlike the other methods, this approach only takes 5 minutes to process and does not require any pre-generated machine learning training datasets. This method is also designed with a virtual reality system that makes the process dynamic and automated.

5.9. Summary of the Calibration Chapter

This chapter started by reviewing the existing calibration methods for the data glove, including neural network, genetic algorithm, and regression analysis. Later, the advantages and limitations of these methods in relation to the project aims and system applicability was discussed. Following this, an advanced calibration method was provided, based on the regression analysis. This included the different finger movement constraints and sensor dependencies. The method uses a dynamic procedure that incorporates an adaptive set of postures to measure the different constraints of the hand.

The calibration was validated by comparing the results from the initial postures to another test set. The result showed high inter-subject repeatability across all the sensor readings, and high correlation between both sets' indices. The mean correlation difference was less than 0.05.

Chapter 6 Results

The proposed method for the project is different from other approaches as it includes new measurement methodologies and technological devices. The applied validation and verification process uses a different procedure (described in Experimental Chapter 4) from the analytical methods currently available for hand rehabilitation. This approach rather focuses on verifying the efficiency and reliability of the system in hand assessment.

This chapter presents the results obtained from all the subjects in the experiment. It starts by listing the subjective assessment criteria for the subjects' performance during the experiments, including the level of motivation and skills in interacting with the system. It then presents the objective measurement for the fingers' performance, known in the project as finger performance value (FPV). The statistical analysis results are given for the various methods used to verify the data intra-subject repeatability, inter-subject reliability, and variability. This is followed by a description of the outliers and abnormalities in the subjects' 8 performance.

The chapter concludes with the EMG data results and analysis, and the overall hardware and software validation tests.

6.1. Subjective Assessment

The obtained subjective assessment, explained in section 4.3.1.2.4, showed that none of the subjects reported any technical (devices, VR impacts, motion sickness, etc.) or physical problems during the experiments. The users quickly adapted to the speed of the audio instructions, with fewer repetitions required to learn the tasks' steps as the experiment progressed.

The subjects gave positive feedback on the VR interface, finding it 'user friendly' and immersive. It included both assistive interaction methods and perspective projections for both subject and front views. The front camera was used during the performance of fine finger movements to assist with accurately grasping the virtual objects.

The remarks from each subject are listed below. The notes describe the level of interaction with the system and other subjective factors:

Table 6-1 User subjective assessment notes

Subjects	Motivation	Compliance with the Instructions	Notes
1	High	High	
2	High	High	
3	Average	Average	Found tremor session unpleasant, but completed without noticeable issues.
4	Low	Average	
5	Average	Average	
6	Average	Low	In the VR, the subject was not accurately grasping the virtual objects, the fingers were flexing in some trials inside the shape of the objects.
7	Average	High	Found tremor session unpleasant, but completed without noticeable issues.
8	Low	Low	Middle finger DIP sensor did not perfectly fit on the subject's finger. In the VR sessions, the subject did not follow the audio instructions, but rather waited for the graphical rendering to move the virtual arm. The subject then complied with the task procedures. The subject did not fully extend the hand and fingers when coming back to the relax position.

Subjects	Motivation	Compliance with the Instructions	Notes
9	High	Average	Index finger DIP sensor did not perfectly fit the subject's finger. The sensors were extending when the subject grasped the object due the gap in the tip of the glove for the index finger. In the VR, the subject was not accurately grasping the virtual objects. In some trials the fingers were flexing inside the shape of the objects.
10	High	High	Subject detected the patterns of the tasks and the sequence of the objects. However, in the VR session the subject was focusing more on the hand formation in the model.

The 'motivation' rank is calculated from the subject's concentration, their interaction level with the system and their compliance with the instructions. During the experiment, the motivation generally varies from high to low; low is inattentive and unmotivated, usually bored; average is attentive and motivated. The motivation is defined by the level of attention and immersion while performing the tasks in the VR environment.

'Compliance with the instructions' is the level of careful consideration taken by the subject to perform a task with accurate fine movements. Subjects might not express high motivation but still show high attention to the task timing and finger formations. High is very compliant with the instructions, average is following the instructions to a standard level, and low is not following the instructions at all. The latter could be due to tiredness, boredom, or very quickly picking up the patterns in the experiment's tasks.

6.2. Objective Assessment

The objective measurements of the results are provided below. It begins by detailing finger performance results, and followed by the EMG measurement and analysis.

In this section, the fingertip displacement is displayed in 2D and 3D, along with the inverse kinematic of the grand average subject performance. The grand average finger performance value (FPV) is then displayed with reference to all the tasks, sessions and fingers' involvements. Finally, the analytical methods are displayed. It lists the correlation values between 'VR' and 'RL' FPVs, the intra-subject repeatability of the FPVs grand average, and the inter-subject reliability across the group.

It is important to note that in the data analysis, the finger joint displacement assumption is Gaussian distribution.

6.2.1.1. Fingers Tip Vertical Displacement

The finger joint's lengths, presented in Table 6-2, are used to obtain the mean average lengths of all subjects finger's joints, which are implemented in the fingertip position calculation method. This helps to compare between individual subjective performance and the grand average length.

Table 6-2 Distance between the Joints of three fingers (Index, Middle and Thumb); the unit is cm. "tip" is the tip end of the finger.

Subject	Joints	Index	Middle	Thumb
1	MCP - PIP	6	7	5
	PIP - DIP	4	5	5
	DIP - "tip"	3	3.5	4
2	MCP - PIP	5	5	4
	PIP - DIP	3	3	4
	DIP - "tip"	2	3	3
3	MCP - PIP	4	5	4
	PIP - DIP	2	3	4
	DIP - "tip"	2	2	3
4	MCP - PIP	4.5	4.5	3
	PIP - DIP	2.8	3	3
	DIP - "tip"	1.9	2.1	2.9
5	MCP - PIP	5	6	4
	PIP - DIP	3	3	4
	DIP - "tip"	2	2	3
6	MCP - PIP	4	4.2	3.5
	PIP - DIP	2	2.5	3.5
	DIP - "tip"	2.1	2.3	2.8

Subject	Joints	Index	Middle	Thumb
7	MCP - PIP	5	5	4
	PIP - DIP	2	3	4
	DIP - "tip"	2	3	3
8	MCP - PIP	5	6	5
	PIP - DIP	3	4	5
	DIP - "tip"	2	2	3
9	MCP - PIP	4	4.3	3.7
	PIP - DIP	2.6	2.7	3.7
	DIP - "tip"	2.1	2.1	3.1
10	MCP - PIP	5	6	5
	PIP - DIP	3	4	5
	DIP - "tip"	2	3	3

The graphs in Figure 6-1 and Figure 6-2 show the displacement of the three fingertips. Each graph shows the fingertip displacement, in cm, during the performance of the task. The graphs show the four different tasks involved in the experiment, each raw represents a session conducted from the three fingertips (index, middle and thumb).
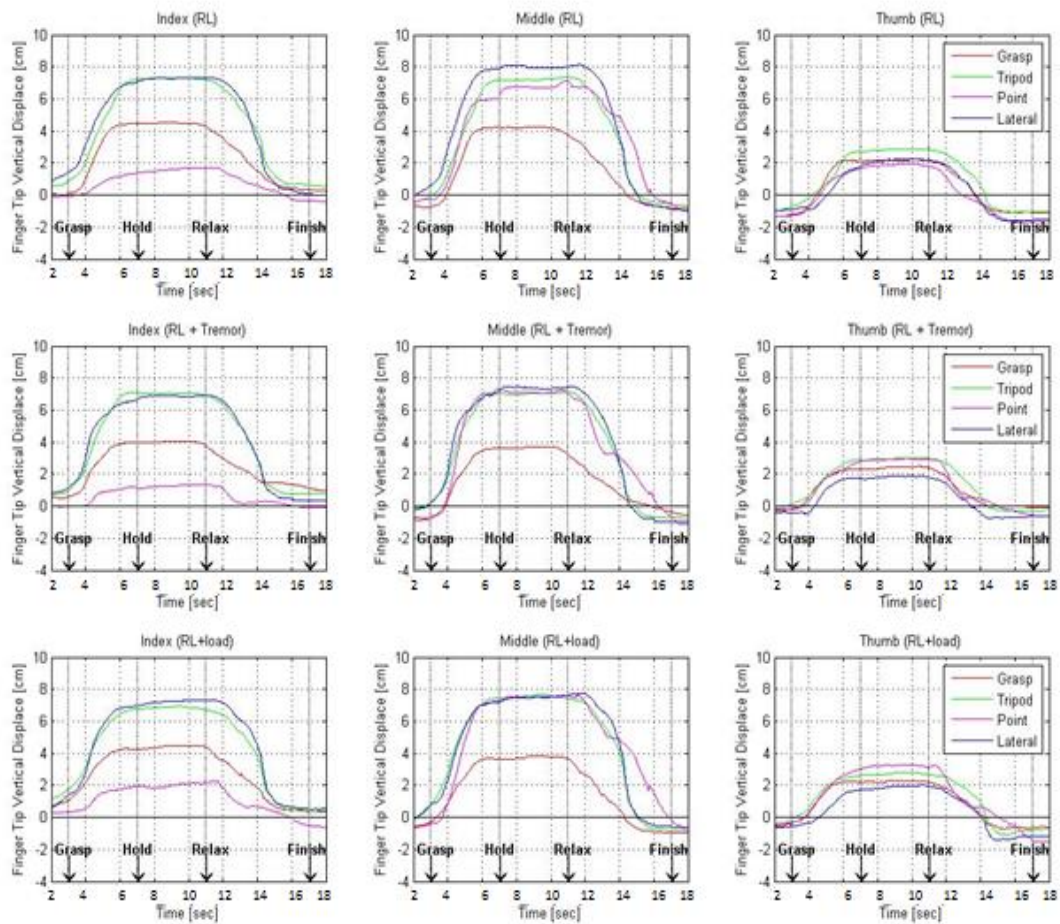
Figure 6-1Grand average of the three fingerstips' (index, middle and thumb) vertical displacement during the RL sessions of the experiment; each graph represents the finger movement in the four different tasks; the three graphs in the first raw represent the data during the real life session; second raw represent the real life with tremor session; and last raw represent the real life with load session.

The displacement is divided into multiple events that demonstrate the variation in the tip position over time. The hand starts from the relax position, increasingly flexing to grasp the object until it reaches the maximum finger flexion position. The hold phase stabilises the movement of the fingertips by holding the object in the last position. The task ends by relaxing the hand back to the start position and decreasing the flexion positions to the minimum. This variation is displayed consistently across the different sessions and tasks, which contributes to validating the efficiency of the recorded data in synchronising the fingers' movements and tasks' event occurrence.
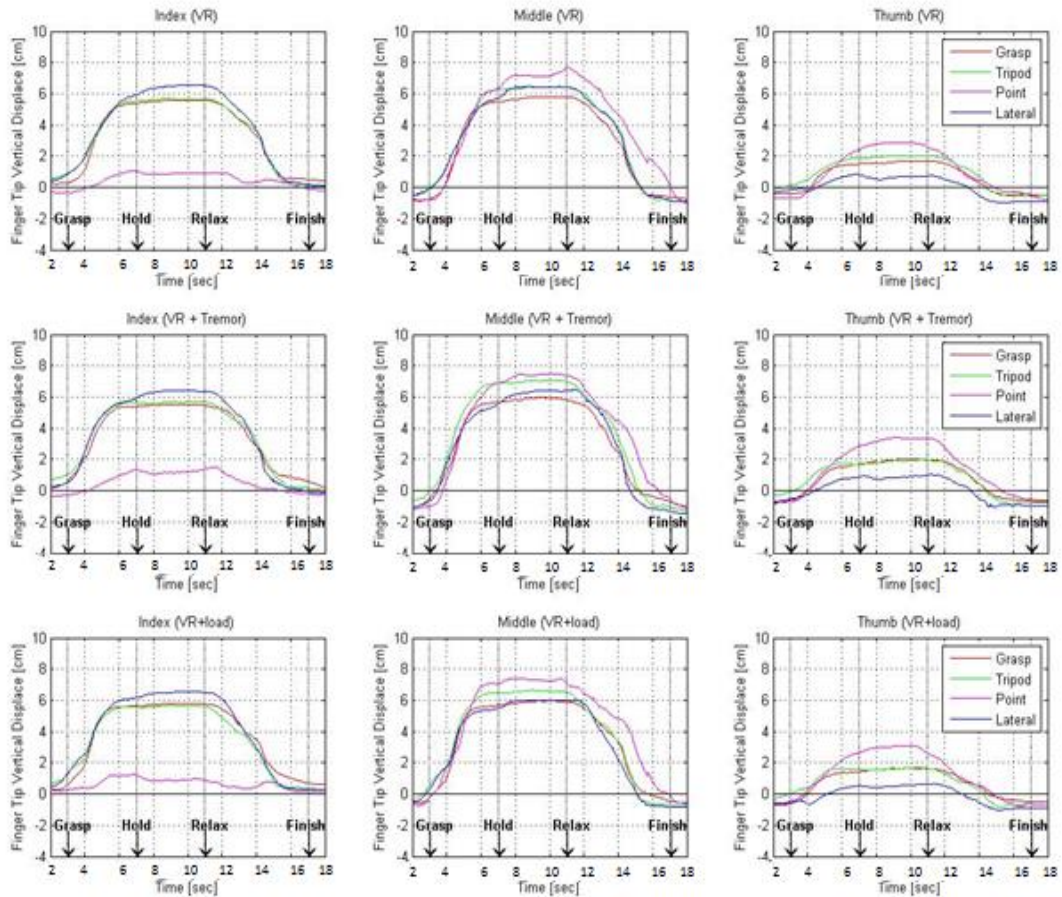
Figure 6-2 Grand average of the three fingertips' (index, middle and thumb) displacement during the VR sessions; each graph represents the finger movement in the four different tasks; the three graphs in the first raw represent the data during the virtual reality session; second raw represent the virtual reality with tremor session; and last raw represent the virtual reality with load session.

6.2.1.2. Fingertip's Displacement in 3D Representation

The presentation of the fingertips' displacement in 3D is based on the calculation of the fingers' inverse kinematic, using D-H parameters (see section 4.1.3.4).

In the following, the inverse kinematic method results for the 3 DoF (Figure 6-3) is provided. The finger joints' lengths are taken from the average of all the subjects' hand sizes, measured in Table 6-2. The graphs display the flexion positions during the trials for each task, where each finger's motion can be easily visualised and qualified in relation to the other two fingers. The level of contribution (flexion) during the particular task, and

association with the adjacent fingers can also be seen. The display shows the three fingers, ordered from top to bottom in the Z-axis (thumb, index, and middle), at certain positions of the simulation, modelling the average movement (blue points) in all the trials (red points).
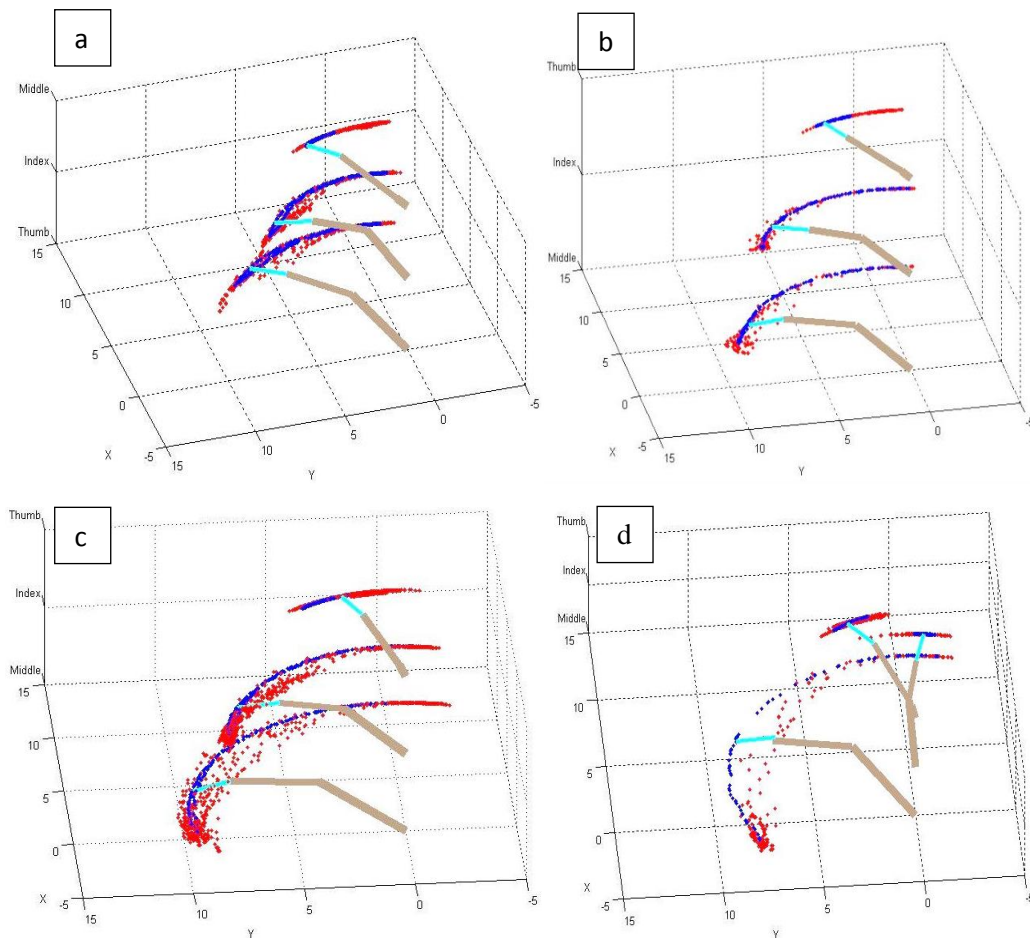
Figure 6-3 Simulation of the inverse kinematic for the three fingers (thumb, index and middle) during the four tasks: (a) Grasp Task, (b) Tripod, (c) Lateral Task, and (d) Point Task in Real Life session. Y-axis represents the horizontal displacement of the fingers in cm, X-axis is the vertical displacement of the fingers in cm; and Z-axis represent the finger displayed; each finger (middle, index, thumb) is displaced with three lines (joints); the red dots represent the grand average of the fingertip displacement; and the blue dots represent a single subject's average fingertip displacement (in this graph it is subject 1).

Figure 6-3 is extracted from a simulation during a specific time frame. The finger simulator is developed by the author in Matlab®, and can be configured with any dataset. Each graph displays the three fingers, which are represented by three lines: distal, middle and

proximal. The lines' lengths are configured by the subjects' average joint lengths, from Table 6-2.

This figure adds an extra perspective to interpret the finger displacement, as it represents the virtual replication of the subject's finger movement. This corresponds accordingly with the finger kinematics and displacement. Abnormal movements will reflect on the simulation and display a mismatch between the joints' line lengths and the tip position. The simulator distinguishes between the compact and the spread parts of the tip positions. This distribution of the tip positions represents the smoothness in the finger movements and the time taken to move from the start to the final position. For example, graphs (a) and (c) show more concentration of the red and blue dots at the end part of the middle and index movement, while this is spread in graphs (b) and (d). It also illustrates the distance travelled by each finger to perform the particular task and provides a comparison of the subject's performance with the total average. In all the graphs the subject's fingers movements closely match the average movement. The graph (c) in Figure 6-4 pinpoints that the subject's finger extensions are shorter than the total average.   The 3D representations of the fingertips' displacement, based on the above simulation, are produced below. This presentation visualises the covariance of the fingertips' movements. Figure 6-4 shows the index and middle fingertip movements in the "RL + Load" and "VR + Load" sessions. Tasks are displayed across the Z axis to highlight the level of finger flexion for each task, as well as the expected curve shape of the finger's motions in compliance with the kinematic (section 2.2).
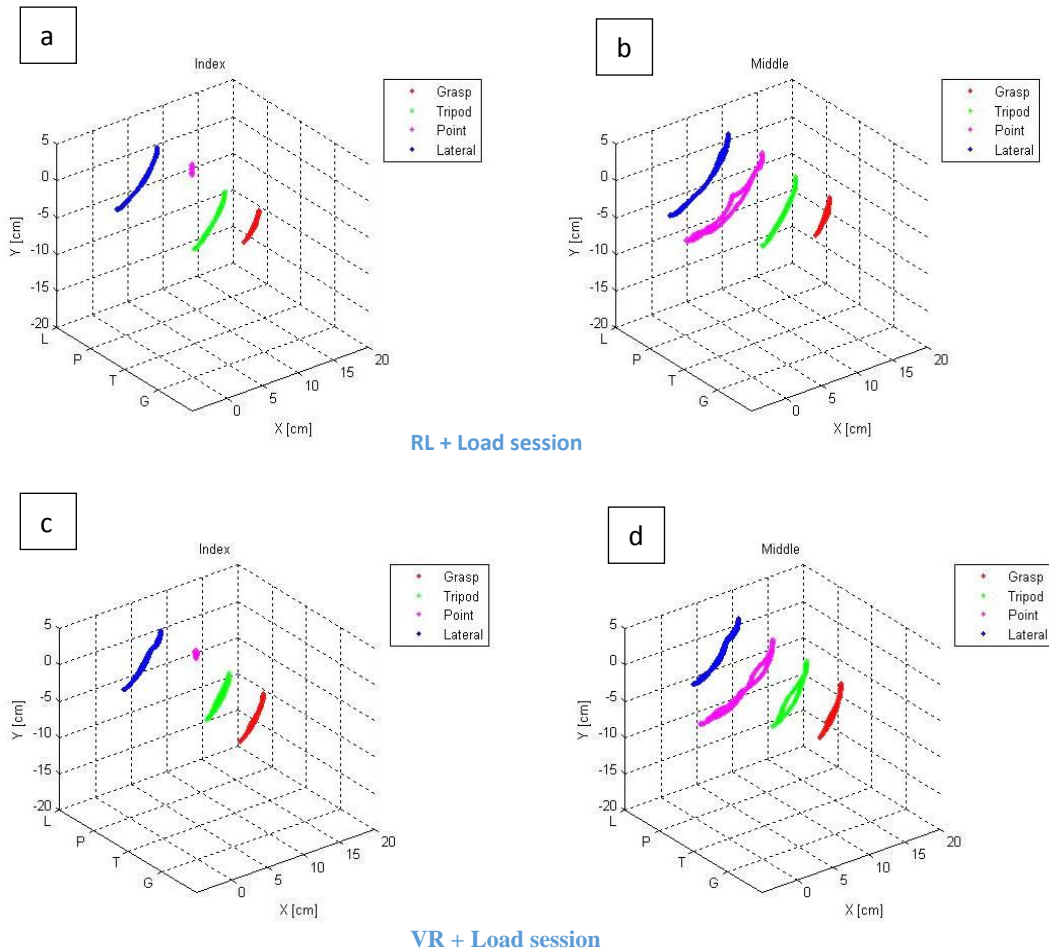
Figure 6-4 Grand average fingertip displacement in 3D space for the RL+Load and VR+Load sessions; Y-axis represents the vertical displacement of the fingertip in cm, and X-axis represents the horizontal displacement in cm; the left column shows the index finger and the right column shows the middle finger; each graph includes the four different tasks, displayed with different colors. (Red – Grasp, Green – Tripod, Magenta – Point, and Blue – Lateral)

 In Figure 6-4, the middle finger shows greater displacement than the index finger, especially in the point task (magenta). There appear to be variations in the middle finger displacement while moving to the destination position and returning to the start position; this is evident in the point task (magenta) in graphs (b) and (d) and tripod task (green) in graph (d). The tip position displacements, plotted in the 3D graphs, display a consistent arc shape between the different fingers and tasks.

184

6.2.1.3.Intra-subject repeatability of the Fingertip Displacement

To test the reliability of the data collected for DoF across the group, an intra-subject repeatability test is performed on the DoF angle values, using Pearson's r auto-correlation method (David et al., 2015).

Table 6-3 Intra-subject repeatability data test showing the grand average of auto-correlation values for each subject across the sessions and tasks. Highlighted in green the low correlations with values <0.5.

				Sessions				
			RL	RL + Tremor	RL + Load	VR	VR + Tremor	VR + Load
Tasks	Index	Grasp	0.728	0.639	0.677	0.542	0.561	0.562
		Tripod	0.873	0.880	0.898	0.857	0.864	0.801
		Point	0.624	0.472	0.414	0.528	0.313	0.209
		Lateral	0.882	0.870	0.874	0.808	0.861	0.837
	Middle	Grasp	0.680	0.497	0.572	0.534	0.538	0.562
		Tripod	0.877	0.883	0.907	0.861	0.881	0.830
		Point	0.709	0.743	0.739	0.715	0.684	0.708
		Lateral	0.884	0.864	0.865	0.810	0.834	0.812
	Thumb	Grasp	0.504	0.643	0.768	0.777	0.666	0.504
		Tripod	0.780	0.775	0.762	0.685	0.619	0.374
		Point	0.808	0.418	0.690	0.548	0.744	0.719
		Lateral	0.760	0.759	0.826	0.615	0.652	0.510

The results displayed in Figure 6-5 and Table 6-3 show high confidence in the level of repetition between the tasks and sessions. The minimum value of ρ was noted on the Point Index task through the ''VR+Tremor'' and ''VR+Load'' sessions (ρ = 0.313 and ρ = 0.209 respectively), and Tripod Thumb task in the ''VR+Load'' session (ρ =0.374). However, in average, the ρ value of the Point Index results is remarkably smaller than the other tasks with the same and different finger (Point Index average ρ for all session = 0.426). The RL and VR sessions with normal movements show large ρ (0.624 and 0.528 respectively).

Furthermore, Table 6-3 shows that the average correlation value for the tasks in the "RL" session is 0.76, the average for "RL + Tremor" session is 0.704, "RL + Load" session average is 0.749, "VR" session average is 0.69, "VR + Tremor" session average is 0.685, and "VR + Load" session average is 0.619. The total average of correlation, for all the sessions, tasks and fingers, is 0.7.

The lowest average correlation is observed whilethe index finger in the point task, during the RL and VR with tremor and load sessions.

The ρ averages for the ''RL'', ''RL+Tremor'', ''RL+Load'' sessions are larger than the ''VR'', ''VR+Tremor'', ''VR+Load'' sessions ranging from 0.02 to 0.13 differences. Both the ''RL'' and ''VR'' average ρ values are bigger than the rest of sessions with Tremor and Load. However, in the VR sessions, it is noted that the ''VR+Load'' is smaller than then ''VR+Tremor'' (by approximately 0.06), while RL's are opposite as the ''RL+Tremor'' is smaller than the ''RL+Load ''(by approximately 0.045).

The data is also presented in Figure 6-5. This displays the box plot of the auto-correlation average for both the VR and RL sessions. The negative outliers are the effects of abnormality from subject 8's fingers' performance.
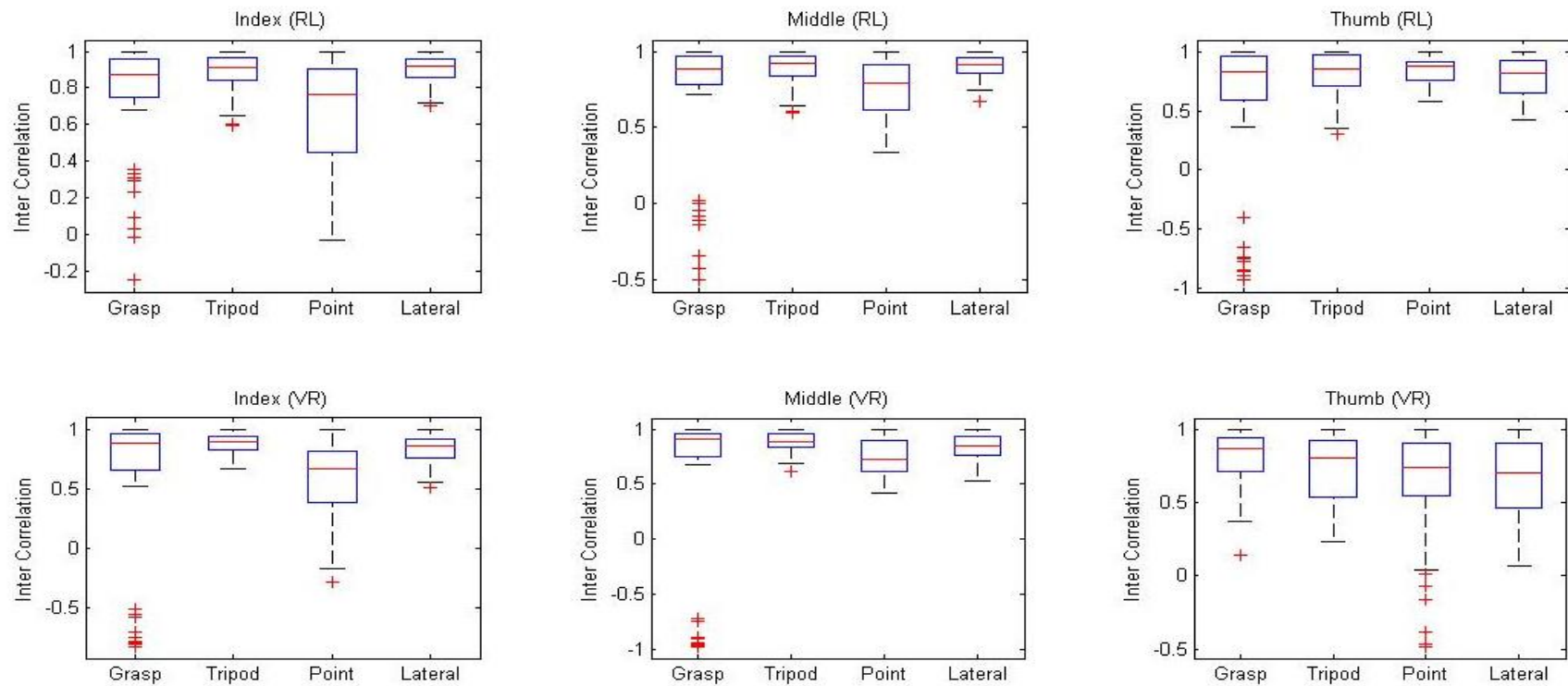
Figure 6-5 Box plot of FPV Grand average intra-repeatability of all subjects values for the RL and VR sessions of the three fingers;

As previously describe, the FPV values illustrate the acceleration level in the fingers' formation, smoothness in following certain trajectory, stability of the fingers in hold status, level of contributions of the three fingers in performing certain tasks, speed of the movement and the fatigue effect.

The total grand average results of finger performance value (FPV) are shown in Figure 6-6. These values are also shown metrically in Table 6-4.The FPV value calculates the performance of each finger in each task by considering the speed, time, smoothness and stability of the finger's performance.

The maximum speed value used for normalisation is 6 cm/s (see chapter Experimental section 4.3.1.2.1 for clarification). The maximum smoothness value calculated from the experiments in this study (including tremor and load) is 4cm, and the maximum stability is 5.5 cm. The calculation of the maximum values for the smoothness and stability excludes the outlier values in the experiments because they were due to incorrect measurements taken while the subject was not following the instructions.

Therefore, the maximum FPV value is 23.25 and the minimum value is 0. The minimum speed is 0 and minimum smoothness and stability is 0.008.

The minimum-maximum threshold is displayed in Figure 6-6 as a red dotted line in each histogram graph.

The benchmark data for the RL session varies between the minimum 0 and maximum 23.5, consistent with the fingers' contributions and normal task performance for the group.
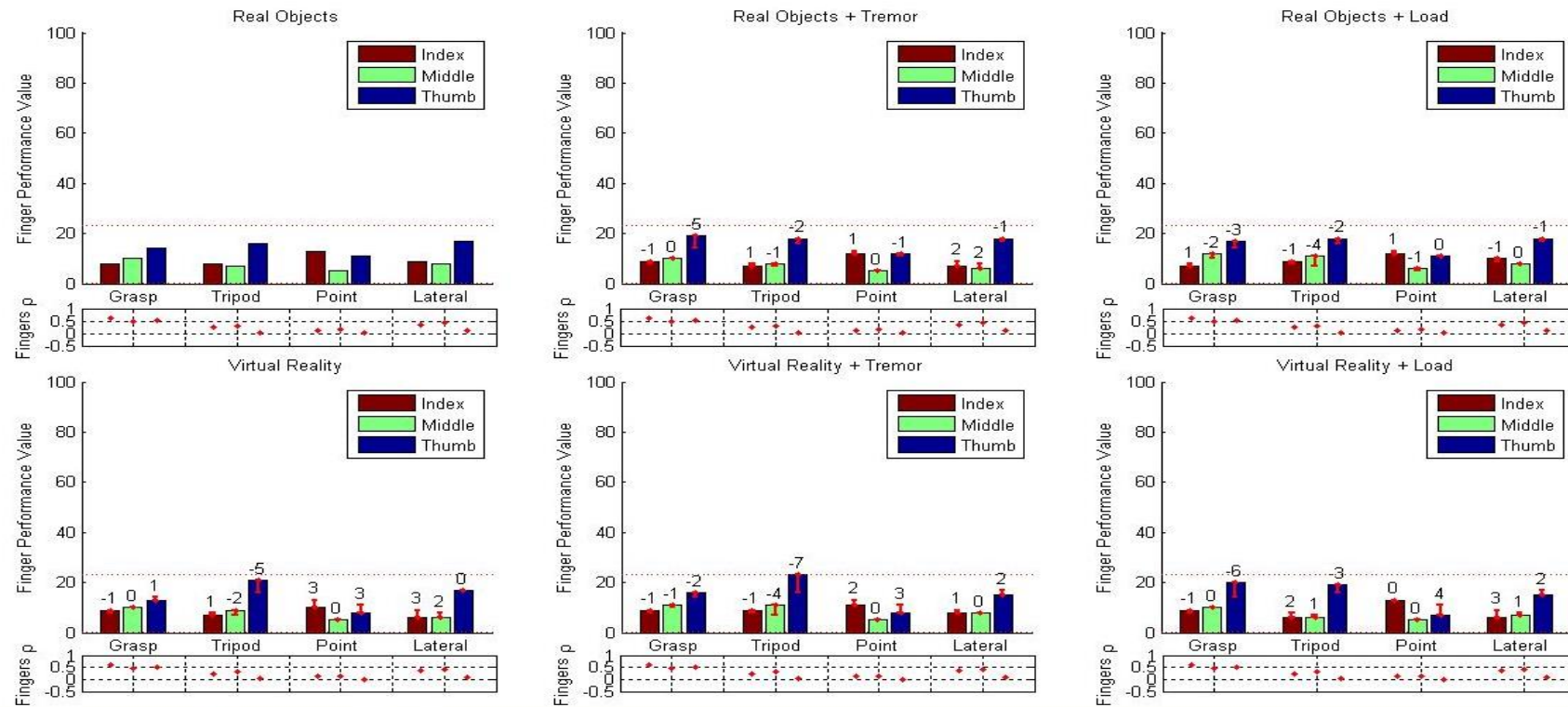
Figure 6-6 Grand average of finger performance values; each graph represents the results for each session of the experiment. The bar colour indicates the finger measured. Data are distributed into four sections representing the tasks (Grasp, Tripod, Point, and Lateral). The dotted line in each graph represents the maximum value of the FPV. The charts below each graph show the cross-correlation value for each finger, representing the level of contribution of the finger in the performance of the task. The red lines display the difference from the benchmark value, which is also noted numerically above each bar. Y-axis is the FPV value and the X-axis is the fingers (coloured red for index, green for middle and blue for thumb) distributed on the four tasks (Grasp, Tripod, Point and Lateral). The graphs are for each session RL, RL+Tremor, RL+Load, VR, VR+Tremor, VR+Load.

On average, the FPVs of the grasp task vary from 7.5 to 9.4 for index, 9.6 to 12.4 for middle, and 13.3 to 19.5 for thumb. The tripod FPVs vary from 5.6 to 8.8 for index, 6.3 to 11.5 for tripod, and 15.8 to 23.2 for thumb. The point FPVs vary from 10 to 13.4 for index, 5 to 6.5 for middle, 7.3 to 12.1 for thumb. The lateral FPVs vary from 6.1 to 9.6 for index, 6.2 to 8.4 for middle, and 15.3 to 18.3 for thumb.

The RL data results are used as the benchmark for all the sessions' data values.

The grand average of the FPVs for all the three fingers varies in an ascending sequential order across all the sessions. In terms of the total average, the thumb FPVs are higher than the middle FPVs, and successively higher than the index FPVs. Moreover, the thumb has higher FPVs than the index and middle fingers, while the FPV for the point task is smaller than the others.

Table 6-4 Grand average of the Finger Performance Value Data. Colour coded by the Finger (Red –Index, Green-Middle, Blue-Thumb).

Last four columns are the subtraction between the different sessions. The last row is the average

Tasks			RL	RL + Tremor	RL + Load	VR	VR + Tremor	VR + Load	Finger Task Contribution	RL + Load-RL	VR + Load-VR	RL + Tremor-RL	VR + Tremor-VR
	Index	Grasp	7.9	9.3	7.5	8.7	9.4	8.5	0.61	-0.24	-0.12	0.85	0.42
		Tripod	8	6.9	8.8	6.8	8.6	5.6	0.24	0.19	-0.29	-0.26	0.43
		Point	12.6	12.1	12.3	10	11	13.4	0.11	-0.03	0.38	-0.06	0.11
		Lateral	8.4	6.8	9.6	6.3	8.3	6.1	0.36	0.43	-0.07	-0.57	0.71
	Middle	Grasp	10.1	10.3	12.4	10.2	11.1	9.6	0.47	1.08	-0.28	0.09	0.42
		Tripod	7.1	7.6	11	9	11.5	6.3	0.31	1.20	-0.83	0.15	0.77
		Point	5.5	5.3	6.5	5.1	5	5.1	0.14	0.14	0.00	-0.03	-0.01
		Lateral	8.4	6.4	8.2	6.2	8	6.7	0.41	-0.08	0.21	-0.82	0.74
	Thumb	Grasp	14.5	18.5	17	13.3	15.9	19.5	0.50	1.25	3.11	2.00	1.30
		Tripod	15.8	18.3	18.5	21.2	23.2	19.56	0.04	0.11	-0.06	0.10	0.08
		Point	10.4	12.1	11.2	8.1	8.3	7.3	0.01	0.01	-0.01	0.02	0.00
		Lateral	16.7	18	18.3	17.3	15.4	15.3	0.10	0.16	-0.20	0.13	-0.19
		Average	10.45	10.97	11.78	10.18	11.31	10.25		0.35	0.15	0.13	0.40

The three 'VR' sessions show very close similarities with the 'RL' sessions, where the 'RL'-'VR' graph (shown in Figure 6-6), of the total FPV average between both sessions, returns very low mean difference of '1.73' and Standard Deviation of '1.42'. However, this difference increases insignificantly in the Tremor sessions, with mean '2.08' and Standard Deviation '1.51', and the Load sessions with mean difference 2.47 and Standard Deviation 1.25.

The 'Tripod' Thumb FPV showed larger difference than the rest, mainly due to the difficulty in visualising the VR position of the thumb in accordance with the Tripod shape object. While the 'Tremor' graph shows small differences of 2.08 averages, the 'Load' graphs, on the contrary, shows bigger differences with 2.47 averages. Furthermore, the 'VR + Load' has lower mean FPV (10.25) than the 'RL + Load' (11.78).

In addition, the total average of the FPVs per sessions shows a similar dispersal to the intra-subject reliability data, as the RL average of the FPVs is smaller than the 'RL+Tremor' and, consecutively, than the 'RL+Load'. However, the VR average FPVs is smaller than the 'VR+ Load', but the 'VR+Tremor' is smaller than the 'VR+Load' and bigger than the VR.

The mean difference of the 'RL' with the 'RL+Load' is 0.35, the 'RL' with the 'RL+Tremor' is 0.13, the 'VR' with the 'VR+Tremor' is 0.4, the 'VR' with the' 'VR+Load' is 0.15, shown in Table 6-4. This is calculated by averaging the difference between the two sessions, then multiply it with the contribution index, listed under the Finger Task Contribution column. The level of correlation of the FPVs data between sessions is presented in Table 6-5. This is mainly to test the relation between VR and RL sessions and verify the system variability. This variation is also presented in Figure 6-7, Figure 6-8 and Figure 6-9.

Table 6-5 Correlation of FPV grand average values between the different sessions

Correlation	RL + Tremor	RL + Load	VR	VR + Tremor	VR + Load
RL	0.7277	0.5754	0.3864	0.4652	0.5658
RL + Tremor	-	0.7375	-	0.4604	-
RL + Load	-	-	-	-	0.5886
VR	-	-	-	0.6201	0.6461
VR + Tremor	-	-	-	-	0.6821

Table 6-5 lists the correlation of FPV grand averages between different sessions. The sessions are contrasted based on the results from the same group, if they are VR or RL; or

the same type, if they are with load, tremor or normal. The sessions of the same group (i.e. "RL"-"RL+Tremor" or "VR"-"VR+Load") have lower correlation, while the sessions with same type (i.e. "RL"-"VR", "RL+Tremor"-"VR-Tremor" and "RL+Load"-"VR-Tremor") have higher correlation.

Although the "RL+Tremor" FPV results showed high correlation with "RL" and "RL+Tremor" (≈0.73), the "RL+Load" showed a lower value than the "RL" (0.5754). The "RL" relationship with the "RL+Load" is close to that with "VR+Load" (0.5658).
In contrast, the "VR" and "VR+Tremor" showed less of a relationship in comparison with the "RL" (≈0.4) but this was higher when compared to each other, as the relationship of the "VR" with the "VR+Tremor" and "VR+Load" is >0.6.

Using the RSQ (root square of the Pearson correlation coefficient), the average distance for the same groups is 0.07 and for the same type is 0.665.
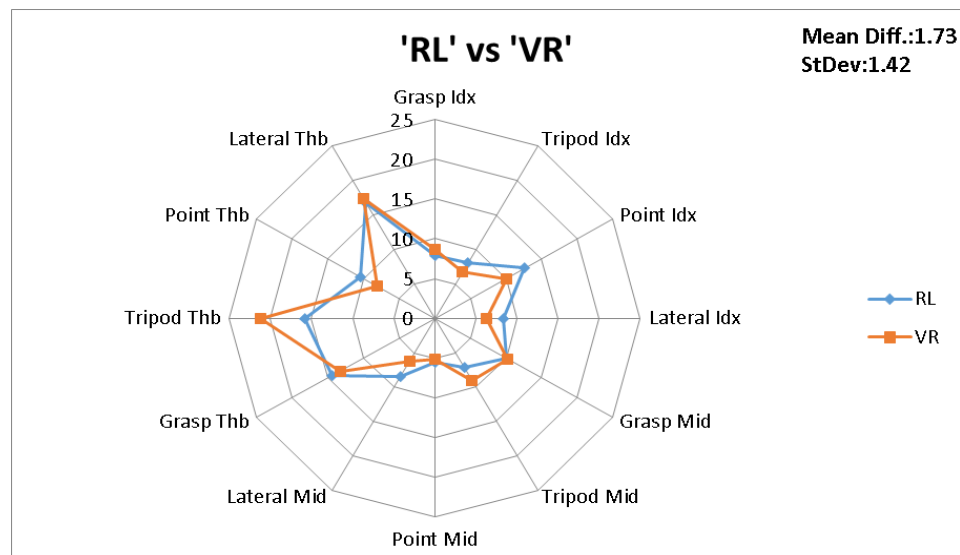
Figure 6-7 Plot of the grand average FPV values for the RL and VR sessions with the standard error; the values are plotted on separate lines, which each correspond to the finger; the range is from 0 to 25; Idx is the index finger, Mid is the middle finger and Thb is the thumb; there are no connections between the fingers' values, the connecting lines in the graph are for visualisation purposes only, to help in signifying the variation between the two sessions.

Figure 6-7 shows very close scattering of the grand average FPV values between "RL" and "VR". The mean difference between both sets of data is 1.73. The FPV value for the thumb in the tripod task shows larger differences than the rest.
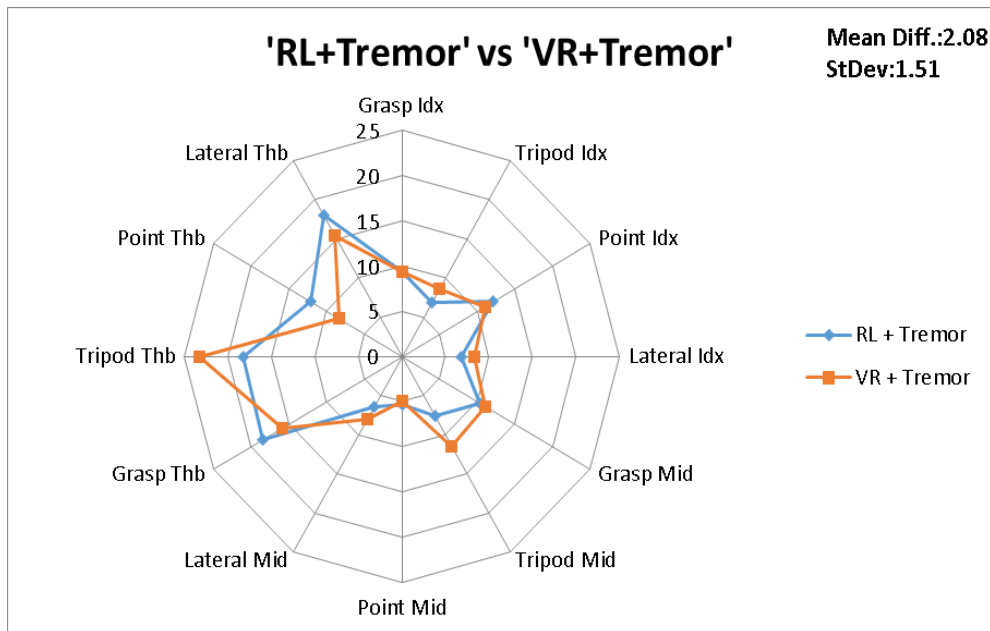
Figure 6-8 Plot of the FPV values' grand average for the "RL + Tremor" and "VR + Tremor" sessions with the standard error; the values are plotted on separate lines, which each correspond to the finger; the range is from 0 to 25; Idx is the index finger, Mid is the middle finger and Thb is the thumb; there are no connections between the fingers' values, the connecting lines in the graph are for visualisation purposes only, to help in signifying the variation between the two sessions.

Figure 6-8 shows a close scattering of the grand average FPV values between the "RL+Tremor" and "VR+Tremor", with a mean difference 2.08. The FPV value for the thumb in the tripod task also shows a greater difference than the rest.
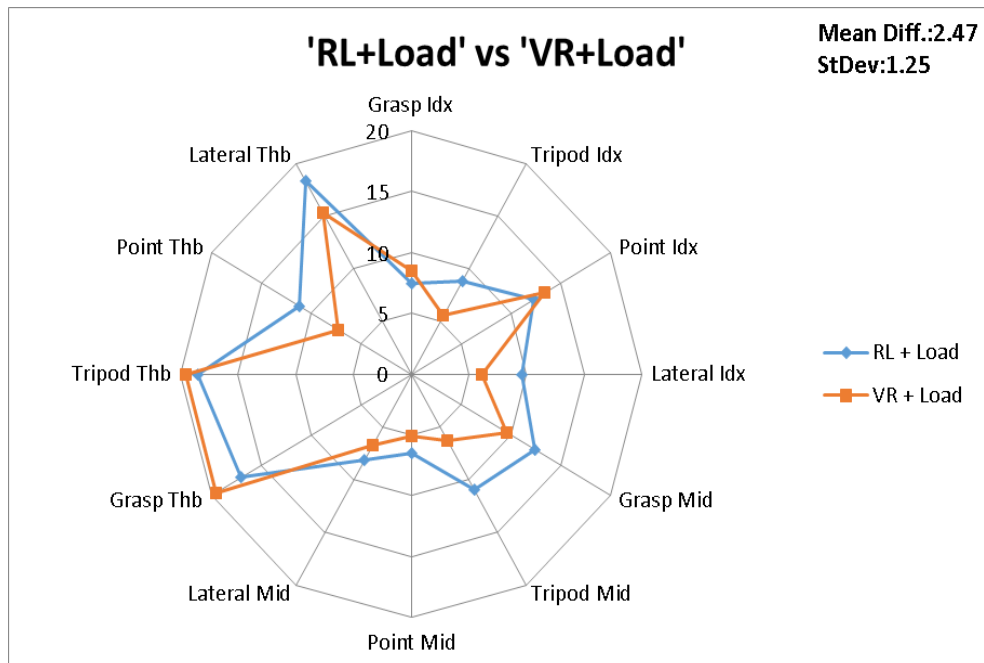
Figure 6-9 Plot of the FPV values' grand average for the "RL + Load" and "VR + Load" sessions with the standard error; the values are plotted on separate lines, which each correspond to the finger; the range is from 0 to 25; Idx is the index finger, Mid is the middle Finger and Thb is the thumb; there are no connections between the fingers' values, the connecting lines in the graph are for visualisation purposes only, to help in signifying the variation between the two sessions.

 In Figure 6-9 the FPV values are still closely scattered, but not as much as in the normal and tremor sessions. The mean difference reflects this, with a value of 2.47. However, the FPV value of the thumb in the tripod task closely matches the other values. Most of the FPV values for the "RL + Load" are bigger than the "VR + Load"; this is the reverse of the other sessions.

6.2.1.5. Finger's Contributions Between Tasks

Finger contribution in the tasks is measured using the fingers' correlation ρ. Table 6-6 shows the correlation ρ of each finger calculated in relation to the task. These values are calculated using the Pearson's r cross-correlation method on the total FPV average values of all the subjects. The minimum ρ for the index is 0. 110788 in the point task and the maximum is 0.606933 in the grasp task. The middle finger's minimum ρ is 0.137756 in the point task and maximum is 0.470565 in the grasp task. The minimum ρ for the thumb is 0.010566 and 0.0394 for the tripod and point tasks, and the maximum ρ is 0.501063 for the grasp task.

Table 6-6 Finger contribution per task

	Index	Middle	Thumb
Grasp	0.606933	0.470565	0.501063
Tripod	0.237771	0.306505	0.0394
Point	0.110788	0.137756	0.010566
Lateral	0.356773	0.410126	0.097896

6.2.2. Inter-subject reliability

A separate procedure is employed to test the reliability of the collected data across the group of subjects. The analysis of variance test (ANOVA) (Lane, 2015) studies the variation of the FPV values across the group data results. The considered null hypothesis is that there are no significant differences in the FPV values between subjects (with 99% confidence).

The calculated ANOVA test analyses are shown in Table 6-7.

Table 6-7 ANOVA test for FPV values across subjects. Highlighted in yellow the values of significant differences with p < 0.01.

		RL	RL + Tremor	RL + Load	Virtual Reality	VR + Tremor	VR + Load
Index	Grasp	0.643	0.203	0.464	1.60E-03	0.363	0.679
	Tripod	0.058	4.16E-04	0.493	0.228	0.458	0.643
	Point	0.643	0.170	0.211	0.023	1.66E-04	0.654
	Lateral	0.354	1.15E-03	0.433	0.023	4.52E-04	0.562
Middle	Grasp	0.667	0.146	0.412	5.08E-03	1.35E-03	0.654
	Tripod	7.22E-04	0.625	0.211	0.225	1.46E-03	0.643
	Point	0.659	0.293	0.392	0.026	0.466	0.345
	Lateral	0.643	0.276	0.326	8.83E-03	0.798	0.455
Thumb	Grasp	0.266	0.622	0.211	0.166	1.50E-08	1.93E-18
	Tripod	0.133	0.276	9.34E-06	9.41E-121	2.07E-97	1.94E-23
	Point	0.109	1.01E-10	5.30E-04	1.67E-99	0.466	0.316
	Lateral	0.276	0.276	0.211	3.33E-62	1.53E-37	5.62E-27

Real Objects:

The Finger Performance Value (FPV) of the three fingertips during the real objects sessions shows no significant difference, other than in the middle-tripod tasks (p = 7.22E-04).

Real Objects with Tremor:

The index fingertip shows significant differences between the tripod and lateral tasks (p = 4.16E-04, and p=1.15E-03). In contrast, the thumb only shows significant difference in the point task (p = 1.01E-10).

Real Objects with Load:

No significant difference is observed in this section, apart from in the thumb tripod and point tasks (p=9.34E-06, p=5.30E-04).

Virtual Reality (VR), VR with Tremor, VR with Load:

Unlike the real objects sessions, the VR data shows significant differences in the FPV for the three fingers. The p values range between 1.66E-4 and 8.83 E-3 in the different tasks, specifically for the index and middle fingers.

The VR results return significant differences in the grasp task for the index finger, and both the grasp and lateral tasks for the middle fingers. The virtual reality with tremor displays significant differences in the index-point, index-lateral, middle-grasp, and middle-tripod tasks.

The thumb has significant differences for most of the tasks in the VR sessions. The P value ranges from p=1.5E-08 to p=9.41E-121. Smaller differences are seen in the thumb results in the point and grasp tasks of the VR with tremor.

6.2.3. Repeatability

In order to study the repeatability, the mean difference versus the average graph plot on repeated measurements on all the subjects is used, (Bland and Altman, 1999) . The other commonly used method is the regression line equality plot, (Bland and Altman, 1986). However, the main concern about the relation between the different session measurements in 'RL', and the regression line fitting calculates the correlation coefficient (r) to show the strength of a relation between variables and not the agreement. Hence, for this analysis the high correlations can produce poor agreements between variables and requires a very specific definition of the correlation's context.

On the other hand, the mean difference against the average plot illustrates the agreement between the measurements to better illustrate the difference between the methods results.

In this section, the repeatability is studied in Figure 6-10.
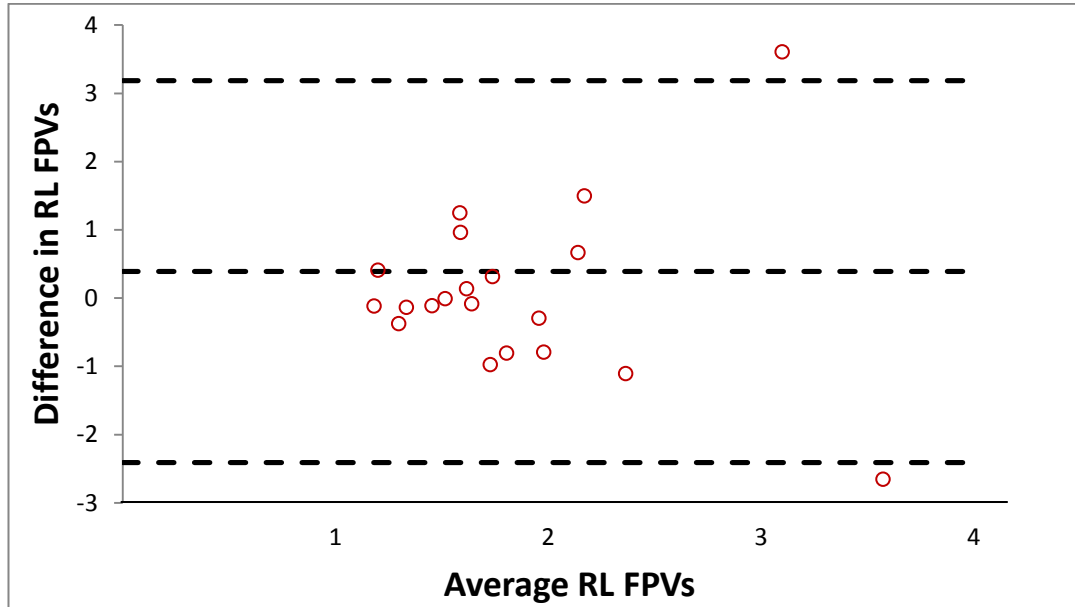
Figure 6-10 FPV total average: Difference between RL repeated measurements against the average values.

Further analysis to study repeatability and agreement between the 'RL' and 'VR' methods is performed in Figure 6-11. By plotting the subtraction of both methods data measurement against the mean, the graph displays a positive agreement between them. Furthermore, the rank correlation of the compared measurement between the absolute differences and the average; calculated using Spearman's rank ((Sedgwick, 2014)) correlation coefficient is $r_s = 0.6$. It illustrates this positive relation, where an increase in the differences between the sessions results in an increase in the average FPVs of the measurements.
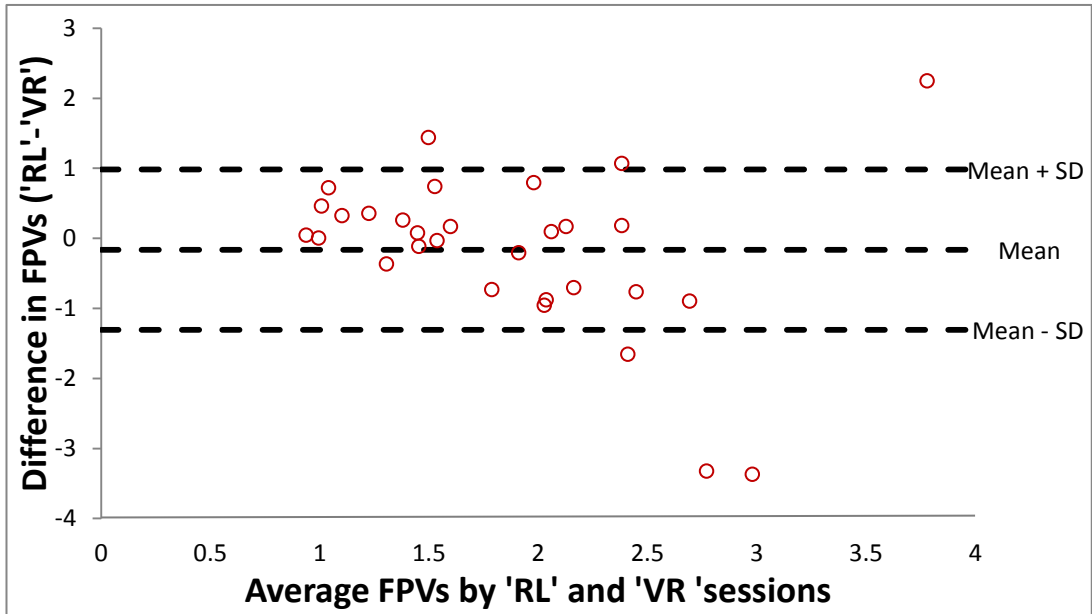
Figure 6-11 FPV total average: Difference between 'RL' and 'VR' sessions versus average of values

Also, another conclusion can be derived from Figure 611. The outliers observed with the large FPV averages illustrate that there are additional factors in one of the methods' data measurements. The following section describes the data outliers noticed across the data results in this chapter.

6.2.4. Outliers

During the process of generating the data results and investigating the FPV for each subject, subject 8's results returned abnormal distance compared to the average and showed outliers across multiple analytical graphs.

In light of this, further details on subject performance and the outlier are included below.
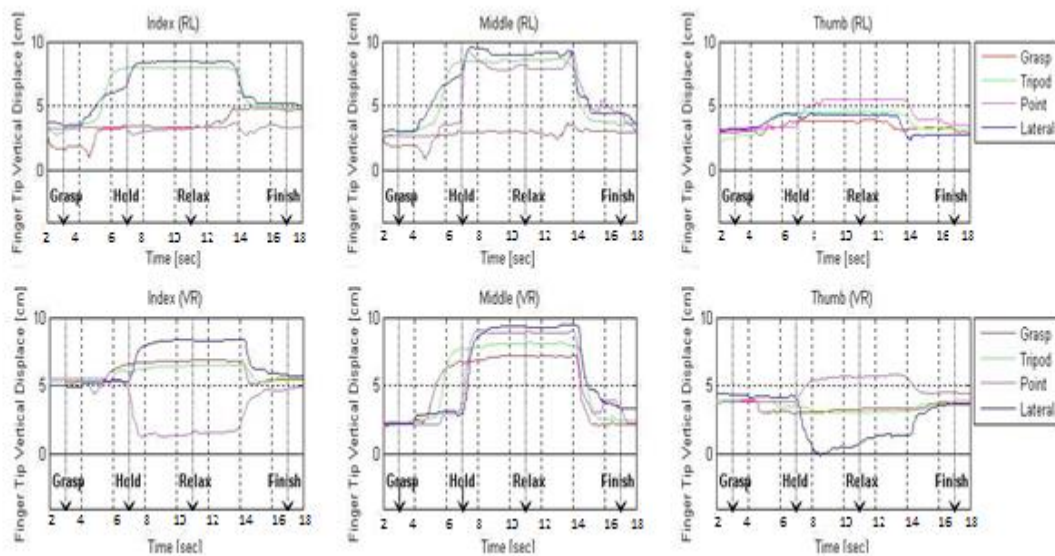
Figure 6-12Fingertip vertical displacement (in cm) of subject 8; the first raw represents the fingers' movements in RL session and the second raw represents the fingers' movements in VR session.

 The abnormal performance of subject 8 is apparent in the vertical Y displacement (Figure 6-12), where the fingertips contradict the changes expected during the events. A decrease in the fingertips' vertical Y displacement is noted at the beginning of the 'grasp' event followed by an increase. This is in contrast to the continuous increase that is expected. In the graph of the index (RL), the grasp task (red line) increases further after the 'relax' event. This inconsistency is displayed across the graphs, where different variations are observed. The small extension/flexion in the finger movement also outlines the abnormality of this particular subject's results in the experiment.

The FPVs of the abnormal results of subject 8 are shown in Figure 6-13. It is evident that thumb FPVs exceed the maximum threshold in multiple sessions, with greater differences than the benchmark values (displayed in the red lines on the histogram of Figure 6-13). In the RL session the thumb FPV exceeds the threshold in the grasp task; in the RL + tremor session it exceeds in in both the grasp and tripod tasks; in the RL + load it exceeds in the grasp and tripod sessions, with significantly larger differences in the lateral task when compared to the index and middle. It also exceeds the threshold limit in the VR + tremor and VR + load sessions during the grasp task, with noticeably larger values in the tripod and lateral tasks for the latter session than that of the other two fingers.
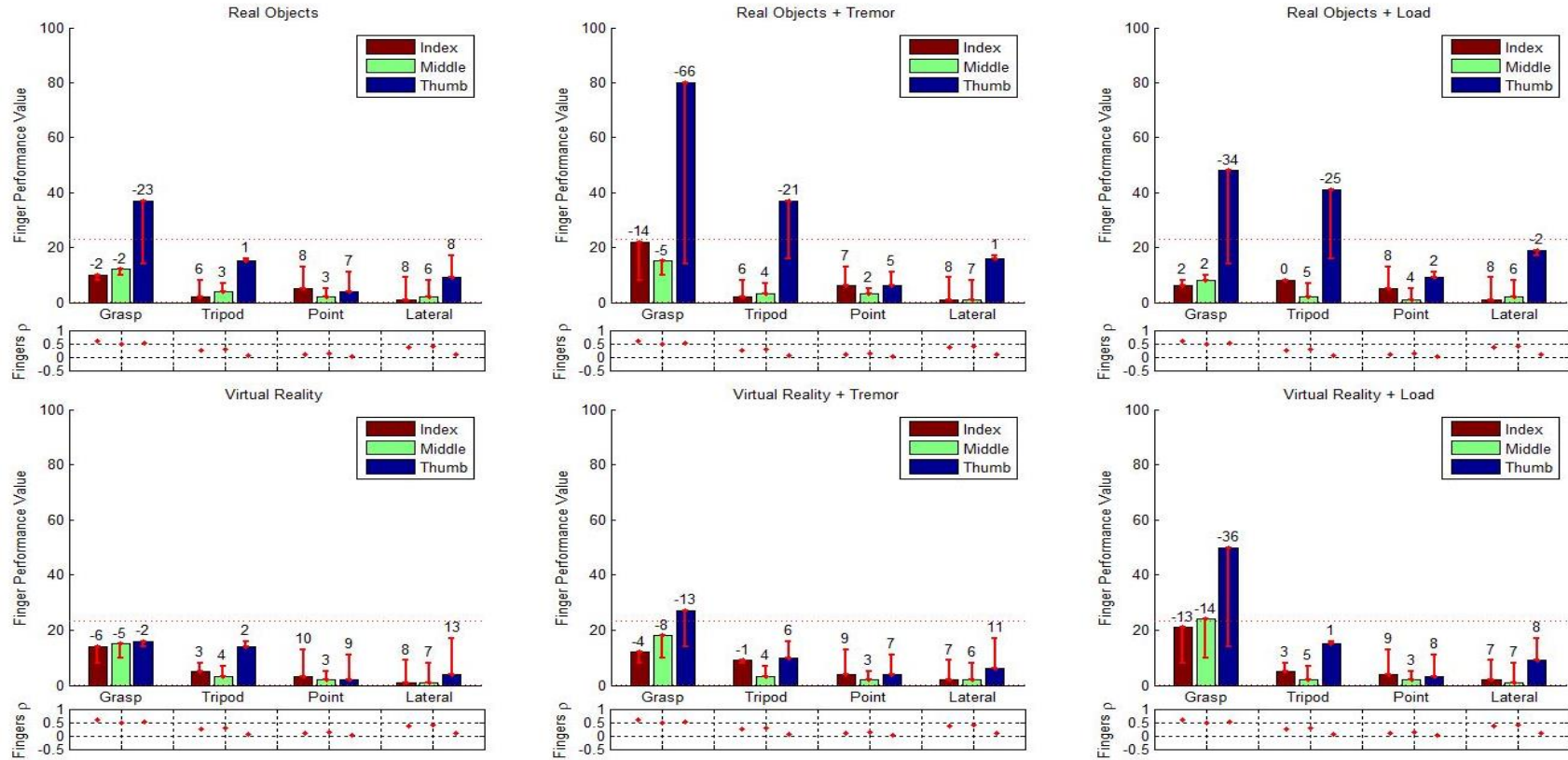
Figure 6-13 6-14 Subject 8 finger performance values; each graph represents the results for each session of the experiment. The bar color indicates the finger measured. Data are distributed into four sections representing the tasks (Grasp, Tripod, Point, and Lateral). The dot line in each graph represents the maximum value of the FPV. The bottom charts below each graph show the cross-correlation value for each finger, representing the level of contribution of the finger in task performance. The red lines display the difference from the benchmark value, which is also numerically noted above each bar. Y-axis is the FPV value and the X-axis is the fingers (colored red for index, green for middle and blue for thumb) distributed on the four tasks (Grasp, Tripod, Point and Lateral)

The Thumb FPV in 'RL' – Grasp task is 37.5, in 'RL+Tremor'-Grasp is 80.5, in 'RL+Tremor'-Tripod is 36.8, in 'RL+Load'-Grasp is 48.5 and 'RL+Load'-Tripod is 40.8. And in the 'VR+Tremor' – Grasp task is 27.5 and in 'VR+Load'-Grasp is 50.5.

The interaction plot between subject 8's FPV values and the total average (excluding subject 8) of all the other subjects' FPVs is shown in Figure 6-15. It shows the difference in the "RL", "VR", "RL+Load" and "VR+Load" sessions. "VR+Tremor" and "RL+Tremor" sessions are not included due the session type – this can include intentional abnormal variations across all the subjects' fingers' vertical displacements.
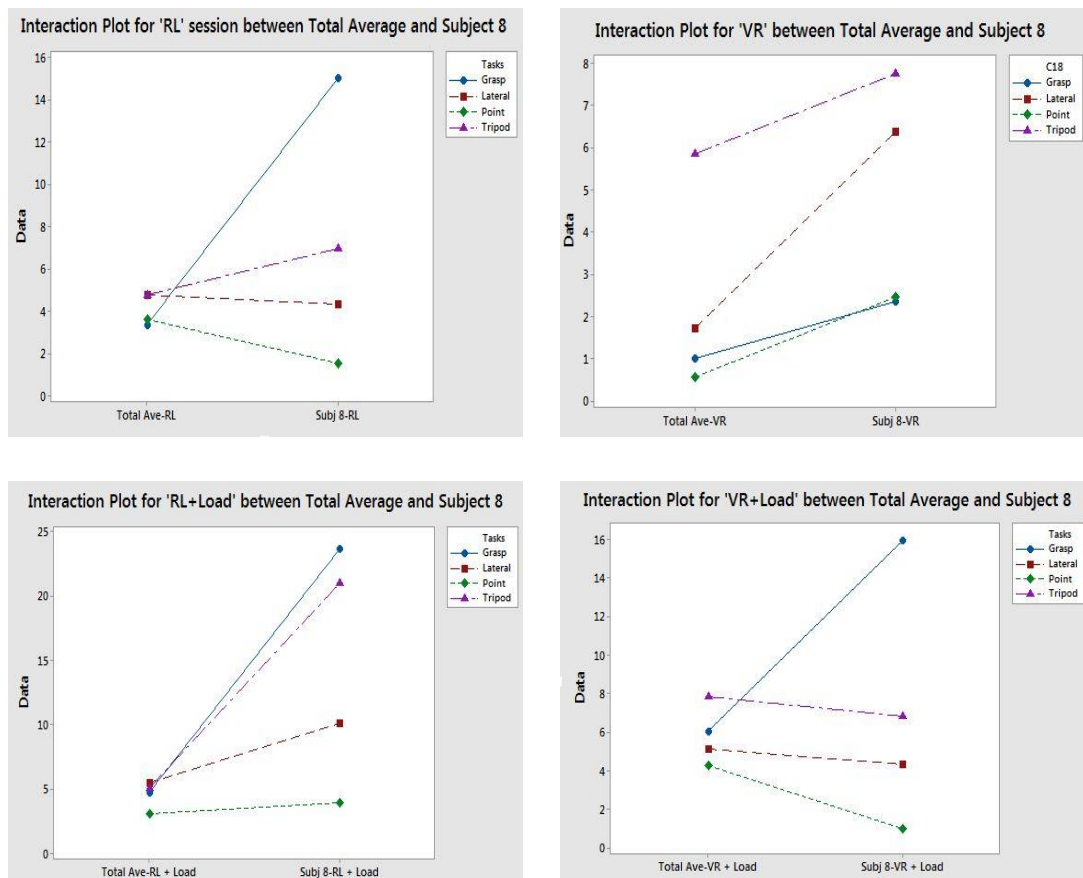
Figure 6-15 Interaction plot for the subject 8 FPV data results in comparison with the grand average of all the other subjects' FPVs. Data comparison is performed on "RL", "VR", "RL+Load" and "VR+Load" sessions; Y-axis (Data) represents StDev of the FPV values in each task

Figure 6-15 shows the clear variation of subject 8's results in comparison to the total average of all the subjects.

In all the graphs, the total average of the tasks' FPV values are closely scattered, while subject 8's FPV results are spread. The VR session graph shows a larger difference only in the tripod task compared to the rest of the tasks, in both the total average and subject 8's FPVs.

It is worth to note that the data of subject 8 is excluded from the normative dataset, inter-subject reliability, and total FPV analysis, as it causes large deviation to the normal results. However, it is included in the Intra-subject reliability in order to verify that the subject has maintained the same movements during the experiment, and in the repeatability studies in order to note the outlier and validate the efficiency of the method in detecting it.

6.2.5. Electromyography Data Results

Figure 6-16 and Figure 6-17 display the EMG signals of the four selected muscles' (dorsal interosseous muscle (DIM), right abductor pollicis (RAP), right flexor digitorum (RFD) and right extensor digitorum (RED)) activities, after they were processed through multiple digital signal filters (rectification, smoothing, enveloping and noise elimination).
The signal electrodes of the last two muscles (right flexor digitorum and right extensor digitorum) show higher intensity than the first two. The signal is segmented using digital markers to synchronise the saved data with the event occurrence and other recording devices. Each graph includes all four tasks to allow comparison of the variations between them. They are grouped by sessions in order to clearly see the deviations occurring in between each.

The EMG signals, presented in Figure 6-16 and Figure 6-17, show consistency in the event occurrence and signal variations. The electrode DIM and RAP had lower intensity in comparison to the RFD and RED. This is mainly due to the skin's interference and muscle size.
The RFD and RED electrode signals show opposite variation. This is expected because the former performs the flexion of the fingers while the latter performs the extensions. This is noted through all the different VR and RL sessions.

The VR RFD electrodes, in contrast to the RL RFD electrode signals, show no immediate decrease at the end of the task. This is because subjects were waiting for the VR animation to finish before performing the instruction. Removing the animation and adding tracking sensors on the wrist could easily eliminate this.

Although the RFD shows a slight difference in the tremor sessions of the RL/VR in comparison to the other sessions, the RED electrode signals show much higher variation that can be noted qualitatively.
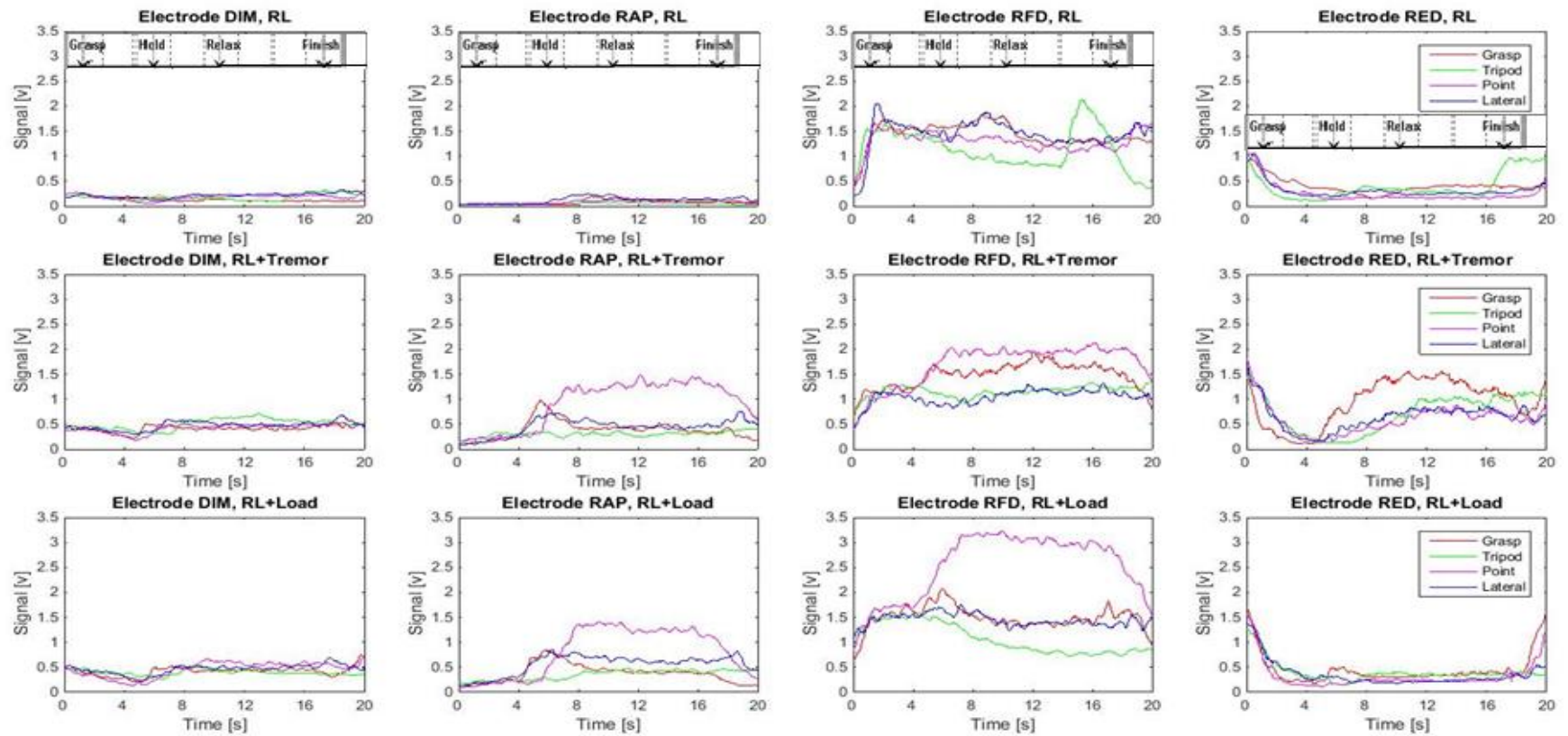
Figure 6-16 Graph display of the four EMG electrodes signals, which are placed on: dorsal interosseous muscles, right abductor pollicis, right flexor digitorum and right extensor digitorum. The graphs present the data signals recorded during the RL, RL+Tremor, and RL+Load sessions.
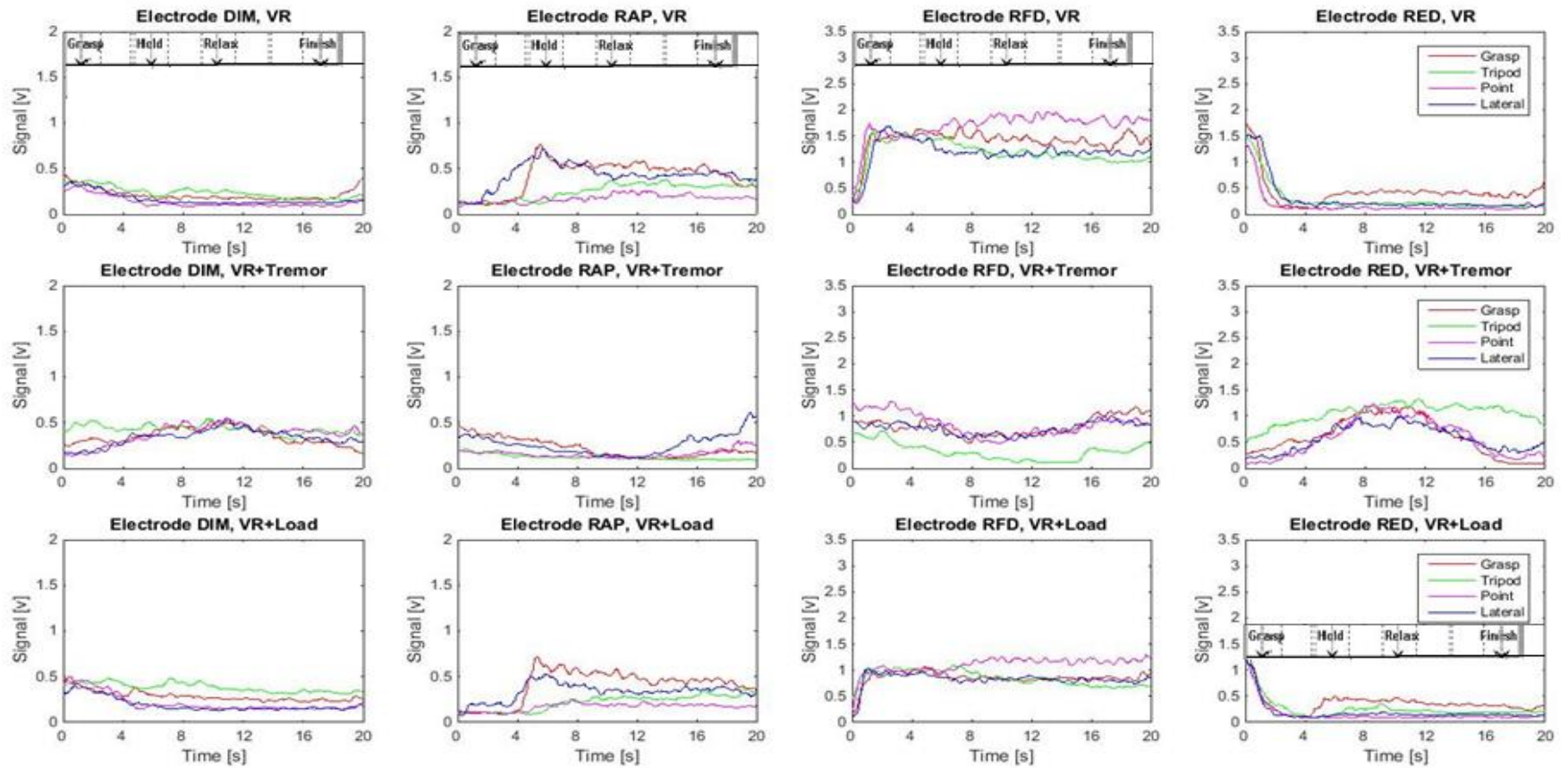
Figure 6-17 Graph display of the four EMG electrodes signals, which are placed on: dorsal interosseous muscles, right abductor pollicis, right flexor digitorum and right extensor digitorum. The graphs present the data signals recorded during the VR, VR+Tremor, and VR+Load sessions.

The spectral analysis of the EMG signals is displayed in Figure 6-18. Each graph compares the power density in relation to the frequency for three sessions in both RL and VR. The four tasks for each session are combined to represent the session deviation and the effect of fatigue and tremor on the muscles.
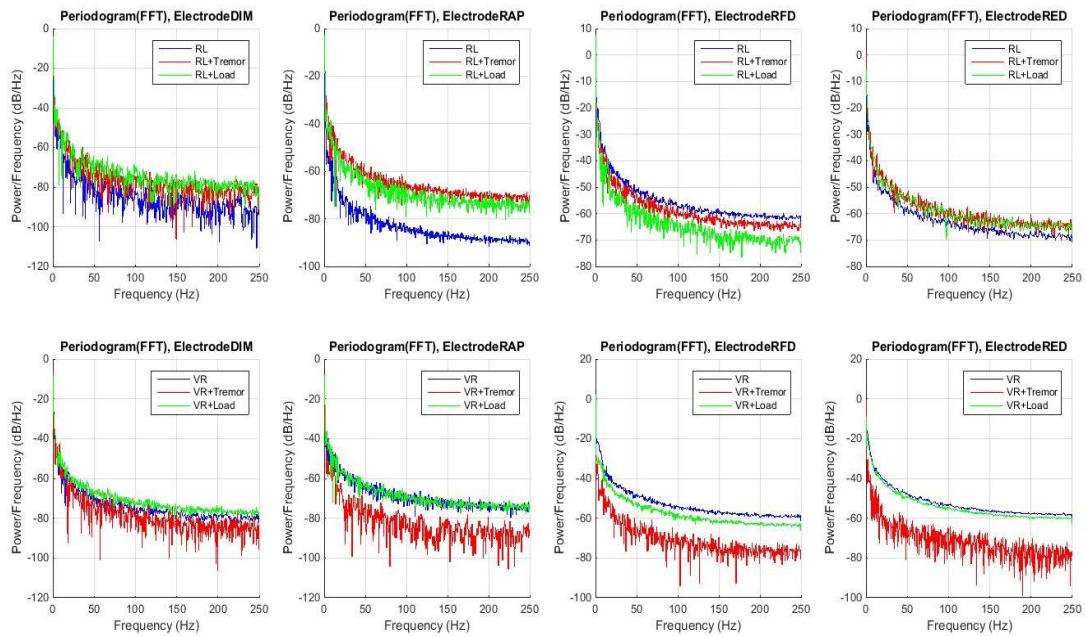
Figure 6-18 Peridogoram of power spectral density for the EMG signals; the graphs show the data signals for the four electrodes: dorsal interosseous muscles, right abductor pollicis, right flexor digitorum and right extensor digitorum; graphs in first raw represents the three sessions in real life and second raw represents the three sessions in virtual reality.

Figure 6-18 shows that the tremor difference (displayed in red) is more apparent in all the electrodes during the VR sessions than in those of the RL.

The calculated mean power frequency (MPF) from the above PSD, used to measure the influence of fatigue and tremor on muscle activity, is shown in the interval plot in Figure 6-19.
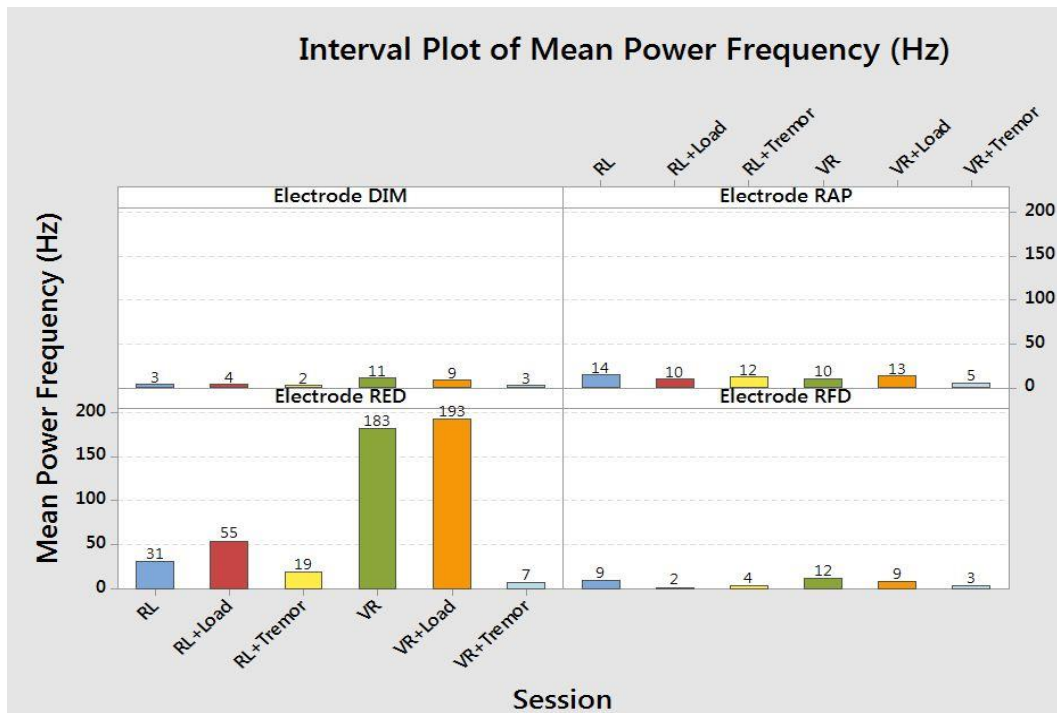
Figure 6-19 Interval plot of the mean power frequency (MPF) for the signals of each electrode; the graph displays the MPF for the six experimental sessions: RL, RL+Tremor, RL+Load, VR, VR+Tremor,VR+Load.

The interval plot of the mean power frequency (MPF), in Figure 6-19, shows quantitative measurement for the signals. Each electrode is presented in a panel that includes the multiple sessions.

Notably, the VR and VR+Load sessions in the RED electrodes data signal have returned much higher results than the rest (183,193 Hz). This is due to the non-decreasing state of the signal back to the normal position at the end of the task, which contributes to increasing the level of PSD for these electrodes.

6.3. System Validation

As the application development is based on software and hardware interaction, it is important to include stress testing of the application before data recording begins.

The data glove device was tested using calibration and statistical analysis methods. The first method examines the consistency of the subject's coefficient values and visual display performance. In the case of discrepancies in the data glove device readings, the calibration will show inconsistencies in the cross-correlation results of the subject's performance.

The above assumption is proven to be invalid as the cross-correlation data has displayed high efficiency and reliability in the data results between the different tasks and sessions. The visual display and representation in Figure 5-7 also show matching outcomes between the VR display and real hand movement.

The software of the application was validated using the black box approach. This validation method was selected due to the following elements:

1- The software is a simulator application that is highly dependent on graphical simulation and user interactions. The user interaction is mainly processed using external applications that directly manipulate the visual display. Therefore, validation of this type of application is mainly dependent on calibration.

2- The application for this study is expected to be operated during the experiment by the researcher and not the end user. The involvement of the end user is in the manipulation of the virtual world rather than the application configurations.

An approach to the validation of this software is the use of stress tests that ensure the functionality of the system as well as consistency in recording and displaying graphical updates.

The following Table 6-8 lists the test cases performed in the application stress test:

Table 6-8 Stress test on the virtual reality application

Case	Expected	Actual	Comment
Loss of user calibration files (delete/remove) while in experiment.	Run with the appropriate calibration.	Application uses live calibration data, which is not affected by deleting or moving the file.	The software stores the application in live data that won't be replaced until a new calibration is performed or the programme is closed.
Inappropriate data calibration.	Warn user.	Abnormal display in the hand manipulation.	Requires new calibration as the test calibration has low coefficient index.
Connection problems with the data glove.	Warn user and stop experiment.	An error message is thrown notifying that the device is disconnected, and the experiment is halted.	Data of the experiment is saved in real time, so the user data will include the last recording position before the connection problem.
Crash/closure of system in the middle of experiment.	Data is saved up to last position before crash.	Data is saved up to last position before crash.	The user data files are updated in real time (in 50 sampling ratio) and hence a crash won't affect the recorded data before the crash.
Memory issues (leakage, overwrite, pointers).	Warn user.	An error handling warning message is thrown notifying the user.	Data is stored in the user file up to the error occurrence.
Pause in the middle of the experiment.	Pause and resume where it stops when 'start' is clicked.	Pause the visual display of the instructions and recording. The audio instruction might continue to play the last instruction until it finishes. A closure to	After closing the dialogue and opening a new one, the user will be notified to store the data in a different file in order to connect them with previous recording later, if applicable.

Case	Expected	Actual	Comment
		experiment dialogue is necessary to restart the timing.	
Create new experiment following previous one.	New recording files and calibration.	New recording files. The user has to redo the calibration; otherwise it will continue to manipulate the virtual hand using the previous user's calibration.	Every time a new session is created the program opens a new dialogue to select the path of the file to record the user data.
Application selection of tasks during the experiment.	Random selection.	Random selection.	
Audio instructions and data recording.	Consistent.	Consistent. Data is recorded and tagged by time and task name.	The experiment class in the application is developed using multi-threading to record data and control other graphical/audio processes in parallel.
Audio instructions and visual displays (tasks, objects, timing, and virtual hand position).	Consistent.	Consistent.	The application is programed with multi-threading to consistently control the instruction cues, and the visual updates and rendering. Object and arm transformations are tagged with ID to consequently execute the instruction phase and duration.
VR and RL experiments.	Consistent.	Consistent.	Both experiments are developed with the same function structure to process the designed experimental procedure.

6.4. Summary of the Results Chapter

In this chapter the results of the experiment are presented. The chapter started by providing a subjective assessment of the results followed by the objective measurements.

The objective measurement section detailed the fingers' vertical displacement signals, which were used to calculate the FPV values. The inverse kinematic method was used to calculate the fingertip position from the DOF angle values of each finger. Intra-subject repeatability tests were then performed on the fingertips' displacement.
Following this, the section displayed the finger contributions in each task, with the FPV results and extensive statistical analysis. This included cross-correlation analysis between the sessions, the inter-subject reliability (performed by using the FPV values), and the repeatability of the data distribution along with the outliers.

Then the EMG results were represented using the power density spectrum and mean power frequency in order to show the results' correlation between task performances and finger movements, and the efficiency in detecting the repeatability between sessions.

The chapter ends with the validation tests of the hardware and software components in order to ensure the robustness and reliability of the system.

Chapter 7 Discussion

This chapter discusses the data results with regards to the reliability and efficiency of the proposed method for measuring finger performance (especially by including the multiple features of the signal: speed, smooth, time). Also, it illustrates the data measurements consistency using the intra-subject repeatability and inter-subject reliability tests. This is associated with description of the results repeatability and the observed outliers.

The system outcome is then compared with the other available systems and the hypotheses, which were established in the Introduction Chapter 1.
At the end of this chapter, a list of system improvement and future work is produced.

It is important to note, before discussing the results, there are different motion tracking systems available as reviewed in Literature Review Chapter 3.In this project, the CyberGlove® device was validated based on the statistical data reliability and consistency of the measured data (Calibration Chapter 5). However, there are multiple methods that could also be used to validate the data sensors reading of the data glove, such as Vicon motion capture device (Vicon, 2015).

But the motion tracking methods, and in particular Vicon system, have different drawbacks; as the passive sensors (markers) must be placed on top of the data glove for tracking and validating the data glove sensors readings. This step introduces variations in the sensors position from the caused displacement in the soft skin, the glove cloth and the bending sensors. Hence, inaccurate data recording may affect the output results as the sensors are not fixed to the joint.
Also, the Vicon system requires two passive sensors placed on each joint to calculate the coordinate differences and measure the angle of the joint. The sensors positions may be inconsistent between the subjects and joints, which is mainly due to the physiological differences. This variation makes the data inconsistent in comparison with the data glove device.

Moreover, the current application monitors the fingers' movements using the data glove only. But in general, task performance highly depends on the wrist orientation and displacement. Therefore, an additional system can complement the data glove device reading such as the inertial accelerometer sensors (Hamed et al., 2014).

Also, motion sensing devices, such as Xbox Kinect (Kinect, 2015) are applicable in reading the hand movements. Metcalf et al. have incorporated Xbox Kinect device to model the hand movements with hand motion capture, and provide interactive display for rehabilitation (Metcalf et al., 2013).

In addition, the stereovision 3D tracking device is an alternative to Vicon system since it does not rely on allocated passive sensors, which can be displaced by the soft skin. These methods have multiple advantages as, unlike the data glove, they are note fixed with hand size, and can be used on hands with significant deformity.
However, it is worth to note that the camera and reflective sensors can be obstructed by objects and surrounding environment, and does restrict the user to work within a limited work volume.

Hence by noting the above devices, it can be noted that additional work can be implemented to further validate the accuracy and consistency of the implemented algorithm and complement the data glove reading.

7.1. Finger Performance

The consistency of the fingertip displacement, displayed in the graphs Figure 6-1 and Figure 6-2, reflects the expected movements of the finger during task performance. The variance of the amplitude is due to the variation in the level of the fingers' involvement in the task and the level of flexion required for grasping the object (or making the posture). The displayed line of the Point task, (pink colour, Figure 6-1) for the index finger, shows small amplitude that corresponds with the low level of flexion of the index fingertip during the Point task.

Furthermore, replicating the finger displacement in 3D by applying the inverse kinematic method provides a demonstrative visualisation that outlines the movement speed and other features. In addition, it provides a visual comparison of the subject's performance in comparison to the total average (normative dataset). Furthermore, it outlines efficiently the difference between the extension and flexion performance. This is illustrated in Figure 6-3 and Figure 6-4.

In the following, a list of the multiple conclusions derived from the results of finger performance is provided.

7.1.1. Intra-subject repeatability

In order to verify the repeatability of the tasks for each subject, the calculated cross-correlation of the FPV values between sessions should return a ρ value higher than 40% (Dancey and Reidy, 2004), indicating a moderate or strong positive relationship.

The end results of the tasks ρ averages, displayed in Table 6-3, for the three VR sessions are smaller than the cross-correlation (ρ or 'rho') averages of the three RL sessions with 0.07 average differences. This is as the VR interactions involve more variations in the finger displacement, and due to the absence of haptic feedback while grasping a virtual object.

However, the results in Table 6-3 showed that all the sessions have average intra-subject repeatability ρ >0.6.

7.1.2. Fingers' Contributions between Tasks

Moreover, the finger contributions shown in Figure 6-6 and Table 6-6 display the expected variation in the level of contribution for each finger in the task.

This is where in the Tripod task, the two fingers (index and middle) are the major contributors to the posture formation, with very small flexion in thumb MCP. Hence, Thumb ρ is 0.0394 and the Index ρ = 0.237, Middle ρ = 0.3.

In the Point task, the main contributor was the index finger. However, in this particular task, the level of contribution is not based on the movement of the Index finger or any of the adjacent fingers, it is rather measured based on the stability of the Index finger after full extension. Hence, very small rho values are shown of the three fingers with ρ < 0.14.

Alternatively, in the Lateral task, all three fingers are involved, but only a small movement is noticed in the thumb, which is reflected in the rho value. Thumb ρ = 0.09, Index ρ =0.357 and Middle ρ = 0.41 (Table 6-6).

Likewise, in the Grasp Task, all the three fingers had large contributions. The rho values reflect this variation with average ρ value = 0.52.

Hence, it is valid to use the finger contribution correlation values of the FPVs as it meets the contributions expected from the fingers' involvement in the tasks.

The finger contribution data results showed similar observations to the literature review, where the index and middle fingers contributions were 25% and 35% (Talsania and Kozin, 1998), and the total average difference with the obtained results is 0.07. However, although the data presented close similarities with the literature review, the study still

requires including the force factor in finger performance. The Force is a very important element in the hand synergy to grasp, hold and interact with objects. In the posture tasks, such as Point, force can be neglected as it requires only fingers motion, but in contrast other tasks, such as Grasp, do largely involve exerting force to grasp and hold the object. In addition, some tasks require small movement for particular finger but larger force. This is observed in the Tripod task where thumb movement is very small but it adds large force to hold the grasped object.

7.1.3. Finger Performance Value:

On the other side, a number of conclusions can be drawn from the FPV results:

- **FPV: Rehabilitation tasks to ADL activities**

  The FPV illustrates the transfer from the rehabilitation tasks to ADL activities.
  The normalised grand average FPV of all the sessions have varied between the minimum 0 and maximum 23.5 thresholds. The ascending variation of FPV, present in all the tasks apart from Point task, is maintained across the sessions. The average cross-correlation between the trials is 0.7.

  The FPV also returns objective measurement details of the finger motion. They are extracted from the variations of the speed during the task, the smoothness of gesture formation, and stability while on hold position. This measurement helps to illustrate the restoration phase and the rate of transfer from the rehabilitation tasks to ADL activities. This is where the 'stability' component in the Middle Point Task- RL session is smaller than the Middle Grasp Task-RL session's (shown in Figure 6-1 with more noises during Hold event) and hence the FPV value of Middle Point Task = 5.5 < than the FPV value of the Middle Grasp Task =10.1.
  Furthermore, the 'smoothness' component in the Middle Point- RL+Tremor was smaller than the other tasks (shown in Figure 6-1 with more noises on the Relax event) and this caused the FPV value to decrease to 5.3 and be smaller than the other tasks FPVs.
  In addition, the 'speed' component of the Index Grasp –RL session in the Relax event is smaller (or slower) than the Index Lateral-RL session's (shown in Figure 6-1 in the Relax event part). Hence, the FPV value of the former is 7.9 < than the lateral FPV = 8.4. Also, to note that because the Index Grasp finger displacement amplitude (or flexion) is smaller than the Index Lateral finger displacement amplitude, therefore the FPV values

didn't show the greater difference and that reflects accurately the type of tasks and fingers involvements.

Furthermore, throughout all the tasks and sessions, apart from the Point task, the FPV values (Figure 6-6) of thumb are larger than the other two fingers. This is because the thumb does not have a contribution in the Point task, and it reaches the destination position faster than the other two fingers. Figure 6-1 and Figure 6-2 demonstrate that the thumb has moved shorter distances than the other fingers. It also shows that the FPV depicted accurately the speed variation and the distance travelled (level of contribution) during the task.

- **FPV: VR's FPV distribution is equal to the RL's FPV distributions**

The VR method in hand assessment returned similar FPV distribution result to those of the RL, and also to the sessions with tremor and load.

The maintained variations order of the fingers FPV values between the 'RL' sessions and 'VR' sessions (shown in Figure 6-6) demonstrates that the VR method had high accuracy in replicating the 'RL' performance measurement. This is depicted visually in Figure 6-6, and numerically the FPV values showed close correlated variation with the finger contributions (Table 6-4).

In the Grasp tasks, the three fingers are expected to have high contributions, and this is proved by the results where the Index, Middle and Thumb fingers contributions were 0.61, 0.47 and 0.5, respectively. Also, the lateral task mainly had Index and Middle fingers involvement while the thumb made very small motion from its home position. This is also proved in the numeric data results where the Index, Middle and Thumb contributions were 0.36, 0.41 and 0.1, respectively.

On the other hand, the sequential variation order of the FPVs is shown in the Grasp RL task, where the FPV fingers variation order was Index (7.9), Middle (10.1) and Thumb (14.5). The SDV (Standard Deviation) was 3.36. Likewise, the Grasp VR tasks FPV fingers variation order was Index (8.7), Middle (10.2) and Thumb (13.3) with a SDV of 2.35.

The above variation orders of the Fingers FPV values is shown also in all the other tasks and sessions apart from the Lateral Index FPVs, wherein the "RL+Load" it is bigger than the other fingers FPVs while in the "VR+Load" is smaller with 0.6 difference.

Furthermore, Table 6-5 shows high correlations in the grand average FPVs for the sessions of the same groups ('RL'-'RL+ Tremor' ρ = 0.7277; 'VR' -'VR+Tremor' ρ = 0. 6201; 'RL'-'RL+Load' ρ = 0. 5754; and 'VR' -'VR+Load' ρ = 0. 6461).

Figure 6-7, Figure 6-8 and Figure 6-9 further illustrate this with similar data scatterings for both sessions and an average mean difference of 2.1.

The RSQ average distance for the sessions compared within the same group was 0.07. However, the RSQ average distance of the sessions compared with the same type was 0.665. This is due to the interaction differences between the real and virtual objects, caused by the VR's absence of tactile feedbacks and difference in visual perception.

- **FPV : Load effect**

In addition, the FPV can effectively show the changes in finger performance when a 0.5 kg weight is added to the forearm. The weight had increased the FPV in the 'RL+Load' session by 0.35 and by 0.15 in virtual reality. This can also be noticed in Figure 6-9 where the values are larger and more scattered than in Figure 6-8 and Figure 6-7.

However, the FPV results have highlighted that the 0.5 kg is not effective enough to cause a fatigue effect on the subjects hand performance. Therefore, increasing the weight on the forearm, or on each finger, with longer session duration, would demonstrate the influence of fatigue on finger performance with higher differences.

On the other side, the EMG data analysis (Figure 6-18 and Figure 6-19) showed large values in the mean power frequency during the load sessions. This is due to the increase of the force applied by the forearm muscles in the movement. But, the data results still displayed close correlations with the finger contributions in the different tasks.

- **FPV: Sensitivity in Detecting Abnormal Movements**

Furthermore, the FPV method had detected the abnormal behaviour of the subjects' finger performance with high reliability, illustrated in the subject 8's case (Figure 6-13). The RL sessions of the subject 8 showed an unexpected increase, over the maximum threshold, in the FPVs for the thumb, particularly in the grasp and tripod tasks, an increased average of 36.325. And an unexpected decrease of the index and middle FPVs

was seen in other tasks of the RL sessions, with an average of 3.33, and for the VR session, with an average of 1.6.

This abnormality is further demonstrated in the interaction plots in Figure 6-15. This data was generated based on the standard derivation (SDV) of the total average and subject 8. It does clearly show the large spread of the scattering for the subject's SDVs in comparison to the total average.

Following this abnormality, a further investigation was performed. The recorded video, during subject 8 experiment, showed that the data deviation happens during different trials. The subject did not extend the fingers to the home position at the start of the task and on the relax state. This caused to have a small range of motion (see Figure 6-12) in the finger movement during task performance, and also to have an increase instead of a decrease in the finger horizontal displacement at the Relax event. Figure 6-12 shows that the fingertip displacement amplitude difference was less than 3 cm in most of the fingertip displacement signals, in comparison to the subjects grand average 8cm. Also, the start position in all graphs was larger than 0 cm with small increases in the grasp and point tasks of RL sessions and decreases in the Point task of index VR and laterals VR. This explains that the difference between Subject 8 performance and the rest of the group, and demonstrate that the FPV calculation methods were able to depict the abnormality in the subject's performance.

7.1.4. Inter-subject variability

The ANOVA test, used for the inter-subject reliability, validates that the overall assessment adheres to a fundamental level of repeatability. This applies to the RL sessions as well as most of the VR sessions and tasks.

Table 6-6 showed that there was no significant difference in most of the RL sessions' (RL, 'RL + Load', 'RL + Tremor') tasks, with p>0.01. A variation appears in the two VR sessions (VR, 'VR + Tremor') with p<0.01, but higher confidence of repeatability is apparent in the 'VR+Load' for the index and middle fingers.

The tactile feedback and constraints on the fingers while interacting with real objects justify the higher confidence of repeatability in the RL sessions in comparison to the VR sessions. These factors have increased the accuracy of repetition in forming similar postures and

joint movements.

In the VR sessions, these elements do not exist, and the subject must rely on the front and back camera visual displays to estimate the level of flexion required to grasp the object virtually and manipulate the VR hand. This may have caused the discrepancies that are observed between the trials.

Both the low repeatability shown in some of the VR tasks and the high intra-subject reliability correlation average (ρ =0.66) of the VR sessions indicated that there are different skill levels between the subjects in interacting with the 3D virtual world. This variation was associated with the subject's age and previous experience with VR applications.

By providing further training on the VR to the subject at the start of the experiment the skills of the user will be improved. Using haptic feedback supports on the fingers to describe the collisions in the virtual world would enhance the accuracy in grasping/holding objects. This would result in higher consistency in the inter-subject reliability results for the VR tasks.

7.1.5. Repeatability

The data scatter, in Figure 6-10, shows that more than 95% of the differences is less than two standard deviations (1.14). Hence, based on the British Standards Institution, this outcome shows repeatability in the data measurement performed across subjects (British Standards Institution, 1975). Furthermore, Figure 6-11 displays the difference between the 'RL' and 'VR' sessions, where the Spearman's $r_s = 0.6$. This describes a positive relationship between the measurement, and a 95% confidence interval. The 'VR' can be used interchangeably with 'RL' for test and studies to measure the FPV.

7.1.6. Electromyography

The EMG data analyses were efficient in distinguishing the influence of tremor on finger performance during the VR session and on the muscles associated with the RFD and RED electrodes specifically.

The power density of the EMG data results showed clear variation in the VR + Tremor session (Figure 6-18). The mean power frequency (Figure 6-19) of this session had a smaller value than the other VR sessions, with a mean difference of 49.5 Hz. The RED electrode had the largest difference between the 'VR' and 'VR+Tremor', with a difference of 176.

The mean tremor MPF between all the electrodes was 4.5, which is inside the expected tremor frequency range 4 to 12 Hz (WeMove, 2008). However, this cannot be considered highly accurate as it is based only on the movements that resemble the tremor, but it serves the requirement of the research.

The 'RL+Load' effect was apparent on the RFD electrode where the MPF value was much smaller than the 'RL', with a difference of 8Hz. This was not seen in the other electrodes.

7.2. System Validation

The data glove calibration performed at the start of each experiment validates the functionality of the software in reading and rendering the sensorial data to the virtual world. This is in addition to the stress test carried out on the virtual system, in Table 6-8. The coefficient index, obtained from the test calibration (Calibration Chapter 5), validates both the calibration result and the reliability of the visual display for rendering the hand postures in accordance with the real hand movement.

Therefore, the VR system was found to be very reliable in measuring finger performance during the experiment and synchronously recording the data from the measurement devices at the task-event's occurrence, without data loss or disruptions.

7.3. Comparison to others

The outcome results of this research project showed that the FPV method is highly efficient and reliable for measuring the finger performance. This was performed by extending the SHAP procedures and including numerous approaches to the hand assessment. The method showed high intra-subject repeatability for each subject of the controlled group, and high inter-subject repeatability in the 'RL' sessions. The calculation method shows efficiency in detecting abnormalities and variations between the normal sessions and the sessions involving constraints on the hand (load).

Consideration of the different signal properties (speed, time, smoothness of finger formations and stability) in the calculation method provided extensive measurements to analyse the multiple dexterities and variations in hand performance.

This method has, for the first time, automated the process by including the sensorial data glove device to measure the fingers' motions and be independent from subjective

assessment. It is easy to setup and comfortable on the patient's hand, modular, safe, portable (can be easily moved to different location), and motivating (as it includes VR interaction).

The method, uniquely, provides a scoring system for finger performance, with objective assessment of each individual finger. It also compares the new results with the normative datasets (generated from the healthy group).

This method doesn't rely on subjective assessment, as it uses original and novel methods to extract the features in the finger movements which describe accurately. It includes the acceleration level of the fingers' movements while forming a gesture, the smoothness of finger displacement on defined trajectories, the stability of the fingers in hold positions, the contributions of the three fingers (index, middle and thumb) in performing classification tasks, and the speed plus time duration.

This method has added an extra dimension to the hand assessment process through the inclusion of VR and the robotic simulator. In contrast to other methods, the present provides higher awareness for the subject by displaying visual information of hand kinematics and functionality. It also provides different visual perspectives (front/subject cam), see-through, and easy to adjust with the patient's characteristics.

7.3.1. Potential Benefits to Clinical Settings

This system offers for the therapists: an automated and dynamic hand assessment system that is easy to setup, and continuously records patient's performance throughout the experiment. It is modular as it can adapt to different measurement devices (i.e. data glove devices, muscle activity measurements, ROM tracking devices, visual display and other biotechnological tools). The system does not require intensive training as it incorporates a user friendly interface, and very clear instructions and tasks.

The system calibration is very simple, robust and requires short setup time (<5mins). The system is also mobile and can be used from home, clinics and research labs.

At the end of the session, the software tool generates a compiled report with statistical analysis describing the performance of the patient's hand, objective measurements of each finger individually, comparisons with previous sessions and the normative dataset; it also scores the rates of the finger's performance in total.

7.3.2. System Setup procedures

In order to setup and use the system, a therapist must follow the below procedures:

1. Set up the measurement and data acquisition devices: PC to analyse and visualise the VR, EMG electrodes on the patient's forearm involved muscles, software, visual display unit. Let the patient wear the data glove device and place the SHAP tools in front of him/her.

2. Train the subject on the equipment and procedures: VR interaction, data glove device, and the tasks/instructions involved in each process of the assessment session.
These include: demonstrating the correct gesture and posture of the hand movement to grasp a real object and interact with the VR and the different events in each task (Ready, Grasp, Hold, Release).

3. Run the calibration procedures and ask the patient to perform the presented postures.

4. Configure the session hand assessment test procedures or load a predefined set that is generated by the program.

5. Run the hand assessment procedures.

6. After the program finishes, ask the patient to relax and dismount the system. A report is generated with statistical data analysis of the patient's hand performance. This can be stored and used for later session as the program can evaluate the patient's hand performance between sessions and elevate the tasks level in each session to accommodate improvement.

7.4. Comparison to hypotheses

In light of the discussion above, the following can be derived in relation to the project's initial considered hypotheses:

a. The newly developed method, FPV, has provided a consistent data measurement system that efficiently extrapolates the significant features in finger performance. This includes the speed, time, smoothness and stability of the fingers' movements.
The method produced an automated process system that doesn't rely on assessor input to control the experiment or to measure the features.

The system presented enough sensitivity to detect the load effect on hand performance during the 'RL+Load' and 'VR+Load' sessions.

b. The VR hand assessment system provides an efficient outcome measurement procedure that closely correlates with the 'Real Life' measurement ('RL'-'VR' mean difference is 1.73).

The VR sessions showed that they are more adaptable and adjustable to the user's needs than the RL sessions. This is due to the inclusion of a see-through and second camera (front view). These features have contributed in improving the system feasibility and interaction level.

7.5. What could have been done differently

The project could be improved in various areas to increase the reliability of the results. A number of improvements to the project procedures are listed below:

a. The results provide elementary analysis for deriving the subject's hand performance. However, the experiment needs to be conducted on a larger group of controlled subjects in order to establish a normative data set.

b. The tremor session requires an additional system to track the variation of the hand from the base (wrist/palm). A solution to this is mounting inertial or accelerometer sensors and synchronising these with the tasks. Movement can significantly highlight the tremor effects and variations and this can be combined with the FPV calculation.

c. Using a 1kg weight on the forearm during the load session may return better results in demonstrating the paresis effect on the subject's hand from the FPV.

d. High density EMG signals can be used with advanced data signals classification in order to detect hand gestures and assess finger movements. This could be achieved by using neural network methods with specified postures. The high density EMG will cover a larger surface of the muscle and return more detailed analysis on the area responsible for the joints' control of the flexion/extension muscles. This is an efficient method to control the virtual hand and prosthetic arms using the EMG electrodes. It also allows for study of the muscle's memory contributions in the motor control process of the hand functionality.

e. Including extra SHAP classification procedures in the experiment can reduce the pattern-learning factor of the hand movement during repetitive trials. It can also increase the list of random task selections.

f. Providing more illustrative training on the virtual reality system to each subject before running the experiment can improve the performance values and improve the inter-subject repeatability between the subjects. This will be of particular benefit to those subjects with no previous experience in this type of applications.

Chapter 8 Conclusions and Future Work

8.1. System Objective Review

This thesis has presented a unique method for objective measurement that can efficiently assess hand performance and reliably be used in hand assessment and rehabilitation. The project studied the implementation of the latest technologies for dynamically measuring the objective performance of the hand. The assessment system can be incorporated during the evaluation phases before or after each rehabilitation session. This will give a dynamic analysis of the finger improvement throughout the rehabilitation process. The assessment system is only compliant for patients who are capable of performing voluntary movements with their hands, or advanced stages in the rehabilitation, after the other assessment devices, such as ARAT and SHAP, are used.

As explained in the Discussion Chapter 7, this project provides a unique measuring value FPV (Finger Performance value). Unlike other scoring systems, such as IoF (Index of Functionality) (Light et al., 2002), the FPV includes new parameters (smoothness of the fingers' motion trajectories, stability of the fingers in the hold positions) and addresses each finger individually. This makes the FPV scoring unit different from the other existing scoring standards and requires a different approach or new evaluation procedures by the therapists. As this project has covered only the first phase to run experiments on healthy subjects, further tests are required to be performed on people with hand dysfunction by therapists to evaluate the FPV.

On the other hand, this system offers multiple advantages; it is portable and can be used in different places. It is fully automated and doesn't require the therapists to set any timer or data inputs for measuring the performance. It is comfortable on the patients' hands and does not involve intensive tasks. It is motivating as it includes virtual interaction and visual illustrations, and it provides dynamic measurement of each finger's performance. This allows the system to be easily adjusted with the patient's requirement and improvement;

In addition, it highlights the level of details for each finger. The system is modular and the measuring or display devices can be replaced with different devices to suit the requirements (costs, accuracy, etc.). The estimated cost of the system might vary from £1,000 to £20,000 (without the EMG system), depending on the quality of the used devices.

In summary, the present research has contributed to the following:
(the sentences presented with quotations below are extracted from previous chapters: Chapter 2, section 2.3 and Chapter 3, section 3.2)

- Developing and implementing for the first time (to the best of the author's knowledge) a unique and advanced robotic simulator that combines the data glove CyberGlove® for biomechanical and hand assessment research. The application meets the below specifications which were specified in the Background Chapter 2, section 2.3:

  o **"The application must show very reliable and robust calibration between the actual hand and the virtual model movement. This is in order to build the confidence level in analysing the reliability of the measured data. "**
  An improved design to the hand kinematic was implemented in the VR application to operate the multiple control mechanisms. Further to this, a thorough investigation for the various calibration methods used in robotic and VR research was performed to produce the most adequate and robust algorithm.

  o **"The virtual models should show very similar representation of the real world hand and classification procedure objects. "**
  Existing limitations in VR, in comparison to the real world, were addressed by using different approaches (such as see-through mode to compensate the sensory feedbacks in object grasp, and virtual hand/object animation to adjust the world to the desired transformation and meet the task requirements). The VR advantages were explored in order to produce an efficient application by eliminating the constraints that exist on actual hand movement.

  o **"The simulator application should be developed with consideration of future implementation in hand rehabilitation. "**
  The adaptability of the virtual hand control with different data formats and the feasibility of the calibration method allow the use of different third party devices (i.e. data gloves, sensors, classified muscle or brain activities data) in combination with the virtual hand manipulation application. This offers a more robust and

feasible system than the prosthetic test platforms.

The application has a user-friendly interface and adaptable robotic structure. This allows new models to be easily loaded and new kinematics and algorithms to be used for different purposes, such as gesture recognition, classifications, grasp optimisation, and automatic postures formation.

o **"The application should also include other experimental types of sensory inputs and simulation."**

The collision detection method developed in this project, allows control commands to be sent to the haptic feedback systems, targeting the specified digits and joints.

The application includes a dynamic engine that can be developed to simulate real world physics and interaction forces.

The specifications listed above are explored in the Background, Chapter 2.

▪ **"SHAP classification procedure should be appropriately included to validate and study the multiple aspects of the proposed method."**

This project selects four SHAP tasks to address the three main digits during hand rehabilitation. In addition to the multiple factors included in data measurement and analysis, the system allows for the creation of an autonomous and objective measurement procedure. This removes uncontrolled variability and subjective influences.

The VR system presented a similar environment and experimental procedures to real world interactions. This validates the feasibility of employing virtual reality applications in the rehabilitation spectrum, and in hand assessment specifically. A new application was produced to be used as a test platform for further studies and research on the VR, by exploring its efficiency in monitoring and contributing to the patient's progress and adaptability.

▪ **"The developed method should be adaptable with new tasks and sessions."**

The uniquely developed algorithm in this project covers the essential characteristics of the finger's movements that contribute to the performance of daily and abstract activities. Further explanation of this method is provided in the Experimental Chapter 4. This includes the considerations used to provide robustness in measuring the motion as

well as important features in the fingers' movements.

This method is proven to be reliable and flexible and can therefore be employed in different fields outside the field of bioengineering. This includes the psychology field, where the classification procedures can be adjusted to involve the measurement of emotional gestures. It can also be employed in ergonomics, to address human-to-machine interactions as preliminary steps towards designing more adequate hand tool devices. Also, this application can be used in system controls and gesture recognitions.

The project provided a configured human hand model for the biomechanical application. In the Calibration Chapter 5, a robust calibration method was developed to efficiently manipulate the virtual hand model using the data glove device sensorial outputs. The calibration method has multiple advantages in comparison to other methods. It doesn't take a long time or require a pre-generated dataset. It is adaptive with each subject's physiological and performance configurations, and the calculations take the dependent sensors into consideration.

This project also covers the various disciplines that are used in hand rehabilitation, and provides substantial reviews on their drawbacks and advantages. It explores the significant motor control factors involved in hand functionality (see Background, Chapter 2). The project outlines the appropriate methods, using brain activities and visual feedback sensory inputs, that can be used to implement this application for hand posture classifications.

In the Literature Review, Chapter 3, an extensive review of different data glove applications is provided. This can be used to justify the need to develop an alternative data glove device that is less expensive, has higher feasibility in tracking the multiple DoF of the hand kinematic, and can be adapted to different hand sizes.

8.2. Future Research Directions

The focus of the project has been to develop an advanced VR application that efficiently measures hand performance. During the research and development work, various areas have been highlighted to improve and extend the system's outcome and applicability. A number of factors to consider and incorporate in future research are detailed below:

- In order to obtain more efficient and clinical results, the application should be tested on patients with hand dysfunctions. An anticipated continuation of the current project is to conduct experiments on patients during the hand rehabilitation process. This would also involve consulting with surgeons and rehabilitation experts to assess the calculated values and closely monitor variations during the rehabilitation sessions. This method has proven to be efficient on healthy subjects. There were time restrictions due to the extensive software development required to produce an efficient interactive simulator and new algorithm equations for kinematics and hand assessment. However, the experiment did cover some aspects of hand dysfunction by simulating paresis during the load and tremor sessions.

- Adding haptic feedback to the hand is essential, since it can increase the accuracy level in interacting with the virtual world. It can also extend the capability of the system to exert forces on targeted hand digits, which can provide consistent and reliable exercises for rehabilitation of specific dexterities in the hand dysfunction. However, the addition of the haptic devices can also cause discomfort for the patient, and can restrict the system's portability and flexibility with the complex tasks. It can also increase the cost and time taken to setup and calibrate the device.

The developed simulator supports collision detection algorithms. By retrieving the collision area of the involved joints in the virtual model, it can be used to program the haptic device and activate the fingers' resistance wires to provide force feedback for describing the virtual object bounding shape.

CyberGrasp® is a haptic system available in the Bioengineering Lab in the University of Strathclyde. It provides individual resistive forces on the multiple joints of the fingers and can be controlled by sending specific commands through the network, using the interface unit. However, this system is not implemented in this project, as it is cumbersome and complex to control. It also imposes a large number of restraints on the hand.

In this thesis, multiple hand exoskeletons were reviewed in the Literature Review Chapter 3. These can be used for developing an adequate and compliant haptic feedback device.

- As discussed in the Background Chapter 2, the dynamic engine in the simulator is fragile and requires significant development. A number of robust and advanced physics engines have recently been developed, such as PhysX (PhysX-Nvidia, 2015) and Bullet (Bullet). These can be employed in the virtual simulator to provide realistic graphical behaviour in relation to the numerous forces in the environment. These engines are extensively used in industrial simulations and can provide an effective imitation that resembles the actual experimental setup. An accurate representation of the real life setup is significant for effectively performing biomechanical and rehabilitation analysis.

  The dynamic engine can expand the system's applicability and reduce the level of controls needed to interact with the real world experimental setups.

- An interesting area of rehabilitation research, which relates closely to this project, is the examination of the motor control EEG signals used to perform certain ADL tasks. Ciocarlie and Allen have developed an Eigengrasp algorithm (Ciocarlie and Allen, 2009), based on Santello's study, to reduce the dimensionality of the motor control signals by identifying the hand postures from a defined set (Santello et al., 2002). (Jonathan et al., 2015) produced an application of the simulator, in combination with the brain computer interface, to plan and select a specific grasp gesture from pre-planned grasps. Their project aimed to provide a flexible grasp planning system for assistive robotic manipulation, with less complexity in comparison to human hand kinematics.

  The CyberGlove® can be combined with this to provide a comparison between actual hand movements and simulated movements. The simulator application can also contribute significantly to reducing the complex kinematic structure of the hand and the high level task planning, by visualising a more adaptive and sustainable hand model representation.

  Further explanation of the features selection and data classifications were provided in the Background Chapter 2.

8.3. Conclusion

In this project, we have developed a unique virtual reality system that provides efficient outcome measurements of the hand rehabilitation. The materials (CyberGlover®, SHAP, Dome®, and EMG), and system applications (Robotic Simulator) adequate to obtain robust and reliable data outputs were specified. Also, an advanced calibration method was developed that can return a vigorous system in reading and manipulating the virtual model.

On the other hand, experimental studies were designed and conducted on a controlled group to validate this approach. They involved selecting specific classification tasks and altering the relevant attributes, such as weight and tremor, to evaluate the effects of fatigue and system sensitivities on the hand measurement. Noticeably, the results showed high evidence to support the thesis hypotheses. In addition, the virtual reality was found reliable in simulating the numerous features of hand performance. The Finger Performance Value (FPV) method demonstrated high reliability and efficiency to objectively measure the performance of the involved fingers.

The combination of the SHAP hand classification procedure with the interactive system, consisting of a graphical simulator and a data glove manipulation device, produced a powerful approach for hand rehabilitation applications. The new algorithm, developed in this project, has proved to be reliable and efficient to measure hand performance. And the implemented algorithm illustrates the various restoration phases of the hand by analysing specific fingers' elements: speed, motion, and coordination.

At the end of this thesis, different plausible approaches and techniques that can be used in order to either improve the system and data measurement were provided. This included integrating a motion capture sensor for the wrist and arm movements, increasing the weight for heightening the fatigue effect, adding other classification tasks to reduce the effect of learning patterns, and using high density EMG to increase the data reading of the multiple involved muscles; or the total research outcome in the medical rehabilitation field, by performing clinical tests and taking therapists' assessments to the FPV scores.

In comparison to the other available hand assessment systems, this approach offers a universal procedure that is cross-compatible with different rehabilitation techniques. In addition, the method dynamically measures the fingers' improvements during hand

recovery, and allows therapist to compare with other normative data sets and review previous performance. It also measures the competencies of the patient's hand motions in the VR and real world.

Hand rehabilitation is certainly a very substantial subject in medical rehabilitation. The author hopes that the work produced in this project will efficiently assist future researchers in developing an effective and adaptable application to rehabilitate the hand.
The method in this project also seeks to provide significant support in enhancing the rehabilitation process and removing the difficulties in hand dysfunction, which can lead to physical and emotional distress.

Bibliography

3DSMAX. 2015. *3d Design Software | 3ds Max | Autodesk* [Online]. Available: http://www.autodesk.co.uk/products/3ds-max/overview.

ADAMOVICH, S. V., FLUET, G. G., MATHAI, A., QIU, Q., LEWIS, J. & MERIANS, A. S. 2009a. Design of a complex virtual reality simulation to train finger motion for persons with hemiparesis: a proof of concept study. *J Neuroeng Rehabil,* 6**,** 28.

ADAMOVICH, S. V., FLUET, G. G., MERIANS, A. S., MATHAI, A. & QIU, Q. 2009b. Incorporating haptic effects into three-dimensional virtual environments to train the hemiparetic upper extremity. *IEEE Trans Neural Syst Rehabil Eng,* 17**,** 512-20.

AGUIAR, R. D. C. 2007. *Concepção e Desenvolvimento de um jogo 3D para Computador utilizando o software VIRTOOLS e Tecnologiade Seguimento.*

AL-JUMAILY, A. & OLIVARES, R. A. Electromyogram (EMG) driven system based virtual reality for prosthetic and rehabilitation devices. Proceed. of the 11th Int. Conf. on Information Integ. and Web-based Applications & Services, 12/14/2009 2009. ACM, 582-586.

ALBANI, G., PIGNATTI, R., BERTELLA, L., PRIANO, L., SEMENZA, C., MOLINARI, E., RIVA, G. & MAURO, A. 2002. Common daily activities in the virtual environment: a preliminary study in parkinsonian patients. *Neurol Sci,* 23 Suppl 2**,** 49-50.

ALTSCHULER, E. L., WISDOM, S. B., STONE, L., FOSTER, C., GALASKO, D., LLEWELLYN, D. M. & RAMACHANDRAN, V. S. 1999. Rehabilitation of hemiparesis after stroke with a mirror. *Lancet.* England.

AMADEO. 2015. *Tyromotion â€" Therapy* [Online]. Available: http://tyromotion.com/en/products/amadeo/therapy.

AMIRABDOLLAHIAN, F., ATES, S., BASTERIS, A., CESARIO, A., BUURKE, J., HERMENS, H., HOFS, D., JOHANSSON, E., MOUNTAIN, G., NASR, N., NIJENHUIS, S., PRANGE, G., RAHMAN, N., SALE, P., SCHÄTZLEIN, F., VAN SCHOOTEN, B. & STIENEN, A. 2014. Design, development and deployment of a hand/wrist exoskeleton for home-based rehabilitation after stroke - SCRIPT project. *Robotica,* 32**,** 1331 - 1346.

AN, K. N., CHAO, E. Y., COONEY, W. P., 3RD & LINSCHEID, R. L. 1979. Normative model of human hand for biomechanical analysis. *J Biomech.* United States.

ANDREW, M. & MATEI, C. 2015. *GraspIt!* [Online]. Available: http://www.cs.columbia.edu/~cmatei/graspit/.

ANYKODE. 2015. *anyKode Marilou - Modeling and simulation environment for Robotics* [Online]. Available: http://www.anykode.com/index.php.

ASSH. 2015. *ASSH.org and Hand About ASSH* [Online]. Available: http://www.assh.org/About-ASSH.

AUTOCAD. 2015. *CAD Software| CAD Design | AutoCAD For Mac & Windows | Autodesk* [Online]. Available: http://www.autodesk.co.uk/products/autocad/overview.

AZZURRA, C., FRANCESCO, G., NICOLA, V., EMANUELE, C., STEFANO, R., FABRIZIO, V. & MARIA, C. C. 2009. HANDEXOS: Towards an exoskeleton device for the rehabilitation of the hand. *2009 IEEE/RSJ International Conference on Intelligent Robots and Systems, St. Louis, MO, USA*.

BANIASAD, M. A., FARAHMAND, M. & ANSARI, N. N. 2011. Wrist-RoboHab: a robot for treatment and evaluation of brain injury patients. *IEEE Int Conf Rehabil Robot,* 2011**,** 5975506.

BARBAY, S. & NUDO, R. J. 2009a. The effects of amphetamine on recovery of function in animal models of cerebral injury: a critical appraisal. *NeuroRehabil,* 25**,** 5-17.

BARBAY, S. & NUDO, R. J. 2009b. The effects of amphetamine on recovery of function in animal models of cerebral injury: a critical appraisal. *NeuroRehabilitation,* 25**,** 5-17.

BELL, C., HAN, V., SUGAWARA, Y. & GRANT, K. 1997. Synaptic plasticity in a cerebellum-like structure depends on temporal order. *Nature***,** 278-281.

BERLIM, M. T., VAN DEN EYNDE, F. & DASKALAKIS, Z. J. 2013. High-frequency repetitive transcranial magnetic stimulation accelerates and enhances the clinical response to antidepressants in major depression: a meta-analysis of randomized, double-blind, and sham-controlled trials. *J Clin Psychiatry,* 74**,** e122-9.

BILLINGSLEY, J. 2006. *"Essentials of Mechatronics". ,* Hoboken, NJ. 2006 ISBN 978-0-471-72341-7 John Wiley & Sons. .

BIONICS, T. 2013. *Home - Touch Bionics* [Online]. Available: http://www.touchbionics.com/.

BIRCH, B., HASLAM, E., HEERAH, I., DECHEV, N. & PARK, E. J. 2008. Design of a continuous passive and active motion device for hand rehabilitation. *Conf Proc IEEE Eng Med Biol Soc,* 2008**,** 4306-4309.

BLAKEMORE, S., FRITH, C. & WOLPERT, D. 1999. Perceptual modulation of selfproduced stimuli: The role of spatio-temporal prediction. *J. Cognitive Neurosc***,** 551-559.

BLAND, J. & ALTMAN, D. 1986. Statistical methods for assessing agreement between two methods of clinical measurement. *Lancet. ,* 1**,** 307-10.

BLAND, J. & ALTMAN, D. 1999. Measuring agreement in method comparison studies. *Stat. Methods in Med. Res.,* 8**,** 135-60.

BLENDER. 2015. *Blender 3D modeling and animation platform* [Online]. Available: http://www.blender.org/.

BOUZIT, M., PISCATAWAY, N., POPESCU, G., BURDEA, G. & BOIAN, R. 2002. The Rutgers Master II-ND force feedback glove. *Haptic Interfaces for Virtual Environment and Teleoperator Systems, 2002. HAPTICS 2002. Proceedings. 10th Symposium on*.

BOVEND'EERDT, T. J., DAWES, H., JOHANSEN-BERG, H. & WADE, D. T. 2004. Evaluation of the Modified Jebsen Test of Hand Function and the University of Maryland Arm Questionnaire for Stroke. *Clin Rehabil,* 18**,** 195-202.

BOWMAN, T. & SPEIER, J. 2006. Videoconferencing, Virtual Reality and Home-Based CIMT-Opportunities to Improve Access and Compliance through Telerehabilitation. *2006 Int. Workshop on Virtual Rehabil*.

BRITISH STANDARDS INSTITUTION, B. 1975. Prec. of test methods 1: Guide for the determ. and reprod for a standard test method. London: BSI

BROOKS, B. M. 2010. Route Learning in a Case of Amnesia: A Preliminary Investigation into the Efficacy of Training in a Virtual Environment. *Neuropsychological Rehabilitation,* 9**,** 63-76.

BROSSEAU, L., JUDD, M. G., MARCHAND, S., ROBINSON, V. A., TUGWELL, P., WELLS, G. & YONGE, K. 2003. Transcutaneous electrical nerve stimulation (TENS) for the treatment of rheumatoid arthritis in the hand. *Cochrane Database Syst Rev***,** CD004377.

BSSH. 2015. *BSSH - The British Society for Surgery of the Hand* [Online]. Available: http://www.bssh.ac.uk/.

BUCHHOLZ, B. & ARMSTRONG, T. J. 1992. A kinematic model of the human hand to evaluate its prehensile capabilities. *Journal of Biomechanics,* 25**,** 149-162.

BULLET. *Bullet Physics Simulation* [Online]. Available: http://www.bulletphysics.org/.

BURDEA, G., POPESCU, V., HENTZ, V. & COLBERT, K. 2000. Virtual reality-based orthopedic telerehabilitation. *IEEE Trans Rehabil Eng,* 8**,** 430-2.

BURDEA, G. C., JAIN, A., RABIN, B., PELLOSIE, R. & GOLOMB, M. 2011. Long-term hand tele-rehabilitation on the PlayStation 3: benefits and challenges. *Conf Proc IEEE Eng Med Biol Soc,* 2011**,** 1835-1838.

BUTTERFASS, J. G., M

LIU, H & HIRZINGER, G. DLR-Hand II: Next Generation of a Dextrous Robot Hand. Proceedings of the IEEE Int. Conference on Robotics and Automation, 2001.

CALLENDER, N. 2015. *Gravity Climbing Centre* [Online]. Available: http://nigelcallender.blogspot.co.uk/.

CARROLL, D. 1965. A QUANTITATIVE TEST OF UPPER EXTREMITY FUNCTION. *J Chronic Dis,* 18**,** 479-91.

CED. 2015. *CED Products | Spike2 life sciences data acquisition and analysis system* [Online]. Available: http://ced.co.uk/products/spike2.

CHALON, M., GREBENSTEIN, M. & WIMB, T. 2010. The thumb: Guidelines for a robotic design. *The 2010 IEEE/RSJ International Conference on Intelligent Robots and Systems October 18-22, 2010, Taipei, Taiwan*.

CIOCARLIE, M. T. & ALLEN, P. K. 2009. Hand Posture Subspaces for Dexterous Robotic Grasping. *The International Journal of Robotics Research,* Volume 28 Issue 7

851-867

COIN3D. 2015. *Coin3D* [Online]. Available: https://bitbucket.org/Coin3D/coin.

CONNELLY, L., JIA, Y., TORO, M. L., STOYKOV, M. E., KENYON, R. V. & KAMPER, D. G. 2010. A pneumatic glove and immersive virtual reality environment for hand rehabilitative training after stroke. *IEEE Trans Neural Syst Rehabil Eng,* 18**,** 551-9.

CONNELLY, L., STOYKOV, M. E., JIA, Y., TORO, M. L., KENYON, R. V. & KAMPER, D. G. 2009. Use of a pneumatic glove for hand rehabilitation following stroke. *Conf Proc IEEE Eng Med Biol Soc,* 2009**,** 2434-7.

CONOLLY, W. 2015. *Rehabilitation of the hand and upper limb - University of Strathclyde*.

CYBERGLOVE-SYSTEMS-SPEC. 2013. *Specifications | cyberglovesystems* [Online]. Available: http://www.cyberglovesystems.com/products/cyberglove-ii/specifications.

CYBERGLOVE. 2013. *Homepage | CyberGlove* [Online]. Available: http://www.cyberglovesystems.com/.

CYBERGRASP. 2015. *Overview | CyberGrasp* [Online]. Available: http://cyberglovesystems.com/products/cybergrasp/overview.

DAMUSH, T. M., PLUE, L., BAKAS, T., SCHMID, A. & WILLIAMS, L. S. 2007. Barriers and facilitators to exercise among stroke survivors. *Rehabil Nurs,* 32**,** 253-60, 262.

DANCEY, C. & REIDY, J. 2004. *Statistics without Maths for Psychology: using SPSS for Windows,* London, Prentice Hall.

DATABASE, C. G. *Columbia Grasp Database large dataset of precomputed grasps on thousands of 3D models, is available for download as a PostgreSQL database backup file* [Online]. Available: http://grasping.cs.columbia.edu/.

DAUD, O., BIRAL, F., OBOE, R. & PIRON, L. 2010. Design of a haptic device for finger and hand rehabilitation. *IECON 2010 - 36th Annual Conf. on IEEE Industrial Electronics Soc.*

DAVID, L., HEBL, M., OSHERSON, D. & ZIEMER, H. 2015. Online Statistics Education: An Interactive Multimedia Course of Study. Pearson r-correlation Coefficient

DAVIES, R., LÖFGREN, E., WALLERGÅRD, M., LINDÉN, A., BOSCHIAN, K., MINÖR, U., SONESSON, B. & JOHANSSON, G. 2002. Three applications of virtual reality for brain injury rehabilitation of daily tasks *Proc. 4th Intl Conf. Disability, Virtual Reality & Assoc. Tech., Veszprém Hungary*.

DAVIS, R., PHILLIPS, R., ROSCOE, J. & ROSCOE, D. 2000. *Physical Education and the study of sport,* Spain: Harcourt.

DE LUCA, G. 2001. Fundamental Concepts in EMG Signal Acquisition. DelSys Inc.

DESROSIERS, J., BRAVO, G., HEBERT, R., DUTIL, E. & MERCIER, L. 1994. Validation of the Box and Block Test as a measure of dexterity of elderly people: reliability, validity, and norms studies. *Arch Phys Med Rehabil,* 75**,** 751-755.

DIDJIGLOVE. 2013. *Didjiglove from Inition* [Online]. Available: http://inition.co.uk/3D-Technologies/didjiglove.

DIPIETRO, L., SABATINI, A. M. & DARIO, P. 2008. A survey of glove-based systems and their applications. *IEEE Transactions on Systems Man and Cybernetics Part C-App. and Reviews,* 38**,** 461-482.

DUNCAN, P. W., BODE, R. K., MIN LAI, S. & PERERA, S. 2003. Rasch analysis of a new stroke-specific outcome scale: the Stroke Impact Scale. *Arch Phys Med Rehabil,* 84**,** 950-63.

DUNNE, L., B., S. & B., C. 2007. A Comparative Evaluation of Bend Sensors for Wearable Applications. *11th IEEE International Symposium Conference on Wearable Computers*.

EARHART, G. M., CAVANAUGH, J. T., ELLIS, T., FORD, M. P., FOREMAN, K. B. & DIBBLE, L. 2011. The 9-hole PEG test of upper extremity function: average values, test-retest reliability, and factors contributing to performance in people with Parkinson disease. *J Neurol Phys Ther,* 35**,** 157-63.

EASY-ROB. 2015. *EASY-ROB Simulator* [Online]. Available: http://www.easy-rob.com/produkt.html.

EDGAR SS, A. P., FRANCESC MN. 2014. *IRI - Kinematic Model of the Hand using Computer Vision* [Online]. Available: http://www.iri.upc.edu/pfc/show/74.

ELETHA, F. G., T.;ETTORE, C.;FRANCESCA, IC.;JOEL, CP.;THIERRY, K.; 2008. Improving patient motivation in game development for motor deficit rehabilitation. *ACE '08 Proceed. of the 2008 Int. Conf. on Adv. in Computer Entert. Tech., New York, NY, USA ©2008**,*** 381-384

ELKOURA, G. & SINGH, K. Handrix: animating the human hand. Proceedings of the 2003 ACM SIGGRAPH/Eurographics symposium on Computer animation, 07/26/2003 2003. Eurographics Association, 110-119.

EMEDICINEHEALTH. 2013. *Hand Injuries, Stats, Causes, Treatments, Pictures - eMedicineHealth.com* [Online]. Available: http://www.emedicinehealth.com/hand_injuries/article_em.htm.

EMG 2015. EMG: Electromyography | Research | BIOPAC.

ENDO, T., KAWASAKI, H., MOURI, T., DOI, Y., YOSHIDA, T., ISHIGURE, Y., SHIMOMURA, H., MATSUMURA, M. & KOKETSU, K. Five-fingered haptic interface robot: HIRO III. Proceedings of the World Haptics 2009 - Third Joint EuroHaptics conference and Symposium on Haptic Interfaces for Virtual Environment and Teleoperator Systems, 03/18/2009 2009. IEEE Computer Society, 458-463.

FAKESPACELABS. 2015. *Fakespacelabs* [Online]. Available: http://www.fakespacelabs.com/.

FELDMAN, A. 1966. Functional tuning of the nervous system with control of movement or maintenance of a steady posture. III. Mechanographic analysis of execution by arm of the simplest motor tasks. *Biophysics**,*** 766-775.

FERENC, K., GABRIEL, Z. & REINHARD, K. Visual-fidelity dataglove calibration. in Proc. of the Computer Graphics International (CGI'04), 2004, 2015.

FIFTH-DIMENSION-TECHNOLOGIES. 2013. *5DT Products* [Online]. Available: http://www.5dt.com/products/pdataglovemri.html.

FISCHER, H. C., STUBBLEFIELD, K., KLINE, T., LUO, X., KENYON, R. V. & KAMPER, D. G. 2007. Hand rehabilitation following stroke: a pilot study of assisted finger extension training in a virtual environment. *Top Stroke Rehabil,* 14**,** 1-12.

FLASH, T. & HOGAN, N. 1985. The co-ordination of arm movements: An experimentally confirmed mathematical model. *J. Neurosc,* 5.

FLORENCE, S. C. & JANE, B. L. 1988. Hand rehabilitation in occupational therapy (Occupational therapy in health care). New York and London: Routledge.

FLORENCE, S. C. & JANE, B. L. 2015. Hand rehabilitation in occupational therapy - University of Strathclyde.

FOGG, Q. 2015. *Professional Anatomist* [Online]. Available: http://www.bbc.co.uk/programmes/profiles/4SvFhFxFDNjyYFmk2SWrqjB/anatomist-quentin-fogg.

FOK, S., SCHWARTZ, R., WRONKIEWICZ, M., HOLMES, C., ZHANG, J., SOMERS, T., BUNDY, D. & LEUTHARDT, E. 2011. An EEG-based brain computer interface for rehabilitation and restoration of hand control following stroke using ipsilateral cortical physiology. *Conf Proc IEEE Eng Med Biol Soc,* 2011**,** 6277-80.

FORRESTER, G., QUARESMINI, C., LEAVENS, D., MARESCHAL, D. & THOMAS, M. 2013. Human handedness: An inherited evolutionary trait. *Behav Brain Res.,* 237**,** 200–206.

FUENTES, J. P., ARMIJO OLIVO, S., MAGEE, D. J. & GROSS, D. P. 2010. Effectiveness of interferential current therapy in the management of musculoskeletal pain: a systematic review and meta-analysis. *Phys Ther,* 90**,** 1219-1238.

GAN, L. S. & PROCHAZKA, A. 2010. Properties of the stimulus router system, a novel neural prosthesis. *IEEE Trans Biomed Eng,* 57**,** 450-9.

GAN, L. S., PROCHAZKA, A., BORNES, T. D., DENINGTON, A. A. & CHAN, K. M. 2007. A new means of transcutaneous coupling for neural prostheses. *IEEE Trans Biomed Eng,* 54**,** 509-17.

GAZEBO. 2015. *Gazebo Simulator , OSRF* [Online]. Available: http://gazebosim.org/.

GEFORCE. 2015. *DirectX 11 | GeForce* [Online]. Available: http://www.geforce.co.uk/hardware/technology/dx11.

GISZTER, S., MUSSA-IVALDI, F. & BIZZI, E. 1993. Convergent force fields organized in the frog's spinal cord. *J. Neurosc***,** 467–491.

GIZMO3D. 2015. *GizmoSDK* [Online]. Available: http://www.gizmosdk.com/.

GLADSTONE, D. J., DANELLS, C. J. & BLACK, S. E. 2002. The fugl-meyer assessment of motor recovery after stroke: a critical review of its measurement properties. *Neurorehabil Neural Repair,* 16**,** 232-40.

GNU. 2015. *GNU License Policy* [Online]. Available: http://www.gnu.org/copyleft/gpl.html.

GOCKLEY, R. & MATARIĆ, M. J. Encouraging physical therapy compliance with a hands-Off mobile robot. Proceedings of the 1st ACM SIGCHI/SIGART conference on Human-robot interaction, 03/02/2006 2006. ACM, 150-155.

GODFREY, S. B., SCHABOWSKY, C. N., HOLLEY, R. J. & LUM, P. S. 2010. Hand function recovery in chronic stroke with HEXORR robotic training: A case series. *Conf Proc IEEE Eng Med Biol Soc,* 2010**,** 4485-8.

GOFFREDO, M., BERNABUCCI, I., SCHMID, M. & CONFORTO, S. 2008. A neural tracking and motor control approach to improve rehabilitation of upper limb movements. *J Neuroeng Rehabil,* 5**,** 5.

GONZÁLEZ-QUIJANO, J., JAVIER.GONZALEZ, Q., WIMBÖCK, T., BENSALAH, C. & ABDERRAHIM, M. Analysis and Experimental Evaluation of an Object-Level In-Hand

Manipulation Controller Based on the Virtual Linkage Model. ROBOT2013: First Iberian Robotics Conf., Adv. in Intell. Sys. and Computing 2015 253. 675-686.

GRAY, H. 2015. *Gray's Anatomy – The Anatomical Basis of Clinical Practice 41st edition*.

GREALY, M. & NASSER, B. 2013. The use of virtual reality in assisting rehabilitation. *Adv in Clinical Neurosc and Rehabil,* 13**,** 19-20.

GREGSON, J. M., LEATHLEY, M., MOORE, A. P., SHARMA, A. K., SMITH, T. L. & WATKINS, C. L. 1999. Reliability of the Tone Assessment Scale and the modified Ashworth scale as clinical tools for assessing poststroke spasticity. *Arch Phys Med Rehabil,* 80**,** 1013-1016.

GRITSENKO, V. & PROCHAZKA, A. 2004. A functional electric stimulation-assisted exercise therapy system for hemiplegic hand function. *Arch Phys Med Rehabil,* 85**,** 881-885.

GROUP-VISUALIZATION-SCIENCES. 2015. *Open Inventor | FEI Visualization Sciences Group* [Online]. Available: http://www.vsg3d.com/open-inventor/sdk.

H., J. 2015. *R-Station: Product* [Online]. Available: http://robotics.snu.ac.kr/r-station/product/product.html.

HAMED, N., STIJN, B., RACHEL, S., BERND, G. & IDE, H. 2014. Towards routine motion analysis in clinical practice: inertial sensor versus optoelectronic motion capture system. *AHORSE, Atrium Medical Centre, Heerlen, The Netherlands*.

HANDCORPUS. 2014. *HandCorpus is an open access repository for sharing and retrieving human and robot hand data.* [Online]. Available: http://www.handcorpus.org/.

HARTIGAN, I. 2007. A comparative review of the Katz ADL and the Barthel Index in assessing the activities of daily living of older people. . *Int. J. of Older People Nurs.,* 2**,** 204-212.

HERNANDEZ-REBOLLAR, J. L., KYRIAKOPOULOS, N. & LINDEMAN, R. W. The AcceleGlove: a whole-hand input device for virtual reality. ACM SIGGRAPH 2002 conference abstracts and applications, 07/21/2002 2002. ACM, 259-259.

HESSE, S., KUHLMANN, H., WILK, J., TOMELLERI, C. & KIRKER, S. 2013. A new electromechanical trainer for sensorimotor rehabilitation of paralysed fingers: A case series in chronic and acute stroke patients. *Journal of NeuroEng and Rehabil,* 5**,** 1-6.

HESSE, S., SCHULTE-TIGGES, G., KONRAD, M., BARDELEBEN, A. & WERNER, C. 2003. Robot-assisted arm trainer for the passive and active practice of bilateral forearm and wrist movements in hemiparetic subjects. *Arch Phys Med Rehabil,* 84**,** 915-20.

HESTER, T., SHERRILL, D. M., HAMEL, M., PERREAULT, K., BOISSY, P. & BONATO, P. 2006. Identification of tasks performed by stroke patients using a mobility assistive device. *Conf Proc IEEE Eng Med Biol Soc,* 1**,** 1501-4.

HO, N. S., TONG, K. Y., HU, X. L., FUNG, K. L., WEI, X. J., RONG, W. & SUSANTO, E. A. 2011. An EMG-driven exoskeleton hand robotic training device on chronic stroke subjects: task training system for stroke rehabilitation. *IEEE Int Conf Rehabil Robot,* 2011**,** 5975340.

HOBBYTRONICS. 2015. *http://www.hobbytronics.co.uk/flex-sensor-2-2* [Online].

HOGAN, N. 1984. An organizing principle for a class of voluntary movements. *J. Neurosc,* 4.

HOLDEN, M. K. 2005. Virtual environments for motor rehabilitation: review. *Cyberpsychol Behav,* 8**,** 187-211; discussion 212-9.

HOLDEN, M. K., DYAR, T. A., SCHWAMM, L. & BIZZI, E. 2005. Virtual-environment-based telerehabilitation in patients with stroke. *Presence: Teleop. and Virtual Env.,* 14**,** 214-233.

HOLMES, S. 2000. *Introductory Statistics - Root Mean Square Error* [Online]. Available: http://statweb.stanford.edu/~susan/courses/s60/split/node60.html.

HONG, K., JEONG, H., FATIMA, N., JAMES, C. & RAYE, C. 2015. A Soft Exoskeleton for Hand Assistive and Rehabilitation Application using Pneumatic Actuators with Variable Stiffness. *2015 IEEE Int. Conf. on Robotics and Automation (ICRA)*.

HOUSMAN, S. J., SCOTT, K. M. & REINKENSMEYER, D. J. 2009. A randomized controlled trial of gravity-supported, computer-enhanced arm exercise for individuals with severe hemiparesis. *Neurorehabil Neural Repair,* 23**,** 505-14.

HUANG, Y. Y. & LOW, K. H. 2008. Initial analysis and design of an assistive rehabilitation hand device with free loading and fingers motion visible to subjects. *IEEE Int. Conf. on Systems, Man, and Cybernetics - SMC* 2584-2590.

HUBER, M., RABIN, B., DOCAN, C., BURDEA, G., NWOSU, M. E., ABDELBAKY, M. & GOLOMB, M. R. PlayStation 3-based tele-rehabilitation for children with hemiplegia. Virtual Rehabil., 2008, 25-27 Aug. 2008 2008. 105-112.

HUENERFAUTH, M. & LU, P. 2010. Accurate and Accessible Motion-Capture Glove Calibration for Sign Language Data Collection. *ACM Transactions on Accessible Computing (TACCESS),* 3**,** 2.

IDROGENET, S. 2015. *Gloreha* [Online]. Available: http://www.gloreha.com/.

IMPRESSUM. 2015. *ProGlove - Wearables for Professionals* [Online]. Available: http://www.proglove.de/.

INMOTION. 2015. *Interactive Motion Technologies | InMotion HAND* [Online]. Available: http://interactive-motion.com/healthcarereform/upper-extremity-rehabilitiation/inmotion-hand/.

IWATA, H. & SUGANO, S. Design of human symbiotic robot TWENDY-ONE. Proceedings of the 2009 IEEE international conference on Robotics and Automation, 05/12/2009 2009. IEEE Press, 3294-3300.

JACK, D., BOIAN, R., MERIANS, A. S., TREMAINE, M., BURDEA, G. C., ADAMOVICH, S. V., RECCE, M. & POIZNER, H. 2001. Virtual reality-enhanced stroke rehabilitation. *Ieee Transactions on Neural Systems and Rehabilitation Engineering,* 9**,** 308-318.

JEANNEROD, M. & FRAK, V. 1999. Mental imaging of motor activity in humans. *Curr Opin Neurobiol,* 9**,** 735-9.

JEBSEN, R. H., TAYLOR, N., TRIESCHMANN, R. B., TROTTER, M. J. & HOWARD, L. A. 1969. An objective and standardized test of hand function. *Arch Phys Med Rehabil,* 50**,** 311-319.

JOHNSON, M. J., WISCONSIN, M. C. O., MILWAUKEE, W., FENG, X., JOHNSON, L. M., RAMACHANDRAN, B., WINTERS, J. M. & KOSASIH, J. B. 2006. Robotic Systems that Rehabilitate as well as Motivate: Three Strategies for Motivating Impaired Arm Use. *IEEE / RASEMBS Int. Conf. on Biomedical robotics and Biomechatronics, BioRob 2006***,** 254-259.

JOHNSON , R. & WICHERN, D. 1992. Applied multivariate statistical analysis. *Englewood Cliffs, NJ: Prentice Hall.*

JONATHAN , W., CARMINE , E. & PETER , K. 2015. A user interface for assistive grasping.

KANADE, R. A. 2009. DEXterous and autonomous dual-arm/hand robotic manipulation with sMART sensory-motor skills: A bridge from natural to artificial cognition. *DEXMART*.

KATZ, S. 1983. Assessing self-maintenance: Activities of daily living, mobility and instrumental activities of daily living. . *JAGS,* 31**,** 721-726.

KATZ, S., DOWN, T. D., CASH, H. R. & GROTZ, R. C. 1970. Progress in the development of the index of ADL. . *The Gerontologist,* 10**,** 20-30.

KAWASHIMA, N., POPOVIC, M. & ZIVANOVIC, V. 2013. Effect of intensive functional electrical stimulation therapy on upper-limb motor recovery after stroke: case study of a patient with chronic stroke. *Physiother Can,* 65.

KAWATO, M., FURAWAKA, K. & SUZUKI, R. 1987. A hierarchical neural network model for the control and learning of voluntary movements. *Biol. Cybern. ,* 56.

KHANICHEH, A., MINTZOPOULOS, D., WEINBERG, B., TZIKA, A. A. & MAVROIDIS, C. 2008. MR_CHIROD v.2: magnetic resonance compatible smart hand rehabilitation device for brain imaging. *IEEE Trans Neural Syst Rehabil Eng,* 16**,** 91-8.

KIKUUWE, R., TAKESUE, N. & FUJIMOTO, H. 2007. Passive Virtual Fixtures Based on Simulated Position-Dependent Anisotropic Plasticity. *Robotics and Automation, 2007 IEEE International Conference on*.

KIM, D., HILLIGES, O., IZADI, S., BUTLER, A. D., CHEN, J., OIKONOMIDIS, I. & OLIVIER, P. Digits: freehand 3D interactions anywhere using a wrist-worn gloveless sensor. Proceedings of the 25th annual ACM symposium on User interface software and technology, 10/07/2012 2012. ACM, 167-176.

KINECT. 2015. *Kinect for Windows* [Online]. Available: http://www.microsoft.com/en-us/kinectforwindows/.

KINOSHITA, H., KAWAI, S. & IKUTA, K. 1995. Contributions and co-ordination of individual fingers in multiple finger prehension. *Ergonomics,* 38**,** 1212-30.

KIVELL, T. L., BARROS, A. P. & SMAERS, J. B. 2013. Different evolutionary pathways underlie the morphology of wrist bones in hominoids. *BMC Evolutionary Biology,* 13**,** 229.

KLEIN, J., OBRADOR, M., GASCONS, N. & REINKENSMEYER, D. 2008a. The effect of dynamic arm support on grip forces and steering errors during simulated driving. *Int Journal of Heavy Vehicle Syst,* 15.

KLEIN, J., SPENCER, S., ALLINGTON, J., MINAKATA, K., WOLBRECHT, E., SMITH, R., BOBROW, J. & REINKENSMEYER, D. 2008b. Biomimetic orthosis for the neurorehabilitation of the elbow and shoulder (BONES). *Proceed. of the 2nd Biennial IEEE/RAS-EMBS Int. Conf. on Biomedical Robotics and Biomechatronics*

Scottsdale, AZ, USA, .

KOHONEN, T. 1997. *Self-Organizing Maps SOM,* New York, Springer-Verlag.

KOWALCZEWSKI, J., GRITSENKO, V., ASHWORTH, N., ELLAWAY, P. & PROCHAZKA, A. 2007. Upper-extremity functional electric stimulation-assisted exercises on a workstation in the subacute phase of stroke recovery. *Arch Phys Med Rehabil,* 88**,** 833-9.

KOWALCZEWSKI, J., RAVID, E. & PROCHAZKA, A. 2011a. Fully-automated test of upper-extremity function. *Conf Proc IEEE Eng Med Biol Soc,* 2011**,** 7332-7335.

KOWALCZEWSKI, J. J., CHONG, S. L. S., GALEA, M. M. & PROCHAZKA, A. A. 2011b. In-home tele-rehabilitation improves tetraplegic hand function. *Neurorehabil Neural Repair.,* 25**,** 412-22.

KOZAK, J. J., HANCOCK, P.A., ARTHUR, E.,, AMP & CHRYSLER, S. 1993. Transfer of Training From Virtual Reality | Peter Hancock. *Rapid Communication,* 36.

KREBS, H. I., VOLPE, B. T., WILLIAMS, D., CELESTINO, J., CHARLES, S. K., LYNCH, D. & HOGAN, N. 2007. Robot-aided neurorehabilitation: a robot for wrist rehabilitation. *IEEE Trans Neural Syst Rehabil Eng,* 15**,** 327-35.

KRISHNA, S., BALA, S., MCDANIEL, T., MCGUIRE, S. & PANCHANATHAN, S. VibroGlove: an assistive technology aid for conveying facial expressions. CHI '10 Extended Abstracts on Human Factors in Computing Systems, 04/09/2010 2010. ACM, 3637-3642.

KUTNER, N. G., ZHANG, R., BUTLER, A. J., WOLF, S. L. & ALBERTS, J. L. 2010. Quality-of-Life Change Associated With Robotic-Assisted Therapy to Improve Hand Motor Function in Patients With Subacute Stroke: A Randomized Clinical Trial. *Phys Ther,* 90**,** 493-504.

LAKE , D. 1992. Neuromuscular electrical stimulation. An overview and its application in the treatment of sports injuries. *Sports Med,* 13**,** 320-36.

LAM, W.-C., ZOU, F. & KOMURA, T. Motion editing with data glove. Proceed. of the 2004 ACM SIGCHI Internat. Conf. on Adv. in Computer Entert. Tech., 09/02/2004 2004. ACM, 337-342.

LANE, D. M. 2015. *Introduction to Analysis of Variance* [Online]. Available: http://onlinestatbook.com/2/analysis_of_variance/intro.html.

LANGHAMMER, B. & STANGHELLE, J. K. 2000. Bobath or motor relearning programme? A comparison of two different approaches of physiotherapy in stroke rehabilitation: a randomized controlled study. *Clin Rehabil,* 14**,** 361-9.

LEASTSQUAREFITTING. *Least Squares Fitting* [Online]. Available: http://mathworld.wolfram.com/LeastSquaresFitting.html

LEIGH, S. J., BRADLEY, R. J., PURSSELL, C. P., BILLSON, D. R. & HUTCHINS, D. A. 2012. A simple, low-cost conductive composite material for 3D printing of electronic sensors. *PLoS ONE,* 7.

LI, J., ZHENG, R., ZHANG, Y. & YAO, J. 2011. iHandRehab: an interactive hand exoskeleton for active and passive rehabilitation. *IEEE Int Conf Rehabil Robot,* 2011**,** 5975387.

LIGHT, C. M., CHAPPELL, P. H. & KYBERD, P. J. 1999. A critical review of functionality assessment in natural and prosthetic hands. *. British Journal of Occupational Therapy,,* 62**,** 7-12.

LIGHT, C. M., CHAPPELL, P. H. & KYBERD, P. J. 2002. Establishing a standardized clinical assessment tool of pathologic and prosthetic hand function: Normative data, reliability, and validity. *Archives of Physic. Med. and Rehabil.,* 83**,** 776-783.

LIGHTGLOVE. 2013. *Bridging the gap w/ light* [Online]. Available: http://www.lightglove.com/.

LIN, J., WU, Y. & HUANG, T. S. Modeling the constraints of human hand motion. Proceedings of the Workshop on Human Motion (HUMO'00), 12/07/2000 2000. IEEE Computer Society, 121.

LINDE, V. D., LAMMERTSE, P., FREDERIKSEN, E. & RUITER, B. 2002. The HapticMaster, a new high-performance haptic interface. *FCS Control Systems, The Netherlands*.

LIU, W. K., HWANG, W. Y., YEH, S. C. & HUANG, T. C. 2013. Virtual Reality Applications Force Feedback Device in Hand Rehabilitation Training. *Applied Mechanics and Materials,* 303-306**,** 2449-2452.

LO, A., GUARINO, P. & RICHARDS, L. 2010. Robot-assisted therapy for long-term upper-limb impairment after stroke. *The New Engl Jof Med,* 362**,** 1772-83.

LOUREIRO, R., AMIRABDOLLAHIAN, F., TOPPING, M., DRIESSEN, B. & HARWIN, W. 2003a. Upper Limb Robot Mediated Stroke Therapy—GENTLE/s Approach. *Autonomous Robots,* 15**,** 35-51.

LOUREIRO, R., AMIRABDOLLAHIAN, F. & W., H. 2003b. A Gentle/S approach to robot assisted neuro-rehabilitation - Research Database - University of Hertfordshire. *Springer 8th International Conference on Rehabilitation Robotics (ICORR 2003)*.

LU, P. & HUENERFAUTH, M. Accessible motion-capture glove calibration protocol for recording sign language data from deaf subjects. Proceedings of the 11th international ACM SIGACCESS conference on Computers and accessibility, 10/25/2009 2009. ACM, 83-90.

LUM, P. S., GODFREY, S. B., BROKAW, E. B., HOLLEY, R. J. & NICHOLS, D. 2012. Robotic approaches for rehabilitation of hand function after stroke. *Am J Phys Med Rehabil,* 91**,** S242-54.

LUO, X., KLINE, T., FISCHER, H., STUBBLEFIELD, K., KENYON, R. & KAMPER, D. 2005. Integration of augmented reality and assistive devices for post-stroke hand opening rehabilitation. *Conf Proc IEEE Eng Med Biol Soc,* 7**,** 6855-8.

MACHINELEARNING. 2015. *Machine Learning â€"Wolfram Language Documentation* [Online]. Available: http://reference.wolfram.com/language/guide/MachineLearning.html.

MAGEE, D. 2007. *Orthopedic Physical Assessment, 5e (Orthopedic Physical Assessment (Magee))*, Saunders.

MARIA , C., CAROLINA, R., DIANA, M. & TANIA, F. 2010. Effect of high-voltage pulsed current plus conventional treatment on acute ankle sprain. *Brazilian Journal of Physical Therapy,* 14.

MASCARO, S. & ASADA, H. Photoplethysmograph fingernail sensors for measuring finger forces without haptic obstruction. IEEE Trans. Robot. Autom, 2001.

MATEI, C., COREY, G. & PETER, A. 2007. Dimensionality reduction for hand-independent dexterous robotic grasping. *IEEE / RSJ Conference on Intelligent Robots and Systems (IROS)*

MATHEMATICS, E. O. 2015. *Linear interpolation - Encyclopedia of Mathematics* [Online]. Available: http://www.encyclopediaofmath.org/index.php/Linear_interpolation.

MATLAB-SMOOTH. 2015. *Filtering and Smoothing Data - MATLAB & Simulink - MathWorks United Kingdom* [Online]. Available: http://uk.mathworks.com/help/curvefit/smoothing-data.html.

MATLAB, R. *Robotics Toolbox for MATLAB* [Online]. Available: http://uk.mathworks.com/matlabcentral/linkexchange/links/2961-robotics-toolbox-for-matlab.

MAYA. 2015. *3D Animation Software, Computer Animation Software | Maya | Autodesk* [Online]. Available: http://www.autodesk.co.uk/products/maya/overview.

MCLAUGHLIN, M. 2007. VR Aided Motor Training for Post-Stroke Rehabilitation: System Design, Clinical Test, Methodology for Evaluation. *Virtual Reality Conf., 2007. VR '07. IEEE***,** 299-300.

MEARY, D. & BAUD-BOVY, G. Toward a robot-assisted assessment of the control processes of the motor system. Proceedings of the World Haptics 2009 - Third Joint EuroHaptics conference and Symposium on Haptic Interfaces for Virtual Environment and Teleoperator Systems, 03/18/2009 2009. IEEE Computer Society, 368-373.

MEDITOUCH. 2015. *HandTutor: active exercise glove with biofeedback* [Online]. Available: http://www.handtutor.com/.

MELLO , R., OLIVEIRA , L. & NADAL , J. 2007. Digital Butterworth filter for subtracting noise from low magnitude surface electromyogram. *Biomedical Engineering Program-COPPE,* 87**,** 28-35.

MERIANS, A. S., FLUET, G. G., QIU, Q., SALEH, S., LAFOND, I., DAVIDOW, A. & ADAMOVICH, S. V. 2011. Robotically facilitated virtual rehabilitation of arm transport integrated with finger movement in persons with hemiparesis. *J Neuroeng Rehabil,* 8**,** 27-27.

METCALF, C., ROBINSON, R., MALPASS, A., BOGLE, T., DELL, T., HARRIS, C. & DEMAIN, S. 2013 Markerless motion capture and measurement of hand kinematics: validation and application to home-based upper limb rehabilitation. *IEEE Trans Biomed Eng. 2013 Aug; ,* 60**,** 2184-92.

METHOT, J., CHINCHALKAR, S. & RICHARDS, R. 2010. Contribution of the ulnar digits to grip strength. . *Can J Plast Surg.,* 18**,** 10–4.

MIALL, R. & WOLPERT, D. 1996. Forward models for physiological motor control. *Neural Networks*, 1265–1279.

MICHAEL, L. T. 2015. *CyberGlove Calibration. Telemanipulation - Dexterous Manipulation Laboratory* [Online]. Available: http://www-cdr.stanford.edu/touch/tele_projects/telesys_cglovecal.htm.

MILTNER, W. H., BAUDER, H., SOMMER, M., DETTMERS, C. & TAUB, E. 1999. Effects of constraint-induced movement therapy on patients with chronic motor deficits after stroke: a replication. *Stroke,* 30**,** 586-92.

MIMUGLOVES. 2015. *MimuGloves* [Online]. Code. Available: http://mimugloves.com/.

MORROW, K., DOCAN, C., BURDEA, G. & MERIANS, A. 2006. Low-cost Virtual Rehabilitation of the Hand for Patients Post-Stroke. *IEEE, Virtual Rehabil., 2006 Int. Workshop on*.

MOURI, T. & KAWASAKI, H. 2008. A Novel Anthropomorphic Robot Hand and its Master Slave System. *In Humanoid Robots, Human-like Machines (July 2007), pp. 29-42*.

MUIR, S. R., JONES, R. D., ANDREAE, J. H. & DONALDSON, I. M. 1995. Measurement and analysis of single and multiple finger tapping in normal and Parkinsonian subjects. *Parkinsonism Relat Disord.* England.

MUNIH, M. & BAJD, T. 2011. Rehabilitation robotics. Technology & Health Care. 19**,** 483-495.

MUSICGLOVE. 2016. *MusicGlove, Flint Rehabilitation Device* [Online]. Available: https://www.flintrehab.com/.

NATHANIEL, I. & ANNE, S. 1994. *Virtual Reality: Scientific and Technological Challenges,* US, National Academies Press.

NEF, T., MIHELJ, M. & RIENER, R. 2007. ARMin: a robot for patient-cooperative arm therapy. *Med Biol Eng Comput,* 45**,** 887-900.

NEURALNETWORK. *Applications of neural networks* [Online]. Available: http://cs.stanford.edu/people/eroberts/courses/soco/projects/2000-01/neural-networks/Applications/index.html.

NHS. 2014. *Stroke* [Online]. Available: http://www.nhs.uk/conditions/stroke/Pages/Introduction.aspx.

NIH. 2015. *National Institute of Arthritis and Musculoskeletal and Skin Diseases* [Online]. Available: www.niams.nih.gov.

O'HAVER, T. 2015. *A Pragmatic Introduction to Signal Processing - Peak Finding and Measurement* [Online]. Available: http://terpconnect.umd.edu/~toh/spectrum/PeakFindingandMeasurement.htm December 1, 2015].

OCHOA, J. M., LISTENBERGER, M., KAMPER, D. G. & LEE, S. W. 2011. Use of an electromyographically driven hand orthosis for training after stroke. . *Rehabil Robotics (ICORR) -IEEE Int. Conf.***,** 1-5.

ODE. 2015. *Open Dynamics Engine - home* [Online]. Available: http://www.ode.org/.

OGRE3D. 2015. *OGRE " Open Source 3D Graphics Engine* [Online]. Tools. Available: http://www.ogre3d.org/.

OPENGL-PERFORMER. 2015. *SGI - OpenGL Performer* [Online]. Available: http://web.archive.org/web/20071224141002/www.sgi.com/products/software/performer/.

OPENGL. 2015. *SGI - OpenGL* [Online]. Available: http://www.sgi.com/tech/opengl/?/overview.html.

OPENRAVE. 2015. *OpenRAVE | databases Package | OpenRAVE Documentation* [Online]. Available:

http://openrave.org/docs/latest_stable/openravepy/openravepy.databases/#package-databases.

OPENSIM. 2015. *Overte Foundation* [Online]. Available: http://opensimulator.org/wiki/Main_Page.

OSHA. 2015. *Occupational Safety and Health Administration* [Online]. Available: https://www.osha.gov/.

OTTOBOCK. 2013. *Ottobock - SensorHand Speed* [Online]. Available: http://www.ottobock.co.uk/cps/rde/xchg/ob_com_en/hs.xsl/5735.html?openteaser=1.

OUJAMAA, L., RELAVE, I., FROGER, J., MOTTET, D. & PELISSIER, J. Y. 2009. Rehabilitation of arm function after stroke. Literature review. *Ann Phys Rehabil Med,* 52**,** 269-93.

PHYSX-NVIDIA. 2015. *NVIDIA DRIVERS 9.14.0702* [Online]. Available: http://www.nvidia.com/object/physx-9.14.0702-driver.html.

PLATZ, T. 2003. [Evidence-based arm rehabilitation--a systematic review of the literature]. *Nervenarzt,* 74**,** 841-9.

POPESCU, V. G., BURDEA, G. C., BOUZIT, M. & HENTZ, V. R. 2000. A virtual-reality-based telerehabilitation system with force feedback. *IEEE Trans Inf Technol Biomed,* 4**,** 45-51.

POPOVIĆ, D. & SINKJÆR, T. 2000. *Control of Movement for the Physically Disabled,* London, Springer

POPOVIC, N., SCHUBART, A., GOETZ, B. D., ZHANG, S.-C., LININGTON, C. & DUNCAN, I. D. 2002. Inhibition of autoimmune encephalomyelitis by a tetracycline. *Ann Neurol,* 51**,** 215-223.

PRANGE, G. B., JANNINK, M. J. A., GROOTHUIS-OUDSHOORN, C. G. M., HERMENS, H. J. & IJZERMAN, M. J. 2006. Systematic review of the effect of robot-aided therapy on recovery of the hemiparetic arm after stroke. *J Rehabil Res Dev,* 43**,** 171-184.

QUICK-QT. 2015. *Introduction to Qt Quick | Documentation | Qt Project* [Online]. Available: http://qt-project.org/doc/qt-4.8/qml-intro.html.

RACHEL, Y. 2015. *Data Glove* [Online]. Available: http://www.rachelyalisove.com/.

REINER, R. 2005. Control of Robots for Rehabilitation. *EUROCON 2005*.

REINKENSMEYER, D. J., PANG, C. T., NESSLER, J. A. & PAINTER, C. C. 2002. Web-based telerehabilitation for the upper extremity after stroke. *IEEE Trans Neural Syst Rehabil Eng,* 10**,** 102-8.

RING, H. & ROSENTHAL, N. 2005. Controlled study of neuroprosthetic functional electrical stimulation in sub-acute post-stroke rehabilitation. *J Rehabil Med,* 37**,** 32-6.

ROVETTA, A. 2009. Daphne system for neuromotor control evaluation: reconfiguration concepts. *Adv. Tech. for Enhanced Quality of Life, 2009. AT-EQUAL '09***,** 3 - 14.

ROVETTA, A., XIUMIN, F., VICENTINI, F., MINGHUA, Z., GIUSTI, A. & QICHANG, H. 2009. Early detection and evaluation of waste through sensorized containers for a collection monitoring application. *Waste Manag,* 29**,** 2939-2949.

SAEBO. 2016. *SaeboGlove* [Online]. Available: http://www.saebo.com/.

SAGGIO, G., LATESSA, G., DE SANTIS, F., BIANCHI, L., QUITADAMO, L. R., MARCIANI, M. G. & GIANNINI, F. 2009. Virtual reality implementation as a useful software tool for e-healthapplications. *IEEE*.

SAGISAKA, T., OHMURA, Y., KUNIYOSHI, Y., NAGAKUBO, A. & OZAKI, K. 2013. High-density conformable tactile sensing glove. *Humanoid Robots (Humanoids), 2011 11th IEEE-RAS International Conference* 537 - 542.

SAKURAI, K., MIURA, T., SAGISAKA, T., HATTORI, M., MATSUKAWA, N., MASE, M., KASAI, H., ARAI, N., KAWAI, T., SHIMOHIRA, M., YAMAWAKI, T. & SHIBAMOTO, Y. 2013.

Evaluation of luminal and vessel wall abnormalities in subacute and other stages of intracranial vertebrobasilar artery dissections using the volume isotropic turbo-spin-echo acquisition (VISTA) sequence: a preliminary study. *J Neuroradiol,* 40**,** 19-28.

SALE, P., MAZZOLENI, S., LOMBARDI, V., GALAFATE, D., MASSIMIANI, M. P., POSTERARO, F., DAMIANI, C. & FRANCESCHINI, M. 2014. Recovery of hand function with robot-assisted therapy in acute stroke patients: a randomized-controlled trial. *Int J Rehabil Res,* 37**,** 236-42.

SANCHEZ, R. J., LIU, J., RAO, S., SHAH, P., SMITH, R., RAHMAN, T., CRAMER, S. C., BOBROW, J. E. & REINKENSMEYER, D. J. 2006. Automating arm movement training following severe stroke: functional exercises with quantitative feedback in a gravity-reduced environment. *IEEE Trans Neural Syst Rehabil Eng,* 14**,** 378-89.

SANTELLO, M., FLANDERS, M. & SOECHTING, J. 2002. Patterns of hand motion during grasping and the influence of sensory guidance. *J of Neurosc***,** 1426-1435.

SATHIAN, K., GREENSPAN, A. I. & WOLF, S. L. 2000. Doing it with mirrors: a case study of a novel approach to neurorehabilitation. *Neurorehabil Neural Repair,* 14**,** 73-6.

SATOSHI, I., HARUHISA, K., YASUHIKO, I., MASATOSHI, N., TETSUYA, M. & YUTAKA, N. 2011. A design of fine motion assist equipment for disabled hand in robotic rehabilitation system. *Journal of the Franklin Institute,* 348**,** 79–89.

SCHABOWSKY, C. N., GODFREY, S. B., HOLLEY, R. J. & LUM, P. S. 2010. Development and pilot testing of HEXORR: hand EXOskeleton rehabilitation robot. *J Neuroeng Rehabil,* 7**,** 36.

SEDGWICK, P. 2014. Spearman's rank correlation coefficient. *BMJ; 349 g7327*

SHAP. 2013. *SHAP: Southampton Hand Assessment Procedure* [Online]. Available: http://www.shap.ecs.soton.ac.uk/index.php.

SHECHTMAN, O., GUTIERREZ, Z. & KOKENDOFER, E. 2005. Analysis of the statistical methods used to detect submaximal effort with the five-rung grip strength test. *J Hand Ther,* 18**,** 10-8.

SHELKEY, M. & WALLACE, M. 2000. Katz Index of Independence in Activities of Daily Living (ADL). 21**,** 109.

SHEN, Y., ONG, S. K. & NEE, A. Y. C. An augmented reality system for hand movement rehabilitation. Proceed. of the 2nd Int.Convention on Rehabil. Engi. & Assistive Tech., 05/13/2008 2008. Singapore Therapeutic, Assistive & Rehabilitative Technologies (START) Centre, 189-192.

SHUAI, J., YI, L., GUANGMING, L., JIANXUN, L., WEIDONG, C. & XIAOXIANG, Z. 2011. Interaction and Control with the Auxiliary of Hand Gesture. *IEEE International Conference on Information Science and Technology*.

SHUAI, J., YI, L. & WEIDONG, C. 2010. A novel dataglove calibration method. *Computer Science and Education (ICCSE), 2010 5th International Conference on***,** 1825 - 1829.

SHURTLEFF, T. L., STANDEVEN, J. W. & ENGSBERG, J. R. 2009. Changes in dynamic trunk/head stability and functional reach after hippotherapy. *Arch Phys Med Rehabil,* 90**,** 1185-95.

SIVAK, M., MURRAY, D., DICK, L., MAVROIDIS, C. & HOLDEN, M. 2012. Development of a Low-Cost Virtual Reality-based Smart Glove for Rehabilitation. *Int. Conf. Series on Disability, Virtual Reality and Associated Tech.*

SOLLERMAN, C. & EJESKAR, A. 1995. Sollerman hand function test. A standardised method and its use in tetraplegic patients. *Scand J Plast Reconstr Surg Hand Surg,* 29**,** 167-76.

SOUZA, A. M. D. C. & SANTOS, S. R. D. Handcopter Game: A Video-Tracking Based Serious Game for the Treatment of Patients Suffering from Body Paralysis Caused by a Stroke. Proceedings of the 2012 14th Symposium on Virtual and Augmented Reality, 05/28/2012 2012. IEEE Computer Society, 201-209.

SPIKE2 Spike2 Configuration http://ced.co.uk/img/Spike7.pdf.

STAUBLI, P., NEF, T., KLAMROTH-MARGANSKA, V. & RIENER, R. 2009. Effects of intensive arm training with the rehabilitation robot ARMin II in chronic stroke patients: four single-cases. *J Neuroeng Rehabil,* 6**,** 46.

STEIN, R. B. & PROCHAZKA, A. 2013. Impaired Motor Function: Functional Electrical Stimulation. 3047-3060.

STRETCHSENSE. 2015. *New fabric sensor StretchSense* [Online]. Available: http://www.stretchsense.com/.

STRINGLOVE. 2015. *StrinGlove* [Online]. Available: http://www.kk-teiken.co.jp/products/StrinGlove/index.htm.

STUDIOROBOTICSDEVELOPER. 2015. *Microsoft Robotics Developer Studio* [Online]. Available: https://msdn.microsoft.com/en-us/library/bb648760.aspx.

STUTZ, M. 2012. Measurement of AC Magnitude. *BASIC AC THEORY*.

SU, Y., ALLEN, C. R., GENG, D., BURN, D., BRECHANY, U., BELL, G. D. & ROWLAND, R. 2003. 3-D motion system ("data-gloves"): application for Parkinson's disease.

SUN, Z., BAO, G., LI, J. & WANG , Z. 2006. Research of Dataglove Calibration Method Based on Genetic Algorithms. *6th World Congress on Intelligent Control and Automation*.

SUN, Z., MIAO, X. & LI, X. 2011. Design of a bidirectional force feedback dataglove based on pneumatic artificial muscles. *In Mechatronics and Automation, 2009. ICMA 2009. International Conference on (aug 2009), pp. 1767-1771, doi:10.1109/ICMA.2009.5246223*.

SUNG, K. 2000. SKK Hand Master-hand exoskeleton driven by ultrasonic motors. *IEEE/RSJ International Conference on Intelligent Robots and Systems,* 2.

SZELITZKY, E., ALUTEI, A.-M., CHETRAN, B. & MANDRU, D. 2013. Data glove and virtual environment — A distance monitoring and rehabilitation solution. *E-Health and Bioengineering Conf. (EHB), 2011***,** 1 - 4.

TAI, E. 2007. *DESIGN OF AN ANTHROPOMORPHIC ROBOTIC HAND FOR SPACE OPERATIONS.* Master of Science, University of Maryland.

TAKAHASHI, C. D., DER-YEGHIAIAN, L., LE, V., MOTIWALA, R. R. & CRAMER, S. C. 2008. Robot-based hand motor therapy after stroke. *Brain,* 131**,** 425-37.

TALSANIA, J. & KOZIN, S. 1998. Normal digital contribution to grip strength assessed by a computerized digital dynamometer. *J Hand Surg Br. ,* 23**,** 162-6.

TAUB, E. & MORRIS, D. M. 2001. Constraint-induced movement therapy to enhance recovery after stroke. *Curr Atheroscler Rep,* 3**,** 279-86.

TERRI, M. S., LEE, O., JANE, F. & PETER, C. A. 2003 *Rehabilitation of the hand and upper limb*, Elsevier.

TIM, M. J. 2015. *Simbad 3d Robot Simulator* [Online]. Forge Summary. Available: http://simbad.sourceforge.net/.

TOUCH-TYPING, K. H. 2015. *KITTY* [Online]. Available: http://gram.eng.uci.edu/~cmehring/KITTY/about-kitty.html.

TRIANDAFILOU, K., OCHOA, J., KANG, X., FISCHER, H., STOYKOV, M. & KAMPER, D. 2011. Transient impact of prolonged versus repetitive stretch on hand motor control in chronic stroke. *Top Stroke Rehabil,* 4**,** 316-24.

TZEMANAKI, A., RAABE, D., DOGRAMADZI, S., TZEMANAKI, A., RAABE, D. & DOGRAMADZI, S. 2011. Development of a novel robotic system for hand rehabilitation. *The 21st IEEE Int. Symposium on Computer-Based Medical Systems.*, 1-6.

UEKI, S., NISHIMOTO, Y., ABE, M., KAWASAKI, H., ITO, S., ISHIGURE, Y., MIZUMOTO, J. & OJIKA, T. 2008. Development of virtual reality exercise of hand motion assist robot for rehabilitation therapy by patient self-motion control. *Conf Proc IEEE Eng Med Biol Soc,* 2008**,** 4282-5.

UNO, Y., KAWATO, M. & SUZUKI, R. 1989. Formation and control of optimal trajectories in human multijoint arm movements: Minimum torque-change mode. *Biol. Cybern,* 89-101.

V-REP, C. R. 2015. *V-REP: Create. Compose. Simulate. Any Robot* [Online]. Available: http://www.coppeliarobotics.com/.

VAN DER SMAGT, P., GREBENSTEIN, M., URBANEK, H., FLIGGE, N., STROHMAYR, M., STILLFRIED, G., PARRISH, J. & GUSTUS, A. 2009. Robotics of human movements. *J Physiol Paris,* 103**,** 119-32.

VIAU, A., FELDMAN, A. G., MCFADYEN, B. J. & LEVIN, M. F. 2004. Reaching in reality and virtual reality: a comparison of movement kinematics in healthy subjects and in adults with hemiparesis. *J Neuroeng Rehabil,* 1**,** 11.

VICON. 2015. *Vicon Motion Systems Ltd* [Online]. Available: http://www.vicon.com/products/software/tracker.

VIRTOOLS. 2015. *3DVIA Virtools* [Online]. Available: http://www.3dvia.com/products/3dvia-virtools/.

VOLPE, B. T., KREBS, H. I., HOGAN, N., EDELSTEIN, O. L., DIELS, C. & AISEN, M. 2000. A novel approach to stroke rehabilitation: robot-aided sensorimotor stimulation. *Neurology,* 54**,** 1938-44.

VRML, W. D. 2015. *Web3D Consortium | Open Standards for Real-Time 3D Communication* [Online]. Available: http://www.web3d.org/.

WADE, D. & CONIN, C. 1988. The Barthel ADL index: a standard measure of physical disability? *Int Disabil Stud,* 10**,** 64-7.

WANG , B. & DAI , S. 2009. Dataglove Calibration with Constructed Grasping Gesture Database. *IEEE VECIMS 2009 - International Conference on Virtual Environments, Human-Computer Interfaces and Measurements Systems*.

WANG, H.-S., HSU, C., CHIU, D. & TSAI, S.-N. 2010. Using augmented reality gaming system to enhance hand rehabilitation. *2nd Int. Conf. on Edu. Tech. and Computer (ICETC).*

WANG, J., LI, J., ZHANG, Y. & WANG, S. 2009. Design of an exoskeleton for index finger rehabilitation. *Conf Proc IEEE Eng Med Biol Soc,* 2009**,** 5957-60.

WANG, R. Y. & POPOVIC, J. 2009. Real-time hand-tracking with a color glove. *Acm Transactions on Graphics,* 28**,** 8.

WARNICK, R. 2015. Robotic Hands, Grasping and Manipulation - IEEE Robotics and Automation Society.

WEBOTS. 2015. *Webots: robot simulator - Overview* [Online]. Available: http://www.cyberbotics.com/overview.

WEGE, A., BERLIN, T. U., AWEGE@CS.TU-BERLIN.DE, KONDAK, K., BERLIN, T. U., KONDAK@CS.TU-BERLIN.DE, HOMMEL, G., BERLIN, T. U. & HOMMEL@CS.TU-BERLIN.DE 2013a. Development and Control of a Hand Exoskeleton for Rehabilitation. 149-157.

WEGE, A., K., K. & G., H. 2013b. Mechanical design and motion control of a hand exoskeleton for rehabilitation.

WEMOVE. 2008. *Essential Tremor: A Clinical Review CME ©* [Online]. Available: http://www.medscape.org/viewarticle/572015.

WESTON, B. G., RYAN, P. F., MICHAEL, L. T. & MARK, R. C. 2000. Calibration and Mapping of a Human Hand for Dexterous Telemanipulation. *ASME IMECE 2000 Conference*.

WOLF, S. L., CATLIN, P. A., ELLIS, M., ARCHER, A. L., MORGAN, B. & PIACENTINO, A. 2001. Assessing Wolf motor function test as outcome measure for research in patients after stroke. *Stroke,* 32**,** 1635-9.

WORSPACE5. 2015. *Workspace Robot Simulation Software* [Online]. Available: http://www.workspacelt.com/.

WRIGHT, J. 2013. *Robotic Technology Lends More Than Just a Helping Hand* [Online]. http://www.nasa.gov/. Available: http://www.nasa.gov/mission_pages/station/main/robo-glove.html#.VJNzZf-b8A [Accessed March 13, 2012.

WU, C. W., SEO, H.-J. & COHEN, L. G. 2006. Influence of electric somatosensory stimulation on paretic-hand function in chronic stroke. *Arch Phys Med Rehabil,* 87**,** 351-357.

XU, Z., YU, H. & YAN, S. Motor rehabilitation training after stroke using haptic handwriting and games. Proceed. of the 4th Int. Convention on Rehabil. Eng. & Assistive Tech., 07/21/2010 2010. Singapore Therapeutic, Assistive & Rehabilitative Technologies (START) Centre, 31.

YAMAURA, H., MATSUSHITA, K., KATO, R. & YOKOI, H. 2009. Development of hand rehabilitation system for paralysis patient - universal design using wire-driven mechanism. *Conf Proc IEEE Eng Med Biol Soc,* 2009**,** 7122-5.

YASUMURO, Y., GRADUATE SCH. OF INF. SCI, N. I. O. S., AMP, TECHNOL, J., CHEN, Q. & CHIHARA, K. 3D modeling of human hand with motion constraints. Int. Conf. on Recent Adv. in 3-D Digital Imag. and Model., 1997. , 12-15 May 1997 1997. IEEE, 275-282.

YAVUZER, G., SELLES, R., SEZER, N., SUTBEYAZ, S., BUSSMANN, J. B., KOSEOGLU, F., ATAY, M. B. & STAM, H. J. 2008. Mirror therapy improves hand function in subacute stroke: a randomized controlled trial. *Arch Phys Med Rehabil,* 89**,** 393-8.

YOSHIYUKI, T., TORU, S., TOSHIO, T. & NOBUAKI, I. 2013. Robotic rehabilitation system using human hand trajectory generation model in virtual curling task. *IEEE/RSJ Int. Conf. on Intell. Robots and Systems, IROS 2011*.

YOUGRABBER. 2015. *YouRehab - YouGrabber* [Online]. Available: http://yourehab.com/yougrabber/.

ZARIFFA, J., KAPADIA, N., KRAMER, J. L., TAYLOR, P., ALIZADEH-MEGHRAZI, M., ZIVANOVIC, V., WILLMS, R., TOWNSON, A., CURT, A., POPOVIC, M. R. & STEEVES, J. D. 2011. Effect of a robotic rehabilitation device on upper limb function in a sub-acute cervical spinal cord injury population. *IEEE Int Conf Rehabil Robot,* 2011**,** 5975400.

ZARIFFA, J. & STEEVES, J. D. 2011. Computer vision-based classification of hand grip variations in neurorehabilitation. *IEEE Int Conf Rehabil Robot,* 2011**,** 5975421-5975421.

Appendix I Experiment System Setup

The hardware and software setup steps to run the experiment.

1. Run the Virtual application by launching "graspit.exe" file in the 'bin' folder. Note to run GraspIt! Application specific libraries need to be set up on the machine first.
2. Load the "startPosition.xml" from 'worlds' directory of the GraspIt! project. This file refers to all the virtual world models and environment setup used in this experiment.
3. Connect CyberGlove® interface unit with the serial port of the machine and switch it on.
4. Enable CyberGlove® sensors reading from the application, by choosing "sensors" from the menu and going to "CyberGlove-> On".
5. Connect CED Micro 1401 EMG recording device with both the USB cable (for reading data) and parallel port cable (for synchronisation) to the machine running the VR application.
6. Make sure the cables are connected properly between the Filter-Isolators-Amplifiers. Adjust Notch filter of each Isolator to 50 Hz low-pass filter cut-off and 500 Hz High-pass filter cut-off to correspond with the EMG signal bandwidth(Al-Jumaily and Olivares, 2009) . See for setup.
7. Run Spike2 (version 5 and above) and configure samples to include four data reading channels, and one digital marker.
8. Connect the Dome® to the machine via the projector VGA cable.
9. Use speaker or headset for audio instructions.
10. Take measurements of the subject physiology: - size of the hand (using the Chart with different standard hand sizes), length of the forearm, - length of the elbow, - Height, - Weight.
11. Ask subject to wash both hands. (for Hygienic considerations across different users)
12. Locate the four muscles and place the EMG electrodes in the appropriate structure, with reference point electrode on the wrist bone 'Pisiform'.
13. Connect the electrodes to the CED1401 wires from the amplifier NL824.
14. Test electrodes read by running Spike and checking the signals.
15. Ask subject to wear the CyberGlove® glove on top of the white nylon glove. Hands should be clean and dry. (The nylon glove helps to maintain hygiene and facilitates the wearing and removing of the glove, as it provides lubricating surface)
16. Tight the subject elbow to the chest with an elastic band, this is to isolate the arm muscles involved in gross movement and be able to produce more accurate results in the tasks requiring fine movements.

Experiment Process

The experiments are performed in the following sequences:

At the start of each experiment, the subjects are asked to read and sign a Consent form, which contains description and details about the experiments, their involvement and the risks involved.

After setting up the system, the data glove reading was calibrated on the subject hand by using the system procedure of software calibration.

This method was done by clicking on "New Calibration" in the "Glove Calibration" dialogue box. Then the subject followed the instructions for calibration by performing specific gestures using the right hand with the glove. (The calibration is by default saved in the '\Poses\Calibration.csv' location)

To verify the calibration a "Test Calibration" was performed after the calibration. This would measure the efficiency of the calibration method and validate the virtual reality mapping values of the sensors data by measuring the Coefficient Index for the sensors and DoFs.

In case of Real Life sessions, the subject is presented with the real objects on the table, placed on top of the Foam board, and would move the object to the relevant marked positions.
In case of Virtual Reality sessions, the subject is presented with Virtual display on the Dome®, where the interactions were all performed virtually. Subject would see two views: "Front Camera" displaying the front view of the scene, where better perceptions of the object's size and dimension in relevance with the Virtual Hand size and shape were displayed; the "Back Camera" displaying the subject view to give the immersive perception for manipulating the virtual hand and objects.

Due to the expected variations between different subject skills in interacting with the VR and instructions comprehension, the subject was given before the experiment a detailed training to explain the terminologies used in the instructions and the tasks correct performance.
For instance the following explanation was given to the subject:
"Move hand – fingers are stable but hand is moving only", "Grasp – formation of fingers", "Hold –holding the object in the current finger positions without moving", "Positions X and Y on the SHAP board, and unavailability on VR as the virtual hand is automatically controlled", "Relax Hand – gesture as the start position relaxed on the table", Demo all the tasks performance individually with clarification of the fingers involvements to maintain consistency between tasks performances and subjects.
The training ensured, as well, the repetitions and consistency of the data measured between subjects while performing the different tasks.

The EMG data was simultaneously recording with the data glove through the CED application Spike2.

After finishing, the subject was asked for feedback. The data collected through the experiment was stored confidentially, and used later in mining and analysis.

Glove Size Chart for Men, obtained from CELTEK http://www.celtek.com/size-chart/.
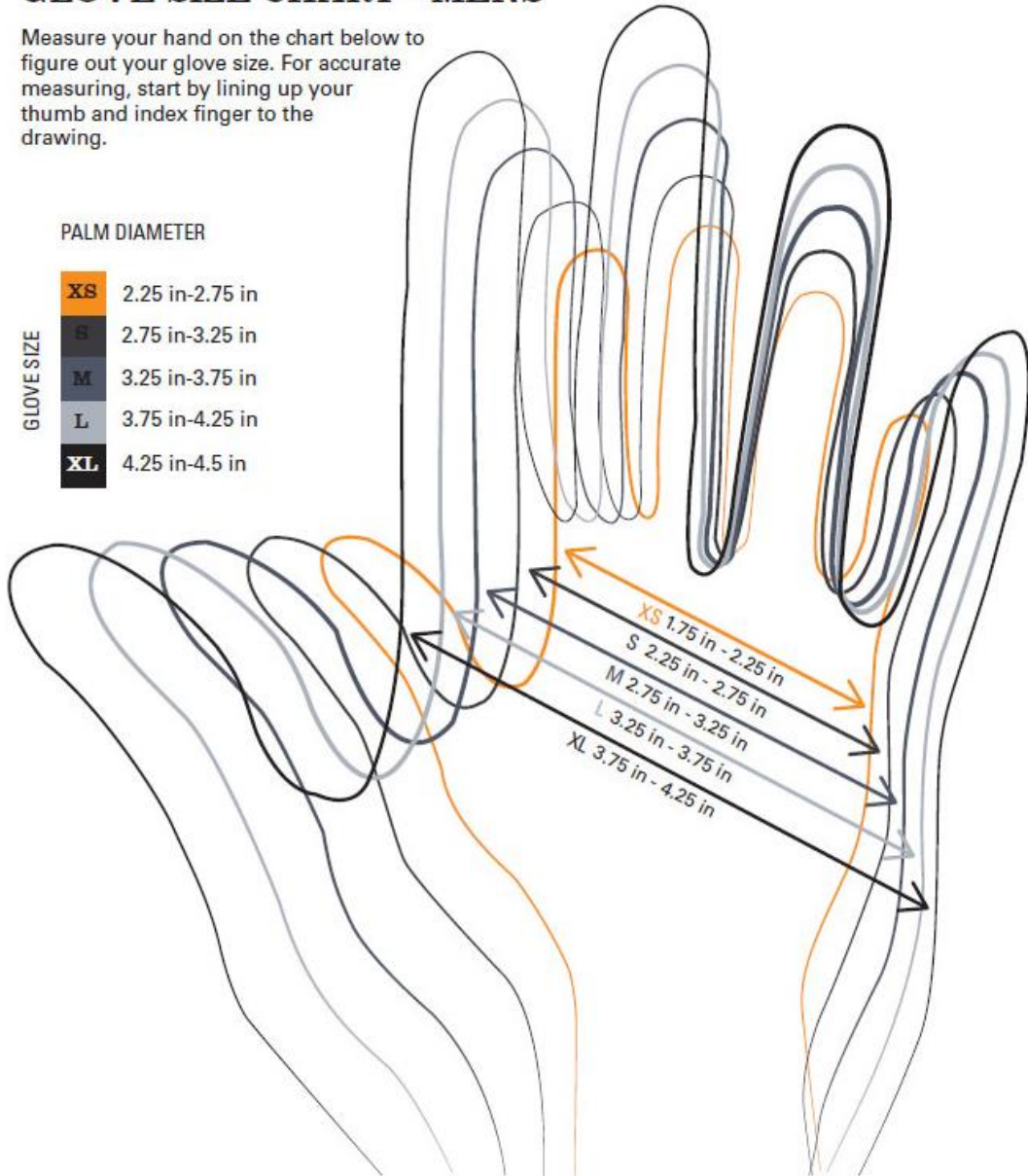
Figure II-1 Glove Hand Size for Men
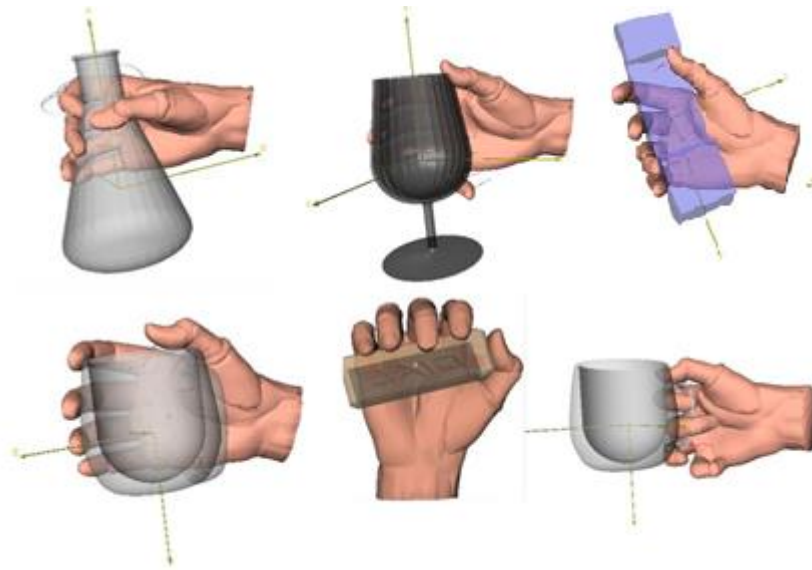
Figure III-1 Virtual Hand Models showing the multiple grasping postures for different objects of variant shape and size; It displays the flexibility and extension of virtual hand in forming the multiple complex shapes.

```
// Defining the robot type whether Human Hand or others.
<robot type="Hand">

// Starting by definition on the palm base of the robot
 <palm>palm.xml</palm>
 <chain>
// The orientation of the palm and its location in the
virtual world
  <transform>
   <translation>-50.6241 -11.5082 18.9317</translation>
   <rotationMatrix>-0.1486 -0.9003 0.4089 0.2665 0.3618
0.8933 -0.9522 0.2418 0.1862</rotationMatrix>
  </transform>

// After definition of the base the connected joints are
```

```
deffined
// hierachically from the parent joint in the finger to the
end
// effector


// The D-H parameters are then applied in the following to
define the
// kinematics of each joint. This explained in the followed
parts of
// this section
// The below are list of constraints defined on the joints
movements
  <joint type="Revolute">//primitive types:Revolute,prism,
universal
    <theta>d16</theta>
    <d>0.0</d>
    <a>0.0</a>
    <alpha>90.0</alpha>
    <minValue>-10</minValue>
    <maxValue>50</maxValue>
  </joint>
  <joint type="Revolute">
   <theta>d17+49.5</theta>
   <d>0.0</d>
   <a>52.1193</a>
   <alpha>44.0</alpha>
   <minValue>0</minValue>
   <maxValue>25</maxValue>
  </joint>
  <joint type="Revolute">
   <theta>d18+5.0</theta>
   <d>0.0</d>
   <a>40.7638</a>
   <alpha>0.0</alpha>
   <minValue>0</minValue>
```

```xml
    <maxValue>40</maxValue>
  </joint>
  <joint type="Revolute">
   <theta>d19+85.0</theta>
   <d>0.0</d>
   <a>0.0</a>
   <alpha>90.0</alpha>
   <minValue>0</minValue>
   <maxValue>30</maxValue>
  </joint>

// defining the links to the 3D model and joints type
obtained from
// one or many degree of freedoms to constitues the various
primitive
// types.
// In this case the first 2 Revolute DoFs are used for the
firt
// Universal link. The second 2 Revolute DOFs are used for
each link
  <link dynamicJointType="Universal">thumb1.xml</link>
  <link dynamicJointType="Revolute">thumb2.xml</link>
  <link dynamicJointType="Revolute">thumb3.xml</link>
 </chain>
</robot>
```

CodeSnippet III-1 Human Hand Model description file

The CodeSnippet III-1 shows a part of the description file for the human hand model which contains set of outlines for the kinematics interactions of each model, the transformation rules from the base and the joint properties (i.e. Revolute, Universal, parameters etc.). This file is related with other configuration files in GraspIt!.

The above CodeSnippet, particularly, displays the Thumb configuration. It starts by defining the type of the robot as "hand" and the transformation matrix for the finger base from the palm in the <translation> and <rotationMatrix> nodes; then it initializes the link between the three joints in the <link> nodes, where the type of joints is assigned as parameter for

this case the first joint is "Universal" and the other two are "Revolute"; and the rest of joints configurations in the <joint> nodes.

These nodes are placed in a sequential order from base joint to last, and they include the type of the joint, the minimum and maximum variation, and the Denavit-Hartenberg parameters: joint angle, joint distance from the previous, link length and link twist.

Appendix IV Data Glove Sensor Values for the Calibration Postures

Table IV-1 Grand average sensor Values for the 15 postures of the calibration process

	Postures	1	2	3	4	5	6	7	8	9	10	11	12	13	14	15
S1	Thumb Rotate	82	101	96.8	92.2	73.6	78.8	80	73.2	78.7	68.4	81.5	83.4	129.2	131.6	93.7
S2	Thumb MCP	94.2	168.6	102.4	111.9	72.2	73.3	102.3	103.6	106	79.1	108.6	119.3	119.4	122.4	127
S3	Thumb IP	107.8	180.6	169.6	101.6	102.3	96.7	105.7	103.6	104.1	98	91.7	103.2	117	128.2	130.3
S4	Thumb Abd	124.1	116.5	88.9	144.5	104.4	104.1	135	135.3	135.8	120.5	159.2	140.4	70.9	61.9	128.8
S5	Index MCP	77.5	141.9	143.9	92.5	73.7	80.9	80.4	83.7	86.7	69.4	160.1	156.5	126.7	109.2	146.7
S6	Index PIP	211.3	254.2	254.1	201.9	204.5	206.5	197.4	201.4	201.4	254.4	234.3	254.5	254.5	206.8	254.6
S7	Index DIP	59.4	157	126.2	64.8	63	63.2	64.1	62.1	62.3	175.8	70	98.7	67.8	76.2	155.2
S8	Middle MCP	89.8	147.4	154.8	99.1	84.3	92.1	88.6	92.4	95	88.3	161.1	158.9	101.1	120.7	149
S9	Middle PIP	54.9	138.1	121.5	46.8	52.6	49.6	53.6	46.4	46.6	152.7	71.3	147.3	62.8	140.2	150.2
S10	Middle DIP	68.5	139.2	116.4	82.5	74.5	75.9	74.5	72.2	70.3	166.5	79.1	79.5	81.9	61.8	127.4
S11	Mid-Index Abd	167.7	129	133.6	185.9	125.5	177.3	103.1	180.6	181.9	141.1	167.9	150.2	133.8	106.7	153
S12	Ring MCP	83.5	140.2	147.1	91.6	78	87.4	82.2	84	88.8	81.8	151.9	153.5	90.3	104.3	146.1
S13	Ring PIP	60	150.7	122.9	51.7	57.3	52.3	54.1	56.1	54.3	156.2	68.9	150.1	58.6	57.8	155.4
S14	Ring DIP	60.9	160.4	119.8	64	62	62	63.8	62	66.4	196.4	75.7	97.8	71.2	64.6	185
S15	Ring-Mid Abd	114.1	85.3	86	129.1	85.7	126.4	115.1	48.7	130.7	100.3	120.8	94.2	103.5	105.4	89.6
S16	Pinkie MCP	70.4	126	134.6	79.4	63	75.6	71	67.2	67	65.6	128.2	141.6	69.9	67.2	137.9
S17	Pinkie PIP	51.9	137.7	105.6	49.8	45	48.4	48.2	47.6	42.4	141	69.9	134.4	50.4	46.3	138.9
S18	Pinkie DIP	95.9	169.6	140.4	96	94.1	94.1	93.1	93.2	93.6	186.8	95	135.9	98.5	96.1	179.3
S19	Pink-Ring Abd	145	141.5	138.8	166.7	106.5	167.5	160.8	148.4	95.9	150.1	153.3	143.2	140.1	137.4	143
S20	Palm arch	133.1	125.3	125	136	136.8	139.4	136.2	140.8	135.1	144.8	135.4	122.6	141.2	143.4	121.6
S21	Wrist Flexion	144.3	111.6	106	144	149.6	148.4	151	149.8	148.2	146.8	102.3	99.6	105.7	93.9	108
S22	Wrist Abd	74.6	77.8	82.9	66.9	72.2	67.6	68.4	72	74.3	72.3	71	74.6	78	82.2	78.2

Appendix V Code Organisation for configuring the Virtual Environment

The code used for the Virtual Environment setup. It applies an XML structure to define the locations, orientations, links, properties and relations of the virtual objects.

```xml
<?xml version="1.0" ?>
<world>
// Include static objects in the virtual environment:Floor,Table
 <obstacle>
  <filename>models/obstacles/simpleFloor2.xml</filename>
  <transform>
// Position and Orientation relative to the world reference
   <fullTransform>(+1 +0 +0 +0)[+0 +0 +0]</fullTransform>
  </transform>
 </obstacle>
 <obstacle>
  <filename>models/obstacles/table.xml</filename>
  <transform>
   <fullTransform>(+1 +0 +0 +0)[-10.381 +162.405 -
0.00101096]</fullTransform>
  </transform>
 </obstacle>
// Include static objects in the virtual environment:the Robot
Stand // (Base)
 <obstacle>
  <filename>models/obstacles/puma_stand.xml</filename>
  <transform>
   <fullTransform>(+1 +0 +0 +0)[+0 +0 -1]</fullTransform>
  </transform>
 </obstacle>


// Include dynamic objects in the virtual environment:Tripod,
Sphere, Plate
 <graspableBody>
  <filename>models/objects/tripod.xml</filename>
  <transform>
   <fullTransform>(+1 +0 +0 +0)[-817.445 +710.57 -
459]</fullTransform>
  </transform>
 </graspableBody>
 <graspableBody>
  <filename>models/objects/sphere.xml</filename>
  <transform>
```

```xml
    <fullTransform>(+1 +0 +0 +0)[+782.758 +726.483 -
459]</fullTransform>
   </transform>
  </graspableBody>
  <graspableBody>
   <filename>models/objects/plate.xml</filename>
   <transform>
    <fullTransform>(+1 +0 +0 +0)[-694.87 +406.234 -
459.996]</fullTransform>
   </transform>
  </graspableBody>
// Include the robot joints models
 <robot>
  <filename>models/robots/Puma560/Puma560.xml</filename>
// Configure each DoF default position when it is loaded
   <dofValues>+1.70887 -2.04238 +0.546504 +0.00906244 +0.127617 -
0.535178 </dofValues>
   <transform>
    <fullTransform>(+1 +0 +0 +0)[+122.779 +0
+8.49962]</fullTransform>
   </transform>
  </robot>
  <robot>
// Include the Human Hand model

<filename>models/robots/HumanHand/HumanHand20DoF.xml</filename>
// Configure each joint default position
   <dofValues>+0.213955 -0.118538 +1.5708 -0.174533 +0.106554 -
0.174533 -0.174533 +0.036828 -0.0872665 -0.054422 -0.157483
+0.022301 -0.143688 -0.174533 -0.174533 +0.0330681 +0.872665 +0
+0.461594 +0.341308 </dofValues>
   <transform>
    <fullTransform>(+0.509822 +0.502387 -0.516462 -
0.47006)[+231.683 +265.489 -375.77]</fullTransform>
   </transform>
  </robot>
// Specify the parental connection in order to mount the hand at
the // end effector of the Puma Robot Model.
// The sequence of defining which robot first is critical in
order  // to select the parent robot controling the child
movement
 <connection>
  <parentRobot>+0</parentRobot>
  <parentChain>+0</parentChain>
  <childRobot>+1</childRobot>
  <transform>
```

```
    <fullTransform>(-0.303316 +0.520209 -0.423588 -0.676723)[-5
+2.47 +47.9]</fullTransform>
  </transform>
 </connection>
// Include camera with the position, orientation and focal
distance // configurations in the scene
 <camera>
  <position>-331.02 -152.199 -19.7425</position>
  <orientation>+0.56436 -0.0970323 -0.147562
+0.806417</orientation>
  <focalDistance>+792.983</focalDistance>
 </camera>
</world>
```

Pre-considerations: (Healthy, no neurological, no medical issues, no skin damage on the hand and forearm, no allergy to the used EMG electrodes, healthy visual perception, no motion sickness, their dominant hand and let are the right side, no hearing issues, no history of epilepsy, no neuromuscular damage, no surgeries to the right side upper limb, and no current health problems)

- **How often do you use tactile hand typing devices?**

Seldom/Never	
Occasionally	
Regularly	

- **How often do you use computer at home?**

Seldom/Never	
Occasionally	
Regularly	

- **For each of the following activities please indicate whether you participate in each of the activities regularly, occasionally or never.**

Team activities	Never	Occasionally	Regularly
Cricket			
Basketball/ Volleyball			
Martial Art			
Bowling			
Hockey			
Goal Keeper			
Gymnastic/Yoga			
Musical Instrument (Please specify)			
Biking			
Video Games			

If others (mainly with hand activities) please specify:

- **Do you do any employment work involving heavy hand functions?**
- **How many hours per week do you do this work?**

- **How many hours per week you attend in university?**
- **How much do you spend time in the day standing?**

Seldom/Never	
Occasionally	
Regularly	
All the time	
Not applicable	

- **How much do you spend time in the day sitting?**

Seldom/Never	
Occasionally	
Regularly	
All the time	
Not applicable	

Regarding your back, please rank from 1 to 10 (where 5 is troublesome, uncomfortable rate) the intensity of any back pain you may experience along with the location and type of pain

- **Where is the location of the identified back pain?**

Considering the dominant side of your body, rank from 1 to 10 (where 5 is troublesome, uncomfortable rate) the intensity of pain at the various location

- **Please specify the kind of the pain.**

Considering the non-dominant side of your body, rank from 1 to 10 (where 5 is troublesome, uncomfortable rate) the intensity of pain at the various location

- **Please specify the kind of the pain.**

Please indicate when your pain is the most bothersome (1), second most bothersome (2) and least bothersome (3).

(Team sport, indvidual recreational activities, work/university, relaxing, morning when you wake up, others)

.

.

.

- **Please indicate the location of the most bothersome (1), second most bothersome (2) and least bothersome (3).**

  (Back, Neck, Shoulder, Elbow, Wrist/forearm, Hand/Thumb)

  .

  .

  .

- **General Questions**

  Age
  Tall
  Weight
  Right forearm length
  Right Upper arm length
  Right hand Size medium

- **Other Notes:**

  The information in this survey and the photos, videos will be kept confidential and stored with anonymous identifications.

Name of department: Bioengineering

Title of the study: A Virtual Hand Assessment System for Efficient Measures of Hand Rehabilitation

Introduction

I am Bilal Nasser, PhD student in Bioengineering. And I am deducting this experiment for my research. Please feel free to contact me for any query on this address
bilal.nasser@strath.ac.uk

What is the purpose of this investigation?

In this experiment we are studying the efficiency of using Virtual Reality system in assessing the kinetic performance of the hand in performing abstract tasks. The existing clinical techniques used in assessing hand performance have many drawbacks as they are subjective to eye observation only, do not offer quantitative analysis and does not support dynamic adjustment with patient's performance.

The developed approach consists of a data glove to measure the finite hand joints movements using 22 flex sensors circumscribed on the hand. The data glove is connected with an operable Virtual Hand model in an interactive Virtual Reality Environment.

Furthermore, EMG (Electromyography) electrodes are placed on the forearm and hand to read specific muscles activities and behaviour in synchronisation with the data glove reading. This is in order to analyse the muscle activities and validate the dataglove readings harmonised with the hand movements.

In addition, paresis simulations are performed in different trials by adding extra weight on the forearm or asking to simulate a tremor movement. This is mainly to study the fatigue effectiveness during the performed tasks and simulate defined form of paresis functions.

The project aim is to provide a robust and consistent outcome measurement of the patient's hand performance during rehabilitation. And support of a thorough investigation for obtaining inclusive details in the hand kinematics and the segmental restoration of its functionality. The suggested approach considers the cross-compatibility with different techniques involved in ADL (Activities of Daily Living) tasks and their existing rehabilitation methods.

Do you have to take part?

This study will conduct experiments on 10 to 12 subjects, in which participants are asked to do sequential movements with their right hand while recording the fingers movements and arm muscles; Participation in this study is voluntary and refusing or withdrawing from experiment is the participant's right which is permitted at any time of the experiment without giving justifications.

What will you do in the project?

In this experiment you will wear a data glove, CyberGlove®, device to measure the movement of your finger joints. And you will be asked to follow visual and audio instructions which detail the form and steps of the hand movements.
The experiment is composed of two randomly selected sections of tasks: 1- virtual reality where you will be asked to perform tasks with virtual objects on the screen by manipulating a Virtual Hand that is connected to the dataglove. 2- Standard system where you will be asked to perform tasks with real objects.
This is repeated with 0.5kg weight placed on the forearm of the right hand to study the fatigue impact on the fingers formation and the adaptability of the application with the changes.

Then the tasks would be repeated with tremor simulation where you will be asked to perform the following procedure: "Please perform the following procedures while pretending you have what you consider a tremor in the right hand. With your arm in position, please mimic this tremor". The last trial is for studying the feasibility of analysing the fingers motions with tremor causalities.

EMG (Electromyogram) electrodes will be placed on the forearm and the thumb muscle so to read the muscle activities during the experiment.

After finishing you will be asked to fill in an evaluation questionnaire for the developed system. The full experiment will take approximately 2.5 hours.

There will be video recording in the background and photo shooting to your right hand (all endorsed in privacy protection and used under your permission). Besides, we will do arm and hand measurement to define the size of the subject's kinematic, height and weight measurement cause it relates with the hand/fingers dimensions.
This is to help in the data analysis process and associate it with the hand variability for every individual.

Why have you been invited to take part?

Required participants for this experiment are healthy male subjects; don't have any reported medical issues on their arm or hand motor functionality.
Skin on the forearm and palm must have no damage to permit effective EMG data reading of the muscle, and don't have allergy to the electrodes.

Subject must have healthy visual perception to interact with the Virtual Graphics display on the screen while the tasks are performed, and don't suffer from motion sickness.
They have the right hand and leg dominant limbs. They must be plus eighteen years old. Have no: hearing issues, history of epilepsy, neuromuscular damage, surgeries in upper limbs, neurological disorders or current health problems or illness.

The contribution in this experiment is a great help to collect the required data in order to experimentally prove the hypotheses of the project and validate the efficiency of the provided data outcome for hand assessment.

What are the potential risks to you in taking part?

The CyberGlove data glove device worn in the right hand during the experiment is approved by CE, FCC and Japan Technical Regulations Conformity Certification of Specified Radio Equipment.
The EMG electrodes, placed on the forearm and palm, are passive electrodes. The electrodes along with other used materials in the experiment have no known risks involved in this procedure.

But there is chance of skin reaction to the gels or pastes used to fix the hypoallergenic electrodes in position. If the electrodes cause any irritation or a burning sensation the test will be terminated, electrodes will be removed and the skin will be carefully cleaned.

What happens to the information in the project?

The results will be finalized by the end of 2014 and written up as part of my PhD Thesis. We will also seek to produce at least one paper from the results of the experiment, and it is hoped that it will provide a basis to carry out further research in the future.
The data we collect will only be accessible by the researcher(s) and supervisor(s) involved in this study. Any data obtained during the course of the experiment will be Stored securely on computer at the Neurophysiology lab in Bioengineering Unit in an anonymised format.

The University of Strathclyde is registered with the Information Commissioner's Office who implements the Data Protection Act 1998. All personal data on participants will be processed in accordance with the provisions of the Data Protection Act 1998.

Thank you for reading this information – please ask any questions if you are unsure about what is written here.

What happens next?

After reading the above information of the experiment and your part of contribution, if you are happy and interested in participating please sign the below consent form. After completing the data collection from the experiments and computing the analysis, participants will be able to access information regarding the study outcome related with their individual contributions. And they will be notified if the data results are published.

This investigation was granted ethical approval by the University of Strathclyde ethics committee.

If you have any questions/concerns, during or after the investigation, or wish to contact an independent person to whom any questions may be directed or further information may be sought from, please contact:

Secretary to the University Ethics Committee

University of Strathclyde

McCance Building

16 Richmond Street

Glasgow

G1 1XQ

Telephone: 0141 548 2752

Email: ethics@strath.ac.uk

Researcher Contact Details:

Bilal Nasser,

PhD student in Bioengineering, University of Strathclyde

Address: 27 1/1 Summertown road, Glasgow G512QA
tel: 07817654317

Email: bilal.nasser@strath.ac.uk

Chief Investigator Details:

This should include the name of the Chief Investigator and the University of Strathclyde contact details (address, phone number and email address).

Consent Form

Title of study:
A Virtual Hand Assessment System for Efficient Measures of Hand Rehabilitation

- I confirm that I have read and understood the information sheet for the above project and the researcher has answered any queries to my satisfaction.
- I understand that my participation is voluntary and that I am free to withdraw from the project at any time, without having to give a reason and without any consequences.
- I understand that I can withdraw my data from the study at any time.
- I understand that any information recorded in the investigation will remain confidential and no information that identifies me will be made publicly available.
- I consent to being a participant in the project

- I consent to being audio and video recorded as part of the project [delete which is not being used] Yes/ No

I (PRINT NAME)	Hereby agree to take part in the above project
Signature of Participant:	 Date